Comparison of nanofiltration and reverse osmosis processes for a selective desalination of brackish water feeds

Hanane Dach

▶ To cite this version:

Hanane Dach. Comparison of nanofiltration and reverse osmosis processes for a selective desalination of brackish water feeds. Engineering Sciences [physics]. Université d'Angers, 2008. English. tel-00433513

THÈSE DE DOCTORAT
Pour obtenir le grade de
DOCTEUR DE L'UNIVERSITÉ D'ANGERS
Spécialité : SCIENCES POUR L'INGÉNIEUR ET CHIMIE ANALYTIQUE
ÉCOLE DOCTORALE D'ANGERS

COMPARAISON DES OPÉRATIONS DE NANOFILTRATION ET D'OSMOSE INVERSE POUR LE DESSALEMENT SELECTIF DES EAUX SAUMATRES : DE L'ÉCHELLE DU LABORATOIRE AU PILOTE INDUSTRIEL

Présentée et soutenue publiquement

le : 6 mai 2008
à : l'Université de Fès
par : **Hanane DACH**

Mr. BOURSEAU Patrick   **Rapporteur**
Professeur, Université de Nantes, France

Mr. ELMIDAOUI Azzedine   **Rapporteur**
Professeur, Université de Kénitra, Maroc

Mr. BENTAMA Jilali   **Examinateur**
Professeur, Université de Fès, Maroc

Mr. LEPARC Jérome   **Examinateur**
VEOLIA, France

Mr. HAFSI Mahmoud   **Examinateur**
ONEP, Maroc

Mr. IJJAALI Mustapha   **Président du Jury**
Professeur, Université de Fès, Maroc

Mr. PONTIE Maxime   **Directeur de thèse**
Professeur, Université d'Angers, France

Mr. LHASSANI Abdelhadi   **Co-Directeur de thèse**
Professeur, Université de Fès, Maroc

Abstract

A competing membrane process to Reverse Osmosis (RO) for brackish water desalination in the near future is Nanofiltration (NF). In this study, we tried to determine when apply of NF instead of RO for brackish water desalination is of a good relevance. In order to predict and compare NF and RO membranes performance, a fundamental study in laboratory scale was performed to a better understanding of the retention mechanisms of salts by several NF and RO membranes. The performance of the tested membranes was measured in terms of fluxes and rejection under different operating conditions (Feed solution composition, ionic strength, Hydrostatic pressure, recovery rate). The results showed that the rejections of salts increased with the feed pressure and decreased with the salt concentration and recovery rate. The Spiegler-Kedem-Katchalsky model (SKK) was used to analyse the experimental data of filtration experiments. The validation of the model applied allowed us to quantify the mass transfer parameters and to determine the mass transfer occurring in NF and RO (Convection and/or hydration diffusion). The membranes were also characterized using Atomic Force Microscopy, Streaming potential and Contact angle measurements with the goal of relating fluxes and salts retention behaviour with the membrane surface properties.

The second part includes a technico-economical study comparing RO and NF processes for Tan Tan brackish water (4 $g.L^{-1}$) desalination on pilot scale in Tan Tan BWRO plant. In this study, the performance of number of NF and RO modules was evaluated in terms of productivity, desalination efficiency and energy requirements. It was found that the RO modules sharply reduced the TDS of Tan Tan water (rejections > 90%). NF was observed to be an effective method to perform partial desalination of Tan Tan brackish water at higher permeates fluxes and lower applied pressures. The degrees of mineral salt removal with the NF90 and NE90 membranes were in the range of 72 and 95%. The results of pilot plant tests were compared with softwer projections. Significant deviations between pilot experiments and the simulations are obtained for some softwares, and pilot studies are required for the elements corresponding.

This part also investigated the application of nanofiltration for demineralization of model solution simulating moderately brackish waters (salinity range of 4-10 $g.L^{-1}$), and defluoridation of Tan Tan brackish water doped with fluoride at high concentrations. The results indicate the effectiveness of NF membranes (NF90 and NE90) in the treatment of brackish water feed of TDS lesser than 6 $g.L^{-1}$. These membranes were also effective for fluoride removal at a satisfactory value.

Key words : Nanofiltration, Reverse Osmosis, Dessalination, Brackish water, Characterization, Defluoridation, Selectivity, Mass transfer, Simulations, technico-economical optimization.

Résumé

Le dessalement des eaux saumâtres et de l'eau de mer peut faire face à la problématique de pénurie d'eau qui menace certains pays tel que le Maroc. Actuellement, la technique la plus utilisée pour le dessalement des eaux saumâtres est l'Osmose inverse. La nanofiltration peut remplacer, dans les années avenir, l'Osmose inverse, mais la méconnaissance du comportement du matériau membranaire et des phénomènes de transfert limite l'application de la NF. Une meilleure compréhension des mécanismes de transport favoriserait son essor au sein du domaine de dessalement. C'est dans cette optique que nous avons mené ce travail pour contribuer à l'étude du dessalement des eaux saumâtres par NF. L'originalité de ce travail est de comparer les deux techniques de NF et d'OI sur le plan fondamental à l'échelle du laboratoire et de comparer leur performances pour le dessalement d'une eau saumâtre du sud du Maroc à l'échelle pilote.

Dans la partie fondamentale une approche systématique pour la caractérisation des membranes commerciales de nanofiltration et d'osmose inverse à basse pression a été établie, pour aider l'utilisateur au choix d'une membrane pour le dessalement des eaux saumâtres. Nous avons développé deux types de caractérisation : (i) physico-chimique, en terme de Hydrophilie/ Hydrophobie, morphologie et topographie, charge de surface et (ii) transfert de mass en terme de perméabilité hydraulique à l'eau ultra pure et à des solutions salines, rétention de sels monovalents et divalents, détermination du seuil de coupure, détermination des paramètres de transfert de masse σ et P_s respectivement le coefficient de reflexion et la perméabilité au soluté des membranes, compréhension des mécanismes de transfert de masse en NF ; la convection pure et la diffusion pure. Nous avons appliqué cette approche pour des membranes commerciales de NF et d'OIBP afin de comparer leurs performances et les classifier pour aider à la sélection d'une membrane de NF pour le dessalement des eaux saumâtres. La deuxième partie est consacrée à une étude pilote du dessalement d'une eau saumâtre du Sud du Maroc, afin de prouver sur le plan technique et économique, l'efficacité de la nanofiltration pour le dessalement cette eau. La NF s'est avérée efficace pour le dessalement partiel et sélectif de l'eau saumâtre étudiée en un seul étage, avec une consommation énergétique plus faible qu'en OI. Les membranes NF90 et NE90 sont les plus adéquates et les plus concurrentes à la BW30 pour le dessalement d'une eau saumâtre avec un taux de salinité de 4 g/L. Elle permettent un dessalement partiel et permettent aussi de préparer une eau destinée à la consommation humaine (TDS $\leq$ 1000 ppm) à des pressions 2 fois plus faibles et à des taux de conversions plus élevés (90%).

Des essais de dopage de l'eau de TanTan à différents taux de salinité et avec des ions fluorures ont été réalisés. Ces essais ont permis de déterminer la limite d'application des membranes de nanofiltration pour le dessalement des eaux saumâtres ($6 g.L^{-1}$) et confirmer l'efficacité de la NF pour la défluoruration sélective des eaux saumâtres au Maroc.

Mots clés : Nanofiltration, Osmose inverse, Dessalement, Eaux saumâtres, Caractérisation, Défluoruration, Sélectivité, Transfert de mass, Simulations, Optimisation technico-économique.

Acknowledgements

Table of contents

List of figures

List of tables

List of symbols

dp	Pore diameter
ds	solute diameter
C_{conv}	Solute concentration due to convection (mol.L^{-1})
C_m	Solute concentration at the surface membrane
C_{int}	Solute concentration inside the membrane (mol. L^{-3})
C_p	Solute concentration in the permeate (mol.L^{-1})
C_0	Solute concentration in feed (mol.L^{-1})
J_{diff}	Solute flux due to diffusion (mol.m^{-2}.s^{-1})
P_s	Solute permeability versus membrane (L.h^{-1})
J_v	Solvent flux (L.h^{-1}.m^{-2})
J_s	Solute flux (L.h^{-1}.m^{-2})
L_p	Pure water permeability (L.h^{-1}.m^{-2}.bar^{-1})
L_p'	Saline solution permeability (L.h^{-1}.m^{-2}.bar^{-1})
ΔP	Transmembrane pressure (bar)
R_{obs}	Observed retention (%)
R_{real}	Real retention (%)
R_a	Membrane roughness (nm)
ΔC_s	the concentration difference between each side of the membrane C_m-C_p (mol.L^{-1})
Pe	Peclet number
K	mass transfer coefficient
M	molecular weight of a solute
Sc	Molecular weight ut off (MWCO)
r_p	pore radius
$\Delta\phi$	trans-membrane potential difference
ΔP	trans-membrane pressure
$\Delta\phi/ \Delta P$	coefficient of streaming potential
Y	Recovery ratio(%)
E	Energy Consumption in kWh/m^3
r	conversion rate
ΔV	Volume of the permeate in a given time interval (Δt)
Pc	critical pressure

Greek letters

Φ	Polarization factor	
θ	Contact angle	
σ	Reflection coefficient	
□	Permittivity	
ζ	Zeta potential	
μ	Dynamic viscosity	
χ	Ionic conductivity of the electrolyte solution	
κ^{-1}	Debye length	
ψ^0	Surface potential	
ψ^d	Potential at the Stern plane	
η	Global pumping system efficiency	
π	Osmotic pressure	

Abbreviations

NF	Nanofiltration
RO	Reverse osmosis
MF	Microfiltration
UF	Ultrafiltration
LPRO	LPRO
R&D	Research and Development
TDS	Total Dissolved solids
WHO	World Health Organization
MSF	Multi-stage flash process
MED	multi effect distillation
VC	vapor compression
ED	Electrodialysis
SWRO	Sea water reverse osmosis
MENA	Middle East and North Africa
PV–RO	photovoltaic powered reverse osmosis
PA	Polyamide
CA	Cellulose Acetate
IEP	Iso electric point
SKK	Spiegler-Kedem-Katchalsky
TFC	Thin film composite

MD	Membrane distillation
MWCO	Molecular weight cut off
IT	Irreversible thermodynamics
SDI	Silt density index
TMP	Trnasmembrane pressure
AFM	Atomic forces microscopy
SWM	Spiral wound modules
SP	Streaming potential
IDA	International Desalination Association

General introduction

Water, a limited finite resource, vital for the very existence of life on earth and a necessity for economic and social development and for environmental sustainability, is becoming a scarce commodity. This is caused by the population growth, the change of lifestyle, water pollution, inefficient use of water and climatic changes with more frequent extreme events such as droughts and floods. Where the availability of water cannot be increased by using conventional resources or by recycling or cannot be made available by demand management methods, the desalination of sea or brackish water offers an alternative solution. The desalination of water has been practiced since ancient times but was not widely used due to technological limitations, the prohibitive high capital costs, high energy consumption and finally very high unit cost when compared to conventional water. New technological advances in the last 30 years tremendously reduced the capital cost and the energy consumption so that desalination projects can be considered as alternative solutions to water development.

During the last three decades, membrane filtration has emerged as a separation technology for water treatment which is competitive in many ways with conventional separation techniques, especially in comparison to distillation.

According to the World Health Organization (WHO, 2006), total dissolved solids (TDS) should be less than 1000 mg.L^{-1} in drinking water based on taste considerations. By comparison, seawater has an average TDS of about 35000 mg.L^{-1}. Thus the vast majority of the earth's readily available water is too saline for potable use, and yet much of the world's fresh water is trapped in polar icecaps (2.5%) or is located far underground (Bindra *et al.* 2001). It is estimated that 0.014% of the world's water is easily accessible and has acceptable salinity levels. Around 300 major river basins and underground aquifers cross national boundaries. Many of the world's fresh water resources are shared (Medeazza *et al.* 2004).

The principal water problem in the early twenty first century will be one of inadequate and uncertain supplies. Finite quantities of developed water supplies exist, and growing demand has outstripped supply in many regions of the world. Some countries currently suffering from water stress are mostly located in the Middle East and Northern Africa (i.e. their per capita yearly fresh water resources are below 1000 m^3/cap/y). However a few countries are also found in Europe, Asia and the Caribbean. By 2025, approximately 29 countries in the world are expected to experience water scarcity, particularly due to the expected increase in population, which will roughly double in regions where severe water shortages already exist (Bremere *et al.*2001).

The history of membrane demineralization using reverse osmosis (RO) dates from the 1960s. Hence, the high pressures traditionally used in RO resulted in a considerable energy cost was first dedicated to seawater. Thus, RO membranes with lower rejections of dissolved components, but with higher water permeability, appeared to be of great improvement for

separation technology, and low pressure RO membranes appeared dedicated to partial demineralization of brackish waters. By the second half of the 1980s, (Conlon, 1989), the interest in low pressure RO had become established, specially for water softening and the first applications of NF was born, as detailed in a recent review (Hilal, 2004).

NF offers several advantages in comparison to RO such as low operation pressure, high flux, high retention of multivalent anion salts and organics compounds with molecular weight situated between 100 to 1000 Da, relatively low investment and low operation/maintenance costs. Because of these advantages, the applications of NF worldwide have increased. Today 10% of brackish waters market in the world is destined to nanofiltration (NF) membranes (Rovel 2004). While NF is a relatively new membrane process, it is already widely used for water treatment in different parts of Europe, Israel and the US. Striving towards improved quality, efficiency and applicability, research is continuing in an attempt to understand and model the varying parameters involved in NF. A technique that is often used for the evaluation of membranes is the flux and rejection behaviour of uncharged and charged solutes (Krieg, 2004). However, many membranes have to be screened before finding a suitable one.

NF is known to be a suitable process for water demineralization. Through this topic is less studied, it is logical to assume that NF is capable of removing other inorganic and organic compounds from the feed waters specially calcium due to its well-known softening properties Furthermore, there is more interest in NF since it is less susceptible for scaling due to more open pores in comparison to RO. NF interest also comes from its property of partial demineralization of brackish waters without the addition of chemicals, at lower pressure and higher flux. Actually, there are no studies dedicated to a technico-economic comparison between RO and NF for brackish water feeds in the literature. The optimum operating conditions of NF planned to obtain in the initial studies of this project are helpful to the project partner to conduct pilot scale experiments.

The objectives of the present work was to determine the technical and energetic limits in which nanofiltration (NF) operation could replace advantageously or not RO operation in the treatment of brackish water feeds. One case study conducted from the laboratory bench scale experiments to industrial pilot scale in Tan Tan city (South of Morocco) will be related.

The body of the dissertation consists of three chapters:

- The first Chapter provides a literature review on the "state-of-the-art" of the studied domain. It includes also the Moroccan experience in desalination, a review of water defluoridation processes. Detailed descriptions of membrane processes are also presented in this chapter. This is followed by a comprehensive review in NF.

- The second Chapter is dedicated to the description of the operating conditions of experiments carried out from laboratory bench scale experiments to industrial pilot studies.

- The third section is related to results and discussions. The results from this work are presented in two parts. The first part is a fundamental study which reports a novel and original systematic approach in the range of characterization of commercial

nanofiltration (NF) and low pressure reverse osmosis (LPRO) membranes materials. Then we'll developed two sorts of membranes characterization in terms of pure water and saline solution permebilities, hydrophilicity, morphology and topography and by phenomenological parameters determination from Spiegler-Kedem-Katchalsky mass transfer model with monovalent (NaCl) and divalent (Na_2SO_4) solutions. The characterization of NF and LPRO membranes was followed by an application on synthetic brackish waters and real feed water from the south of Morocco (Tan Tan) in a bench scale will help us to illustrate the interest in NF vs LPRO for a selective removal of excess chloride, fluoride and nitrate ions in brackish waters. In the second part, an applied study on a pilot scale in Tan Tan desalination plant (South of Morocco). In this part, the technical and economical feasibilities of NF versus RO process for the production of potable water from Tan Tan water were investigated for a sustainable development of brackish water desalting unit for the future. The main performance indicators of the small NF/RO desalination system used were productivity in the form of flux and recovery, desalination efficiency in the form of retention with regards to total dissolved solids, individual elements and energy requirements.

Chapter one: Literature review

1. Water Desalination: Global overview

1.1 Introduction

Water, a limited finite resource, vital for the very existence of life on earth and a necessity for economic and social development and for environmental sustainability, is becoming a scarce commodity. This is caused by the population growth, the change of lifestyle, water pollution, inefficient use of water and climatic changes with more frequent extreme events such as droughts and floods. Where the availability of water cannot be increased by using conventional resources or by recycling or cannot be made available by demand management methods, the desalination of sea or brackish water offers an alternative solution (Nicos, 2001). A desalination process separates sea or brackish water into two streams: a fresh water stream containing a low concentration of dissolved salts and a concentrated brine stream. The desalination of water has been practiced since ancient times but was not widely used due to technological limitations, the prohibitive high capital costs, high energy consumption and finally very high unit cost when compared to conventional water. The process utilizes several different technologies for separation. Two of the most commercially important technologies are based on the multi-stage flash (MSF) distillation and reverse osmosis (RO) processes (Maurel, 2006). Although the desalination technologies are mature enough to be a reliable source for fresh water from the saline water, a significant amount of research and development (R&D) has been carried out in order to constantly improve the technologies and reduce the cost of desalination. However, desalination projects are still not very cheap to be easily accommodated by the economics of many countries, energy consumption is still comparatively high. This section reviews the current status, practices, and advances that have been made in desalination technologies and their contribution on current water supply needs. Additionally, it provides an overview of R&D activities and outlines future prospects for the state-of the-art water desalination technologies.

1.2 Water availability

The Earth's hydrosphere represents 1.38 billion km^3 of water. As represented on Figure 1, 97.5 % of it is seawater with oceans covering approximately 71% of Earth surface. Among the 2.5 % of the hydrosphere being fresh water, 69.5 % is in the form of ice or permanent snow cover in Arctic, Antarctica and mountainous regions. The other 30.1 % are groundwater estimated at 10 millions km^3 (Bindra *et al.* 2001). At last, lakes and rivers represent 0.4% of freshwater resources, i.e. around one 1/150000th of water on Earth.

The principal water problem in the early twenty first century will be one of inadequate and uncertain supplies. Finite quantities of developed existing water supplies has outstripped the growing demand in many regions of the world.

In order to assess local human needs vs. water availability, the annual renewable water resources ought to be compared with the current and future human withdrawals estimated at the local scale. Water stress indicator is defined as the ratio between annual water withdrawals divided by the annual renewable water resources. In 1995, the UNESCO estimated that 1.7 billion people were under water stress. As shown in Figure 2, the countries currently suffering

from water stress are mostly located in the Middle East and Northern Africa (i.e. their per capita yearly fresh water resources are below 1000 m^3/cap/y). However a few countries are also found in Europe, Asia and the Caribbean. Considering an average population growth (9.3 billion people in 2025) (UNESCO, 2003), it is possible to forecast the evolution of water consumption and to identify future water stress situations. By 2025, approximatively 29 countries in the world are expected to experience water scarcity (Figure 3), particularly due to the expected increase in population, which will roughly double in regions where severe water shortages already exist (Bremere *et al* 2001).
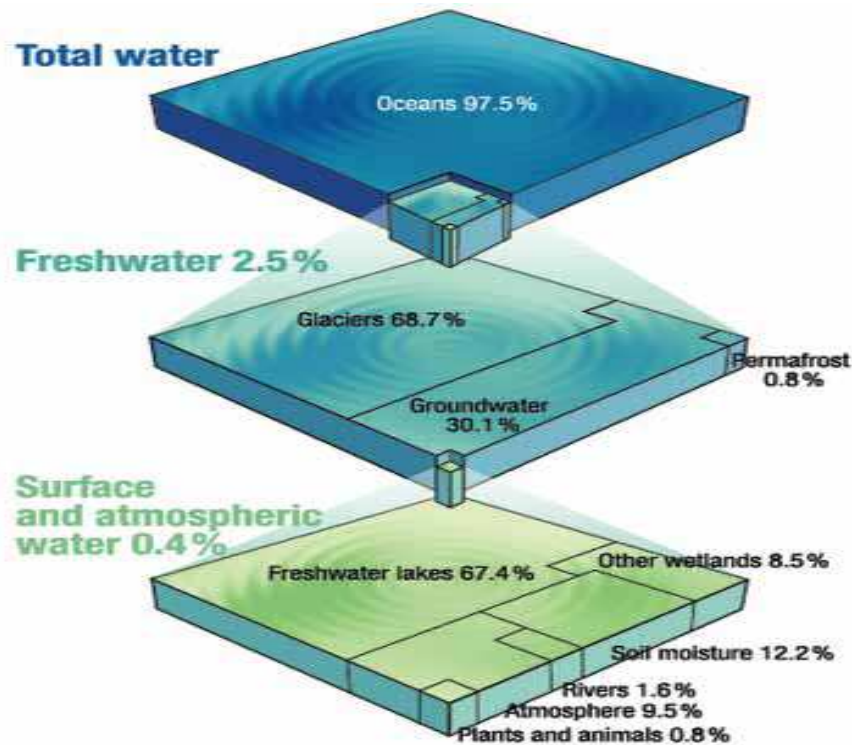
Figure 1: Earth's hydrosphere

Traditional solutions to water scarcity have focused on developing new supplies (e.g. drilling wells, building dams to store water that would otherwise become irretrievable). However, even when options are available for developping new supplies or transferring water from other areas where supplies are more plentiful, water development can be extremely expensive. Water availability includes issues of both water quantity and quality. After all, just as drought conditions can reduce the amount of water available, reductions in water quality can diminish the available water supply for it's entended use. Properly desingned water treatment can transform otherwise non-usable water to usable water, thereby increasing the amount of available water. Desalination technologies offer the potential to add significantly to freshwater supplies in the region of world where water is scarce although these supplies currently are associated with substantial energy and financial costs (Bremere *et al.* 2001). Once considered as an expensive last resort solution for marginal municipal domestic and industrial water supply, desalination technology is becoming increasingly affordable. It is finding new outlets in water scarce regions where it was never previously considered as a

viable long term resource (Bremere *et al.* 2001). The difference between the cost of desalted water and that of conventional supplies has narrowed dramatically in the past 15 years. The growth of the desalination is due to the increase of the cost of development of the conventional water because of water shortage, fewer and not suitable dam sites with higher developments costs, deeper aquifers and water quality deterioration (Nicos, 2001).
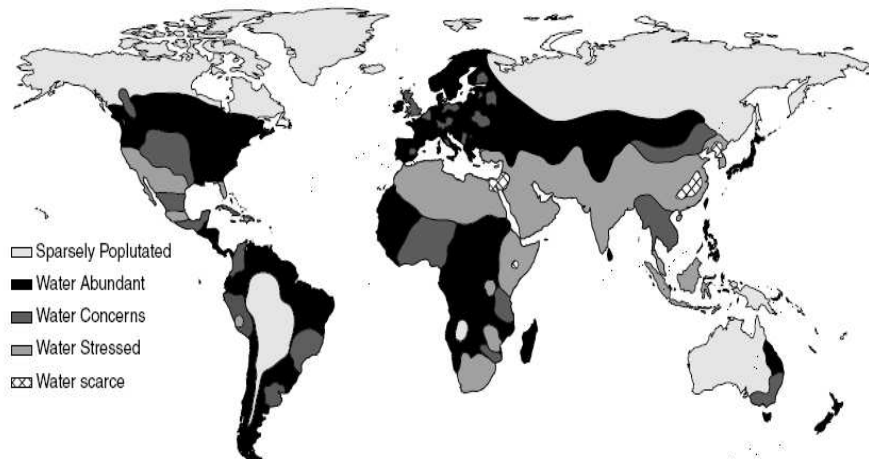
Figure 2: Estimated water availability world wide
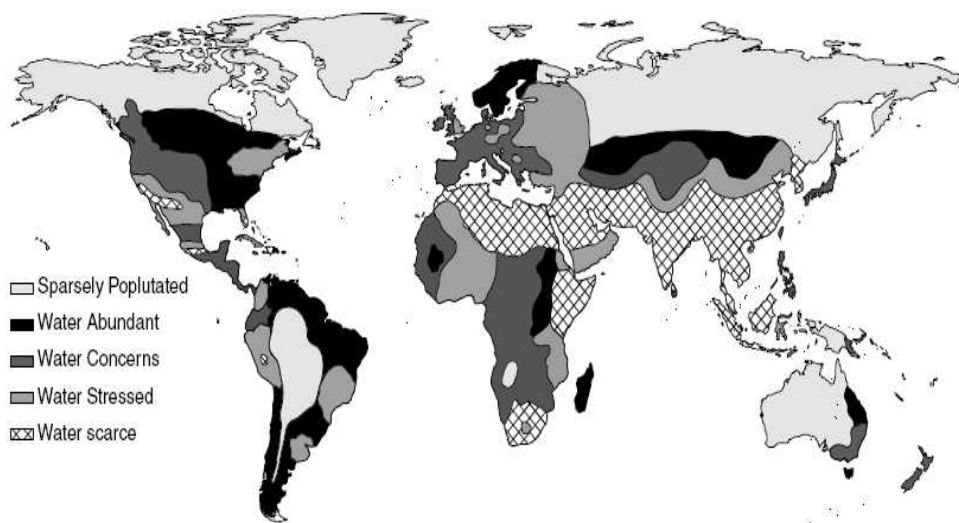
Figure 3: Projected worldwide water scarcity through 2025.
(Source: Committee to Review the Desalination and Water Purification Technology Roadmap, National Research Council, 2004)

1.3 Desalination

Desalination is the process of removing dissolved solids from brackish water and seawater to produce potable water. The amount of salt in water is usually described by the concentration of total dissolved solids (TDS) in the water. TDS refers to the sum of all minerals, metals, cations and anions dissolved in water. Water that contains significant amounts of dissolved salts is called saline water, and is expressed as the amount of TDS in water in mg/L.

1.3.1Brackish water versus seawater

The desalination industry makes a distinction between seawater and brackish water. A classification of source water according to quantity of dissolved solids is given in table 1.

Table1: *Classification of source water according to quantity of dissolved solids*

Water source	Total dissolved solids (milligrams per liter)
Potable water	< 1000
Mildly brackish waters	1000 to 5000
Moderately brackish waters	5000 to 15000
Heavily brackish waters	15000 to 35000
Average sea water	35000

Note: some seas and evaporative lakes can show wide variability in TDS; for example, the Arabian Gulf has an average TDS of 48g.L^{-1}, and the Mediterrannean sea 38g.L^{-1}.

Seawater typically has a salt concentration in the order of 35000 mg/L. More than seventy elements are dissolved in seawater, but only two elements (Chloride and Sodium) make up greater than 85% by weight of all the dissolved water. Seawater is a saline solution of nearly constant composition. Brackish water contains less TDS than seawater but more than freshwater. The TDS concentrations in brackish water can range between 1000 mg/L to 15000 mg/L; most brackish water environments are dynamic and TDS levels in these environments fluctuate spatially and temporally. The salinity of brackish surface water near the coast can vary depending on the tide, the amount of fresh water entering the system as rain or river flows, and the rate of evaporation. Brackish water also occurs in coastal aquifers. Some deep groundwater aquifers contain brackish water that occurs under natural conditions. In costal aquifers, excessive groundwater withdrawals may cause the seawater to move into freshwater aquifers (a phenomenon known as saltwater intrusion) and create brackish water in the aquifer.

1.3.2 Product water specification

An important consideration for any desalination system is the quality required of the product water. Some systems provide very pure water for particular industrial processes, but the majority are designed to provide drinking water. It is clearly important to establish an appropriate upper limit for the concentration of the water delivered to the consumer. In desalination literature, it is often stated that the World Health Organisation (WHO) recommends a limit of 500 mg/L TDS, but the exact origin of this figure is unclear. There is no evidence of a 500-mg/L TDS limit within the WHO Guidelines. Regarding total dissolved solids, the WHO Guidelines (Third Edition, 2006, chapter 12, page 444) say:

…no health-based guideline value is proposed. However, the presence of high levels of TDS in drinking-water may be objectionable to consumer. Water with extremely low concentrations of TDS may also be unacceptable because of its flat, insipid taste. (see chapter 10).

Apparently, the first edition of the guidelines (1984) did suggest a limit of 1000 mg/L for TDS, based on *taste*. This limit was removed in the second edition. There is no mention of any limit at 500 mg/L. Chapter 10 of the Guidelines (page 218) indicates that *The palatability*

of water with a TDS level of less than 600 mg/liter is generally considered to be good; drinking-water becomes significantly and increasingly unpalatable at TDS levels greater than about 1000 mg/liter.

In summary, the acceptable concentration of salt in water is primarily a matter of taste, not health .The acceptable taste will depend greatly on whom the consumers are, what they are accustomed to and what their alternatives are. A product concentration of 500 mg/L remains a useful target, but in areas with no alternative supply, 1000 mg/L may well be perfectly acceptable, especially if this can be produced in greater quantity or with improved reliability.

1.3.3 Growth of desalination capacity worldwide

Desalination technologies and their application have grown substantially over the last fifty years. Today, some countries depend on desalination technologies for the purpose of meeting their fresh water requirements. In particular, in the Middle East, water desalination is a vital and dependable fresh water resource in countries such as Saudi Arabia, United Arab Emirates, and Kuwait. Overall, it is estimated that over 75 million people worldwide obtain fresh water by desalinating seawater or brackish water. The IDA Desalting Inventory 2007 Report shows that at the end of 2006, installed and contracted brackish and seawater desalination plants worldwide totaled 12,791 desalination plants. The current world desalination plant capacity is 43 million m^3/day and the annual average growth rate for the last 5 years is 12% (Khawaji *et al.* 2008).

Desalination plants operate in approximatively 125 countries, with seawater desalination plants contributing 60 percent of the total worldwide desalination capacity (Figure 4).
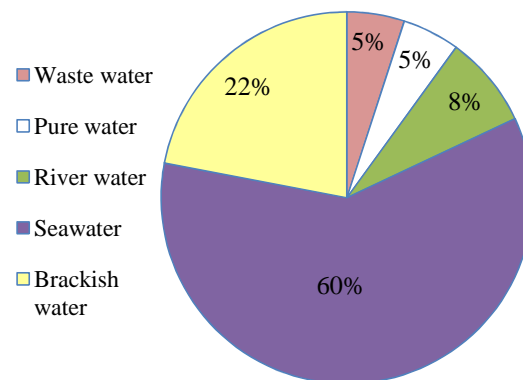
Figure 4: *Chart showing portions of total desalination capacity by source water (IDA Desalination Yearbook, 2007)*

Some arid regions depend heavily on desalination for their water supply. The Middle East countries, mainly the Gulf Cooperation Council States, are the biggest users of desalination technology with 50% of the world's capacity, followed by America then Europe, as shown in Figure5 (Maurel, 2006).
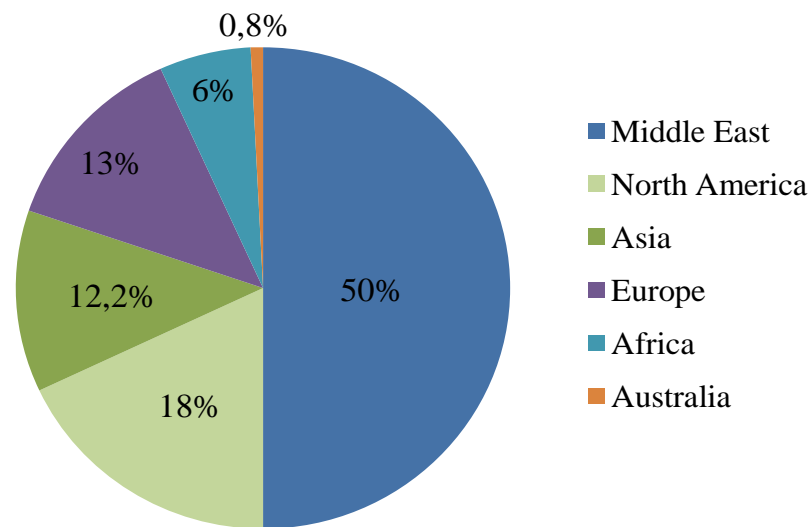
Figure 5: *Chart showing fraction of the worldwide capacity of desalination plants by region.*

1.4 Desalination Technologies

Many different desalination technologies exist to separate dissolved salts from water. The desalinated water is recovered for consumption where the salts are concentrated in a stream of water called the brine reject, disposed either to the sea or to a saline aquifer or in evaporation ponds. A typical flow diagram of the process with inputs and outflows is shown in Figure 6.
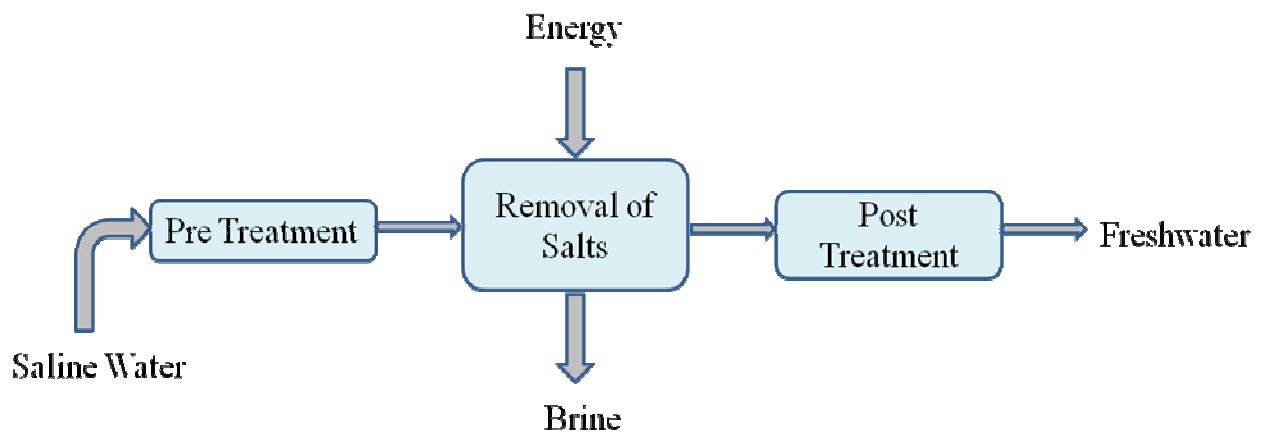
Figure 6: *Typical desalination system (Maurel, 2006)*

The water desalination processes require significant quantities of energy to achieve the salt separation and to get fresh water. The amount and type of the energy required differs according to the used technique (Ahmed *et al.*, 2002).

The choice of technology used for water desalination depends on a number of site specific factors, including source water quality, the intended use of the water produced, plant size, capital costs, energy costs and the potential for energy reuse (Al-Subaie *et al.* 2007). The commercially tested desalination processes are given in Figure 7.

Water desalination can be accomplished by different techniques that can be classified into two categories: thermal and membrane processes. The thermal processes can be subdivided into the following processes:(i) Multistage flash evaporation, (ii) Multiple effect distillation and (iii) Vapour compression. The membrane processes are subdivided into: (i) Reverse osmosis (ii) Electrodialysis and (iii) Nanofiltration. Some basic informations on these processes are shown in Tables 2.
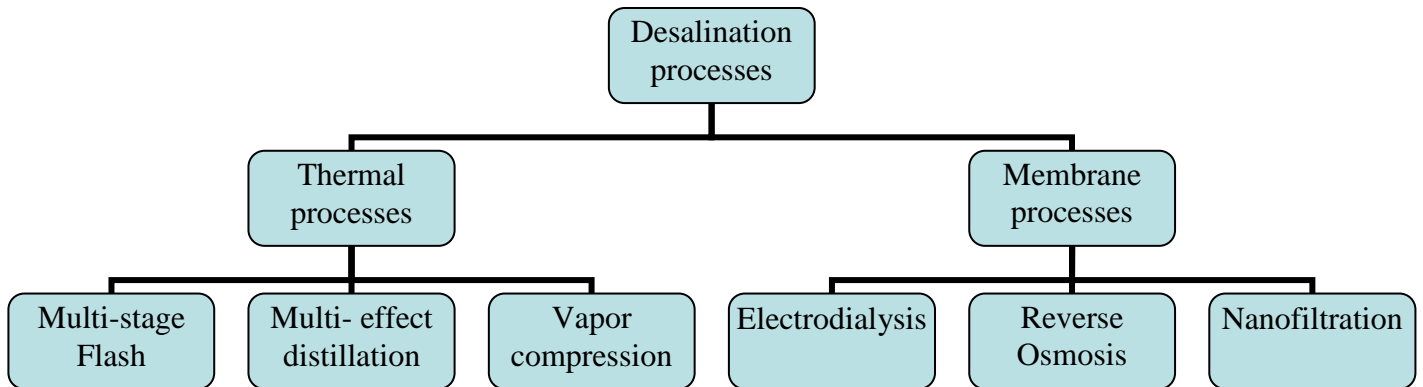
Figure 7: *Industrial desalination processes (Maurel,2006)*

1.4.1 Thermal processes

This method mimics the hydrological cycle in that salty water is heated producing water vapor that in turn condensed to form fresh water free of salts. The fresh water is mineralized to make it suitable for human consumption. The important factors to be considered for this method of desalination are the proper temperature relative to its ambient pressure and enough energy for vaporization for energy minimization and the control of scale formation. The energy needed for vaporization is reduced usually by the use of multiple boiling points in successive vessels, each operating at a lower temperature and pressure, where the scale forming is controlled by controlling the top temperature of the process or by the addition of antiscalants to the seawater. The known thermal methods are the multi-stage flash process (MSF), multi effect distillation (MED) process and the vapor compression (VC) distillation process.

1.4.1.1 Multiple-effect distillation

The multiple-effect distillation (MED) process is the oldest desalination method and is very efficient thermodynamically. The MED process takes place in a series of evaporators called effects, and uses the principle of reducing the ambient pressure in the various effects. This process permits the seawater feed to undergo multiple boiling without supplying additional heat after the first effect. The seawater enters the first effect and is raised to the boiling point after being preheated in tubes. The seawater is sprayed onto the surface of evaporator tubes to promote rapid evaporation. The tubes are heated by externally supplied steam from a normally dual purpose power plant. The stream is condensed on the opposite side of the tubes, and the steam condensate is recycled to the power plant for its boiler feed water. The MED plant's steam economy is proportional to the number of effects. The total number of effects is limited by the total temperature range available and the minimum allowable temperature difference between one effect and the next effect. Only a portion of the seawater applied to the tubes in the first effect is evaporated. The remaining feed water is fed to the second effect,

11

where it is again applied to a tube bundle. These tubes are in turn heated by the vapors created in the first effect. This vapor is condensed to fresh water product, while giving up heat to evaporate a portion of the remaining seawater feed in the next effect. The process of evaporation and condensation is repeated from effect to effect each at a successively lower pressure and temperature.

1.4.1.2 Multi-stage flash distillation (MFS)

In *flash* distillation, the water is heated under pressure, which prevents it from vaporizing while being heated. It then passes into a separate chamber held at lower pressure, which allows it to vaporize, but well away from the heating pipes, thus preventing them from becoming scaled. Like MED, practical flash-distillation systems have compartments and each compartment is called *stage*, hence the term *Multi-Stage Flash* (MSF). When first introduced in the 1960's, MSF offered slightly lower energy efficiency than MED, but this was outweighed by scaling considerations and MSF became the industry standard. The desalinated water produced by the MSF process contains typically 2-10 ppm dissolved solids. Therefore, it is remineralized through the potabilization (or post-treatment) process.

1.4.1.3 Vapour Compression

Compressing water vapour raises its temperature, which allows it to be used at a heat source for the *same* tank of water that produced it. This allows heat recycling in a single effect distillation process. In Thermal Vapour Compression, the compressor is driven by steam, and such systems are popular for medium-scale desalination because they are simple, in comparison to MSF. In Mechanical Vapour Compression, the compressor is driven by a diesel engine or electric motor.

The water produced by the thermal process is very pure with almost no salts, where the feed water quality has almost negligible effect on energy consumption (Nicos, 2001). Thermal processes are the primary desalination technologies used throughout the Middle East because these technologies can produce high purity water from seawater and because of lower fuel costs in the region.

1.4.2 Membrane processes

Membranes have the ability to differentiate and selectively separate salts and water. Using this ability but differently in each case, three membrane desalination processes have been developed for desalting water: Electrodialysis (ED), reverse osmosis (RO) and nanofiltration (NF).

The RO represents the fastest growing segment of the desalination market (Blank *et al.*, 2007). Membrane technologies can be used for desalination of both seawater and brackish water, but they are more commonly used to desalinate brackish water because energy consumption is proportional to the salt content in the source water.

Although thermal technologies dominated from the 1950s until recently, membrane processes now approximatively equal thermal processes in global desalination capacity.

Compared to thermal distillation processes, membrane technologies generally have lower capital costs and require less energy, contributing to lower operating costs. In fact, the most important progress in the area of membrane systems is the reduction of membrane cost by

factor of approximatively 10 over the last 30 years making the pretreatment and the seawater intake as the most expensive items of a membrane system (Khawaji et *al.,* 2008).

However, the product water salinity tends to be higher for membrane desalination (< 500 ppm TDS) than that produced by thermal technologies (< 25 ppm), but when making use of a second RO pass the same quality can be obtained.

Table2: *Characteristics of desalination operations (Mohsen and A1-Jayyousi, 1999)*

Method of desalination	Advantages	Disadvantages
Multi-effect desalination (MED)	High production capacity Low capital cost High purity (< 30ppm) Energy input independent on salinity Minimal skilled operator	Dependence of output on local power availability Long construction period Difficult to control water quality Low conversion of feed water (30%-40%) Labor-intensive Large space and material requirements
Reverse osmosis (RO)	Suitable for both sea and brackish water Flexibility in water quantity and quality Low power requirement compared with MED and VC Flexibility in site location Flexibility in operation start-up and shut-off Simple operation	Low quality (250-500 ppm) Requires high quality feed water Relatively high capital and operating costs High pressure requirements Long construction time for large scale plants
Vapor compression (VC)	High water quality (20 ppm) High operational load Short construction period Operation and production flexibility	High operational costs High energy consumption Lack of water quality control
Electrodialysis (ED)	Low operating and capital costs Flexible energy source High conversion ratio (80%) Low energy consumption Low space and material requirements	Low to medium brackish water capability (3000ppm) Requires careful pretreatment of feed water Low production capacity Purity affected by quality of feed water
Multi-stage flash	Flexibility in salinity of feed water High purity production (< 30ppm) High production capacity Low skill requirement Production of both water and electricity High energy input	Labor intensive Low conversion ratio (30%-40%) High operating costs High construction requirements Limited potential for improvement

1.4.2.1 Reverse osmosis

In the reverse osmosis (RO) process, the osmotic pressure is overcome by applying external pressure higher than the osmotic pressure on the feedwater. Thus, water flows in the reverse direction to the natural flow across the membrane, leaving the dissolved salts behind with an increase in salt concentration. No heating or phase change is necessary. The major energy required for desalting is for pressurizing the seawater feed. A typical large seawater RO plant consists of four major components: feed water pre-treatment, high pressure pumping, membrane separation, and permeate post-treatment.

1.4.2.2 Electrodialysis

Electrodialysis also uses membranes, but unlike RO, the salt ions are deliberately carried through the membranes, leaving behind the freshwater. Two types of membranes are required: one that lets anions through but not cations, and the other that does the opposite. These membranes are stacked alternately and held apart by spacers. The saltwater is fed into the spacer layers on one side of the stack, and a DC voltage is applied to the stack as a whole. The salt ions are attracted through one membrane or the other depending on their polarity, and by the time the water comes out from other side of the stack, it is alternately freshwater and concentrate in separate compartment. Reversing the polarity of the applied voltage reverses the freshwater and concentrate compartments, and this can be done periodically (several times per hour) in order to reduce fouling, and it is termed Electrodialysis Reversal. Electrodialysis was commercialized during the 1960's and is widely used today for desalinating brackish water. The energy consumption depends very much on the concentration of the feed water and so electrodialysis is rarely used for seawater desalination.

1.4.2.3 Nanofiltration

Nanofiltration works similar to reverse osmosis expect, NF needs less pressure. This process can remove some total dissolved solids but is often used to partially soften water and is successful at removing solids and dissolved organic carbon. For low TDS brackish waters, NF may be used as a stand-alone treatment for removing salts. NF is the technology chosen for the system described in this thesis versus RO, and is described in section V.

1.4.3 Current technologies and their merits and demerits

By looking at the total desalination plants installed in the world we simply realize that two major desalination technologies are used: RO with 51% and MSF processes with 33% production (IDA Desalination yearbook, 2007). Figure 8 shows the share of installed desalination capacities by process.
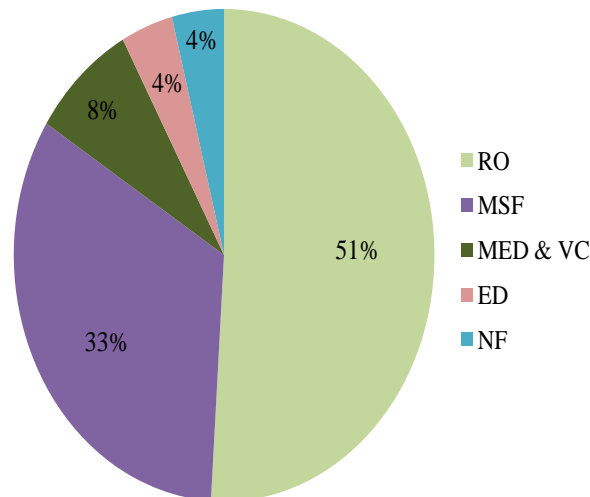
Figure 8: *Installed capacity by process (IDA Desalination Yearbook, 2007)*

<u>*Multi-Stage Flash distillation (MSF)*</u>

MSF uses a series of chambers, each with successively lower temperature and pressure, to rapidly vaporize or flash water from bulk liquid brine. The vapor is then condensed on tubes in which feed water is following, thereby recovering energy from the heat of condensation. MSF is a reliable technology having large production capacities per unit. MSF produces very low TDS product water < 50 mg/L, which is suitable for industries application and it does not depend on feed quality. Despite its large energy requirements, MSF is among the most commonly employed desalination technologies. It is predominantly used in the Middle East.

<u>*Reverse Osmosis (RO)*</u>

Early RO plants were developed for the treatment of brackish water and the membranes were not suitable for seawater desalination. Since the early days, the membranes have been improved in terms of salt rejection, productivity, resistance to higher pressure as well as higher temperature. They are presently used for seawater desalination (SWRO) (Al-Subaie *et al*. 2007). SWRO is typically the lowest capital and operating cost solution for most applications worldwide. It consumes nearly about half of the energy needed for thermal processes (Blank *et al*., 2007) also, the modularity of RO units, their simplicity of operation, their compact sizes and lower environmental impacts give them priority to be used for water desalination in remote areas (Ahmed *et al.*, 2002). SWRO is very much dependent on feed water quality as well as good designing of pretreatment systems. The membranes are very sensitive to suspended solids, certain chemicals and biological fouling. In order to maintain the membranes in good order and to give them reasonable life, better pre-treatment is needed (Andrianne *et al.* 2002).

With the growing trend for hybrid desalination plants, i.e., a combination of thermal and membrane technology, to provide the optimum plant configuration in terms of running cost

and flexibility, SWRO will continue to establish itself as a suitable technology, even in the most difficult locations subject to a good pretreatment plant (Khawaji et *al.,* 2008).

1.4.4 Future processes for brackish water desalination

Other processes for brackish water desalination other than those mentioned earlier are gaining popularity and will come into the market on a large scale within the next years (Bindra *et al*. 2001). Figure 9 presents the installed capacity of brackish water desalination by process. Electrodialysis represents approximatively four percent of worldwide desalination capacity. This process constitutes a more realistic choice for brackish water desalination, since it consumes low energy than RO when feed water salinity is lower than 3000 mg/L (Walha *et al*. 2007, Sahli *et al*. 2008). Considering the feed water quality, pre-treatment is often more strict in the case of RO, since RO membranes are very susceptible to fouling. On the other hand, as ED removes ions from the water, additional measures may be required (disinfection, removal of particles, etc).

A competing membrane process for brackish water desalination in the near future is Nanofiltration (NF). Since reverse osmosis cannot be used for partial and/or selective demineralization, NF is more suitable for producing drinkable water directly without the need for remineralization. The ability of NF membranes to demineralize salty solutions partially or selectively makes it interesting technique in many respects due to the recent development of novel NF membranes.

Million m^3/d

9.8

1.4

Distillation processes   Membrane processes (RO+ED+NF)
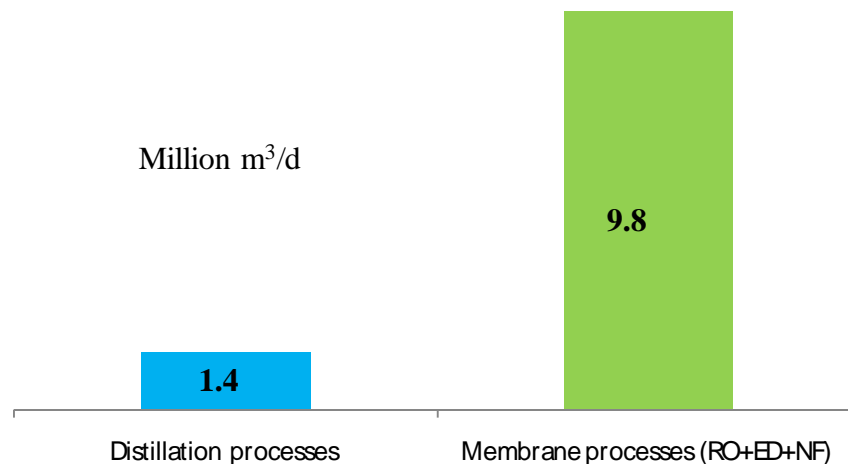
Figure 9: *Installed capacity of brackish water desalination by process (Rovel, 2004)*

NF seems to be the economical desalination process for brackish water desalination due to its low energy consumption. NF offers the great advantage of lower operating costs than RO and ED. Low cost membrane materials have also contributed to its use, making it less expensive than the other method mentioned earlier. Having more open pores and functioning with lower pressures, this process give rise to a high permeate flux and to a selective retention between divalent and monovalent ions (Haddada *et al*. 2004).

In principle, the economic potential of the NF process for brackish water desalination is known and a lot of research was carried out on this process, but considerably more R&D work and pilot plant testing in large scale is required to industrialize it.

1.5 Renewable energy sources for desalination

Desalination is an energy intensive process and energy requirements are huge since desalination plants are high tonnage plants. Presently, these energy requirements are met with very expensive fossil fuels which continue to increase in price and greatly contribute to global warming. It is thus an essential obligation in the future to look for alternative energy sources to meet the growing demand for desalination. The development of a sustainable desalination method requires the minimization of energy consumption, but also the use of renewable energy sources. This could enable less developed countries to have access to sufficient quantities of fresh (desalted) water. Different options can be suggested. The most common renewable energy sources are solar and wind (Van der brugen, 2003). At present, uses of renewable energy sources for desalination are very limited. The world's share of total renewable energy sources used for desalination is only about 0.02% of the total energy used (Lourdes. 2002). Large part of the (MENA) region faces severe water shortage and in some countries have bad water management issues. Renewable energy is the most obvious choice especially solar energy in the Middle East and North Africa (MENA) region which is characterized by arid and semiarid environments (Mahmoudi and Ghaffour, 2008). However, this technology needs to be developed to reduce its limitation since it is presently at least four times more expensive than fossil fuel.

1.5.1 Wind energy

Wind energy rotates windmills creating mechanical energy that can be converted to electrical energy. For better efficiency, the average wind velocity should be above 5m/s. Thus, wind powered desalination is a feasible option for windy islands, for example, such as the Canary Islands where wind energy is used partially for electrical power generation and partly for sea water desalination (Carta *et al.* 2003). Electrodialysis and MVC systems are well suited to operate using wind energy. Using this energy to power RO systems is not feasible because RO systems have to be operated continuously. Operating costs of a wind powered system are minimal, but a significant investment has to be made (Lourdes. 2002).

1.5.2 Solar energy

Many coastal and inland areas around the world have plenty of sunshine and lack fresh water supply. The logical answer to the problem is solar desalination using available seawater or brackish water. Solar energy can be used as an improved combination of solar distillation and MED (El-Nashar, 2001, Hrayshat *et al.* 2008). Among the different systems, salt gradient solar ponds and the parabolic trough are the most common. Possible uses are to be found in the preheating of the seawater and stream generation. To this date , solar energy for MED is still not able to compete with fossil energy at current crude oil market prices, except for (sunny) remote areas where solar energy can be an attractive alternative (Van der brugen, 2003).

Currently, the most promising solar energy technology is photovoltaic (PV) arrays. Photovoltaic arrays convert solar energy into electricity through the transfer of electrons. Hundreds of small photovoltaic power plants have been developed. Reverse osmosis systems connected to photovoltaic plants are already commercialized and considered the most promising combination of solar energy with desalination. Many examples of photovoltaic powered reverse osmosis (PV–RO) treatment systems can be found in the literature (Herold *et al 1998;* Richards *et al.* 2004; Coté *et al.* 2001; Thomson *et al.* 2003; Gotor *et al.* 2003; Bouchekima *et al.* 2003). The successful adaption of such systems to remote locations, where maintenance facilities are generally not available, is largely a question of robust system design and socio-economic integration. The coupling with photovoltaic systems also may be feasible with electrodialysis.

1.5.3 Geothermal energy

Geothermal energy resources exist in three forms: thermal, hydraulic and methane gas. Geothermal can be harnessed and applied to produce electricity that is sent to local grids or to directly power thermal desalination plants.

1.5.4 Nuclear energy

Using nuclear energy to power desalination plants is a developing technology. Currently, research is being conducted to determine the feasibility of developing dual purpose power and desalination plants. Combining nuclear power plants with desalination plants is economical because 2/3 of thermal power generated is waste heat. Researchers have found that it is economical to use this heat in desalination plants. Also power plants are able to provide immediate electricity to the desalination plant.

1.6 Concentrate disposal

Desalination and membrane-based water purification technologies do not eliminate the water constituents of concern. Rather, these constituents are concentrated in a fraction of the water, thus improving the water quality of the other fraction. Designing a desalination plant to eliminate concentrate production is not technologically feasible. However, the volume of water containing concentrated salts can be reduced through various technologies.

The concentrate must be handled in a manner that minimizes environmental impacts. At present, most of desalination plants dispose their concentrate to surface waters. Other concentrate disposal options include deep well injection, land application, evaporation ponds, brine concentrators and zero liquid discharge (ZLD) technologies. Planners consider a variety of factors to choose the best disposal option and it depends on the volume or quantity of the concentrate, the quality of the concentrate, the location of the desalination plant and the environmental regulations. Other factors include public acceptance, capital and operating costs and the ability of future plant expansion.

Several current or future concentrate management alternatives are summarized below.

• **Disposal in a Saline Water Body** is a reasonable option when the desalination plant is located close to a very salty water body such as the ocean. In this case the main constraint is to meet environmental concerns. In most cases, appropriate dilution of the concentrate can be

achieved to reduce or eliminate its impact on the environment (Huang *et al.* 2003), but saline water disposal could become an issue if the concentrate contains elements with toxic effects on aquatic organisms or on wildlife that feed on aquatic organisms. Pretreatment prior to disposal consists of aeration by adding oxygen to the concentrate, and degasification to remove hydrogen sulfate from the concentrate (Van der Brugen and Vandecasteele, 2002). Using non-toxic additives and dechlorination techniques limits the toxic chemical concentrations that enter the environment.

• **Deep Well Injection** is often the most viable option for concentrate management at inland desalination facilities when suitable geologic formations are available. Generally, suitable formations must be confined and/or isolated to prevent contamination of adjacent aquifers. Suitable formations for injection often contain water with TDS concentrations in excess of 10,000 mg/L and are located at great depths. Injection wells are expensive to develop and operate.

• **Evaporation Ponds** are constructed ponds where water from concentrate is allowed to evaporate while the remaining salts accumulate in the base of the pond. Evaporation ponds are used in areas that have warm climates and high evaporation rates. The size of an evaporation pond depends on the evaporation rate in the region and the surge capacity, freeboard and storage capacity. It is important for these ponds to have liners in order to prevent saline water from percolating into the groundwater aquifer. Evaporation ponds are a cost effective option for inland plants to dispose of concentrate due to the large surface area required and the associated land and impermeable liner costs. Land costs are a function of location but the cost of liners could be reduced through technological improvements.

• **Zero Liquid Discharge (ZLD) or near-ZLD** employs evaporative/crystallization systems to remove as much water as possible to reduce the cost of concentrate disposal and to improve the options for beneficial use of the salt products. Gypsum is mined at many locations, and sodium chloride can be extracted from high salt content water bodies.

• **Crop Irrigation** is suggested in the Roadmap as a means for disposing of lower concentration desalination waste by application to salt-tolerant plants (halophytes).

• **Solar Energy Ponds** utilize concentrate from desalination plants to capture solar radiation and convert it into useable energy. In a sense, a solar energy pond is simply an evaporation pond with the opportunity to produce energy under the appropriate conditions. Solar radiation penetrating the water heats the lower dense layers of water which remain heavier than the layers above in spite of their rise in temperature. With no convection currents to disburse the temperature gradient due to the dense saline water layer topped by a less concentrated layer, the bottom layer's temperature rises to very high levels. The stored heat from this bottom layer of hot brine is then extracted using a heat exchanger.

Jibril and Ibrahim, 2001, reported their results obtained on disposal studies of the desalination blow-down to the sea which causes detrimental affects to the benthic environment. The blow

down consists of highly concentrated salts. This work proposes an environmentally beneficial process for the production of some chemicals from the salt concentrates. The process involves a serie of chemical reactions to convert the NaCl into Na_2CO_3, $NaHCO_3$ and NH_4Cl. In the initial investigations using a batch gas bubbler, optimum temperature of 22°C and NH3/NaCl ratio of 1.2 were established. At these conditions the highest NaCl conversion of 82,2% was obtained. This work has shown preliminary indications of the feasibility of protecting the environment by utilizing the salt concentrates from desalination plant for chemicals production.

Vedavyasan et al. 2001 detailed how to extract salts by solar evaporation under arid climates for the recovery of calcium, magnesium, barium and strontium salts, from brines solutions. But the use of sequestrants should limit this solution.

Rodriguez et al. 2002, Veza et al. 2003, developed the possibility to reuse the reverse osmosis membrane. In areas where tap water has a high salt content, wastewater is not appropriate for reuse in agriculture, particularly for sensitive crops. One alternative is the reduction, via desalination, of the brackish character to the secondary effluent. A filtration stage is also required before desalination. On the other hand, used reverse osmosis membranes can be recycled and used as filters in the advanced treatment stage in order to reduce suspended matter contained in the secondary effluent- one advantage being the environmental recovery of solid waste. Used membranes can be treated with strong chemical oxidants to peel off the active separation layer in order to transform them into microfiltration or ultrafiltration elements. Preliminary tests have been carried out with 8" elements, aimed at comparing membrane performance before and after the peeling process. An index denoted as peeling effectiveness (high flux, high salt passage) is used for comparison. It was soon observed that potassium permanganate was more effective than others, together with sodium hydroxide. Doses around 1000 mg/L KMnO4 provided the best results. These modified membranes were then used to reduce suspended solids in the tertiary treatment of municipal wastewater.

Côté et al. 2004, reported a comparison of membrane options for water reuse and reclamation. The reuse of effluents for irrigation and indirect potable water uses is rapidly developing as an alternative to seawater desalination. This paper explores two membranes-based options available to treat sewage for water reuse, tertiary filtration (TF) of the effluent from a conventional activated sludge (CAS) process and an integrated membrane bioreactor (MBR). These options are compared from technical, performance and cost points of view using Zee Weed immersed membrane. The analysis shows that an integrated MBR is less expensive than the CAS-TF option. The total life cycle costs for the treatment of sewage to a quality suitable for irrigation reuse or for feeding reverse osmosis decrease from 0.40 dollars UD/m^3 to 0.20 dollars UD/m^3 as plant size increases to 75,000 m^3/d. It is also shown that the incremental life cycle cost to treat sewage to indirect potable water reuse standards (i.e. by ultrafiltration and reverse osmosis) is only 39% of the cost of seawater desalination.

2. Desalination experience in Morocco

Master plans for water resource development in Morocco foresee a shortage in potable water from conventional resources mainly for the southern basins by the year 2017.

As a solution, sea and brackish water could provide a unique and reliable source of potable water for these areas. Therefore, brackish and seawater desalination is being progressively utilized, despite the higher costs in comparison with conventional techniques (Tahiri, 2001). The ONEP (Office National de l'Eau Potable) and the OCP (Office Chérifien des Phosphates) are the main developing agencies. The OCP chose the distillation to produce water for industriel use; this has been performed by Phos-Boukraa firm in Laayoune since TDS sought was 25 ppm. The experience of ONEP in this field is more diversified because of the variability of the process used (Zidouri, 2000).

2.1 ONEP's Background in desalination field

Since 1973, the national Master plan of drinking water supply has given rise to the necessity of resorting to desalination of brackish and seawater as a source of drinking water supply. In 1975, the first demineralization unit was established in Tarfaya. This was electrodialysis unit using brackish water containing 5 g/L of dissolved salts. A production capacity of 75 m^3/d was expected to fulfill the drinking water needs. In 1983, a new demineralization installation based on the reverse osmosis process was built to augment the electrodialysis unit of Tarfaya. This unit has been considered as pilote unit used to allow the ONEP technical staff to be familiar with RO process and also to compare it to other processes based on electrodialysis and steam compression installed in Boujdour (Zidouri, 2000).

Boujdour plant is a mechanical vapor compression plant for seawater desalination. It was set up in 1977 for a 250 m^3/d production capacity and was in operation till 1995. Some components of the compressor were replaced in 1991. Its shut-down was due to its limited capacity that could not meet the actual water needs of Boujdour and particularly to its specific energy consumption (around 20 kWh/m^3 of distilled water). Through 18 years of operation, it was found that the MED-MVC process has a highest availability and reliable.

In 1986 a second reverse osmosis plant was installed in Semara with a 330 m^3/d production capacity, using Dupont B-9 membranes for the demineralization of 10 g/L brackish water (Hafsi 2001).

In order to choose reliable technology that could be adapted to a relatively large capacities and specifications (energy costs) required to solve water shortage problems in the south of Morocco, ONEP formed a committee, which at the end of the 1990s visited several countries that had accumulated experience on research and operation of seawater desalination plants producing potable water (Middle East, Canary, Islands, Malta, etc). As a result, desalination using the RO process was adopted and two SWRO plants (Laayoune, 7000m^3/d and Boujdour, 800 m^3/d) were built in 1995.

The largest desalination plant currently in operation in Morocco is Laayoune seawater reverse osmosis plant. This plant insures the production of 7,000 m^3/d of drinking water. The desalinated water is produced with an average energy cost of approximately 5.3 kWh/m^3. Added to the brackish underground water (5,616 m^3/d with a TDS of 1,600 mg/L), the total capacity is brought up to 12,600 m^3/d of drinking water supply. Pretreatment consists of

chlorination, acidification, coagulation, pressure filtration through a sand filter, acidification to reduce the precipitation of calcium carbonate, at the membrane level, microfiltration and dechlorination. The plant uses brine staging design concept and has four trains, each with a capacity of 1750 m^3/d. the RO section of the plant uses Dupont polyamide hollow fine fibre membrane. Laayoune plant is currently being extended to produce a further 6,500 m^3/d. Tan Tan plant is a Reverse osmosis plant for brackish water desalination. It started up in 2003 with a production capacity of 1700 m^3/d. This plant will be presented in chapter 3. Some basic information about the current and future desalination plants in Morocco are shown in Table 3.

Table3: *Production of current and future desalination in Morocco (Boughriba, 2004)*

City	Process	Raw Water	Capacity (m^3/d)	Implementation's date	Observations
Tarfaya	Electrodialysis	Brackish water	75	1976	Out of duty since 1984
Boujdour	Distilation MCV	Sea water	250	1977	Rehabilitated in 1990 and in 1998
Tarfaya	RO	Brackish water	120	1983	Rehabilitated in 1988
Smara	RO	Brackish water	330	1986	Out of duty since 1994
Boujdour	RO	Sea water	800	1995	Expansion (2400 m^3/d) is in progress
Laayoune	RO	Sea water	13000	1995	-
Tarfaya	RO	Brackish water	800	2000	_
Tan Tan	RO	Brackish water	1700	2003	_
Tan Tan	RO	Sea water	11,300	By 2010	Project
Agadir	RO	Sea water	43,200	By 2020	Project

In order to complement its desalination experience further, ONEP has carried out the following feasibility studies: (1) design of an MSF plant using solar energy from a solar pond. The pilot project size is 300 m ^{3}/d of potable water; (2) design of a vertical tube multiple effect distillation (VT-MED) plant coupled to a nuclear heating reactor (NI-IR) insuring 10MW thermal. The desalination plant was designed to produce 8000 m^3/d of potable water.

These studies show that desalination using nuclear energy or heat extracted from a solar pond is relatively expensive for small capacities of potable water production. Nevertheless, they could be implemented as demonstration plants for future introduction of large-scale desalination units.

2.2 Perspectives of desalination in Morocco

The Tan Tan BWRO which was set up for short term potable water needs in 2003 represents a first phase (Tahiri 2001). A 11,300 m^3/d plant is planned to be built by 2010 for seawater desalination for long term water supply. A largest seawater desalination plant, with a production capacity of 43,000 m^3/d, will be built in Agadir by 2020.

3. *Water defluoridation processes: a review*

Fluorosis caused by high fluoride (F$^-$) intake predominantly through drinking water containing F$^-$ concentrations higher than 1 mg.L^{-1}, is a chronic disease manifested by mottling of teeth in mild cases (dental fluorosis)and changes in bone structure (skeletal fluorosis), ossification of tendons and ligaments, and neurological damage in more severe cases (Sy 1996, Wang 2001, Ghorai 2002).

Today an increasing concern is being expressed that these adverse effects of fluorosis are irreversible, in particular for African, Indian and Chinese populations living in rural areas in which drinking water is supplied from wells and bore holes with high F$^-$ concentrations. The development of a long term solution for the defluoridation of F$^-$ contaminated groundwaters is thus of critical importance. This would require appropriate water treatment procedures. Appropriate technology must be technically simple, cost effective, easily transferable, using local resources and accessible to the rural community.

The removal of fluoride from water using defluoridation techniques is a common practice world-wide, both domestically and industrially. Current methods of fluoride removal from water include adsorption onto activated alumina, bone char and clay, precipitation with lime, dolomite and aluminium sulfate, the Nalgonda technique (Srimurali 1998), ion exchange (Mohan Rao 1988) and membrane processes such as reverse osmosis, electrodialysis and very recently nanofiltration (Pontié *et al.* 1996, 2003, Lhassani *et al.* 2001, Diawara *et al.* 2003, M. Tahaikt *et al.* 2006)

3.1 The origin and distribution of fluoride in groundwaters

High F$^-$ concentrations in groundwater are found in many countries around the world, notably in Africa, Asia and USA (Czarnowski 1996, Azbar 2000). The most severe problems associated with high F$^-$ waters occur in China (Wang 2002), India (Agarwal 2003) and Rift Valley countries in Africa (Du Plessis 1995). Groundwaters with high fluoride contents have been studied in detail in Africa, in particular Kenya and Tanzania (Moges 1996, Chernet 2002, Mjengera 2002, Moturi 2002). The abundance of F$^-$ in Rift Valley groundwaters is due to the weathering of alkaline volcanic rocks rich in F$^-$. Typical fluoride concentrations of towns in the Rift Valley are between 1 and 33 mg.L^{-1}. High fluoride groundwater is also found in the East Upper Region of Ghana (Apambire 1997).The concentration of fluoride is between 0.11 and 4.60 mg.L^{-1}. The hydrogeology and hydrochemistry of ground waters of Senegal has been thoroughly studied by Y. Travi (Travi, 1988). In France two major basins;

Aquitan Basin and Parisian Basin, are concerned with F^- concentrations between 0.6 mg.L^{-1} and 4.2 mg.L^{-1}.

3.2 Fluorosis

Fluoride has certain physiological properties (Sy 1996, Muller 1998, Notcutt 1999) of great importance in human health. The role of fluoride in the process of mineralization of certain tissues is important. At low concentrations fluoride stabilises the skeletal system by increasing the size of apatite crystals and reducing their solubility (Moges, 1996). Although beneficial effects can be demonstrated at low concentrations, it has detrimental effects when concentrations exceed the threshold (Li 2001).

Endemic fluorosis is known to be global in scope, occurring in all continents and affecting many millions of people. Cases of skeletal fluorosis have been reported all over the world (Hillier 2000). According to a report from UNICEF (Susheela 2001), fluorosis is endemic in at least 25 countries across the globe.

The drinking water standards for fluoride ion stipulated by WHO authorities are between 0.8 and 1.5 mg.L^{-1}, the average suggested in USA by US Public Health is 0.7-1.2 mg.L^{-1} and 0.7 - 1.5 in UE.

3.3 Ways of solving the problem: defluoridation techniques

The prevention of fluorosis through treatment of drinking water in rural areas is a difficult task because of economical and technological restrictions. Defluoridation of water is the only measure to prevent fluorosis and many different defluoridation techniques have been developed (Chaturvedi 1990). However, many cannot be easily implemented in areas where the problems occur. This section gives a brief overview of defluoridation methods.

Defluoridation processes can be classified into four main groups: *Adsorption methods*: in these methods sorbents such as bone charcoal, activated alumina, and clay are used in column or batch systems. *Ion exchange methods* : these methods require expensive commercial ion exchange resins. *Co-precipitation and contact precipitation methods*: these methods coprecipitate F^- with for example aluminium sulfate and lime (Nalgonda technique.) or precipitate F^-, for example with calcium and phosphate compounds. *Membrane processes*: these include reverse osmosis, electrodialysis and nanofiltration methods. The last one is very promising for large scale pilots plants in the future.

Taking into account the realities of the problem as outlined in this short review, the provision of an affordable and technologically simple solution must obviously lie in empowering the local communities to construct viable defluoridation systems from local and readily available materials. There is thus a need for developing low cost methods to remove fluoride from water. The removal of fluoride using locally available clays was studied in many countries where the problem occurs and the development of laboratory scale defluoridation columns to study the efficiency of fluoride removal using different sorbents is recommended for local communities.

3.4 Defluoridation processes

3.4.1 Precipitation methods

Precipitation methods can be divided into two categories, those based on coprecipitation of adsorbed F^- and those based on the precipitation of insoluble fluoride compounds.

- Methods based on coprecipitation: Coprecipitation is the process by which aluminium salts (aluminium chloride and aluminium sulphate) are added to F^- contaminated drinking waters (Yang 1999, 2002).

- Methods based on F^- precipitation with calcium and phosphate compounds.

3.4.2 Adsorption methods

Fluoride can be removed by adsorption onto many adsorbent materials. The criteria for the selection of suitable sorbents are: cost of the medium and running costs, ease of operation, adsorption capacity, potential for reuse, number of useful cycles and the possibility of regeneration. Some of the most frequently encountered sorbents are (Activated alumina,Clays and soils, spent bleaching earth, spent catalyst, rare earth oxides, bone charcoal and activated carbon were studied as sorbents for F^-.

3.4.3 Ion exchange resins

Ion exchange resins are effective in removing F^- from water. Mohan Rao and Bhaskaran (1988) studied the removal of F^- using ion exchange materials such as sulphonated material from coconut shell, Carbion, Tulsion and Zeocarb 225. From the results, it was evident that Zeocarb 225 had the highest F^- removal capacity and sulphonated material of coconut shell has the lowest one. It was also indicated that the ion exchange material could be regenerated by aluminium sulphate solution (2-4%). Castel et al (Casterl 2000) studied the removal of F^- by a two way ion exchange cyclic process. This system used two anion exchange columns. The results show that this process can effectively remove fluoride from water. The use of anion exchange resins for F^- removal is not practiced because of their relatively high costs. The presence of other anions such as chloride and sulphate also pose a major problem when using ion exchange resins for F^- removal. Because F^- removal is accompanied by sorption of other anions, the sorption capacity is limited to 0.5 mg.L^{-1} of F^- concentration level in the bulk (Veressinina 2001).

3.4.4 Electrochemical technique

Electrochemical technique (also electrocoagulation) is a simple and efficient method for the treatment of potable water. Recent results reported by Parthasarathy 1986, Yang 2002 have demonstrated that electrocoagulation (EC) using aluminium anodes is effective in defluoridation. In the EC cell the aluminium electrodes are used to form aluminium ions first. Afterwards the aluminium ions are transformed into $Al(OH)_3$ before being polymerized to $Al_n(OH)_{3n}$. The $Al(OH)_3$ floc is believed to adsorb F^- strongly as illustrated by the equation :

$$Al(OH)_3 + xF^- = A(OH)_{3-x} F_x + xOH^-.$$
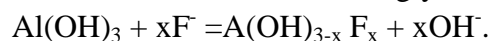
Usually the EC operation is completed by an electroflottation (EF) in order to separate the formed floc from water by floating them to the surface cell (Mameri, 1998, Pouet 1992).

3.4.5 Membrane processes

Membrane processes such as reverse osmosis, nanofiltration, dialysis and electrodialysis have been recently developed methods for F^- removal from drinking waters (Pontié, 1996, Lhassani 2001, Scheoman 1986, Garmes 2002, Durand-Bourlier 1997, Hichour 2000) and brackish waters (Pontié 2003, Diawara 2003, Amor 2001, Tahaikt et al. 2008, Menkouchi *et al.* 2007, Tahaikt 2007)
It is well known that application of defluoridation techniques constitutes a big challenge in third world countries. Unfortunately, of the 25 countries in the world with severe fluoride problems, most have low economies. Then two complementary approaches have to be developed in the future depending on the local conditions: (i) defluoridation using clays for rural areas, (ii) defluoridation using nanofiltration for urban areas.

4. Membrane processes

4.1 Introduction

A membrane is an interphase between two adjacent phases acting as a selective barrier, regulating the transport of substances between the two compartments. The main advantages of membrane technology as compared with other unit operations are related to this unique separation principle, i.e. the transport selectivity of the membrane. Separations with membranes do not require additives, and they can be performed isothermally at low temperatures and compared to other thermal separation processes at low energy consumption. Also, upscaling and downscaling of membrane processes as well as their integration into other separation or reaction processes are easy (Maurel, 1993).
By 1960, the elements of modern membrane science had been developed and the important discovery that transformed membrane separation from a laboratory to an industrial process was the development of the Loeb–Sourirajan process for making defect-free, high-flux, anisotropic RO membranes (Loeb and Sourirajan , 1962). Membrane technologies have now been industrially established in impressively large scale. The markets are rather diverse, from medicine to the chemical industry, and the most important industrial market segments are medical devices and water treatment. Today, membrane technology is used in a wide range of applications and the number of applications is increasing regularly.

4.2 Principle

In membrane processes, a membrane separates two phases. The membrane allows transport of one or few components more readily than that of other components. The driving force for transport can be either a pressure gradient, a temperature gradient, a concentration gradient or an electrical potential gradient. A schematic representation of a membrane process is given in Fig.10. A feed stream is divided into two streams, the retentate or concentrate stream and the permeate stream. Either the retentate or the permeate can contain or be the desired product depending on the application.
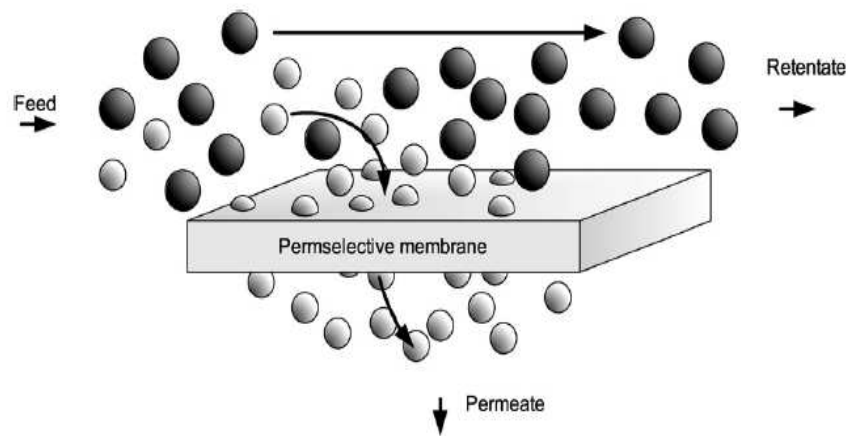
***Figure 10:** Simplified concept schematic of a membrane separation operation*

The objectives of a separation can be classified roughly as follows (Maurel, 1993):
- Concentration: the desired component is present at a low concentration and solvent has to be removed
- Purification: undesirable components have to be removed
- Fractionation: a mixture must be separated into two or more desired components
- Reaction mediation: combination of chemical or biochemical reaction with a membrane separation process to increase the reaction rate

The proper choice of a membrane processes should be determined by the specific application objective: particulate or dissolved solids removal, hardness reduction or ultra pure water production, removal of specific gases/chemicals etc. The end-use may also dictate selection of membranes for industries such as potable water, effluent treatment, desalination or water supply for electronics or pharmaceutical manufacturing. The following sections explain the different membrane processes and the types of membranes commonly used.

4.3 Different membrane operations

4.3.1. Driving forces

Membrane processes can be divided according to their driving forces. As driving forces, gradients in pressure, concentration, temperature and electrical potential are used (see Table 4).

4.3.1.1 Electrically driven processes

The electrically driven processes are electrodialysis and membrane electrolysis (Table 4). The driving force for (ionic) transport in these processes is supplied by an electrical potential difference. Electrically driven processes can be employed only when charged molecules are present, using ionic or charged membranes.

Table 4: *Classification of membrane processes via passive transport (Rumeau, 1990)*

Trans-membrane gradient	Process	Permeate nature
Concentration (ΔC)	Dialysis Osmosis	Liquid
Electrical potential (ΔE)	Electrodialysis Membrane electrolysis	Liquid
Pressure (ΔP)	Micro, Ultra, Nanofiltration Reverse osmosis Pervaporation Gas separation	Liquid Gas
Temperature (ΔT)	Membrane distillation	Gas

4.3.1.2 Concentration driven processes

Concentration driven membrane processes are dialysis and osmosis. In dialysis process, the transfer of the solute across the membrane occurs by diffusion and separation is obtained through differences in diffusion rates because of differences in molecular weight (Pontié, 1996).

Osmosis is the transport of water across a selectively permeable membrane from a compartment of higher water chemical potential to a compartment of lower water chemical potential until the osmotic pressures of both compartments are equal. It is driven by a difference in solute concentrations across the membrane that allows passage of water, but rejects most solute molecules or ions. Osmotic pressure (π) is the pressure which, if applied to the more concentrated solution, would prevent transport of water across the membrane (Cath *et al* 2006).

4.3.1.3 Heat-driven process

Membrane distillation is a separation process for aqueous solutions, based on the use of hydrophobic microporous membranes. The membranes are not wetted by the aqueous phase, until the operating pressure remains lower than the minimum penetration pressure of the membrane, so that the entrance of the pores acts as the physical support for a liquid vapour interface which can originate the separation of components of different volatility.

The driving force for mass transfer across the membrane is a difference in the partial pressure between the two ends of the membrane pores. That can be maintained by acting on the temperature difference across the membrane, as in direct contact MD, by using a sweeping gas on the permeate side, by introducing an air gap or by applying vacuum in the permeate side (Cabassud et al. 2003).

4.3.1.4 Pressure driven processes

Pressure driven membrane processes use the pressure difference between the feed and permeate side as the driving force to transport the solvent through the membrane. Particles and dissolved components are (partially) retained based on properties such as size, shape and

charge. Four membrane processes can be distinguished when the driving force is a pressure difference across the membrane, separating two liquid solutions. These processes are Microfiltration (MF), Ultrafiltration (UF), nanofiltration (NF) and reverse osmosis.

Going from MF through UF and NF to RO, the hydrodynamic resistance increases and consequently higher driving forces are needed. On the other hand the product flux through the membrane and the size of the molecules being retained decreases. The product flux obtained is determined by the applied pressure and the membrane resistance (Shih *et al* 2005). Typical values for applied pressures and fluxes are given in Table 5.

Table 5: *Molecular weight cut off, flux range and used pressure range in MF, UF, NF and RO membrane processes. (Van Der Bruggen et al 2003)*

Membrane operation	Pressure range (bar)	Hydraulic permeability range $(L.h^{-1}.m^{-2}.bar^{-1})$	MWCO (Da)
MF	0.1 - 2	> 1000	$> 10^6$
UF	1 - 5	10 - 1000	1000-300000
NF	3 - 20	1.5 - 30	200-1000
RO	5 - 120	0.05 - 1.5	< 200

4.3.2 Membrane technologies for brackish water desalination

Membrane technologies for desalination operate under one or two driving forces: pressure or electrical potential.

4.3.2.1 Electrodialysis

Electrodialysis is a technique based in the transport of ions through selective membranes under the influence of an electrical field. This technique has proved its feasibility and high performance in the desalination of brackish water.

In a conventional electrodialysis stack, cation and anion –exchange membranes are alternatively placed between the cathode and the anode. When a potential difference between both electrodes is applied, the cations move towards the anode. The cations migrate through the cation exchange membranes, which have positive fixed groups, retain them. On the other hand, the anions migrate through the anion exchange membranes and the cation exchange membranes retain them. This transport produces a rise in the salt concentration in some compartments (concentrate compartments) and a decrease in the adjacent ones (diluate compartments) (Ortigez *et al* 2007).

4.3.2.2 Reverse osmosis

Reverse osmosis membranes are used for salt removal in brackish water application. This operation is a membrane separation process in which brackish water permeates through a membrane by applying a pressure larger than the osmotic pressure of the brackish water. The membrane is permeable for water, but not for the dissolved salts and molecular organic

contaminants from water. In this way, a separation between a pure water fraction (The permeate) and a concentrate fraction (the retentate) is obtained.

Pressures needed for the separation are usually in the range of 20 bar for brackish water. Most RO membranes are thin-film composite membranes and the membranes are usually configured in spiral wound modules.

4.3.2.3 Nanofiltration

Nanofiltration is another pressure driven process that is important to desalination. NF is typically referred to as "loose" RO due to its larger membrane pore structure as compared to the membranes used in RO, and allows more salt passage through the membrane. NF is capable of concentrating, divalent salts, bacteria, viruses and other constituents that have a molecular weight greater than 1000 daltons. Nanofiltration is further discussed below in section V.

4.4 Membranes classification

Membranes can be classified according to the membrane based separation mechanisms, the membrane structure and material, and Membrane configuration, as described in the following section.

4.4.1 Membrane based separation mechanisms

The membrane morphology dictates the mode of permeation and separation. The barrier structure of membranes can be classified according to their porous character (Table 6). The membrane surface can be dense selective skin, permitting only diffusive transport or a porous skin, allowing viscous flow of the permeate. The membrane separation is achieved by the manipulation of these basic morphologies. Active development is also concerned with the combination of nonporous or porous membranes with additional separation mechanisms, and the most important ones are electrochemical potentials and affinity interactions (Nguyen, 1999).

4.4.1.1 Porous membranes

For porous membranes, transport rate and selectivity are mainly influenced by viscous flow and sieving or size exclusion. Nevertheless, interactions of solutes with the membrane (pore) surface may significantly alter the membrane performance. An important example is the rejection of charged substances in aqueous mixtures by microporous NF membranes due to their Donnan potential. Furthermore, with meso- and macroporous membranes, selective adsorption can be used for an alternative separation mechanism, (affinity) membrane adsorbers are the most important example. In theory, porous barriers could be used for very precise continuous permselective separations based on differences in size, shape and/or functional groups (Ulbricht 2006).

Table 6: *Classification of membranes and membranes transfer mechanisms (Ulbricht, 2006)*

Membrane barrier porosity	Transfer mechanism		
	Viscous flow/size exclusion	*solution/diffusion*	*Electrochemical exclusion*
Non-porous		Reverse Osmosis (RO) Pervaporation (PV) Gas separation (GS)	Electrodialysis (ED)
Microporous pore diameter $d_p \leq 2$ nm	Nanofiltration (NF)	Nanofiltration (NF)	Dialysis (D)
Mesoporous pore diameter $d_p = 2$–50 nm	Ultrafiltration (UF)	Dialysis	Electrodialysis
Macroporous pore diameter $d_p = 50$–500 nm	Microfiltration (MF)		

4.4.1.2 Dense membranes

For non-porous membranes, the interactions between solutes and membrane material dominate transport rate and selectivity; the transport mechanism can be described by the solution/diffusion model (Pontié, 1996).

4.4.1.3 Ion-exchange membranes

Ion- exchange membranes are normally of three types: (1) negatively charged membranes, (2) postively charged membranes, and (3) bipolar membranes.

Two mechanisms are normally used to describe transport through charged membranes namely:

• Solution–diffusion mechanism with Donnan effect.

• Electrokinetics mechanism.

The first mechanism is based on the assumption that the membrane is nonporous, and in the second models, it is assumed that the membrane is micro-porous.

4.4.2 Membrane structure

Different membrane structures are created through different processing methods. The classification occurs according to the homogeneity of the pore structure along the membrane cross section into symmetric, asymmetric and composite membranes. These are represented in Figure 11.

4.4.2.1 Symmetric membranes

Symmetric membranes have a homogenous pore diameter and/or pore cross section across the thickness of the membrane.
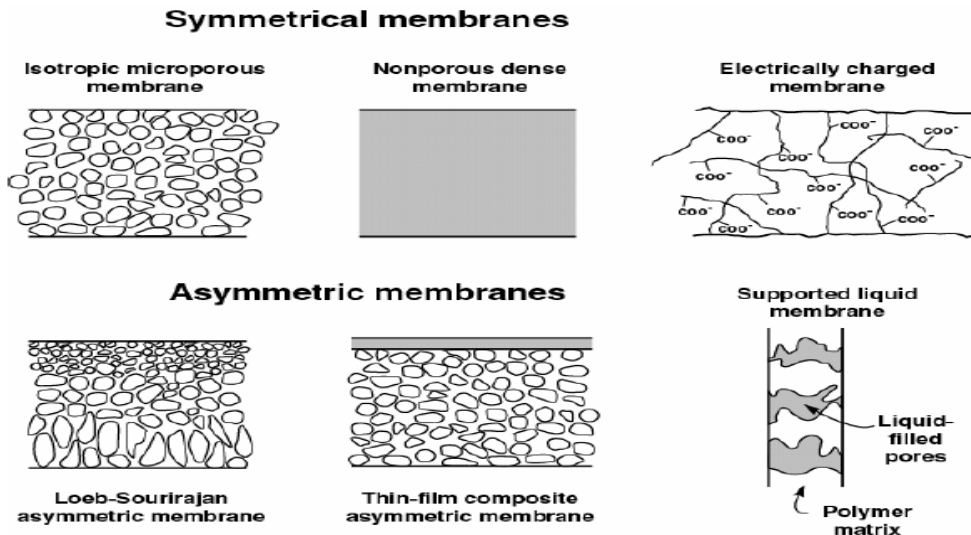
Figure 11: Schematic diagram of symmetric and asymmetric membrane (Cot, 1998)

4.4.2.2 Asymmetric membranes

In industrial applications, symmetrical membranes have been almost completely displaced by asymmetric membranes, which have much higher fluxes. An asymmetric membrane comprises a very thin (0.1-1.0 micron) skin layer on a highly porous (100-200 microns) thick substructure. The thin skin acts as the selective membrane. Its separation characteristics are determined by the nature of membrane material or pore size, and the mass transport rate is determined mainly by the skin thickness. Porous sub-layer acts as a support for the thin, fragile skin and has little effect on the separation characteristics (Maurel, 1993 and Matsuyama et al 2000). In an integral asymmetric membrane, the selective barrier layer and the microporous support always consist of the same polymer. The asymmetric membranes are prepared by the phase inversion process, which can be achieved through four principal methods: immersion precipitation, vapor-induced phase separation, thermally-induced phase separation and dry casting (Altinkaya et al 2004).

4.4.2.3 Thin film composite membranes (TFC)

Composite membranes consist of at least two layers, which differ in structure. The thin dense skin layer of a 0.01 to 0.1 µm is formed over an approximatively 100 µm thick microporous film. Composite membranes differ from asymmetric membranes by the mode of fabrication which consists of two steps: casting of the microporous support and deposition of the barrier layer on the surface of this microporous support layer (Nguyen, 1999). This preparation mode leads to significant advantages of the composite membrane compared to asymmetric membranes: (i) it improves the permeation rate which is inversely proportional to the thickness of the barrier layer and thus composite membranes shows a much higher permeation rate then asymmetric, (ii) increases the rejection rate of the membranes and (iii) minimizes the pressure drop across the membrane (Ulbricht, 2006). The materials used for the support layer and the skin layer can be different and optimized for the best combination of high water flux and low solute permeability.

The TFC membrane structure is especially suitable for reverse osmosis and Nanofiltration which require high flux on one hand and high salt rejection rate on the other.

4.4.3 Types of membranes materials

Membranes can be classified into organic, inorganic and hybrids of organic/inorganic materials.

4.4.3.1Organic membranes

Polymeric membranes account for biggest proportion of installed membranes currently in use. Several different polymers are used to suit the molecular weight cut off required, or achieve the desired resistance to fouling or performance when contacted with a specific process fluid. Organic membranes are commonly made of natural or synthetic polymer. The common materials include; cellulose acetate, polysulfone, aromatic polyamides, polyacrylonitrile (Nguyen, 1999, Suen *et al* 2003 and Ulbricht 2006).

Cellulose acetate

Cellulose acetate (CA) is one of the first polymer membranes that have been used for aqueous based separation, i.e. reverse osmosis and ultrafiltration techniques (Sivakumar *et al* 2006). Being hydrophilic, cellulose acetate offers a good fouling resistance. Cellulose acetate membranes have high water permeability and are also inexpensive and easy to manufacture. However, their asymmetric structure makes them susceptible to compaction under high operating pressures, especially at elevated temperatures, leading to a reduction in product flux. Cellulose acetate membranes are susceptible to hydrolysis and can only be used over a limited pH range (4 to 6). They are vulnerable to microbial attack and also undergo degradation at temperatures above 35°C (Buisson *et al* 1998).

Aromatic polyamides

Polyamides (PA) membranes overcome some of the problems associated with CA membranes; they have better resistance to hydrolysis and biological attack than the cellulosic membranes. They can also be operated over a pH range of 4 to 11and can withstand higher temperature. However, PA membranes are much worse with regard to chlorine tolerance and biofouling tendencies and have lower water permeability than CA membranes. Polyamide is used as the thin film membrane layer in NF and RO membranes. The supporting porous sublayer of these membranes is usually made of polysulfone (Nguyen, 1999).

Polysulfone

Polysulfone is an attractive material for preparing membranes because it possesses excellent film-forming properties and high mechanical and chemical stability. Polysufone is commonly used for UF membranes or coated with aromatic polymers for NF and RO membranes. The use of polysulfone for aqueous phase is restricted due to its hydrophobicity which makes it susceptible to fouling.

4. 4.3.2 Inorganic membranes

Membranes can also be prepared from inorganic materials such as ceramics, metals and glass. Two main classes of membranes can be distinguished: dense (they are made of metals, hybrid organic–inorganic or mixed conductive oxides) and porous (ceramic) membranes. Sol–gel processing, plasma-enhanced chemical vapor deposition and hydrothermal synthesis are methods that can be used for inorganic membrane preparation (Cot, 1998). Inorganic membranes compete with organic membranes for specific applications in drastic conditions. They can operate at elevated temperatures, with metal membranes stable at temperatures ranging from 500 – 800°C and with many ceramic membranes usable at over 1000°C. They are much more resistant to chemical attack and have long life cycle (Caroa *et al* 2006, Caroa *et al* 2007). But on the other hand, their pore properties, cost, capability for surface modification may not be competitive. Accordingly, inorganic materials are infrequently adopted as the affinity membrane supports (Suen *et al* 2003).

4.4.3.3 Hybrid membranes

Organic-inorganic hybrid materials offer specific advantages for the preparation of artificial membranes exhibiting high selectivity and flux, as well as a good thermal and chemical resistance (Sforça *et al* 1999). Hybrid organic/inorganic materials are usually classified in two categories (Cot *et al* 2000):

• Type I in which only interactions like van der Waals forces or hydrogen bonds exist between organic and inorganic parts. Hybrid materials can be described here as micro or nanocomposites in which one part (organic or inorganic) is dispersed in the other part acting as the host matrix.

• Type II in which covalent bonding exists between organic and inorganic parts, resulting either in an homogeneous hybrid material at the molecular level or in high surface area inorganic materials modified through surface grafting of organic groups.

4.4.4 Membrane shapes and module designs

When employed for practical applications, membranes are usually housed in a module. The design of membrane module depends on the membrane shape. Various membrane shapes and module designs have been adopted in different membrane processes. The techno-economic factors for the selection, design and operation of membrane modules include cost of supporting materials and enclosure (pressure vessels), power consumption in pumping and ease of replaceability (Aptel *et al*.1996).

Membranes are manufactured as flat sheets, hollow fibers, tubular and spiral modules. The principal advantages and disadvantages of different modules are given in Table 7.

Table 7: Principal advantages and disadvantages of different modules

Shape of module	Tubular	Hollow fibre	Flat sheet	Spiral
Packing density (m^2/m^3)	Low 10 - 300	High 9000 - 30000	Low 100 - 400	High 300 - 1000
Hydraulic diameter (mm)	5 - 15	0.1 - 1	1 - 5	0.8 -1.2
Membrane material	inorganic Organic	Organic	Organic inorganic	Organic
Replacement of membranes	Tube	Module	Sheet	Cartridge
Risk of clogging	Low	High	Average	High
Cost	High	High	High	Low
Maintenance	Easy	Difficult	Easy	Difficult
Dead volume	High	Low	Low	Low

4.4.4.1 Flat sheet module

The simplest device for packing flat sheet membranes is a plate-and-frame module. Plate-and-frame modules can be constructed in different sizes and shapes ranging from lab-scale devices that hold single, small-size membrane coupons to full-scale systems that hold more than 1700 membranes. Two of the main limitations of plate-and-frame elements for membrane applications are lack of adequate membrane support and low packing density. Lack of adequate membrane support limits operation to low hydraulic pressure and/or operation at similar pressures on both sides of the membrane (requiring relatively high process control). Low packing density leads to a larger system footprint, higher capital costs, and higher operating costs (labor for membrane replacement). Other limitations of the plate-and-frame configuration include problems with internal and external sealing, difficulty in monitoring membrane integrity, and a limited range of operating conditions (e.g., flow velocities and pressures) (Cath *et al* 2006).

4.4.4.2 Spiral wound module

A spiral wound module contains from one to more than 30 membranes leafs, depending on the element diameter and element type. Each leaf is made of two membrane sheets glued together back-to-back with a permeate spacer in between them (Aptel *et al* 1996). A glue lines Seal the inner (permeate) side of the leaf against the outer (feed/concentrate) side. The open side of the leaf is connected to and sealed against the perforated central part of product water tube, which collect the permeate from all leaves. The leaves are rolled up with a sheet of feed spacer between each of them, which provides the channel for the feed and concentrate flow. In operation, the feed water enters the face of the element through the feed spacer channels and exits on the opposite end as concentrate**.** The construction of a spiral wound membrane element is schematically shown in Figure 12.
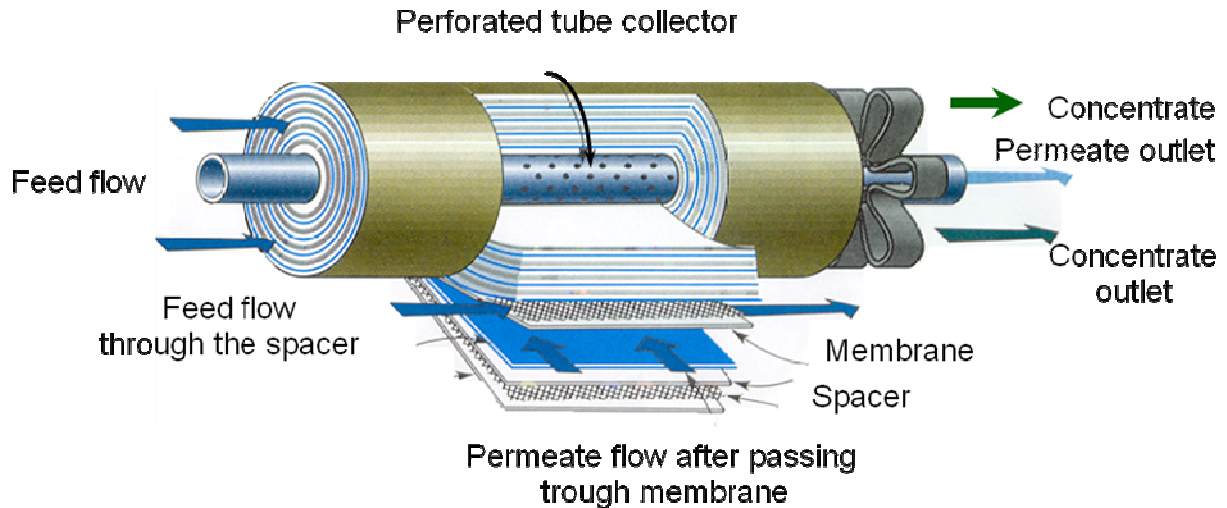
Figure 12: *Construction of a spiral wound element*

Spiral wound designs offers many advantages compared to other module designs. Typically, a spiral wound configuration offers significantly lower replacement costs, easier maintenance, high packing density and higher pressure application. As to the possible problems for the spiral-wound design, there included difficult module cleaning, and the flow complexity caused by the decline in transmembrane pressure drop along the radial direction (Cath *et al* 2006).

Spiral wound configuration is the industry standard for reverse osmosis and nanofiltration membranes in water treatment.

4.4.4.3 Tubular module

Tubular membranes are not self-supporting membranes. They are located on the inside of a tube which is the supporting layer for the membrane. Because the location of tubular membranes is inside a tube, the flow in a tubular membrane is usually inside out. The main problem for this is that the attachment of the membrane to the supporting layer is very weak. Tubular membranes have a diameter of about 5 to 15 mm. The tubes are encased in reinforced fibreglass or enclosed inside a rigid PVC or stainless steel shell. As the feed solution flows through the membrane core, the permeate passes through the membrane and is collected in the tubular housing. Because of the size of the membrane diameter, plugging of tubular membranes is not likely to occur. This type of module can be easily cleaned. A drawback of tubular membranes is that the packing density is low, which results in high prices per module (Bouchard *et al* 2000).

4.4.4.4 **Hollow fibre module**

Hollow fiber membranes are small tubular membranes with a diameter of below 2mm. Hollow fiber membranes are self supporting membranes. The selective barrier is sufficiently strong to resist filtration pressures. Because of this, the flow through these membranes can be either inside out or outside in (Maurel, 1993). The chances of plugging of a hollow fiber membrane are very high. The membranes can only be used for the treatment of water with

low suspended solids content. The packing density of a hollow fiber membrane is very high. The cartridges contain several hundred of fibers.

The key properties of efficient membrane modules are (Starthmann, 1999):

- High packing density
- Good control of concentration polarization and membrane fouling
- Low operating and maintenance costs; and
- Cost efficient production

5. *Nanofiltration versus Reverse Osmosis*

Nanofiltration (NF) is a type of pressure driven membrane with properties in between reverse osmosis (RO) and ultrafiltration (UF). The history of nanofiltration (NF) dates back to the seventies, when reverse osmosis membranes with a reasonable water flux operating at relatively low pressures were developed. Hence, the high pressures traditionally used in reverse osmosis resulted in a considerable energy cost. On the other hand, the quality of the permeate was very good, and often even too good. Thus, membranes with lower rejections of dissolved components, but with higher water permeability would be a great improvement for separation technology. Such ''low-pressure reverse osmosis membranes'' became known as nanofiltration membranes (Van der Bruggen and Vandecasteele, 2003). The term 'nanofiltration' signifies that particles of nanometric dimensions are separated through the NF membranes. NF membranes have low molecular weight cut-offs (200 - 1000 Da) and smaller pore size (~1 nm). They also have a surface electrostatic charge which gives them great selectivity towards ions or charged molecules. More specifically, NF membrane can be used to remove small neutral organic molecules while surface electrostatic properties allowed monovalent ions to be reasonably well transmitted with multivalent ions mostly retained. NF membrane's operating pressure ranged from 3 to 20 bars, which was much lower than RO membranes. (Bowen and Welfoot, 2002). NF offers several advantages, such as low operation pressure, high flux, high retention of multivalent anion salt and organic molecular above 300, relatively low investment, low operation and maintenance cost. By the second half of the eighties, nanofiltration had become established, and the first applications were reported (Conlon and McClellan, 1989; Eriksson, 1988). Nanofiltration has practical applications in water treatment, chemical industry, food and dairy industry. The primary application of NF membranes continues to be in water treatment. NF membranes available in the market show a wide range of properties and thus this variation affects the membrane performances. In general, NF membranes properties can be characterized in terms of the hydrophobicity, membrane roughness, membrane charge, membrane MWCO, retention properties and permeability. Modeling can also be used to analyse and to predict the membranes performances.

5.1 Nanofiltration membranes

5.1.1. *NF Membrane Preparation, Structure and Properties*

Various types of commercial NF membranes are available, and the separation performance of these membranes varies greatly.

The two main kinds of nanofiltration membranes are asymmetric membrane and thin film composite membrane. The latter shows higher water permeability and salt rejection because it consists of a dense (dp < 2 nm), ultra-thin selective layer on the surface of a porous substrate (Yang *et al.* 2007). Figure 13 shows a schematic of this type of membrane.
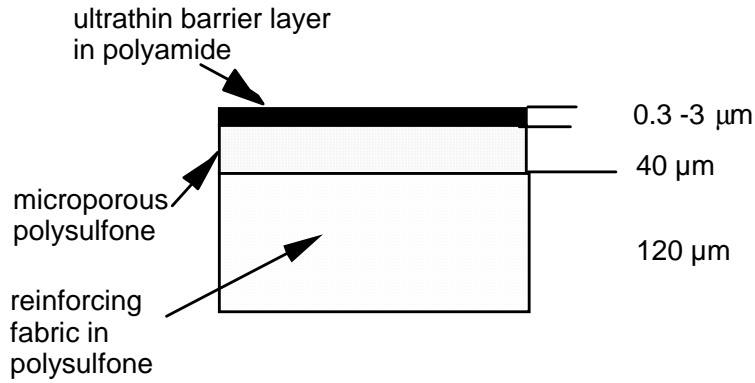
Figure 13: *Schematic diagram of the thin film composite membranes*

It is well known that there are many methods to prepare composite membrane. NF membranes are manufactured using two preparation techniques:
• Polymer phase inversion resulting in a homogeneous asymmetric membrane;
• Interfacial polarisation of a thin film composite layer on top of a substrate ultrafiltration membrane or other porous substrate.
Cellulose acetate and sulfonated polysulfone are two common materials used for making homogeneous asymmetric NF membranes. Thin film composite NF membranes use cross linked polyamide polymers, reacted to carboxylic group or other charged groups. Substrate materials commonly used for thin film composite membranes are polysulfone (PS), polyethersulfone (PES), polyvinyledene fluoride (PVDF), polyacrylonitrile (PAN), and Polyether ether Ketone (PEEK). The structures of the most widely used polymers on nanofiltration membrane preparation are shown in Figure 14.
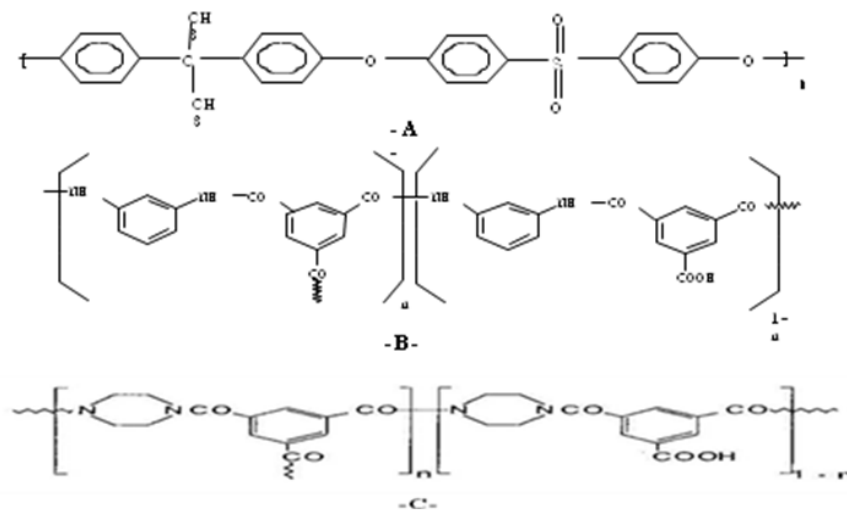
Figure 14: *Chemical structures of the polysulfone (A) the polyamide (B) and the poly piperazineamide (C)*

Nowadays, Most NF membranes are packed into spiral wound elements; however, tubular, hollow fiber and flat sheet/plate and frame modules are also available. One of the main uses of spiral wound membranes is in water treatment for drinking water production (Ben Farès, 2006).

5.1.2. Nanofiltration membranes available in the market

Several NF membranes are available in the market. Presently, NF membranes are commercially supplied by many companies (Table 8). Nanofiltration membranes are a relatively recent development in the field of RO membrane separations. Thus, the research efforts on reverse osmosis and the fast growing of RO technology in the market have had an impact on all of the progress in Nanofiltration technology.

Table 8: *Main manufacturers of nanofiltration membranes (Ben Farès, 2006)*

Manufacturer	Material	Configuration
Advance Membrane Technology (United States)	PSSf	Spiral
Celfa-Daicel (Suisse)	CA or PA	Flat sheet
Dow chemical (Denmark)	PA	Spiral
Filmtec (United States)	Diverse	Diverse
UOP fluid system (United States)	CA-PA	Spiral
Hoechst (Germany)	CA-PES	Flat sheet /spirale
Hydranautics (United States)	Composite	Spiral
Kalle (Germany)	CA-PA	Plat/Spiral
Koch membrane systems (Germany)	Diverse	Diverse
Membrany (Russia)	Diverse	Diverse
Millipore (United States)	PA	Plat/spiral
Nitto-Denko (Nitto Electrical Industriel) (Japan)	PVA-PSf	Diverse
North Carolina SRT (United states)	Diverse	Plat
NWW acumen (United states)	PS	Spiral
Osmonics Desalination Systems (United states)	CA-PA	Spiral
Osmota (Germany)	Composite	Diverse
PCI (Paterson Candy International) (Great Britain)	Diverse ceramic polymers	Tubular
Stork Friesland (Canada)	PA	Tubular
Orelis (France)	Zircon	Diverse
Tami (France)	Ceramic	Tubular
Toray (Japen)	PA-PES	Spiral
Tri-Sep (United states)	PA	spiral
US Filter SCT (United states, France)	Titan	Tubular
Wheelabrator (United states)	PVDf-PS-PAN	Tubular
X-Flow (Nederland)	PES	Spiral

Polysulfone (PSF), polyethersulfone (PES), polyvinyledene fluoride (PVDF), polyacrylonitrile (PAN), Polyamide (PA), Polysulfone sulfunated (PSSf), Polyvinyl alcohol (PVA).

5.1.2. Applications of NF membranes

From the very start, the drinking water industry has been the major application area for nanofiltration. The historical reason for this is that NF membranes were essentially developed for softening, and to this date NF membranes are still sometimes denoted as ''softening'' membranes (Van der Bruggen and Vandecasteele, 2003).The first nanofiltration plants that were developed were essentially meant for softening, and NF became a concurrent to lime softening. Softening was mainly of interest for groundwater in contrast to surface waters, where the major problem is usually a high organic content.

At the present time, nanofiltration is rather seen as a combinatory process capable of removing hardness and a wide range of other components in one step (Schaep,1998). The possibility of replacing many different treatment processes by a single membrane treatment was the engine for intense research and an enhanced interest from drinking water companies.
Due to their unique separation properties, NF membranes are widely used in industry. It is advantageous to use NF membranes when (Rautenbach and Groschel, 1990):
• It is not necessary to retain monovalent salts
• A separation of anions of different valency must be achieved
• A separation between low molecular weight organic material and a monovalent salt is desired: i.e. separation of lactose from ash; separation of dyes from sodium chloride.
• Purification of acids, bases or solvent is being investigated: especially when the contaminants are in the NF MWCO range.
• A reduction in osmotic pressure is required: compared to reverse osmosis membranes.

NF membranes are applied in a variety of industrial applications. NF membranes extremely useful in the fractionation and selective removal of solutes from complex process streams. This development of NF technology as a viable process over recent years has led to a marked increase in its adoption in a number of industries such as treatment of pulp-bleaching effluents from the textile industry (Rosa and de Pinho, 1995, Bes-Pia *et al.* 2005, Gozalvez-Zafrilla *et al.*2008), separation of pharmaceuticals (Tsuru *et al.* 1994; Yoon *et al.* 2007), demineralisation in the dairy industry (Van der Horst *et al.*1995, Balannec *et al.* 2005, Frappart *et al.* 2006), metal recovery from wastewater (Fane *et al.* 1992) and virus removal (Hoffer *et al.*1995).

Nanofiltration (NF) has been progressively used for water and wastewater treatment in order to remove suspended solids and reduce the content of organic and inorganic matters. Many authors have reported the application of NF and RO to highly reduce TDS, salinity, hardness, nitrates, cyanides, fluorides, arsenic, heavy metals, colour and organic compounds, e.g., total organic carbon (TOC), biological oxygen demand (BOD), chemical oxygen demand (COD), and pesticides, besides the elimination of bacteria, viruses, turbidity and TSS from surface water, groundwater, and seawater (Amy *et al.*1990 ; Berg *et al.* 1997; Bertrand *et al.*1997 ; Bohdziewicz *et al.*1999 ; Boussahel *et al.* 2000 ; Choi *et al.* 2001, Ericsson *et al.* 1996 ; Escobar *et al.* 2000 ; Hafiane *et al.* 2000 ; Kiso *et al.* 2000 ; Redondo *et al.* 2001; Van der Bruggen *et al.* 2001; Van der Bruggen *et al.* 1998 ; Van der Bruggen *et al.*1999 ; Ventresque *et al.*1997; Ventresque *et al.* 2000 ; Watson *et al.* 1989 ; Wittmann *et al.*1998).

NF as a desalting process

NF membranes are charged and reject multivalent ions. Monovalent ions are only partly rejected, so that the concentration difference between feed and permeate is smaller than for a complete rejection. This is an advantage for NF: osmotic pressures are lower compared to reverse osmosis, so that lower pressures need to be applied, and the energy consumption is proportionally lower.

Hassan *et al*. (1998) reported the use of NF in an integrated desalination system NF-SWRO (Sea Water Reverse Osmosis) and NF-MSF (Multi Stage Flash). The concentration of monovalent salts was reduced by 40%, and the overall concentration of TDS (Total Dissolved Salts) was reduced by 57.7%.The permeate thus obtained was far superior to seawater as a feed to SWRO or MSF. This made it possible to operate a SWRO and MSF pilot plant at a high recovery (resp. 70 and 80%). The MSF could be operated at a top brine temperature of 120°C without any scaling problem (Al-Sofi et al., 1998). The high water output in both integrated desalination systems, combined with a reduction of chemicals and energy (by about 25–30%) allows producing fresh water from seawater at a 30% lower cost compared to conventional SWRO (Al-Sofi, 2001). Recently, a demonstration plant was built at Umm Lujj, Saudi Arabia, consisting of six spiral wound NF modules (8x40 inches) followed by three SWRO elements (Hassan *et al*.,2000).

Pontie *et al*. 2003, studied the possibility of obtaining a partial demineralization of seawater using two successive NF stages. The treated water (salinity 9 g/L) could be used in the field of human health care (i.e., preparation of nasal sprays, medical dietetics and hot mineral springs).

Al-Zoubi, 2006 reported the use of the Nanofiltration membrane NF90 in the pretreatement of desalination processes and in partial demineralization.This membrane shows its ability to reject both monovalent and divalent ions of seawater of Indian Ocean collected from the coast of Oman with very reasonable values. Moreover, it reduced the salinity of investigated seawater from 38 to 25 g/L using one stage. On the other hand, the NF270 membrane can reject monovalent ions at relatively low values and divalent ions at reasonable values and reduced seawater salinity to 33 g/L at very high permeate flux. The author recommended the use of the NF270 membrane only as pretreatment for desalination processes.

Nanofiltration is a new process that is still little used in the brackish water desalination, and is beginning to compete with the other two membrane techniques (Reverse osmosis and Electrodialysis) for the treatment of brackish water (Rumeau and Pontié, 1998, Haddad *et al.* 2004). Nanofiltration can provide selective desalination and is generally used to remove divalent ions, such as sulfates and calcium ions. But it is also important to determine whether this process can be used to separate ions of the same valency. This technology also offers the great advantage of lower operating costs than reverse osmosis. Low cost membrane materials have also contributed to its spread, making it less expensive than the other two methods mentioned earlier (Pontié *et al*., 1994). Mohsen *et al.* 2003, investigated NF to treat brackish water collected from Zarqa basin, Jordan. The results show that NF is efficient for reducing the organic and inorganic contents and gives a high water recovery up to 95%. M'nif *et al*. 2007, analyzed the performance of coupling both NF and RO membrane units followed by an

inverse RO-NF coupling for a better desalination of brackish water with salinities varying from 3 to 10 g/L. The recovery rate in NF/RO coupling was improved compared to that obtained in RO alone. This coupling also improves salt rejection and thus leads to a decrease in the salinity of water product. Haddad et al. 2004, investigated the use of NF for desalination of two Tunisian brackish waters, with a salt content between 3.5 g/L and 4 g/L. The NF membrane used was prepared with cellulose acetate. The nanofiltration tests revealed that anneled membranes at 75°C and 80°C correspond well to NF needs and are well adapted to desalination needs of Tunisian brackish waters.

Walha *et al*. 2007 studied the possibility of producing drinking water from brackish groundwater using nanofiltration (NF), reverse osmosis (RO) and electrodialysis (ED) processes. Brackish groundwater samples were taken from desalination plants in Gabes (TDS 2.6 g/L) and Zarzis (5.3 g/L) cities, Tunisia. The authors used a Tubular nanofiltration membrane (MPT 03). The results obtained for the Gabes water show that nanofiltration permitted to reduce the concentrations of Ca^{2+}, Mg^{2+} and SO_4^{2-}. The total dissolved salts of the produced water was reduced to 1890 mg.L^{-1}. The Zarzis water is richer in chloride and sodium than the Gabes water. By NF and with Gabes water, Na^+ and Cl^- were not retained and the possibility of producing drinking water from the Zarzis sample using NF under the same conditions was very difficult.

NF can play an important role in some small scale desalination systems, treating brackish groundwater aquifers for isolated or remote communities. There has been several renewable energy-powered desalination systems designed to produce 400 – 1000 L of drinking water per day using RO membranes. Many existing water treatment technologies in remote communities are unsustainable for several reasons. The designer of a successful appropriate technology needs to consider the following issues: variability in membrane choice depending on water quality; NF membranes are designed to operate at lower pressures (5-10 bars) than RO membranes, the salt rejection is sufficient to achieve clean drinking water from brackish water sources and the power requirements are significantly reduced (Richards and Schäfer 2003).

Schäfer et al. 2005 reported the use of NF to treat brackish water collected from Murramarang national park, Austrilia (TDS 1.5-5 g/L). The authors compared the performances of a nanofiltration membrane NF90 with a reverse osmosis membrane BW30 with a solar desalination system using hybrid membrane technology, UF and NF/RO. The results show that the retention of both membranes was very similar while the NF90 membrane permeability was highest. The NF90 membrane retained hardness and multivalent ions at >98% and monovalent ions at >90%. Moreover the specific energy consumption for the NF90 (2.0-3.1 KWh/m^3) was smaller than for the BW30 membrane (3.0-5.5 KWh/m^3) at pressures of 7 to 15 bars.

Schäfer *et al*. 2007 also investigated NF to treat Australian brackish water with a salt content of 5.3 g/L using a photovoltaic powered NF/RO system. Number of operation parameter combinations (transmembrane pressure, feed flow) was investigated to find the best operating conditions for maximum drinking water production and minimum specific energy consumption. The nanofiltration membrane NF90 was able to produce better quality water with the RO membrane BW30, whereas TFC-S membrane has not been able to fulfill the recommended drinking water guidelines.

5.2 Separation mechanisms

As NF membranes spans the gap between UF and RO membranes, while separation is thought to be accomplished via size exclusion or charge repulsion, dielectric exclusion can also contribute the separation process. Depending on the physicochemical characteristics of the solute and the membrane, separation can be achieved by one or several mechanisms. While sieving mechnism and electrostatic interaction often dominate the separation process, physicochemical interactions factors play a subtle but not less critical role. The word 'physicochemical' explicitly implies that separation can be due to physical selectivity (charge repulsion, size exclusion or steric hindrance) or chemical selectivity (solvatation energy, hydrophobic interaction or hydrogen bonding).

The sieving (steric hindrance) effect described that most of the solutes that having larger molecular weight (MW) than the molecular weight cut-off (MWCO) of the membrane are rejected by the membrane and ones having lower MW than the MWCO of a membrane will permeate easily through the membrane. Thus solutes having different MWs can be separated based on sievig effect. Sieving mechanism and non-electrostatic membrane solute interaction (e.g. Van-der-Waals forces) are mostly responsibe for the retention of uncharged molecules and their transport takes place by convection due to a pressure difference and by diffusion due to a concentration gradient across the membrane (Kosutic and Kunst, 2002; Van der Bruggen *et al.*,1999). This mechanism is relatively simple, easy and well understood.

For charged compounds both size exclusion and electrostatic interactions are responsible for separation. Another important parameter in the transport process through NF membranes is the membrane charge along the surface and through the pores (Teixeira *et al.* 2005, Peeters *et al.* 1999, Childress *et al.* 2000). As most NF membranes are charged (mostly negatively), electrostatic interaction takes place between the component and the membrane (Schaep *et al.* 1998).

The ion separation resulting from electrostatic interactions between ions and membrane surface charge is based on the Donnan exclusion mechanism (Childress *et al.* 2000). In this mechanism the co-ions (which have the same charge of the membrane) are repulsed by the membrane surface and to satisfy the electroneutrality condition, an equivalent number of conter-ions is retained which results in salt retention. Donnan effect leads to a difference in rejection according to ion charge. Multivalent ions have a higher rejection in NF than monovalent ions because charge interactions are larger; co-ions in particular are efficiently retained (Van der brugen *et al.* 2004). The Donnan effect is dependant on several factors, e.g.:

- Salt concentration
- Fixed charge concentration in the membrane
- Valence of the co-ion
- Valence of the counter-ion

The salt concentration increase leads to the rejection decrease. With increasing concentration, the shield effect of the cations on the membrane charged groups becomes progressively stronger, i.e. a decrease on the membrane repulsion forces on the anions occurs (Afonso *et al.* 2001).

The Donnan exclusion is marked by a characteristic dependence of rejection on the electrolyte valence type; an increase with the increasing coion charge and a decrease with the increasing counterion charge (Yaroshchuk 2001). However, the degree of retention can decrease with increasing valency of the cations, since highvalency cations cause membrane charge shielding. This would, for example, result in retention sequence following the order: Na_2SO_4 > $CaSO_4$ > $NaCl$ > $CaCl_2$. The charge of the anion, however, still dominates the degree of retention. The rejections order: Na_2SO_4 > $NaCl$ and $CaSO_4$ > $CaCl_2$ corresponds to the decreasing order of the anion charge density, and therefore to the decrease of the repulsion forces of the anions. The rejections order: Na_2SO_4 > $CaSO_4$ and $NaCl$ > $CaCl_2$ corresponds to the increasing order of the cation charge density, and therefore to the increase of the attraction forces of the cations.

For the same valence ions, the rejection sequence could be affected by the difference in ion diffusivities, i.e., an ion is retained more if it has a smaller diffusivity and higher stockes radius. The diffusion coefficient is essentially related to the stockes radius. The stockes – Einstein radius is given by Eq (1):

$$ri = \frac{KT}{6\pi\eta Di}$$

(1)

Where K is the Boltzman constant (J/mol.K), η is viscosity (Kg/m.s), T is temperature (K) and D_i is diffusion coefficient (m^2/s).

Sieving mechanism can also be used for the retention of ions where the hydrated ion radius needs to be considered. In water solutions, ions are surround by fixed water molecules. Table 9 gives the stockes radius and the hydration energy of different ionic types.

Table 9: *Stocks radius and hydration energy of different ionic types*

Ion	Stockes radius (nm)	Hydration energy (KJ.mol^{-1})
Na^+	0.184	407
Cl^-	0.121	376
F^-	0.117	515
NO_3^-	0.128	329
SO_4^{2-}	0.231	1138
Ca^{2+}	0.310	1548
Mg^{2+}	0.341	2018

The ions which have higher hydration energy are more retained. Hydration can be considered as a force, the force necessary to extract the solute from the solvent to put it into the pores. In this way, it whould require more energy to extract ions with higher hydration energy to push it into the pores than ions with lower hydration energy (Pontallier *et al.* 1997). Thus, the degree

of hydration can influence the retention. For example the retention of $NaNO_3$ is lower than of NaCl because the nitrate ion is less hydrated in aqueous solution than the chloride ion. This reduces its effective charge, which in turn reduces the retention (Peeters *et al.* 1998).

Recently, many investigations showed that the dependance of the separation performance of NF membrane for the salts with multivalent cations on the salts concentration was distinguished from that for the salts with univalent cations (Wang et al. 2005; Peeters et al. 1998, Scheap et al. 1999, Wang et al. 2002, Labez et al. 2003, Aleman et al. 2004, Yaroshchuk et al. 2001). The rejection of the salts with Mg^{2+} or Ca^{2+} by negatively charged NF membranes slightly increased with the growth of salts concentration. This phenomenon is expalined by the counter-ion adsorption on the surface of NF membranes, which may yield the reverse of membrane charges. The conter ions of higher valences that are adsorbed by the membrane can completely shield the charged groups in the membrane, hence neutralizing or changing the sign of the effective charge of the membrane. Another explanation is the effect of dielectric exclusion. This phenomena have to be accounted for so as to improve realism of NF transport modeling. That is the reason why the dielectric exclusion has been accorded attention in the recent years (Szymczyk and Fievet 2006). Dielectric exclusion is caused by the interactions of ions with the bound electric charges induced by ions at the interfaces between media of different dielectric constants, in particular, a membrane matrix and a solvant (Yaroshchuk 2000, Szymczyk *et al.* 2006).

The mechanism of retention is more complex in mixed salt solutions. In the case of ion mixtures, electrostatic interactions between co-ions may cause, according to the Donnan exclusion, a decrease in monovalent ions rejection, especially if less permeable co-ions are present in the solution (Moros *et al.* 2007, Tannien *et al.* 2006). For exemple, in a mixed solution with NaCl and Na_2SO_4, the concentration of the divalent anion influences the monovalent anion retention. When Na_2SO_4 is added to a solution of constant NaCl concentration, the retention of Cl^- decreases as the concentration of Na_2SO_4 increases. The Na^+ ions which readily pass through the membrane must be accompanied by a negatively charged ion in order to maintain electroneutrality.The negatively charged ions are, however, repelled by the negatively charged membrane. The Cl^- ions with the lower potential are forced to permeate preferentially compared with the $SO4^{2-}$ ions (Krieg et al. 2004).

There are still a lot of unknowns in the removal mechanisms by NF membranes because the rejections of solutes by NF membrane are rather complicated. Membrane properties such as hydrophobicity, membrane charge, membrane pore size, potential for fouling, resistance to temperature, retention properties and permeability dramatically affect the filtration process. Solute properties such as dipole moment and hydrophibicity also affect the separation efficiency by adsorption or interaction with membrane surface.

5.3 Modelling of nanofiltration membrane

Recently, efforts have been made to predict the performance of NF membranes and membrane systems. But so far little satisfactory results have been achieved. A new way is to use modelling and simulation techniques to achieve this objective, as recently reported by

Palmeri *et al. (2000).* An other approach is to develop a model using the results of experiments in order to guide the choice of the best membrane for a given feed water solution (Lhassani *et al.* 2001, Diawara *et al.*, 2003).

A good predictive model will allow users to obtain membrane characteristics, predict process performance as well as optimize the process. The ability to develop such modelling technique will successfully result in a smaller number of experiments and subsequently save time and money in the development stage of a process (Hilal *et al.*, 2003).

Literature models for high-pressure membranes (NF & RO) are usually based either on a mechanism-independent approaches, such as irreversible thermodynamics (IT), or on the extended Nernst-Plank method. Initial descriptions of the NF process were based upon irreversible thermodynamics. These methods were originally employed as a black box description of dense reverse osmosis membranes (Kedem and Katchalsky, 1958; Spiegler and Kedem, 1963).

5.3.1 Irreversible thermodynamics (IT) models

The irreversible thermodynamics (IT) is the most general approach to the description of transport phenomena in the membrane systems (Staverman, 1952 ; Spiegler, 1958 ; Kedem and Katchalsky, 1963 ; Schlögl, 1964 ; Meares *et al.*, 1972 ; Klinowski *et al.*, 1974 ; Barannowski, 1991)

Most current IT models (Perry and Linder, 1989 ; Schirg and Widmer, 1992) are based on, or derived from, the work of Spiegler and Kedem.

In these models, the membrane is treated as a black box in which relatively slow processes proceed near the equilibrium without specific transport mechanisms and structure of the membrane. The model simply considers that the fluxes of solute and solvent are directly related to the chemical potential differences between the two sides of the membrane.

This approach has been extensively used in predicting the data of the transport of single solute and solvent through the membrane in the reverse osmosis and nanofiltration system (Jain and Gupta, 2004 ; Sutzkover *et al.*, 2000; Pontié et al. 2004; Diawara et al. 2003, Pontié *et al.* 2008).

The Speigler-Kedem approach was usually applied when there was no electrostatic interaction between membrane and solute. This is the case when the membrane is uncharged such as RO membrane or when the solute is neutral (organic compounds). Many authors however (Gilron *et al.*, 2000 ; Diawara *et al.*, 2003 ; Hafiane *et al.*, 2000) used this model in retention of electrolyte with an NF membrane that is charged.

This black-box approach allows the membranes to be characterized in terms of salt permeability (P_s) and the reflection coefficient (σ). This model is in the first instance limited to binary salt systems, and in the limiting case to a binary salt system in the presence of a completely rejected organic ion (Levenstein *et al.*, 1996). Koyuncu and yazgan (2001) found that this model was able to fit well their experimental data (rejection *versus* permeate flux) for different salt mixtures using TFC-S NF membrane. They concluded that σ is constant for each anions and cations in the salt mixture whereas P_s was varied according to the type of the salt ions. Nevertheless, different conclusion has been obtained by other authors (Diawara *et al.*, 2003) for the filtration of single salts showing that both parameters σ and P_s have changed and were dependent on the type of the filtered salt. In a recent study, Al Zoubi, 2006 has the same

conclusion for the values of σ and P_s. In this study, Spiegler-Kedem model was used to fit the filtration of different single salt solutions using three NF membranes (NF90, NF270, and N30F).

Bhattacharya and Ghosh (2004) used the Spiegler–Kedem model while Fukuda *et al.* (2003) used the Kedem–Katchalsky model in predicting the binary solute system when an impermeable ion is present in the salt–water solution.

The Spiegler–Kedem model is mostly used in the single solute system and binary solutes system with one solute is assumed to be impermeable to the membrane and the solute–solute interactions are neglected. However, in the literature, models have been proposed for the multiple solutes system in membrane filtration (Hoppe *et al.*, 1983 ; Slezak *et al.*, 1989 ; Zelman, 1972 ; Ahmad *et al.*, 2005).

In this work, SKK model and a simplified version of this model have been utilized to gain some insight in mass transfer into NF/RO membranes.

5.3.2 Theory

The transport of solutes through a membrane can be described by using the principles of irreversible thermodynamics (IT) to relate the fluxes with the forces through phenomenological coefficients. For a two components system, consisting of water and a solute, the IT approach leads to two basic equations (Spiegler and Kedem, 1966)

$$J_v = L_p[\Delta P - \sigma\Delta\Pi] \qquad (2)$$

$$J_s = P_s.\Delta C_s + (1-\sigma)J_v C_{int.} \qquad (3)$$

where J_v and J_s are respectively the solvent flux and the solute flux, ΔP and $\Delta\Pi$ defined respectively the membrane transmembrane pressure and the osmotic differences between each side of the membrane, Lp is the hydraulic permeability to pure water, σ is the local reflection coefficient, P_s is the solute permeability, $c_{int.}$ is the solute concentration in the membrane and $\Delta Cs = C_m - C_p$ with C_m and C_p the concentrations respectively at the surface of the membrane in the bulk side and in the permeate. We have also defined in the following text Lp' the hydraulic permeability for a saline solution and P_c the critical pressure defined as :

$$P_c = \sigma\Delta\pi \text{ : critical pressure} \qquad (4)$$

The parameter P_c in the Eqn.(4) is the efficient pressure for which the first droplets of permeate solution observed.

With constant fluxes, constant transport parameters (Lp and σ), integration of Eq. (3) on the membrane thickness yields, in term of the real salt rejection, give the following rejection expression (Jain et al. 2004) :

$$R = \frac{\sigma(1-F)}{1-\sigma F} \qquad (5)$$

with $F = e^{-\frac{1-\sigma}{P_s}J_v} = e^{-\frac{1-\sigma}{P_s}J_v}$

From Eq.(5), it appears that the retention increases with increasing water flux and reaches a limiting value σ at an infinitely high water flux, as recently reported (Diawara et al. 2003). As the diffusive flux of the solute can be neglected in the range of the higher water flux, the

reflection coefficient σ is a characteristic of the convective transport of the solute. A σ value of 100% means that the convective solute transport is totally hindered or that no transport by convection takes place at all. This is the case for ideal RO membranes where the membranes have dense structure and no pores are available for convective transport. Eq. (4) however only relates the membrane surface concentration to the permeate concentration. It needs to be combined with concentration polarization if the permeate concentration is to be related to the bulk feed concentration which results in the combined film theory—Spiegler–Kedem (Murthy and Gupta, 1997).

According to the *film theory*, the relation between the observed rejection rate and the true rejection R may be expressed as :

$$Ln\left(\frac{1 - R_{obs}}{R_{obs}}\right) = Ln\left(\frac{1 - R}{R}\right) + \frac{J_v}{K} \quad (6)$$

where K is the mass transfer coefficient.

Substitution of Eq. (5) into Eq. (6) and rearranging results in the following equation (Murthy and Gupta, 1997):

$$R_{obs} = \frac{1}{\frac{1 - \sigma}{\sigma\left(1 - e^{-(\frac{1-\sigma}{P_s})J_v}\right)} e^{\frac{J_v}{K}} + 1} \quad (7)$$

By using a nonlinear parameter estimation method by supplying the data of R_{obs} vs. J_v taken at different pressures but at constant feed rate and constant feed concentration for each set, Eq. (7) may be used to estimate the membrane parameters σ and P_s and the mass transfer coefficient, K, simultaneously (Jain et al. 2004). A wide variation of trans-membrane pressure at a constant feed flow rate are required to prevent poor regression due to too many unknowns (σ, P_s and K) compared to the experimentally obtainable variables (J_v and R_{obs}). Even in this case, poor regression might still be obtained for high values of K. In this particular case, the inequality K >> J_v holds at most values of J_v and this prevent to obtained K with some confidence because R_{obs} = R (Eq. (6) reduces to Eq. (4) for any value of K >> J_v). To the author opinion the best way to determine the σ and P_s values is to work under experimental conditions so that K >> J_v (high tangential rate and low pressure). This allows to directly obtained the true rejection and then σ and P_s using a non-linear least squares estimation procedure that make equation (6) fit the data as closely as possible.

An other way to quantify the both convective and diffusive parts is to expressed equation (3) as :

$$J_{diff} + J_v C_{conv} = C_P J_v \quad (8)$$

where J_{diff} is the solute flux due to diffusion (with $J_{diff.} = P_s \Delta C_s$), and C_{conv} is the solute concentration due to convection [with $C_{conv} = (1-\sigma)C_{int}$]. Note that this equation is identical to the Kedem-Katchalsky model and doesn't imply a linear concentration gradient as it is frequently reported. It may be expressed as well as (Diawara et al. 2003, Pontié et al. 2003):

$$C_P = \frac{Jdiff}{Jv} + C_{conv} \qquad (9)$$

By following C_p versus the reverse of the permeate flux, it is possible to quantify separately both part of the solutes mass transfer occuring in NF : convection and solvation/diffusion as reported recently (Diawara et al. 2003). The results are expected to be valid only in some limited domain of operating conditions with low polarization concentration and with membrane considered having no charge and for the steady state. This approach may be useful for the comparison of the behavior of different NF and RO membranes.

To better compared both contribution of the mass trasnfer we defined a Peclet number, noticed Pe, as :

$$Pe = (J_v C_{Conv.})/J_{diff.} \qquad (10)$$

with a Pe>1 convective mass transfer is dominant, with a Pe <1 diffusionnal mass transfer is dominant.

To determine the MWCO of membrane we can use the Cconv data as reported recently by Lhassani et al. 2000. For porous membranes, membrane selectivity is related to pore size as expressed mathematically by following equation (Perry, 1984):

$$C_{conv.} = C_0 \left[1- ds/dp\right]^2 \qquad (11)$$

with ds = solute diameter; dp = pore diameter and
From the Cconv. values, it is possible to calculate the molecular weight cut-off (MWCO) of the three membranes studied, from the Eq.(11)

$$C_{conv} = C_0 \left[1-(M/Sc)^{1/3}\right]^2 \qquad (12)$$

with $ds/dp \approx (M/Sc)^{1/3}$ where M the molecular weight of a solute, Sc the Molecular weight cutt off (MWCO) of the membrane and C_0 the initial concentration of the solute in the feed.

5.4 Characterization of NF/RO membranes

5.4.1 Surface Characterization

Characterization of membrane surface properties is of great interest to researchers since they greatly influence separation properties. Membrane permeability, rejection ratio and solute selectivity have been related to surface properties. The streaming potential (charge), roughness, hydrophobicity (contact angle) and MWCO are mainly used for membrane surface characterization (Boussu et al. 2006, Norberg et al. 2007, Childress et al. 2000, Singh et al. 1998, Brant et al. 2006, Boussuat al. 2008)

5.4.1.1 Membrane charge (Streaming potential)

The origin of a membrane charge is clear. When brought into contact with an aqueaous electrolyte solution, membranes do acquire an electric charge through several possible mechanisms. These mechanisms may include dissociation of functional groups, adsorption of ions from solution, and adsorption of polyelectrolytes, ionic surfactants and charged macromolecules. This charging mechanism can take place as well on the exterior membrane

surface as on the interior pore surface of the membrane. These surface charges have an influence on the distribution of the ions in the solution due to requirement of the electroneutrality of the system. This leads to the formation of an electrical double layer, so that we have a charged surface and a neutralizing excess of counter-ions in the adjacent solution (Schaep and Vandecasteele, 2001).

In certain conditions (i.e. low molecular weight cut-off membranes) the property of the electrical double layer near the pore walls is an important part of the pore volume. Therefore, the membrane electro-kinetic properties (i.e. streaming potential and surface conductivity) play an important role. When an electrolyte solution is forced to flow through a capillary, an electrical potential is generated which is known as streaming potential (SP). SP measurement gives information about the charge related modifications on the surface/ inside the pores of a membrane.

Ions in an electrolyte solution that is brought in contact with a charged surface will not be distributed randomly. The concentration of counter-ions near the membrane will be higher than that in the bulk of solution. The charges at and adjacent to the surface will cause a potential difference between the region near the surface and the bulk of the solution. The potential decreases within the solution as a function of the distance from the charged surface, as shown in Fig.15.
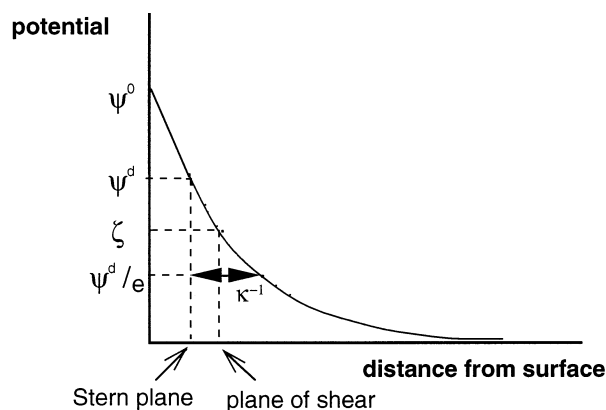
Figure 15: *Schematic drawing of potential decrease as a function of the distance from the surface in an electrolyte solution*

Three different potentials are shown in this figure, the surface potential, ψ^0, the potential at the Stern plane, ψ^d, and the electrokinetic or zeta potential ζ. All these potentials are defined with respect to the potential at infinite distance from the surface. Although the surface potential is an important parameter, the potential at the Stern plan is practically of more importance. This Stern plane is the interface between the fixed part, i.e a layer of immobile ions near the charged surface, and the diffusive (mobile) part of the electrical double layer. The potential at the stern plane is the actual potential influencing the behaviour of the charged species. However, as this potential cannot be measured directly, the electrokinetic potential is often considered as an adequate substitute. The plane at which the zeta potential is located should be outside the stern layer, and represents the potential at the surface of shear between surface and solution where there is a relative motion between them. The position of the surface of shear is close to, and from practical reasons assumed to be identical to, the stern

surface (Peeters et al. 1999). There are four basic types of electro-kinetics effects. Theoretically, each can be utilized to evaluate the zeta potential for a given set of conditions.

1. ***Electrophoresis:*** dealing with mobility of a charged colloidal particle suspended in an electrolyte in which a potential gradient is set up.
2. ***Electro-osmosis:*** denoting a movement of liquid in a capillary or in a system of capillaries (porous plug) under an applied potential.
3. ***Sedimentation potential:*** determining the magnitude of the potential developed by a dispersion of particles settling under the influence of gravity.
4. ***Streaming potential:*** concerned with the magnitude of induced electric potential, generated by a flow of liquid in a single capillary or in a system of capillaries.

A streaming potential is the potential difference at zero current caused by the convective flow of charge due to a pressure gradient through charged capillary, plug, diaphragm or membrane (Childress *et al.* 1996).When an electrolyte solution is forced through a thin slit, the charges on the mobile part of the double layer are carried towards one end. This constitutes a streaming current, and the accumulation of ions of one sign at one end of the slit generates a potential difference between the slit ends. The resulting back flow of current, in the steady state, will be equal to the streaming current and a steady potential difference, the streaming potential, will be established across the slit (Afonso *et al.* 2001).

Streaming potential measurements can be performed in two different ways: by flow through the membrane pores (transmembrane streaming potential measurements) (Nyström *et al* 1989, Ricq *et al*. 2002) or by flow across the top surface of the membrane (tangential streaming potential, TSP) measurements) (Lettmann *et al.* 1999, Van Wagenen *et al*. 1980, Sbaï *et al*. 2003, Szymczyk *et al*. 2007). The first method has the advantage of experimental simplicity but interpretation of experimental data may be difficult when measurements are performed with multilayer membranes (support layer(s) + skin layer) and/or membranes having selective layers. Indeed, the global streaming potential of the membrane does not necessarily reflect the real properties of the skin layer which rules the membrane selectivity, because of the non-negligible pressure drop occurring through the thick support layer(s) (Afonso *et al*. 2001).

Measurement of streaming potential can provide both the zeta potential and the net charge density at the hydrodynamic shear plane.

According to Helmholtz-Smoluchovsky equation (Eq. 13), the streaming potential can be linked to the zeta potential by the equation:

$$\frac{\Delta\phi}{\Delta P} = \frac{\varepsilon\zeta}{\mu\chi} \tag{13}$$

where $\Delta\phi$ is the trans-membrane potential difference, ΔP is the trans-membrane pressure, ε the permittivity, ζ, the zeta potential; μ ,the dynamic viscosity; χ , the ionic conductivity of the electrolyte solution; and $\Delta\phi/\Delta P$ is denoted the coefficient of streaming potential. From the measurements of variations of potential differences between two Ag/AgCl electrodes vs. trans-membrane pressure, it is possible to follow the charge evolution of pore walls of the membrane, because the trans-membrane potential difference per unit pressure is directly proportional to the zeta potential of the filtration medium. SP is the more simple way to

determine the charge carried by a porous material, as reported recently (Kecili, 2006, Pontié *et al.* 2006 and Thekkedath, 2007).

If such SP measurements are made across the top surface of the membrane, then the calculation of the zeta potential from the basic data is generally unambiguous. However, the calculation requires more care if measurements are made by the flow through the membrane (Afonso *et al.* 2001). In this case an electrical double layer is formed by the charged membrane pore walls and the adjacent electrolyte. Rice and Whitehead, 1965, have suggested that a correction in Eq. (13) should be made, with regard to narrow capillaries, which takes into account the double layer thickness on the interface. They proposed the following equations:

$$\frac{\Delta\phi}{\Delta P} = \frac{\varepsilon\zeta}{\chi\mu} F(\kappa^{-1}, r_p, \sigma) \tag{14}$$

with the correction function *F* approaches the value of 1 at $\kappa^{-1} \longrightarrow 0$.

The use of Helmholtz-Smoluchovski equation is restricted to high ionic strengths (Debye length, κ^{-1} should be less than 3 nm) in large capillaries (pore radius, r_p higher than 1.5 nm). If such SP measurements are made across the surface of a membrane, calculation of the zeta potential from the basic experimental data is generally unambiguous (Christoforou *et al.* 1983). However, the calculation requires more care if measurements are made with a flow through a membrane. In this case, an electrical double layer is formed in between the charged membrane pore walls and the adjacent electrolyte solution. It was shown that Eq.14 can be used to the limit of the ratio κ^{-1} / r_p around 10 in the case of high charge density. Thus a correction should be made to Helmholtz-Smoluchovsky equation with regard to narrow capillaries which takes into account of the double layer thickness on the interface. In the case of MWCO under 100 kDa with a concentration of electrolyte 0.001M, κ^{-1} is the double (with 9.7 nm) of the pore radius value (around 1 nm) and overlapping of double layers will occur. Then Eq (14) will not be valid for the calculation of absolute zeta potential but permits a qualitative measurement of the charge. So, we have to specify that our study was focalized only on streaming potential (SP) measurements firstly to qualify the charges bring by NF and LPRO membranes and secondly to determine the isoelectric point (IEP) of the studied membranes.

The pH value of the feed solution can affect the membrane surface potential. In general, streaming potential of amphoteric membranes can change from a positive to a negative value as the solution pH increases. Subsequently, electrostatic interaction between an ionic compound and the membrane surface can also vary according to the solution pH. SP measurements permit to determine the isoelectric point (IEP) of the membrane. The IEPis the pH of zero charge. At this pH, the surface charge and the SP vanished. For our microporous PA membranes, the IEP is dependent on the ionic strength and on the kind of the electrolyte solution in contact with organic membranes materials (Zimmermann et al. 2001, Teixeira et al. 2005).

5.4.1.2 Membrane hydrophobicity

The degree of hydrophilicicity is measured by the contact angle of the water droplet with the surface. As can be seen in Fig. 16, a hydrophilic surface is one which is completely wetted by

water, whilst on a hydrophobic surface, water forms beads or droplets. If completely wetted, the contact angle is zero. For a strongly hydrophobic surface, the contact angle is > 90°C. In water treatment, a hydrophilic membrane has some obvious advantages. Firstly, the membrane is easily wetted, and this results in easy commissioning procedures and high permeabilities relative to the pore size. Secondly, hydrophilic surface tends to resist attachement due to absorption by organics, and such a surface is reffered to as a low fouling surface (Pearce, 2007). However, hydrophobicity is essential for maintaining the membrane's mechanical and chemical stability as well as a high salt retention (Mulder, 2003). Membrane grafeting or chemical surface modification can be used to increase the hydrophilicity of the membrane surface while preserving other essential properties within the sub-layer (Freger et al. 2002; Nabe, et al. 1997). Ahmed et al.2004, reported that the modification of a TFC co-polyamide membrane by addind carboxylic group improved the permeability of the modified membrane about 20%.

| Hydrophilic Membrane | Hydrophobic Membrane |
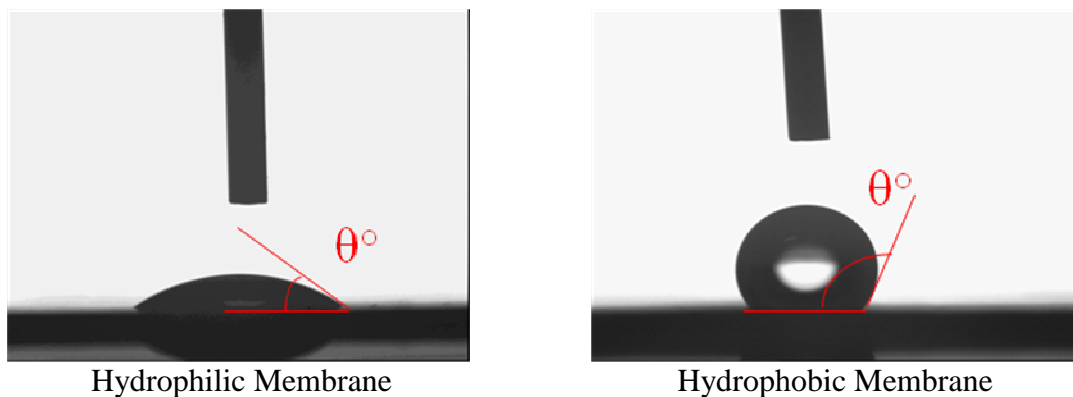
Figure 16: *Water drop contact angle (θ°) as a function of membrane surface hydrophobicity*

While contact angle is commonly used to measure the hydrophobicity of the membrane surface, the data should be used with some caution. Membrane surface roughness can influence contact angle measurement due to capillary effects and results from different measurement methods can vary considerably (Kwok et al. 1999). If roughness is higher than 100 nm, the measured contact angles are meaningless. On very rough surfaces, contact angles are larger than on chemically identical smooth surfaces (Neumann *et al.* 1972, Bain *et al* 1989).

5.4.1.1 membrane roughness (Atomic forces microscopy)

An Atomic Force Microscope is an excellent tool to study the topography of the membrane skin layer. An AFM consists on an extremely sharp tip mounted to the end of a tiny cantilever spring, which is moved by a mechanical scanner over the surface to be observed. Every variation of the surface height varies the force acting on the tip and therefore varies the bending of the cantilever. This bending is measured and recorded line by line (Bowen *et al.*, 1999). The image is then reconstructed by computer software associated with the AFM. Figure 17 shows a schematic demonstration of the principal of AFM operation.
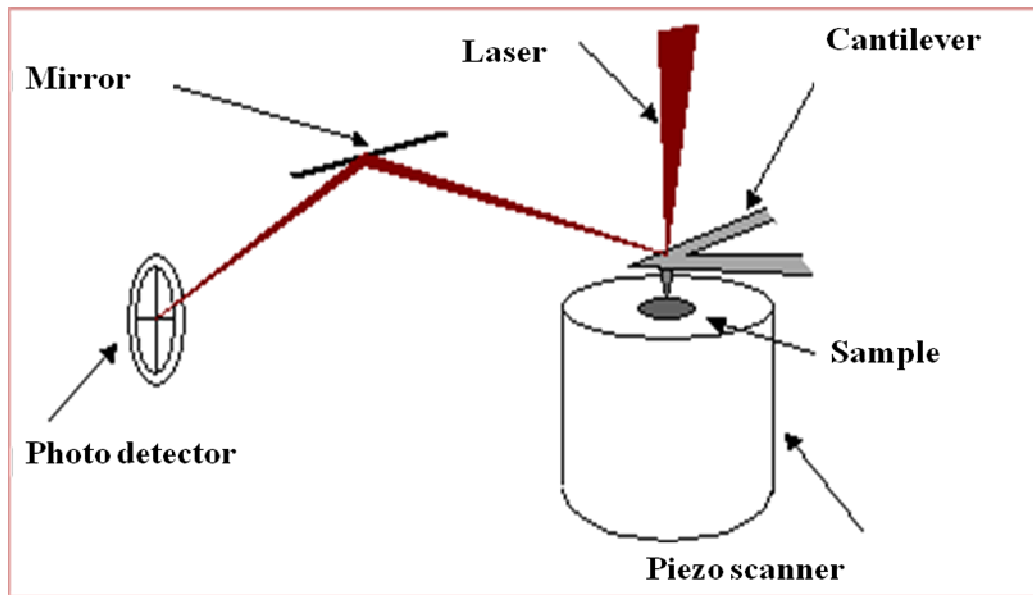
Figure 17: *Schematic demonstration of the principle of AFM operation*

Atomic force microscopie became popular in nineties (Matsuura, 2001). It gives topographic images by scanning a sharp tip over a surface. Figure 18 shows an example of an AFM image of the active surface of the membrane.

(a)

(b)
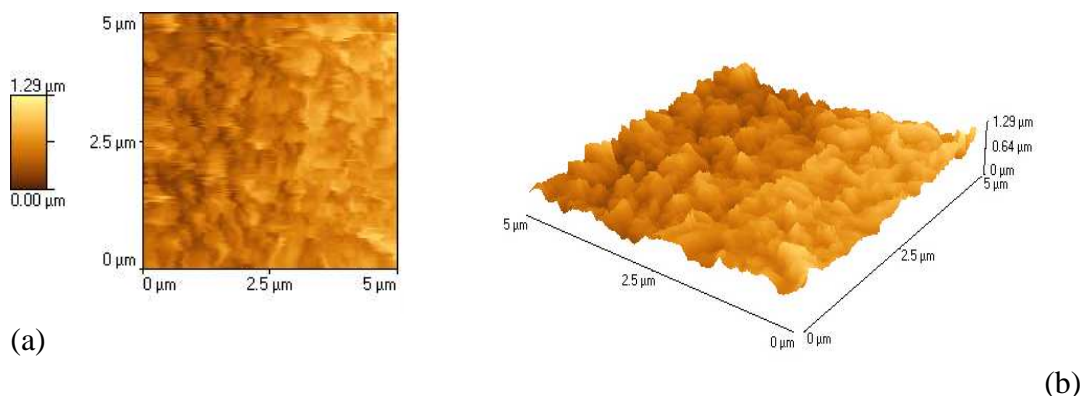
Figure 18: *An example of an AFM image of the active surface of the membrane;*
(a) 2-Dimentional image, (b)3-Dimentional image

AFM has become an important means of imaging the surface of materials at up to atomic level resolution. The study of the surface morphology of membranes can help to explain the separation processes in these membranes such as the characteristics of pore structure, surface roughness (Bowen *et al.*, 1996, Bowen *et al.*, 1997).The technique has therefore attracted the interest of a number of researchers interested in the surface properties of membranes. Many researchers used atomic force microscopy technique to characterize membrane surface and therefore determine key properties of these membranes.

AFM contributed to the developement of high flux reverse osmosis membranes. Hiros et al.1996 found a relationship between the flux of reverse osmosis membranes and their roughness parameters. Singh et al. related the roughness of membrane surface to the MWCO

of the membrane. They explained that membranes of higher MWCO are cast from the solution having lower polymer concentration and, therefore, will have less tightly packed nodules aggregates in the skin layer, which in turn, would contribute to higher degree of roughness on its surface.

Surface roughness has also an important effect in membrane fouling behaviour (Elimelech *et al*. 1997; Zhu and Elimelech *et al*.1997; Vrijenhoek *et al*. 2001). Because of the ridge-and-valley structure of rough membrane surfaces, colloids are thought to be preferentially transported into the valleys (path of least resistance), which results in "valley clogging" and hence in a more severe flux decline in comparison with smooth membranes. Noverberg et al. 2007, used the surface characteristics of 20 NF and RO membranes for the selection of fouling resistant membranes for use in a pilot plant study to treat high brackish water surface. A recent works show up-to-date work carried out on application of atomic force microscopy to nanofiltration membrane surfaces (Hilal *et al*., 2003, Al-zoubi, 2006).

5.4.1.3 Molecular weight cut-off

The rejection characteristic of a specific NF membrane is often quantified by the MWCO. Usually, the MWCO is defined as the MW of a solute that was rejected at 90 percent (Van der Bruggen et al.1999); although, this definition is not explicit and it can vary between 60 and 90 percent depending upon protocols used by various manufacturers. Variations in solute characteristics, solute concentration, solvent characteristics, as well as flow conditions such as dead-end versus cross-flow filtration, make comparison of results from different manufacturers difficult (Cleveland *et al*. 2002).The MWCO concept is based on the observation that molecules generally get larger as their mass increases. As molecules get larger, sieving effects due to steric hindrance increase and the molecule is rejected by the membrane more often than a smaller molecule. It should be noted that the MWCO may also be related to diffusion, because a bigger molecule will diffuse more slowly than a smaller molecule. Definitive MWCO values are often not reported for semi-permeable membranes like RO membranes. Van der Bruggen *et al*. 1998 and Mohammad *et al*. demonstrated that the MWCO of an NF membrane only poorly correlated with rejection of compounds studied, and as a sole number, is only capable of providing a rough estimate of the sieving effect.

5.4. 2 membrane performance

5.4. 2.1 Pure water permeability

Pure water flux through a membrane can be described by the Darcy's law from the Eq. (15):

$$J_v = L_P \, \Delta P \qquad\qquad\qquad (15)$$

with Lp the hydraulic permeability.

The pure water permeability reflects the porous structure of the membrane. A constant value of pure water permeability, i.e. the linear dependence of the pure water flux Jv on pressure, points to unchangeable membrane porosity. If the water flux dependence on pressure deviates from linearity, the pure water permeability of a membrane is not constant, and it indicates the changes in the membrane's porous structure (Kosutic *et al*. 2006). Thus, by measuring a

dependence of the membrane's pure water permeability on pressure, a state of the membrane's active layer porosity can be characterized.

Kosutic et al. reported that in the case of the loose NF membranes, containing in addition to medium size pores a remarkable fraction of large pores, the water flux is prevailingly determined by the large pores. The large pores shrink under pressure only slightly resulting in a minor water flux drop. The pressure effect is the strongest for the tight NF membranes, which active layer accomodates many medium sized pores. The increased pressure appreciably reduces both the dimensions of the medium sized pores and the water flux. The active layer structure of the RO membranes is fairly compact containing numerous very narrow pores. Their size cannot be reduced under pressure significantly due to the resistance of the already shrunk solid polymer matrix. The results whould be small water flux changes and low susceptibility parameter of these membranes. However, it has been also shown that the water flux at higher pressures can be increased due to opening up a number of closed pores to become "active" ones, i.e. by increasing the effective number of pores.

5.4. 2.2 Rejection characteristics

A parameter frequently used to describe the rejection characteristics of a membrane is the desalting degree. The desalting degree of a membrane is commonly reported as the percent rejection of electrolytes such as sodium Chloride, magnesium sulfate and other electrolytes. The desalting degree can be useful parameter in estimating the rejection of some compounds. This parameter is needed to be considered during membrane selection. Many authors have used this parameter to determine the effect of preparation condition on NF membranes performance (Sun et al. 2007, Mio et al.2006, Van Gestel et al. 2002, Yang et al. 2007). Some authors used the membrane permeation tests and the sequence of salt rejection to evaluate the membrane charge (Labez *et al*. 2003, Krieg *et al*. 2004, Schaep *et al*. 2001, Wang, 2005)

Membrane rejection (Robs) is calculated by the following relation:

$$Robs(\%) = (1 - \frac{Cp}{Co}) \times 100$$

(16)

where Cp and Co are the salt concentrations in the permeate and in the feed solution respectively.

5.5 Parameters affecting the performance of NF membranes

When designing a NF process, one should consider several operating parameters. Many authors (Turan, 2004; Ben Farès *et al*. 2005, Ballet *et al*. 2007, Bellona *et al*. 2004) have studied the influence of operating conditions on NF membranes performance The most important operating parameters affecting the performance of NF membranes are similar to those for most crossflow filtration processes:

• **Pressure:** Pressure difference is the driving force responsible for a NF process. The effective driving pressure is the supplied hydraulic pressure less the osmotic pressure applied on the membrane by the solutes. NF provides good separation at net pressures of 10 bar or higher.

• **Temperature:** Increasing the process temperature increases the NF membrane flux due to viscosity reduction. Additionnaly, increasing temperature increases mean pore radii and the molecular weight cut off suggesting changes in the structure and morphology of the polymer matrix comprissing the membrane barrier layer (Ramesh et al 2003). The rejection of NF membranes is not dependent significantly on the process temperature.

• **Crossflow velocity:** Increasing the crossflow velocity in an NF membrane process increases the average flux due to efficient removal of fouling layer from the membrane surface. However, the mechanical strength of the membrane, and construction of the element and system hardware will determine the maximum crossflow velocity that can be applied. Running a NF membrane at too high crossflow velocity may cause premature failure of membranes and modules. Increasing cross flow velocity also increase the pressure drop.

• **Recovery rate:** many authors have reported that an increase of feed water recovery leads to a decrease in rejection (Bannoud. 2001, Lhassani *et al.* 2001, Abouzaid *et al.* 2003). A study by Chellam and Taylor, reported that feed water recovery had a significant impact upon the rejection of total hardness. These findings indicate that diffusion across the membrane which is one of the main driving factors for solute permeation becomes higher when increasing the recovery rate. This increase may, be responsible for stronger concentration–polarisation, membrane–solute interactions and, even, solute adsorption onto membrane surface, all of these phenomena with a deleterious effect on the membrane performance.

• **pH:** pH affects performance of NF membranes in more than one way. The charged sites on the NF membrane surface (i.e. carboxylic group, sulfonic group) are negatively charged at neutral pH or higher, but lose their charge at acidic pH. It is well known that most NF and RO membranes have lower rejection at low pH, or after acid rinse. It should be noted, however, that since different membrane manufacturers use different chemistries to produce their thin film composite layer, the pH dependency of a membrane should be determined for each membrane type. In addition to the effect of pH on the membrane itself, pH can be responsible for changes in the feed solution, causing changes in membrane performance. Two examples are change of solubility of ions at different pH regimes, causing different rejection rate; and change in the dissociation state of ions at different pH ranges (Teixeira et al. 2005, Bellona *et al.* 2004).

• **Salinity:** the effective pore radius of a charged pore will increase as the ionic strength of the surrounding liquid increases. Therefore, the rejection of monovalent ions will decrease as their concentration in the feed solution increases. The rejection of divalent ions will be affected to a lower extent. The shield effect of membrane charge also increases as the ionic strength of feed solution increases.

Chapter two: Materials and methods

1. Membranes studied

1.1 Flat sheet membranes

Seven organic flat-sheet membranes purchased from different companies (Dow Filmtec and Saehan) were studied. The membranes used are thin film composite membranes composed of three layers: a thin film as active layer, a large mesoporous polysulfone as the support layer and an intermediate microporous layer in polysulfone. The studied membranes are four nanofiltration membranes (NF90, NF200, NF270 and NE90) and two low pressure reverse osmosis membranes (BW30 and BW30LE). Table 10 shows the commercial names of the membranes and their suppliers as well as the main polymer used in the manufacture of the membranes.

Table 10: *Properties of the membranes used and their manufacturers*

Membrane	Type	Manufacturer	Polymer
NF90	NF	Dow (Filmtec)	Polyamide
NF200	NF	Dow (Filmtec)	Poly piperazineamide sulfonated
NF270	NF	Dow (Filmtec)	Polyamide
NE90	NF	Saehan	Polyamide
BW30	LPRO	Dow (Filmtec)	Polyamide
BW30LE	LPRO	Dow (Filmtec)	Polyamide

Most of the membranes were made of Polyamide expect for the NF200 membrane that was made of Poly piperazineamide reticulated with sulfonated functional groups.

Flat sheet membranes conditionning

Prior to filtration, the membranes were immersed for 24 h in ultrapure water at 4°C in order to remove preservatives and each membrane was pressurized using pure water at 4 bar for 15 min until the conductivity of the permeate remained below 1μS/cm.

1.2 Spiral wound modules (SWM)

Eight spiral wound modules (4"), denoted BW30, BW30LE, ESPA3, REBLF, NF90, NE90, NE70, ESNA1LF, were studied. These membranes were purchased from DOW Chemical, Hydranautics and Saehan companies. Table 11 shows the commercial names of the membranes and their suppliers.

Table 11: *Names and suppliers of the NF and LPRO SWM*

Manufacturer	LPRO membranes	NF membranes
Dow Filmtec	BW30-4040 BW30 LE-4040	NF90-4040
Hydranautics	ESPA3-4040	ESNA LF-4040
Saehan	REBLF-4040	NE90-4040 NE70-4040

All the membranes used are thin film composite membranes and are made on polyamide. The geometrical area of the spiral wound modules (SWM) is 7.6 m^2.

Pretreatment of the SWR membranes

The membranes were shipped with no preservative solution. A pretreatment technique was required by the manufacturers to accelerate start up performance of the dry elements (FILMTEC technical manual, 2005, Hydranautics technical service bulletins, 2002, SAEHAN technical manual, 2005). A three-step pretreatment technique was used to ensure stabilized performance is achieved.

- Pre-Flushing: the membranes were flushed with feed water at a pressure of 3.5 for 15 minutes. This step was performed with the booster pump. Pre-flushing is critical to avoid permanent flux loss if the membranes have not been operated before.
- Soaking: the membranes were soaked in 1% sodium metabisulfite solution for 14 days.
- Post-Flushing: the membranes were flushed with feed water at a pressure of 3.5 for 60 minutes.

When the pilot unit did not operate longer time (more than 24 h), the membranes were preserved in 1% sodium metabisulfite solution.

1.3 Membranes characteristics

Suppliers have provided informations about the membranes such as the maximum pressure, maximum temperature and salt rejection as shown in Table 12.

Table 12: *Characteristics of the membranes used done by the suppliers*
(FILMTEC technical manual, 2005, Hydranautics technical service bulletins, 2000,
SAEHAN technical manual, 2006)

Membrane	*ΔP (bar) Max*	*pH range*	*T°C Max*	*NaCl Rejection (%)*	*MgSO₄ Rejection (%)*
NF90	41	3 - 10	45	85 – 95 [1]	> 97
NF200	41	3 - 10	45	35 – 50 [2]	97
NF270	41	3 - 10	45	40 – 60 [2]	>97
NE90	41	3 - 10	45	85-95 [3]	99.5
NE70	41	3 - 10	45	60 - 70 [3]	99.5
ESNA 1 LF	41	3- 10	45	75 - 92 [4]	nd
ESPA 3	41	3-10	45	nd	99
RE BLF	41	3 - 10	45	99.2	99
BW30	41	2 - 11	45	99.5 [5]	99
BW30LE	41	2 - 11	45	99 [6]	99

(1) Rejection of NaCl and MgSO₄ at 2000 mg/L, (ΔP = 4.9 bar), T = 25°C, Y = 15%. (2) Rejection of CaCl₂ at 500 ppm and MgSO₄ at 2000 ppm, (ΔP = 4.9 bar), T = 25°C, Y = 15%. (3) Rejection of NaCl and MgSO₄ at 2000 mg/L, (ΔP = 5.2 bar), T = 25°C, Y = 15%. (4) Rejection of CaCl₂ at 500 ppm, (ΔP = 5.1 bar), T = 25°C, Y = 15%. (5) Rejection of NaCl at 2000 mg/L, (ΔP =10 bar) , T = 25°C, Y =15%. (6) Rejection of NaCl at 2000 mg/L (ΔP =15.5 bar), T = 25°C, Y =15%.

It's clear that the manufacturer's data are not organized, since each company gives its proper data. Then it is difficult to compare the data because they have not been established under the same operating conditions.

2. Filtration experiments

2.1 Bench scale flat sheet testing

2.1.1 Experimental set-up

2.1.1.1Single salt experiments

The laboratory scale NF/RO setup used for single salts experiments were supplied by Sepratech (module SEPA II, Separation technology, INC, US), and consisted of: (i) a feed tank with a capacity of 10L , (ii) a pump Wanner (Wanner GP, US) and (iii) a planar module with a membrane area of 472cm^2. The feed tank was equipped with a temperature control system. A picture of the assembled experimental set-up is shown in Fig.19.
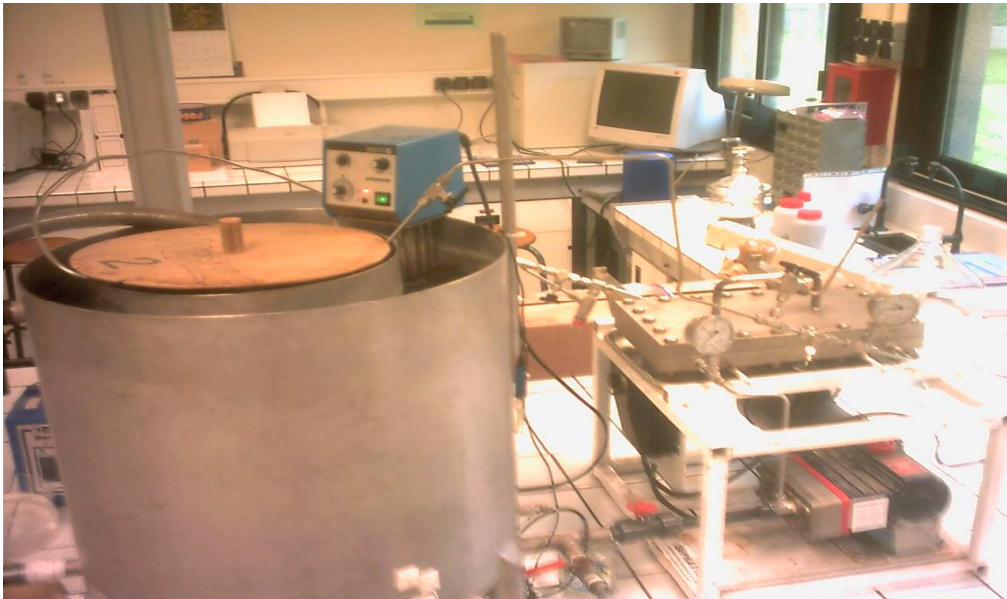
Figure 19: *Picture of the experimental set up used for single salt experiments (Module SEPA II)*

2.1.1.2 Salt mixture and real water experiments

A flat sheet laboratory scale NF/RO setup consisting of a planar cross flow module (Osmonics, Module SEPA CFII, USA), with a membrane area of 138 cm^2, was used in total recycle mode. The total volume of the system was 5 L. The feed tank was equipped with a temperature control system. A gear pump (Wanner GP, US) with variable speed has been used to circulate the feed solution through the module. Two valves were installed at the concentrate outlet and the feed inlet to adjust the transmembrane pressure and the volumetric flow rate. A picture of the assembled experimental set-up is shown in Fig.20, and a schematic representation of the equipment is illustrated in Fig.21.

Figure 20 *: Picture of the experimental set up used for salt mixture and real water experiments (Module SEPA CFII)*
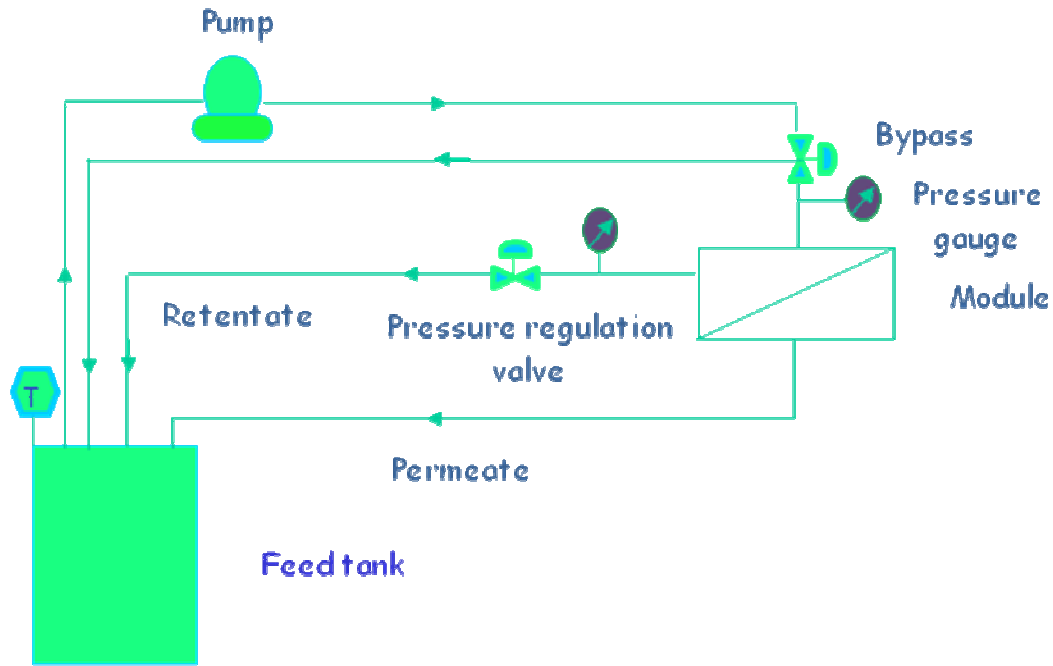
Figure 21: *Schematic representation of the flat sheet RO/NF bench scale setup*

2.1.2 Filtration procedure

Preliminary, filtration experiments with ultra pure water and synthetic brackish water (NaCl at 0.1M, total salinity near 6 g.L^{-1}) at different pressure and at a temperature of 25°C were carried out to determine the membranes permeabilities. The pressure was varied from 0 to 25 bar and for each pressure value the permeate volume with time was measured in order to calculate the flux and determine the hydraulic permeability.

2.1.2.1 Single salt experiments

The filtration experiments were carried out by circulating five liters of the feed solution under pressure into the filtration module. In the filtration tests, both the permeate and the retentate were returned to the feed tank in order to keep a constant concentration. The cross flow velocity was fixed to 4 m.s^{-1}. The transmembrane pressure and volumetric flow rate were adjusted using the valves. The pressure applied was varied from 0 bar to 16 bar. The permeate flux and the salt concentration in the product water were measured for each pressure value. The permeate samples were collected after 15 min of filtration when the equilibrium is reached.

To study the influence of operating conditions (applied pressure, solute concentration and the nature of the salt) in membranes performances, filtration experiments with single salt solutions were carried out. Two salts (NaCl and Na$_2$SO$_4$ were used at various concentrations (10^{-3}, 5.10^{-3}, 10^{-2}, 5.10^{-2} and 10^{-1} mol.L^{-1}). The temperature was maintained to 25°C and no adjustment of the pH was made (pH = 6.7).

During these experiments we have limited the concentration polarization by using a low conversion rate of 5% and a high flow rate (4m.s^{-1}). These conditions were chosen for the

application of the SKK (See Abbreviations) model to determine the membrane transfer parameters.

2.1.2.2 Salt Mixture experiments

Chloride rejection in the presence of Sulfate and Calcium ions was investigated. Two different salt mixtures were used ($NaCl/Na_2SO_4$ and $NaCl/CaCl_2$) at different proportions.

A mixture with common cation was performed by adding Na_2SO_4 to a NaCl solution of 1200 mg/L of chloride (in order to be in similar to Tan Tan water concentration). The effect of the concentration in added salt was observed for values included between 5.10^{-3} M to $3.5 \ 10^{-2}$ M.

A solution mixture with the same anion (Cl^-) was studied by associating $NaCl/CaCl_2$. The total concentration in chloride ions of the solution was fixed at 1200 mg/L. The values of the proportion $NaCl/CaCl_2$ mixture were chosen equal to 1/3, 1 and 2. The filtration of pure NaCl solution was needed in order to determine the effect of the salt addition on Cl^- permeation. The salt mixture experiments were done at 10 bar and a conversion rate of 15%. The temperature was maintained to 28°C.

2.1.2.3 Real brackish water filtration

In the last part of the laboratory scale filtration study, experiments with real water have been carried out. The investigated water was Tan Tan brackish water which has a total salinity above 4000 $mg.L^{-1}$. More details about the characteristics of this water, such as the ion concentration, pH value and temperature, will be presented in details later in chapter three. Before carrying out the desalting experiments, the permeation rate of the brackish waters for each membrane was determined. The permeate flux and salt rejection rate were determined by varying the applied feed pressure at different recovery rates. The cross flow velocity was varied from 0.05 to 0.36 $m.s^{-1}$ (Reynolds criterion: 400 <Re< 2857) to change the conversion rate. Higher feed velocity leads to a smaller recovery rate. This parameter was varied from 15% to 75%. The temperature was maintained at 28 °C in the permeation and the salt rejection tests.

2.2 Pilot scale testing

The pilot scale testing was carried out at Tan Tan Brackish water reverse osmosis plant, located in Tan Tan city (South west of Morocco).

2.2.1 Pilot unit description

The pilot unit was supplied by Veolia (Anjou Recherche). This pilot unit was designed to test a large range of membrane modules could be tested (NF and LPRO) under varying operating conditions, with conversion rates from 10% to 90%. The pilot unit is composed of three main systems:

1. One feed water tank (volume of 2.6 m^3) equipped with a mixing device (figure 22b)
2. The pilot unit and its motor and instrumentation were mounted on a skid having dimensions: L = 250 cm x W = 120 cm x H = 190 cm (figure 22a and 22c)
3. A chilling unit to feed refrigerated water for temperature-control of the feed water used a plate exchanger (not shown).

The photographs of the pilot unit are shown in the figure 22.

(a) Back of the pilote unit	(b) Feed water tank	(c) Front of the pilote unit

Figure 22: *Pictures of the pilote unit drain*

Figure 23 shows the process flow sheet of the skid-mounted unit.

The main components of the pilot unit are the following:
- A booster pump upstream of the high pressure. This pump could also be used for the flushing and chemical cleaning of the membrane module.
- A set of 5µm cartage filters to avoid the carryover of large debris into the membrane system
- A temperature regulating system for the feed water (only for chilling) which is composed of a plate exchange, a chilled water recirculation loop fitted with a three-way valve and an actuator, a chiller, two temperature transmitters for temperature control through the PLC of the pilot unit.
- A high pressure pump equipped with a variable frequency drive
- A pressure vessel housing on standard 4" membrane module
- A manual regulation valve on the concentrate line to adjust the brine backpressure, thereby to control the conversion rate of the system
- An internal concentrate recirculation loop fitted with a manual regulation valve
- An external concentrate recirculation loop fitted with a manual regulation valve.
- An external permeate recirculation loop allowing to recycle the permeate into the feed water tank (possibility to run the unit in batch mode)
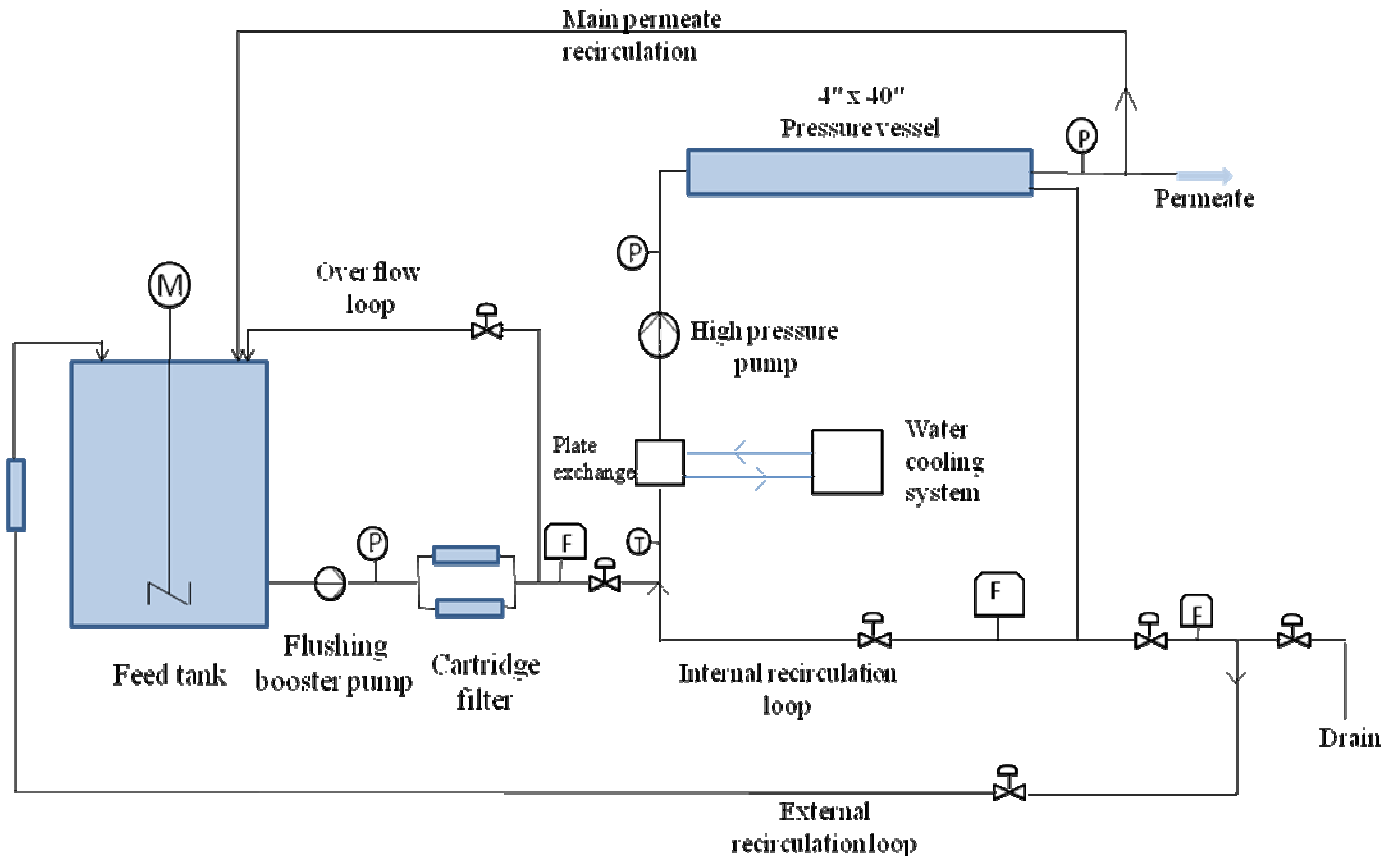
Figure 23: *Process flow sheet of the skid-mounted unit*

With the different recirculation loops, the unit could be operated under the following modes:

No recirculation
- The feed flowmeter is placed just downstream of the two feed cartridge filters
- The concentrate flowmeter is placed in the external concentrate loop
- The conversion rate is the ratio of the permeate flowrate to the flowrate through the booster pump (same flowrate as the one through the high pressure pump)
- Under this configuration, the maximal conversion rate will be about 20%

Internal recirculation
- The feed flowmeter of the system is placed downstream of the two feed cartridge filter
- The concentrate flowmeter is placed on the internal concentrate loop
- A portion of the concentrate is directly recirculated downstream of the two feed cartridge filters
- The conversion rate is the ratio of the permeate flowrate to the flowrate through the booster pump
- For higher conversion rates, the flowrate through the booster pump may be too low for safe operation (< 200 L/h). Under those conditions, the operator could either use the external recirculation mode or use the bleeding loop located downstream of the booster pump, which will allow a higher flow through the booster pump without impacting the conversion rate.

- The feed flowmeter of the system is placed upstream of the feed tank
- The concentrate flowmeter is placed on the external concentrate loop
- A portion of the concentrate is recirculated to the feed tank. The mixer then ensures a fast homogenization of the feed water and the concentrate
- The conversion rate is the ratio of the permeate flowrate to the flowrate of the feed water entering the feed water tank.

2.2.2 Filtration protocol

Preliminary experiments were carried out with Tan Tan brackish water to evaluate the desalting performances of different commercial NF and LPRO membranes. The membrane modules were tested under various operating conditions (feed flow, permeate flow and recovery rate) listed in table 13.

Before carrying out the desalting experiments, the permeation rate of Tan Tan brackish water for each membrane was determined.

Table 13: *The various operating conditions followed for each membrane*

	Conversion rate %			
	10%	45%	70%	90%
Membrane feed flow = 2 m³/h Permeate flow = 0.2 m³/h	Q feed = 2 m³/h Q reci = 0 m³/h	Q feed = 0.44 m³/h Q reci = 1.56 m³/h	Q feed = 0.28 m³/h Q reci = 1.72 m³/h	Q feed = 0.22 m³/h Q reci = 1.78 m³/h
Membrane feed flow = 1.5 m³/h Permeate flow = 0.15 m³/h	Q feed = 1.5m³/h Q reci = 0 m³/h	Q feed = 0.34 m³/h Q reci = 1.16 m³/h	Q feed = 0.22 m³/h Q reci = 1.28 m³/h	Q feed = 0.17 m³/h Q reci = 1.33 m³/h
Membrane feed flow = 1 m³/h Permeate flow = 0.1 m³/h	Q feed = 1 m³/h Q reci = 0 m³/h	Q feed = 0.22 m³/h Q reci = 0.78 m³/h	Q feed = 0.14 m³/h Q reci = 0.86 m³/h	Q feed = 0.11m³/h Q reci = 0.89 m³/h

Q feed: flowrate from the feed water tank to the booster pump
Q recirculation: flowrate on the concentration recirculation loop

The operation of the pilot unit is automated in order to ensure safe operation of the pumps (protection against dry run). The pilot was operated through a touch-screen panel and adjusting the three regulating valves located on the front side of the unit. The feed pressure was fixed by conversion rate and chosen permeate flux. The applied pressure was in the range of 4 and 20 bar.

Samples of permeate, collected every 15 min, allows us to follow the variation of permeate total salinity. When the equilibrium was reached (after 60 min), steady state rejection rate of the membranes was evaluated. The filtration experiments were repeated twice for each module and the mean values of rejection rate and applied pressures are reported in this thesis. The temperature was maintained at 21°C.

Additional experiments were conducted with Tan Tan brackish water to evaluate the impact of salinity on NF and LPRO modules performances. The brackish water was doped at 6 and 10 g.L-1 with NaCl salt.

In a second part of the study, fluoride removal experiments were conducted with Tan Tan water, to compare the defluoridation performances of NF and LPRO membranes. To realized those experiments Tan Tan water was doped at 5, 10 and 15 ppm of fluoride (NaF).
These experiments were performed at three conversion rates (10%, 45%, 70%) and with a permeate flow of 0.2 m3.h-1.

2.3 Calculating parameters

The parameters taken into count are:
The volumetric flux (Jv) was determined by measuring the volume of the permeate or the concentrate in a given time interval by the relation (17):

$$Jv = \frac{\Delta V}{\Delta t \times S}$$
(17)

Jv: Flux (L.h^{-1}.m^{-2})

ΔV: volume of the permeate in a given time interval (Δt)

S: the membrane surface area (m^2)

The hydraulic permeability with the electrolyte solution (Lp') is obtained from the slope of the plot of flux (J_v) versus the increasing trans membrane pressure (ΔP) using the equation (2) and the intercept on x-axis of the plot gives the critical pressure Pc when the transmembrane pressure is equal to the osmotic pressure.

The recovery rate calculated using the following equation

$$Y = \frac{Qp}{Qo}$$
(18)

Where Qo and Qp are the feed and the permeate flow rate respectively.

The Specic Energy Consumption is proportional to the transmembrane pressure. It is calculated by the following relation

$$E = \frac{\Delta P}{\eta.r} . \frac{100}{36}$$
(19)

with E in kWh/m^3,

 ΔP the transmembrane pressure in bar,

η the global pumpingsystem efficiency,

r the conversion rate

3. Streaming potential measurements

The charge of the investigated membranes was evaluated by means of a homemade streaming potential (SP) measurements apparatus. In this work, the measurements of SP are made by flow through the membrane pores. Fig.24 shows a photography of the cell which is used to support the membrane samples for the streaming potential measurements. The cell is a dead-end cell (Model 8050, Amicon) purchased from Millipore (France). The filtration cell with a capacity of 50 ml was used with a flat-sheet membrane (effective membrane area of 14.52

cm^2). The unit was operated at pressure differences up to 5 bar using pressurized nitrogen gas as a driving force. A pair of Ag/AgCl electrodes introduced in the SP device was used to measure the potential difference between both sides of the membrane vs. the transmembrane pressure. The electrodes were connected to a voltmeter (PHM250 from Radiometer Analytical, France) presenting a high impedance (10Mohm). The positive potential to the feed and the negative to the permeate was connected. The sign of the membrane pore walls is the slope. The SP measurements were done at room temperature of 20°C.The membrane samples were cut to fit the measurement cell and then wetted with pure water and stored in a refrigerator at 4°C for 24h.
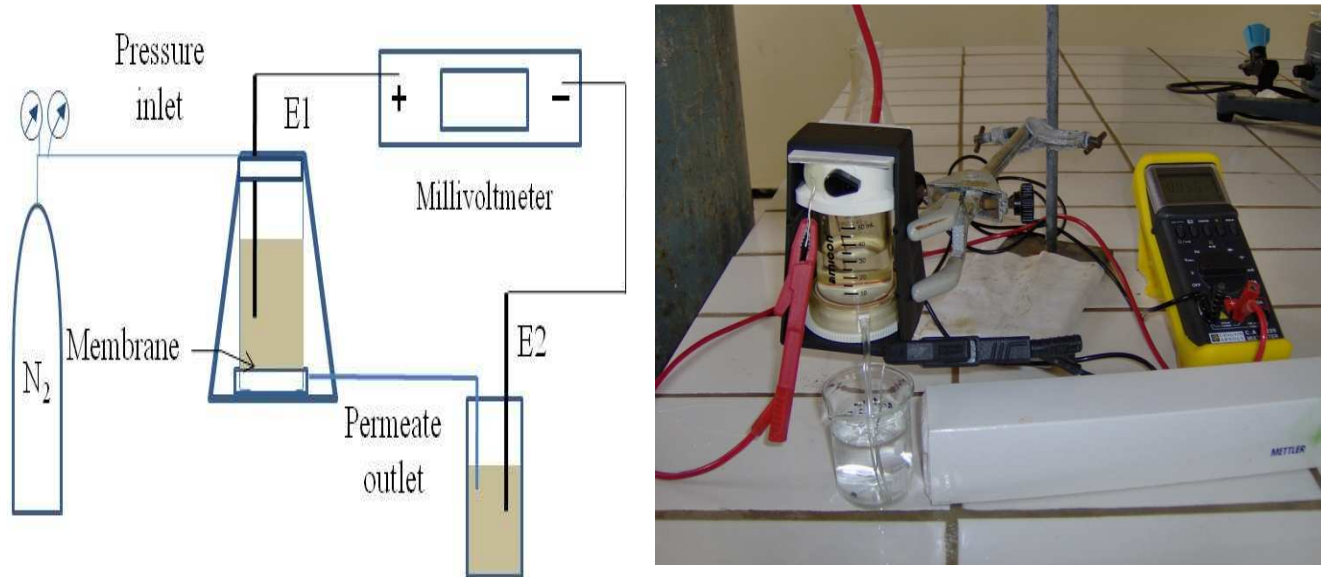
Figure 24: *Schematic representation and photography of the SP measurement device*

Streaming potential design enables characterization of the active layer of the membrane due to decrease in transmembrane pressure occurring in the microporus layer. Furthermore these experiments are planned for qualification of the pore wall charges and not its quantification.
SP was measured with electrolyte solutions of NaCl, KCl and CaCl$_2$ having concentrations in the range of 10^{-4}M to 10^{-1}M.
In order to estimate the membrane isoelectric point, IEP, streaming potential was determined as a function of pH in solutions of KCl, NaCl and CaCl$_2$. Several solutions were prepared at a concentration of 10^{-3}M. The pH was set by adding HCl (1M) or NaOH (1M) to the solutions and was varied in the range from 2 to 10.

4. Atomic force microscopy apparatus

Atomic force microscope (AFM) has been used to investigate the surface morphology of each investigated membranes. Such imaging provides in quantitatifying the surface roughness. The AFM experiments were carried out using a Nanoscope III device from VEECO (USA). Contact mode in air medium was used to characterize the investigated membranes with a scan rate of 1 Hz and 400x400 pixel resolution. The membrane samples were primarily washed and wetted with pure water and stored in a refrigerator for 24hr then dried at room temperature in

a desiccator. The membranes were then attached to steel discs with double side-scotch tape. The cantilever used for this imaging was from Veeco, with a specified spring constant between 0.44 – 0.63 N/m and a resonant frequency of 17-20 KHz.

The images were obtained over a large area of 50µmx50µm and small area of 1µmx1µm. Image analysis was carried out by means of (SPMLab602) software from VEECO licensed for GA&P. The surface analysis software associated with the explorer can give full details about features of the surface such as peak to valley ratio, average roughness and root mean square roughness. The obtained average roughness (Ra) from software which is the mean value of surface relative to the center plane is calculated by

$$Ra = \frac{1}{LxLy} \int\limits_{}^{Lx} \int\limits_{}^{Ly} [f(x,y)]dxdy \qquad (20)$$

5. *Contact angle measurements*

Contact angle has been used as an index of the wettability of the membrane active layer. Contact angles were measured by the sessile drop method, using a goniometer (KRUSS G10 USA) and a camera. Prior to measurement, membranes were stored in a container of pure water for 24 h at 4 °C. The rinsed membranes were dried in a desiccator prior to measurement. Membrane samples were cut into small pieces and mounted in a support. An approximately 2.0 µl droplet of pure water was placed on the membrane specimen and the contact angle was measured with the goniometer via the camera immediately after the drop placement. Reported values are the averages of the contact angles (right and left) of 5 droplets. During the short time of measurement, no change in contact angle was observed.

Contact angle do not give absolute values but allow a comparison between each materials. A variation of 2 degrees in the angle is needed to differentiate each kind of low roughness materials (Ra < 100 nm).

6. *Analytical methods for solutions characterization*

Following analytical methods were used to determine the solute properties in feed and permeate solutions containing: Na^+, K^+, Ca^{2+}, Mg^{2+}, Cl^-, F^-, NO_3^- and SO_4^{2-} ions.

6.1 pH

pH was measured for each sample using a pH- meter (Ecoscan Ion 6). The pH meter was calibrated with two pH buffer standard (pH 4 and 7)

6.2 Total salinity measurement

A TDS meter (ECOSCAN TDS6) was used to measure the total salinity of the feed and permeate sample. The probe is capable of measuring the conductivity of any solution from 1 mg/L to 15 mg/L.

6.3 Chloride, nitrate and fluoride ion selective electrodes

Chloride, nitrate and fluoride ion selective electrodes with a double junction reference electrode were used to measure the ions concentrations in the feed solution and the permeate. These electrodes are connected to a digital Ionometer multiparameter (pH/mV/Ion/°C meter).

The ionometer allows ion concentration measurements of various ions and the electrode potential. The characteristics of the used electrodes are shown in Table 14.

Table 14: *Characteristics of the ions selective electrodes (ISE)*

ISE	Model	Reference Electrode	Linear measurement range	Detection limit
Chloride	Elit 8261	Elit 002 (0.02N KNO_3)	10^{-5}M à 1M	10^{-5}M
Fluoride	Elit 8221	Elit 001 (0.01N AgCl)	4.10^{-6}M à 5.10^{-2}M	4.10^{-6}M
Nitrate	Elit 8021	Elit 003 (0.03N Li acetate)	$3.5.10^{-5}$M à 1M	$3.5.10^{-5}$M

The calibration of each ion electrode is performed by using a corresponding standard solution (NaCl for Cl^-, NaF for F^-, $NaNO_3$ for NO_3^-). Calibration solutions of 1000 mg/L was diluted to prepare the samples for calibrating curve. Three standard samples were prepared for concentration ranging from 0.1 mg/L to 100 mg/L, i.e 1 mg/L, 10mg/L and 100 mg/L for Cl^- and NO_3^- electrodes and 0.1 mg/L, 1mg/L and 10 mg/L for F^- electrode. The electrodes calibration was repeated in every measurement.

6.4 Sulfates dosage

The sulfate ion is precipitated in acid chloridrique containing barium chloride in such a way that it forms crystals of barium sulfate (Rodier.J, 1996). The absorbance of the suspension of barium sulfate is measured with a turbidimeter. A calibration curve between the turbidimeter reading and concentration of standard sulfates solution was prepared which will be linear over the range of concentration studied. This curve will be used to calculate the concentrations of sulfate ion in the feed and permeate samples. Seven samples of sulfate solution were prepared for concentrations ranging from 10 to 80 mg/L.

6.5 Calcium and Magnesium determination

The calcium and Magnesium in the feed and permeate samples were quantitatively analyzed using Colorimetric Method (Rodier, 1996). A spectrophotometer model DR/2010 HACH was used for colorimetric analysis.

6.6 Chemicals and brackish water samples

The salts solutions were prepared from MilliQ water (Millipore system, France). The conductivity of the water was less than 3µS/cm. High purity NaCl, KCl, Na_2SO_4, $CaCl_2$, $MgCl_2$ salts were used (purity higher than 99%). All salts were obtained from Aldrich (France). The pH adjustment was made with HCl (1M) and NaOH(1M) solutions with high grade purity.

The main characteristics of Tan Tan water obtained from the Office National de l'Eau Potable (ONEP, Morocco) are reported in Table 15. The parameters analyzed were ion concentration,

total salinity, pH value, which are typically measured for collected brackish water samples. The measured parameters will be presented in details later in Chapter three.

Table 15 : *Characteristics of Tan Tan water (ONEP)*

	Tan Tan brackish water
T(°C)	25
pH	7.9
TDS(ppm)	3300
Cl^-(ppm)	1200
NO_3^-(ppm)	20
F^-(ppm)	1.1
SO_4^{2-}(ppm)	502
Ca^{2+}(ppm)	384
Na^+(ppm)	584
HCO_3^-(ppm)	237

The Silt density index (SDI) of Tan Tan water has a value of 0.36.

6.7 Simulation softwares

The simulation softwares are design programs that estimate the performances of elements and/or membrane systems. In this study, we used three commercial simulation softwares to project the performances of reverse osmosis and nanofiltration brackish water systems. These software tools are : (i) ROSA 6 (DOW, USA) for the BW30, BW30LE and NF90 membranes, (ii) IMS Design (Hydranautics, USA) for ESPA 3 and ESNA1LF membranes, and (iii) CSMPRO3(Saehan, Korea) for the REBLF, NE70 and NE90 membranes.

The following data are needed to create a system design:

Feed water: water classification type, feed TDS or feed analysis, feed temperature and feed pH

System configuration: Number of stages, number of stages in a pass, number of pressure vessels in stage, number of elements in each vessel, element type, permeate flow, feed flow, and recovery rate.

Chapter three: Results and discussions

1. Fundamental study: Comprehensive characterization of NF and LPRO membranes

A variety of NF and RO membranes exists, each membrane having its own specific characteristics and performance towards aqueous solutions. The relationship between the membrane performance and the membrane characteristics is still not clear and to study this relationship a detailed membrane characterization is needed.

This fundamental study presents a comprehensive characterization of four NF membranes denoted NF90, NF200, NF270 and NE90 and two LPRO membranes denoted BW30 and BW30LE, by their separation performance, morphology and surface charge parameters.
First, the performances of the studied membranes in terms of water flux and salt/ion rejections were investigated. The experiment measurements were used to calculate the mass transport parameters of the membranes by the Spiegler-Kedem model. The sequences of rejection of NF and LPRO membranes were compared and discussed, taking into consideration the separation mechanisms known. Then some important characteristics of the membranes top layer (hydrophobicity, surface charge and surface roughness) were performed. The surface properties were related to the water flux and salt rejection to interpret the performance results. The second part concerned the filtration of salt mixtures and real water from Tan Tan city.

1.2 Membranes performances

1.2.1 Hydraulic permeability

Permeability of the investigated membranes with Ultra pure water (Lp) was measured under different operation pressures. The obtained water flux values of the examined membranes and their dependence on the pressure variations are presented in Fig. 25. The linear evolution of fluxes with the transmembrane pressure shows that Darcy's law is valid (Eq 15). This linear behaviour is described by a slope which corresponds to ultra pure water permeability.

The permeation experiments of NF and LPRO membranes were also performed with a NaCl solution at $6g.L^{-1}$ ($10^{-1}M$). The permeation data are plotted in Fig.26, which gives the dependence of the water flux on the applied pressure. The fluxes increase linearly with the increasing operation pressure for the salt solution as described by the Spiegler-Kedem model. The hydraulic permeability with the electrolyte solution (Lp') is obtained from the slope and the x-intercept of the plot gives the critical pressure Pc when the transmembrane pressure is equal to the osmotic pressure (Eq 2).
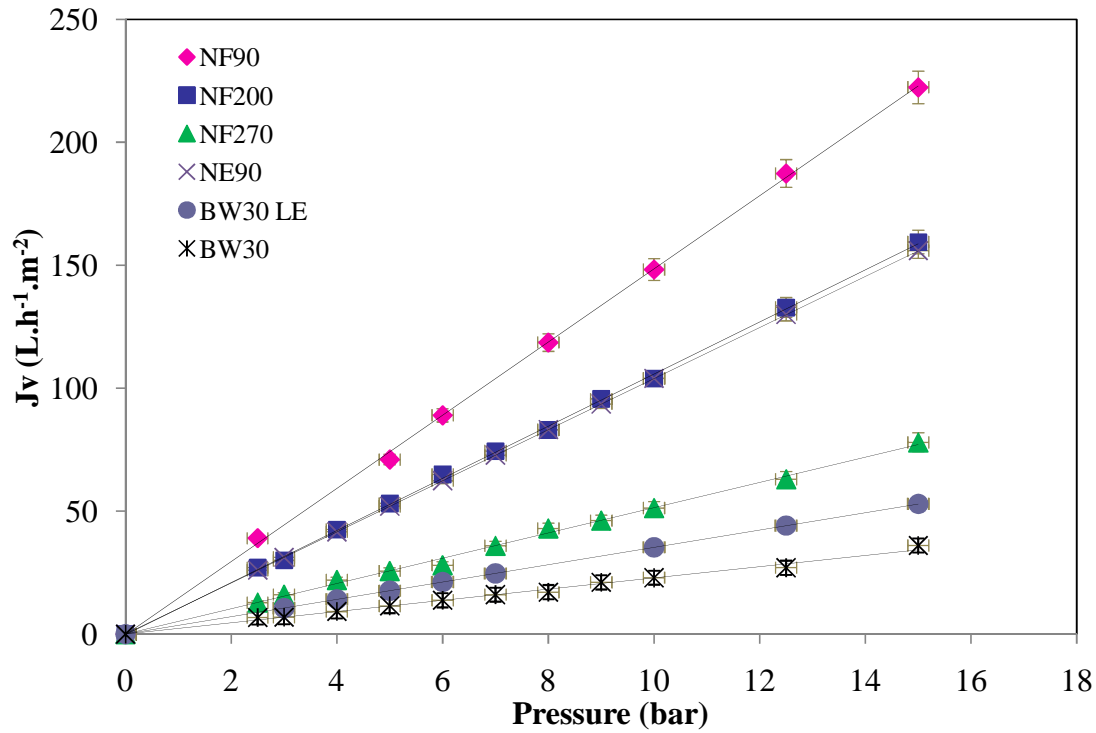
Figure 25: *pure water flux as a function of the applied pressure for the NF and LPRO membranes (T = 25°C, pH =6.4)*
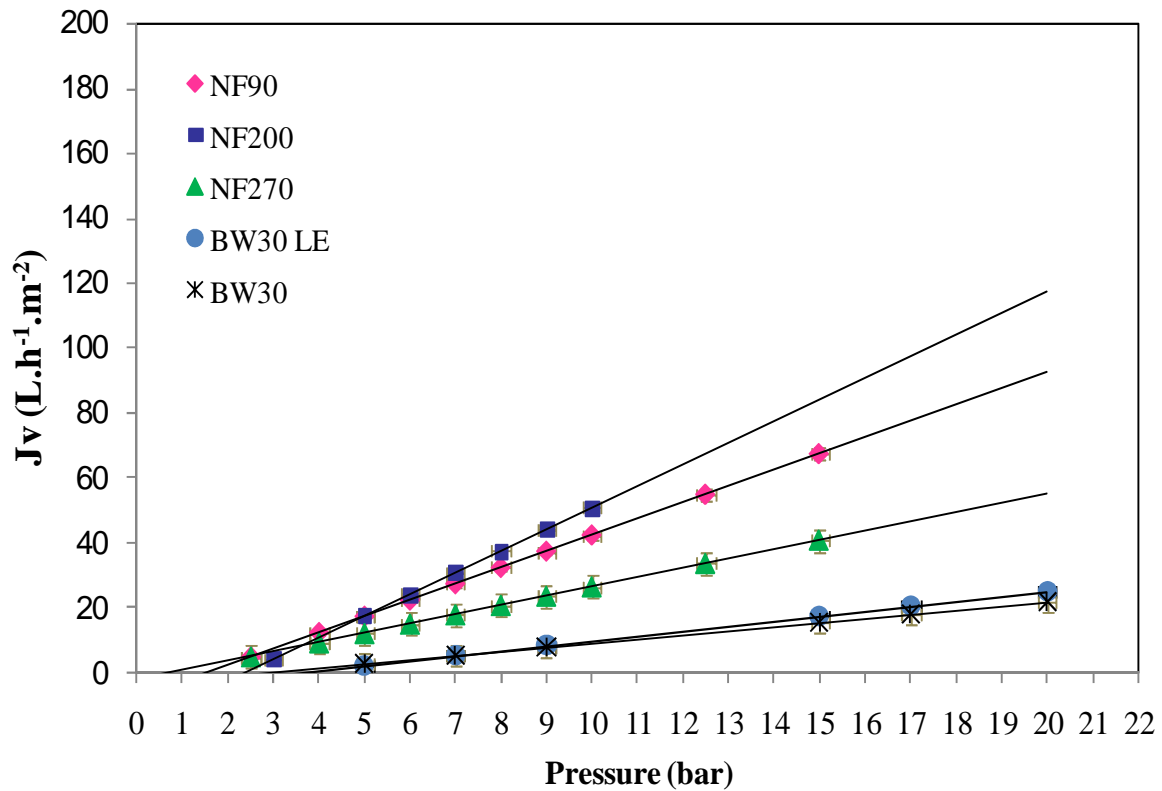
Figure 26: *Effect of operating pressure on the permeate flux of NaCl solution for NF and LPRO membranes (T = 25°C, NaCl 10^{-1}M)*

From Fig.25 and Fig.26, we can see that the lowest slope values are obtained for the examined LPRO membranes, which is expected due to narrowest pores in the skin. The steepest slope values are found for NF membranes indicating that such membranes with the widest pores are more affected by the applied pressure. This can be explained by considering transport through NF membranes as a result of two mass transfer mechanisms: convection and diffusion (Pontié *et al* 1997).

The NF90 membrane exhibits higher permeate flux values to ultra pure water compared to the other NF membranes. The NE90 and NF200 permeabilities do not differ remarkably; these membranes are more permeable than the NF270. For the LPRO membrane, the BW30LE membrane is more permeable than the BW30. The high permeability characteristic generally indicates a high porosity. The MWCO of the investigated membranes which is proportional to the pores size is given in Table 16.

Table 16: *Molecular weight cut off of the NF and LPRO membranes*

Membrane	NF270	NF200	NF90	NE90	BW30	BW30LE
MWCO (Da)	300	200	200	nd	90	nd
References	Mänttäri *et al.* 2004	Essis Tome *et al* 2004	Krieg et al 2004	nd	Darling *et al* 2007	nd

The NF270 membrane has more opened pores compared to the other NF membranes, but its permeability is abnormally lower. The NF200 and NF90 membranes have the same MWCO but their permeabilities are different. The permeability of a membrane is also related to a thickness of selective layer (Mänttäri *et al.* 2004) and surface roughness of the membrane (Hiros *et al.* 1996, Gao and chen 1998).

With the NaCl electrolyte, the LPRO membranes follow the same order of permeabilities, while this order changed for the NF membranes. The NF200 membrane was more permeable to NaCl solution than the NF90, followed by the NF270. The values of the described membrane parameters Lp, Lp' and Pc are listed in Table 17.

Table 17: *Values of pure water and saline solution (NaCl 6 g.L^{-1}) permeabilities, and critical pressures of the NF and LPRO membranes.*

Membrane	$Lp\ (\pm 0.7)$ $(L.h^{-1}.m^{-2}.bar^{-1})$	$Lp'\ (\pm 0.3)$ $(L.h^{-1}.m^{-2}.bar^{-1})$	Pc (bar) (± 0.1)
NF270	5.1	2.9	0.8
NF200	10.6	6.6	2.3
NE90	10.4	nd	nd
NF90	14.8	5.0	1.6
BW30	2.3	1.3	3.8
BW30 LE	3.5	1.5	3.8

It is observed from Table 17 that in the presence of electrolyte solution under the same operating conditions, the saline solution permeability (Lp') is lower than pure water permeability (Lp).

The presence of the electrolyte in the solution makes the membrane surface more compact due to contraction of pores, resulting in the decreasing in the permeability through the membranes (Huang *et al.* 2008). The decrease of the permeability of the LPRO membranes in presence of NaCl salt indicates that these membranes have more open pores than the usual RO membranes. This can be further confirmed using the Pc values.

Conventional theory of RO suggests that no water permeation exists at zero net driving force (Wijmans *et al.*1995). The critical pressures of the NF membranes are lower compared with the LPRO membranes. The flux through the NF membranes starts under 2.5 bars, while with LPRO the permeate flux is obtained by applying a pressure larger than 3.8. The NF membranes, having more open pores, are less dependent on osmotic pressure because of lower rejections (Pontié *et al.* 1997). The osmotic pressure has a great influence on LPRO membranes (Menjeaud *et al.* 1993). The Pc values obtained for these membranes are lower than the theoretical osmotic pressure which is equal to 4.8 bar for a solution of NaCl of 0.1 M suggesting that the LPRO are more opened than RO membranes.

1.2.2 Rejection of ionic components

The performance characteristics of Nanofiltration and LPRO membranes were evaluated using ion retention for different operating conditions and the characteristics of the investigated membranes were compared.

1.2.2.1 Effect of operation conditions on the salt retention

Experiments were carried out to obtain retention data of the NF and LPRO membranes for single salt solutions for qualitatively evaluate the factors that influence the retention.

1.2.2.1.1 Effect of operating pressure on rejection

The rejection of the investigated membranes for NaCl solution was plotted against the operating pressure as shown in Fig.27. The rejections increase with the increasing operating pressure, and some cases reach a threshold. Increasing operating pressure increases the ion rejection efficiency because the water flux increase linearly with increase of operating pressure while ion permeation is only a function of feed concentration and is independent of the operating pressure (Ahmed *et al* 2004, Li *et al.* 2008).

The NaCl rejection in LPRO membranes is almost independent of operating pressure; the rejection tends towards an asymptotic value. While in NF the salt rejection increases gradually with the applied pressure. This can be explained by considering salt transport through the membrane as a result of diffusion and convection, which are respectively due to a concentration and a pressure gradient across the membrane. At a low transmembrane pressure (TMP), diffusion contributes substantially to the salt transport resulting in a lower retention. With increasing TMP, the salt transport by diffusion becomes relatively less important, so that salt retention is higher (Schaep *et al.* 1999, Van Gestel *et al.* 2002).
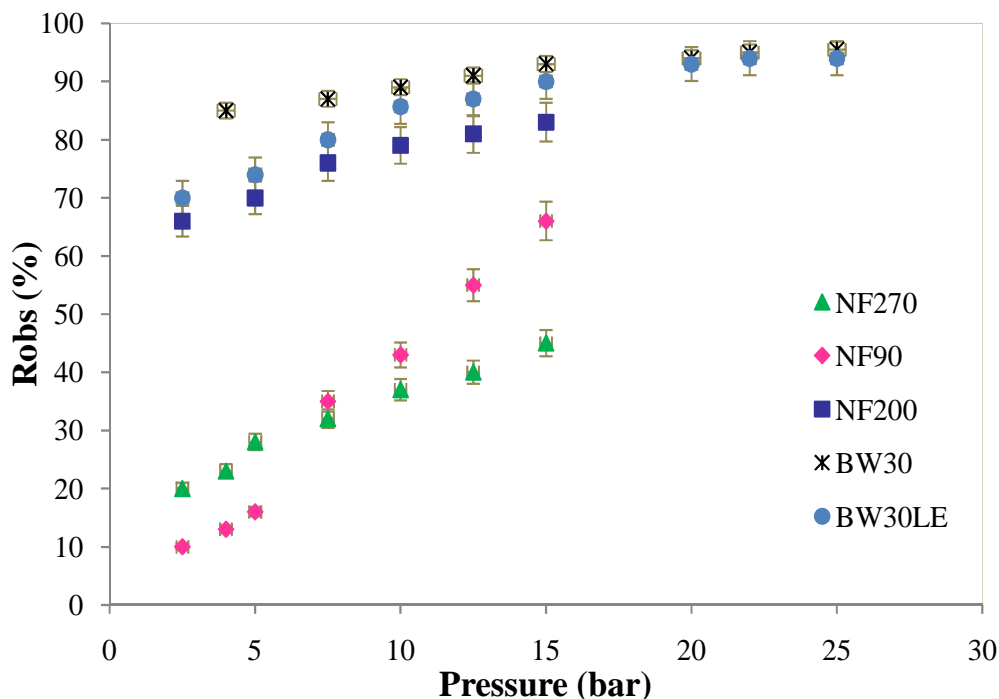
Figure 27: *NaCl retention as a function of transmembrane pressure for NF and LPRO membranes (NaCl 10^{-3}M, pH= 6.4, Y= 5%, T= 25°C).*

The LPRO membranes as expected have shown the best performance. Their rejections for NaCl are the highest and almost identical for both membranes examined. NF membranes, which have larger pores, show lower rejection of NaCl except for the NF200 which shows higher rejection of this salt. The following order was observed for the NF membranes, NF200 > NF90> NF270. This retention sequence is reversed for the NF90 and NF270 at higher pressures. This can be attributed to the inversion of the predominant mass transfer process occurring at low pressure and high pressure (Pontié *et al.* 2002).

1.2.2.1.2 Effect of electrolyte type on rejection

Retention experiments of NF and LPRO membranes were performed for tow electrolytes (NaCl and Na_2SO_4) solutions. The objective was to investigate the effect of the type of salts on the performance of the investigated membranes. The rejection of the membranes for NaCl and Na_2SO_4 solutions at the same concentration ($10^{-3}M$) are plotted against the operating pressure in Fig. 27 and 28, respectively.

Fig.27. and Fig.28 reveal that NaCl has the lowest retention while Na_2SO_4 is the most retained by the membranes. The higher rejection factors of both salts by the LPRO membranes than the NF membranes are evident. The differences of R_{NaCl} and R_{Na2SO4} data in case of LPRO membranes are small in contrast to wide differences of their values for NF membranes. Both facts point to differences in the active layer porosities of the examined NF and LPRO membranes which have been shown earlier in Table 16.
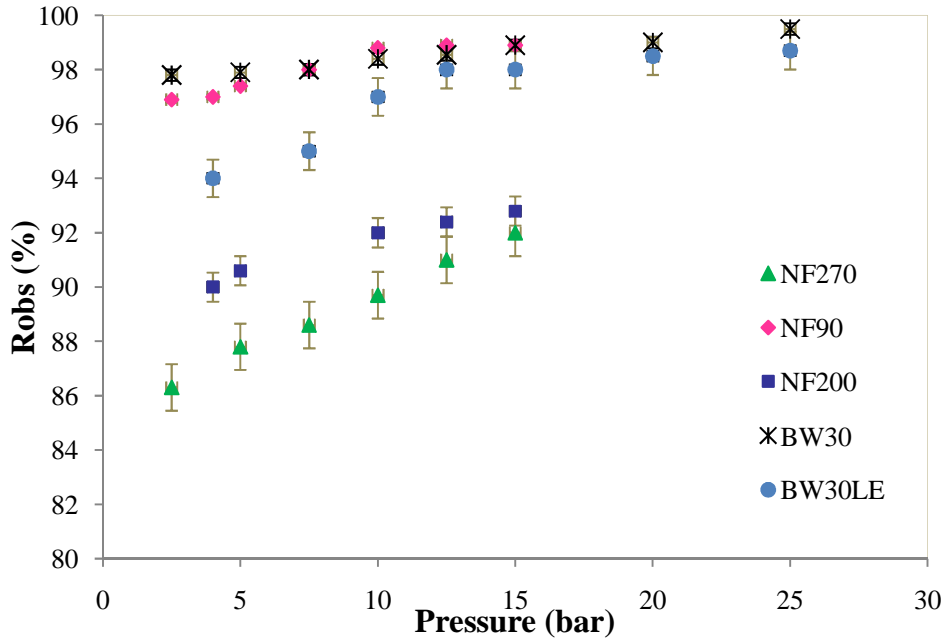
Figure 28: *Na₂SO₄ retention as a function of transmembrane pressure for NF and LPRO membranes (Na₂SO₄ 10⁻³M, pH= 6.4, Y= 5%, T= 25°C).*

For LPRO membranes which have small pores, the retention of the salts depends on the salt diffusion coefficient in water (or molecular dimensions of hydrated ions) (Boussu *et al.* 2006). The dimensions of the hydrated ions show that Cl^- is smaller than SO_4^{2-} (Table 9). Based on these dimensions the low retention of NaCl and the high retention of Na_2SO_4, especially for the BW30LE membrane, can be explained.

The MWCO of all the NF membranes due to evidently for wider pores that are responsible for the lower sodium chloride retention. Thus, the size exclusion mechanism is not prevailing in the sodium chloride retention values. Indeed, the separation properties of the NF membranes are determined by the co-effect of the sieving effect from the surface nano-sized pores and the Donnan exclusion caused by the surface charge of NF membrane (Peterson *et al.* 1993, Dong *et al.* 2007). The high retention values of sodium sulfate, and the wider gap between R_{NaCl} and R_{Na2SO4} values observed with the NF membranes are the consequence of additional charge exclusion resulted from the repelling action of the NF membrane's negative charge on the divalent anion (Kosutic *et al.* 2006).

The NF200 membrane exhibited an excellent retention of both sulphate (95%) and chloride (80%) ions. This membrane is reticulated with sulfonated functional groups which make the membrane surface negatively charged. Thus the salt rejection is mainly determined by charge effect.

For the NF 90, the NaCl retention is moderate (60%), while the retention for the other salt is close to 100%. This result could not be ascribed to charge effects alone because the pores of the NF90 are too small to see only the charge effect. This NF membrane has rather small MWCO, close to the reverse osmosis side of the nanofiltration region. For such membranes the retention of the salts depends on the salt diffusion coefficient in water (or molecular dimensions of hydrated ions).

The NF270 gives a relatively low value of rejection of NaCl ($< 50\%$) and the retention of Na_2SO_4 is fairly high (90%). This membrane has larger pores (MWCO = 300 Da), thus transport by diffusion can be neglected.

1.4.1.3 Effect of feed concentration on rejection

To investigate this effect, the NaCl and Na_2SO_4 concentration was varied from $10^{-3}M$ to $10^{-1}M$. The results of the membranes rejection at two concentrations $10^{-3}M$ and $10^{-1}M$ are listed in table 18.

Table 18: *Retention of NaCl and Na_2SO_4 salts at two pressures and two concentrations for the NF and LPRO membranes*

		Robs (%)			
	Concentration (mol.L^{-1})	0.001		0.1	
		P=5 bar	P=15 bar	P=5 bar	P=15 bar
NaCl	*NF270*	34	49	11	20
	NF90	15	62	5	50
	NF200	70	83	29	53
	BW30	84	94	nd *	93
	BW30LE	74	90	nd	85
		P = 7 bar	P=15 bar	P=7 bar	P=15 bar
Na_2SO_4	*NF270*	87	93	35	60
	NF90	98	99	96	98
	NF200	92	95	60	82
	BW30	98	99	nd	98
	BW30LE	98	99	nd	97

(*) the rejection at this pressure value was not possible to be measured for LPRO membranes as the flux was extremely low

Fig.29. and Fig.30. present the rejection of NaCl solution at different concentrations as a function of the operating pressure for the LPRO and NF membranes respectively. As observed in these figures, the salt concentration increase leads to the rejection decrease. The retention of LPRO membranes for NaCl and Na_2SO_4 electrolytes is almost independent of ionic concentration. The NF membranes retentions were more dependent on the electrolyte concentration of the feed solution than LPRO membranes. In this case higher rejection at lower feed concentration and lower rejection at higher feed concentration was observed, characteristic of charged membranes (Peters et al. 1998). Increasing the concentration of sodium cations of the solution involves the formation of a screen which gradually neutralises the negative charge of the membrane. As the total charge of the membrane decreases, the retention of the anions decreases since the electrostatic effect of the membrane becomes weaker (Childress *et al*. 2000). This means that the effect of membrane charge is completely eliminated when the salt concentration is high enough (Scheap and Vandecasteele, 2001). When charge effects play no role, it can be assumed that ion diffusion is no more hindered and no steric hindrance is taken into count.
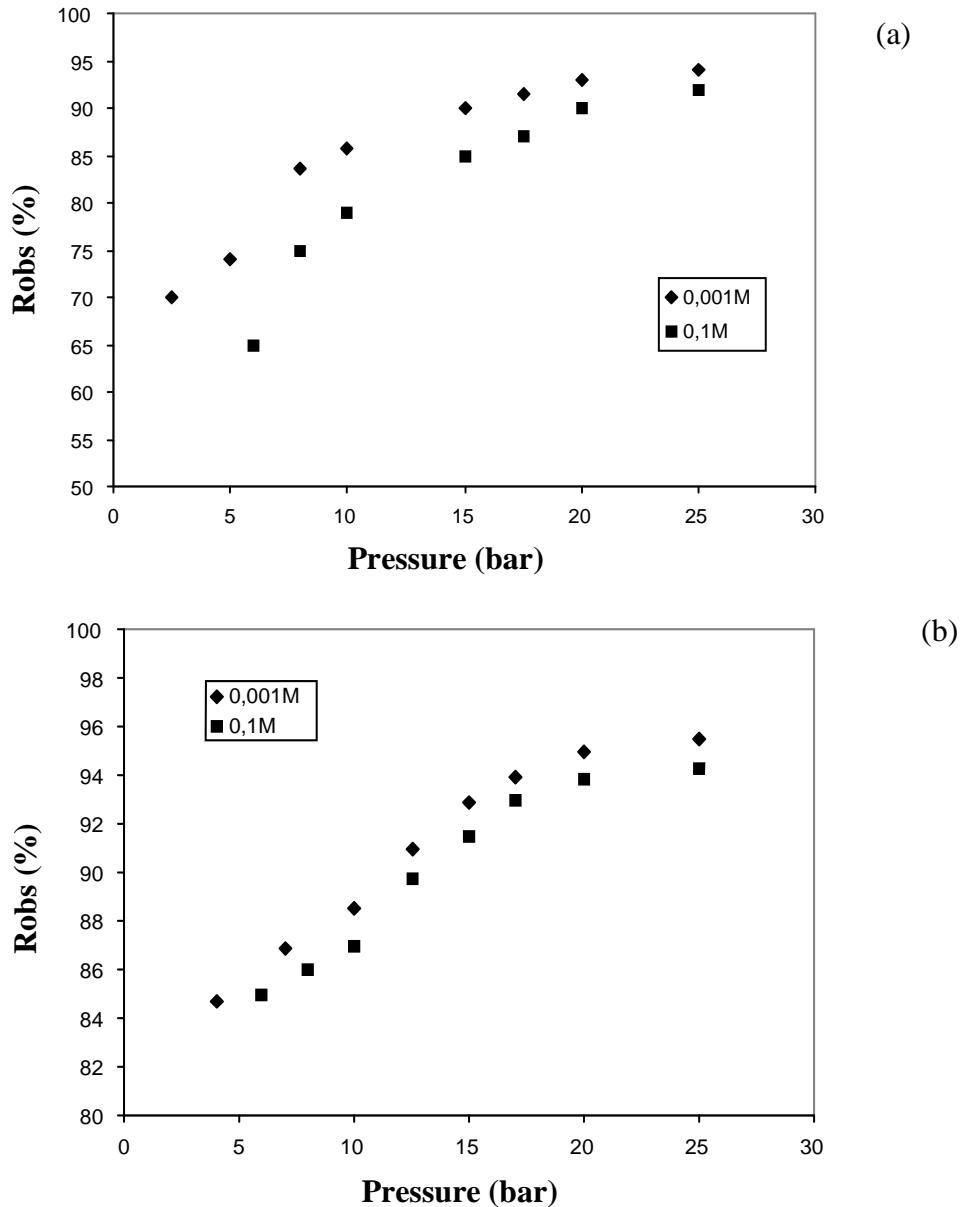
Figure 29: *NaCl retention versus transmembrane pressure for (a) BW30LE and (b) BW30 membranes at two concentrations of $10^{-3}M$ and $10^{-1}M$ (Y= 5%, T= 25°C)*

For the NF90 membrane, generally similar retentions for SO_4^{2-} ion at 10^{-3} and 10^{-1} M was observed. Because NF90 is characterized by very small pores, the effect of increasing concentration on the retention of Na_2SO_4 is very small (Boussu *et al.* 2006). On the other hand, Table 18 shows that the NaCl retention by the NF90 decreases slightly (10%) when the salt concentration increases. This can be explained by considering the thickness of the double layer formed in the pores of the top layer when the membrane is contacted with a salt solution. With increasing salt concentration the thickness of the double layer decreases, resulting in a lower retention (Huisman *et al.* 1998, Van Gestel *et al.* 2002, Li *et al.* 2008).

In the case of the NF200, when the solution concentration increases the charge effects play no role anymore. The moderate retention of NaCl (50%) and relatively high retention of Na_2SO_4 cannot be explained by Donnan exclusion. Most probably size effects play a role for salt separation with this membrane as well (MWCO = 200 Da).
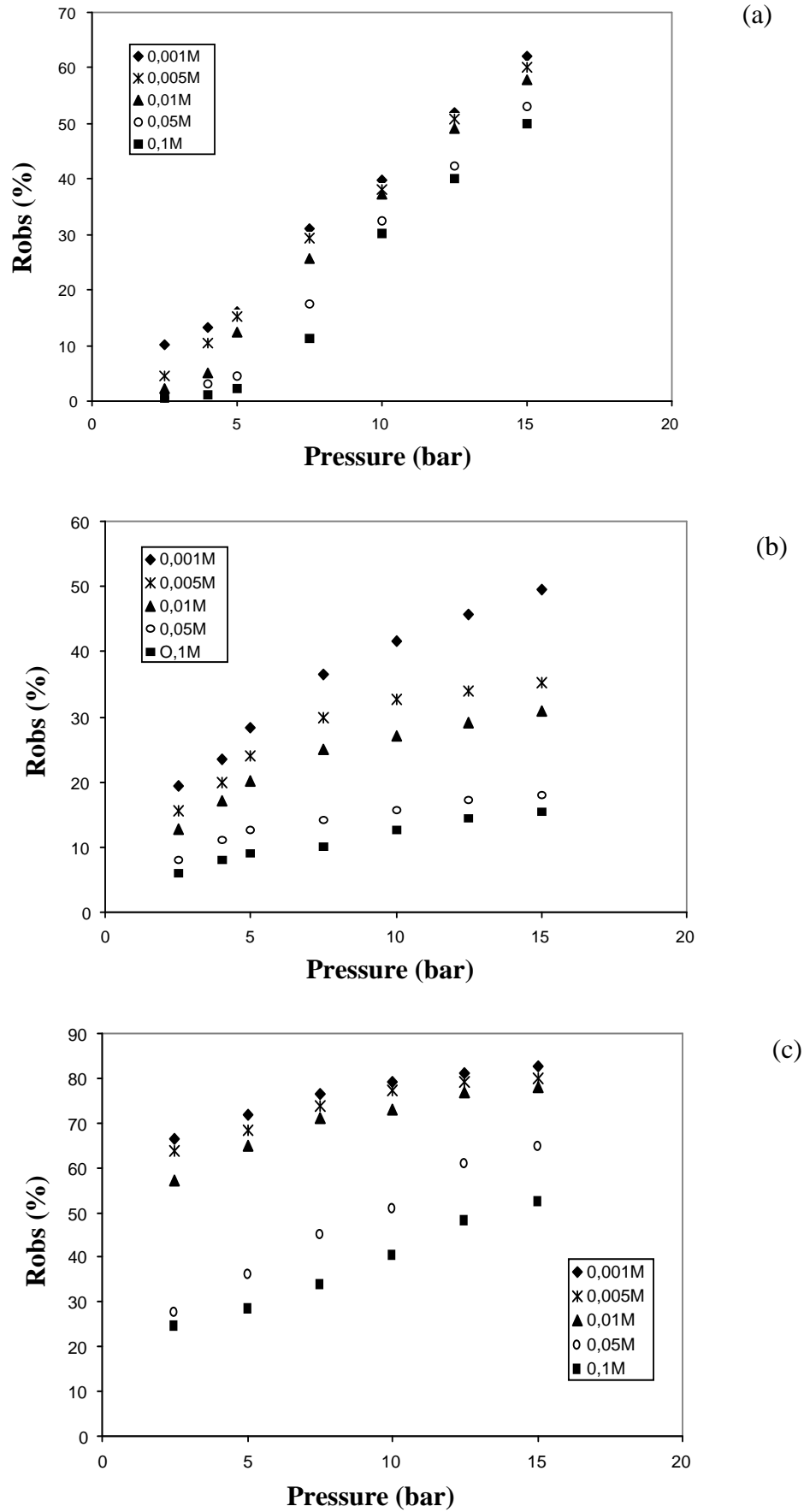
Figure 30: *NaCl retention versus transmembrane pressure for (a) NF90, (b) NF270 and (c) NF200 membranes at different concentrations from $10^{-3}M$ to $10^{-1}M$ (pH= 6.4, Y= 5%, T= 25°C)*

For the NF270 which has the largest pores, the decrease in salt retention, with increasing concentration, is most pronounced when treating a sodium chloride solution. At higher concentrations the smaller ion size of Cl⁻ levels the size effect out, resulting in a considerable decreasing of NaCl retention. The NF270 has the lowest retention of NaCl and Na_2SO_4 compared to the NF90 and NF200. This was also observed in previous publications (Mänttäri *et al*. 2006, Boussu *et al*. 2006).

1.2.2.2 Ion retention in salt mixture

The influence of the sulphate and calcium ions on the level of chloride rejection was investigated here for the NF membranes NF90 and NF200 which gives the best performances in single salt solutions. These experiments were carried out at pressure of 10 bar and a conversion rate of 15%. The chloride concentration was fixed at 1200 ppm.

1.2.2.2.1 NaCl/ Na_2SO_4 mixture

In Fig.31, the rejection of chloride anion for the NaCl/Na_2SO_4 mixture is presented for the NF90 and NF200 membranes. As can be seen from this Figure, an increase of SO_4^{2-} concentration generally decreased Cl⁻ rejection. The retention of chloride anion is lower for the salt mixtures than for the single salt experiment. It seems that the presence of the high valence anion (SO_4^{2-}) drives more chloride into the membrane, thus decreasing its retention (Krieg *et al.* 2004). This is further confirmed by the reasonable high chloride rejection at low sulphate concentrations (85% for the NF90 and 45% for the NF200) compared to the chloride rejection at high sulfate concentrations (75% for the NF90 and 35% for the NF200).
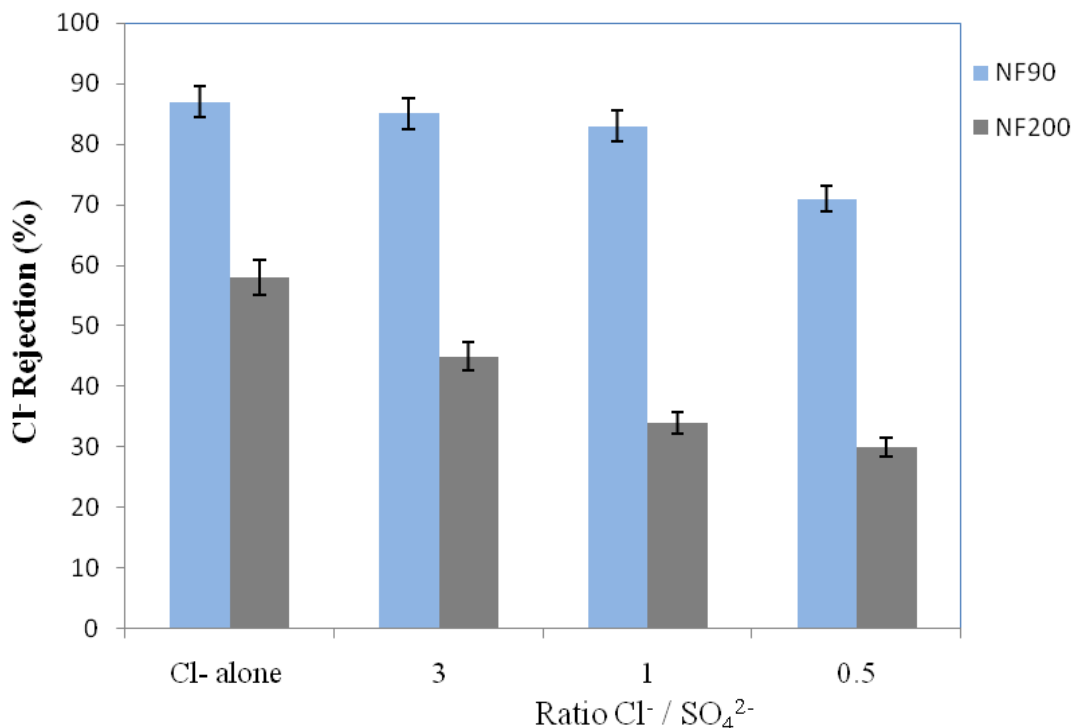
Figure 31: *Cl⁻ rejection of NaCl/Na_2SO_4 mixture*
(Pressure = 10 bar, Y = 15%, Cl⁻ concentration = 1200 ppm, T = 28°C)

The effect of SO_4^{2-} addition on Cl^- rejection varied significantly between the tested NF membranes; The NF200 showed the strongest retention decline of Cl^- while the selectivity for the NF90 did not change much with concentration and it was less impressive than for the other membrane (Rautenbach and Gröschl. 1990). For the more negatively charged membrane due to charge effects, the retention is expected to be highest for sulphate ions. Then chloride must be the lowest retained ion in order to satisfy the electroneutrality requirements. For the NF90 membrane this could further confirm that this membrane is rather tight (Tanninen *et al.* 2006).

1.2.2.2.2 NaCl/ CaCl₂ mixture

In Fig.32, the rejection of Chloride anion for the NaCl/CaCl₂ mixture is presented for the NF90 and NF200 membranes. We can see from this Figure, that the increase of Ca^{2+} concentration generally increased Cl^- rejection.
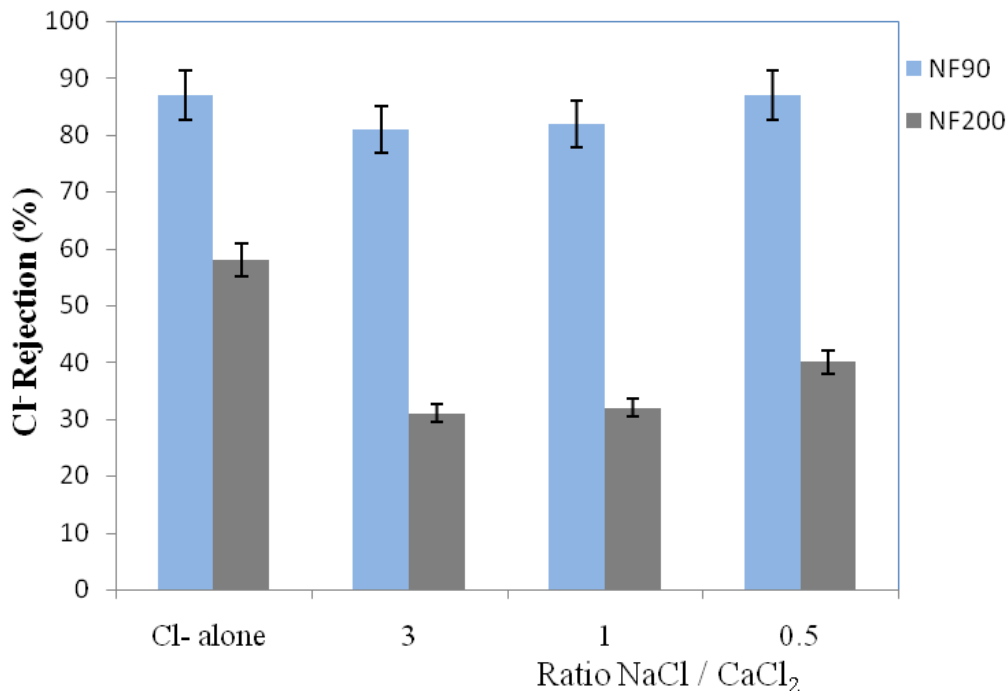
Figure 32: *Cl⁻ rejection of NaCl/CaCl₂ mixture*
(Pressure = 10 bar, Y = 15%, Cl⁻ concentration = 1200 ppm, T = 28°C)

In the case of a NaCl/CaCl₂ mixture, Chloride retention is higher when this ion originates in larger proportion from the CaCl₂ salt. The screen phenomenon of the membrane by the Na^+ ions allows to explain part of the decline of Cl^- retention when the quantity of Na^+ increases in the solution (when the ratio NaCl/CaCl₂ was 3). On the other hand, the Ca^{2+} ions transfer is more difficult than that of the Na^+ because of their different hydration energy and the size of the divalent cation. It is then the monovalent cation transfer that is privileged; their retention is thus weaker in the binary mixture and consequently that of Cl^- too (electroneutrality condition). The Ca^{2+} ions are more retained by the membrane than the Na^+ ions because of their strong energy of hydration. In a logical way, in binary mixture, Chloride ions retention is higher when the quantity of divalent cations is dominating (Paugam *et al.* 2003).

Furthermore, when the proportion of Na$^+$ ions increases in the solution, the screening phenomenon of the membrane also grows; the repulsion effect between the membrane and the Cl$^-$ is therefore decreased and the transfer of the latter in the permeate is then made easier.

1.3 Modelling the retention of single salt solutions

In this study, the filtration experiments carried out for the investigated membranes will be analysed by transport model inspired by the phenomenological approach proposed by Kedem and Katchalsky (KK) and completed by Spiegler (S). Information will be provided about phenomenological transport parameters, and a hydrodynamical approach will help us to quantify separately both parts of mass transfer occurring, the pure convection or and the pure diffusion for three membranes, and to calculate the membranes MWCO.

1.3.1 Determination of the phenomenological parameters Ps and σ

The experimental data of rejection and flux for all investigated membranes and salts were fitted using the Spiegler-Kedem model to determine the Salt permeability Ps and reflection coefficient σ parameters. A good fit was obtained for the rejection values of NF270 membrane for NaCl and Na$_2$SO$_4$ solutions studied. This is shown in Fig.33, which compares experimental results with magnitudes calculated using the best fit values of Ps and σ obtained by regression of data according to (Eq 6). Experimental data used are marked as solid symbols, where as dash lines represent the Spiegler-Kedem model.
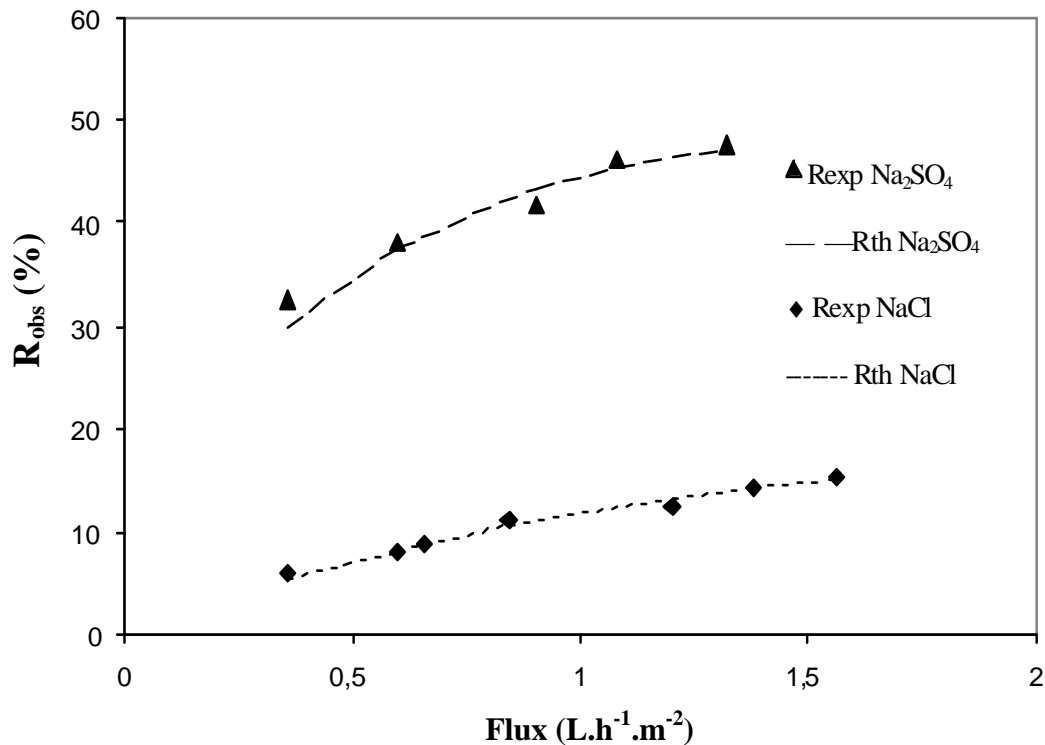
Figure 33: *Experimental evolution of NaCl and Na₂SO₄ rejection with permeation flux for NF270 membrane. the curves were fitted by the Spiegler-Kedem model*

This method was also used for the NF200, NF90, BW30 and BW30LE membranes. The experimental rejection evolution with permeation flux is well-fitted by the model for all the membranes. However, in the case of monovalent salt NaCl, the fit was not good for the NF90 membrane; an unrealistic result was obtained ($\sigma > 1$). A summary of the transport parameters thus determined for the membranes under study at two salinity levels of NaCl and Na_2SO_4 are presented in Table 19.

Table 19: *Summary of the membrane transport parameters determined for various membrane/salt systems*

		NF270		NF90		NF200		BW30		BW30 LE	
	Concentration (mol.L^{-1})	10^{-3}	10^{-1}	10^{-3}	10^{-1}	10^{-3}	10^{-1}	10^{-3}	10^{-1}	10^{-3}	10^{-1}
NaCl	σ ($\pm$ 0.02)	0.43	0.26	nd	nd	0.87	0.62	0.98	0.99	0,98	0,98
	Ps (L.h^{-1}) ($\pm$ 0.01)	1.01	1.32	nd	nd	0.24	1.73	0.11	0.13	0.123	0.103
Na$_2$SO$_4$	σ ($\pm$ 0.02)	0.96	0.51	0.98	0.98	0.94	0.75	0.99	0.99	0.99	0.99
	Ps(L.h^{-1}) ($\pm$ 0.01)	0.04	0.34	0.06	0.03	0.03	0.22	0.00	0.01	0.03	0.07

It is clear that the values of Ps and σ are dependent on the concentration of each studied salt and the type of the membrane. Ps increases with salt concentration due to high amount of salt passing through the membrane while σ decreases due to the reduction of salt rejection (Perry and Linder 1989, Hilal *et al* 2004). Table 19 shows that values of σ are always close to one for both LPRO membranes which means that these membranes give a complete rejection of both salts. Consequently the transport of salts through these membranes and then Ps values are lower. For NF membranes, the values of σ are high for Na_2SO_4 salt at low concentration. At high concentration, the σ value remains constant for the NF90, while it decreases due to the reduction of salt rejection for the NF200 and NF270 membranes. The Ps values of these membranes also increase with salt concentration. The salt permeability of the NF200 membrane with the strong negative charge is more influenced by the high feed salinity than the NF270 with the weaker negative charge.

On the other hand, the NF membranes have lower values of σ for NaCl salt than Na_2SO_4 due to the lower rejection values of the monovalent salt. The NF270 which has a low rejection of NaCl presents the lower reflection coefficient value and the higher salt permeability.

1.3.2 Hydrodynamical approach

The experimental data of rejection and flux for the investigated membranes can be represented in another approch to quantify the transfer parameters: J_{diff}, the solute flux and C_{conv}, the solute concentration due to convection. In the proposed approach the salt concentration in the permeate as a function of the reverse of permeate flow is studied, as shown in Fig 34. The plot of Cp vs. Jv is linear in conforming the relation in Eq (8) except for the NF200 membrane which shows a low correlation coefficient (R^2= 0.85) of the Cp = f(1/Jv) curve. This can be explained by the limitation of the approach considered which

assume that the membranes are not charged. The intercept on Y-axis of the plot gives the C_{conv} value and slope J_{diff}. All the C_{conv} and J_{diff} values obtained for the investigated membranes are reported in Table 20 for two salts at two concentrations.
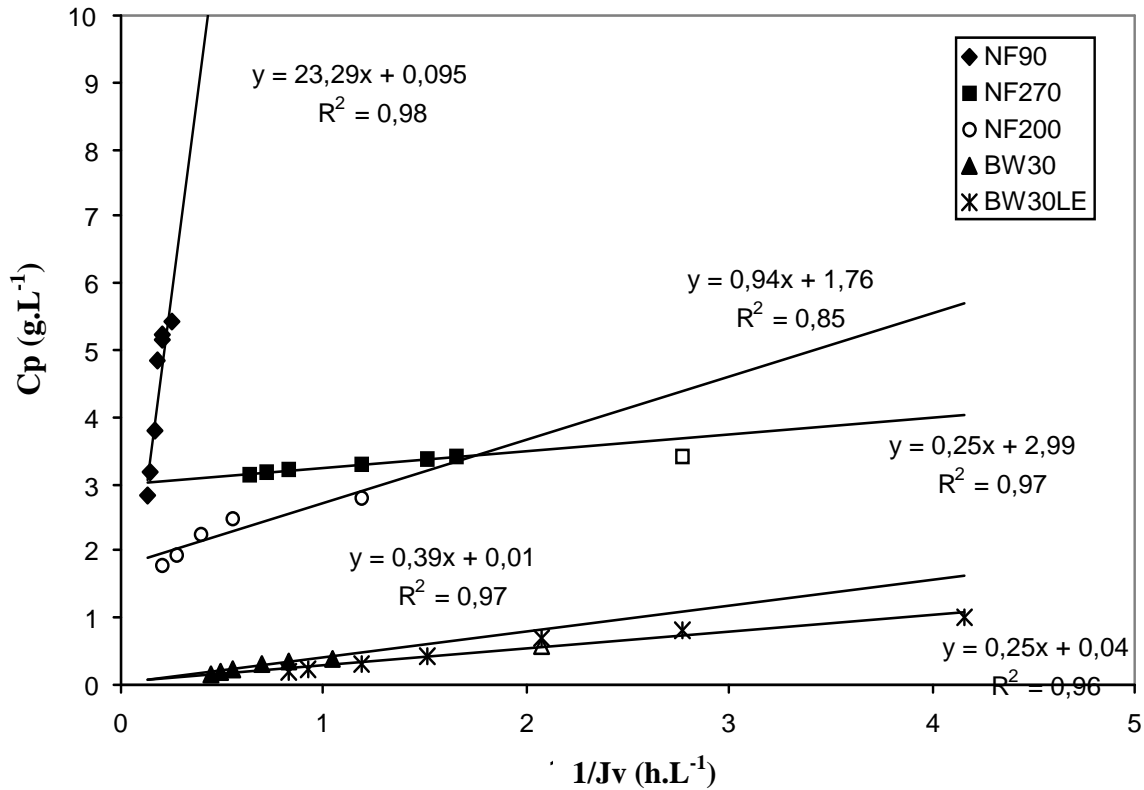
Figure 34: *Permeate concentration evolution as a function of the ratio 1/Jv for NF and LPRO membranes (NaCl 10^{-1}M, pH= 6.4, Y= 5%, T= 25°C).*

The C_{conv} values obtained for the LPRO membranes are close to zero. This can be explained by considering salt transport through these membranes as a result of diffusion. In NF both modes of transfer can be observed: diffusion and convection. From the C_{conv} values of NF membranes it can be concluded that the NF200 and NF270 are more convective compared to the NF90 membranes for both salts studied. The C_{conv} value of the NF90 membrane can be neglected. The slopes obtained for the NF90 confirm that this membrane has high diffusionnal transport than the other NF membranes. It was also observed that the values of slope obtained with sodium sulfate salt are lower than for chloride salt and in reverse to the size order for both Sulfate and Chloride anions and the difference in hydration energy.

In NF both modes of transfer can be observed, the extent of which depends on operating conditions (ionic strength, electrolyte type, transmembrane pressure) and also on the membrane material (Diawara *et al* 2003, Lebrun *et al.* 1999, Szaniawska *et al.* 1995).

The mass transfer properties of the NF90 membrane are very similar to RO membranes. This can explain the high rejection values obtained for the divalent salt. A recent study demonstrated the potential of diffusional NF membranes to selectively separate the following single monovalent salts: NaF, NaCl, NaI, LiF and LiCl. The authors have observed that a

selective defluorination can be effected with tight NF membranes, which have a diffusional mass transfer (Diawara *et al* 2003, Pontié *et al* 2008). Then we can hypothesize that the NF90 membrane will be a good candidate for the treatment of high fluorinated brackish waters.

***Table 20*:** *Cconv and Jdiff values Summary of the membrane transport parameters determined for various membrane/salt systems*

	Concentration (mol.L^{-1})	Cconv (g.L^{-1})	Jdiff (mol.m^{-2}.s^{-1}) 10^{-3}	Cconv (g.L^{-1})	Jdiff (mol.m^{-2}.s^{-1}) 10^{-1}
	NF270	0.0380	$2.5.10^{-6}$ ($\pm 9.10^{-7}$)	2.91	$2.5.10^{-5}$ ($\pm 0.5.10^{-5}$)
NaCl	NF90	0.0008	$0.86.10^{-4}$ ($\pm 8.10^{-6}$)	0.09	$2.3.10^{-3}$ ($\pm 3.10^{-4}$)
	NF200	0.0123	$0.75.10^{-6}$ ($\pm 0,3.10^{-6}$)	1.76	$0.95.10^{-4}$ ($\pm 0.2.10^{-4}$)
	BW30	0.0009	$0.9.10^{-6}$ ($\pm 0.2.10^{-6}$)	0.01	$3.5.10^{-5}$ ($\pm 1.10^{-5}$)
	BW30LE	0.0063	$0.63.10^{-6}$ ($\pm 0.1.10^{-6}$)	0.04	$2.5.10^{-5}$ ($\pm 0.1.10^{-5}$)
	NF270	0.0084	$3.7.10^{-7}$ ($\pm 0.6.10^{-7}$)	4.15	$4.2.10^{-5}$ ($\pm 0.9.10^{-5}$)
	NF90	0.0024	$7.4.10^{-7}$ ($\pm 0.5.10^{-7}$)	0.03	$6.2.10^{-6}$ ($\pm 0.9.10^{-6}$)
Na$_2$SO$_4$	NF200	0.016	$3.8.10^{-7}$ ($\pm 0.2.10^{-7}$)	2.38	$4,7.10^{-5}$ ($\pm 0.8.10^{-5}$)
	BW30	0.0016	$1.0.10^{-7}$ ($\pm 0.1.10^{-7}$)	0.01	$3.7.10^{-6}$ ($\pm 0.7.10^{-6}$)
	BW30LE	0.001	$4.1.10^{-7}$ ($\pm 0.2.10^{-7}$)	0.06	$2,8.10^{-6}$ ($\pm 0,5.10^{-6}$)

The peclet number was calculated from the Cconv and Jdiff values to compare better the contribution of the convection and diffusion on the mass transfer in the membranes studied. The calculated values are given in Table 21.

The Pe values shows that Pe >1 was found for the NF membranes NF200 and NF270. The convective mass transfer is dominant for these membranes. The Pe < 1 found for the LPRO membranes confim that diffusional mass transfer is dominant for these membranes. The mass transfer through the NF90 which is a tight membrane is due to mainly diffusion (Pe < 1).

Table 21: *Values of peclet number for the NF and LPRO membranes for two electrolytes at two concentrations (ΔP = 16 bar)*

		Pe	
	Concentration (mol/L^{-1})	0.001	0,1
NaCl	NF270	3.34	19.42
	NF90	0.01	0.028
	NF200	10	9.42
	BW30	0.24	0.036
	BW30LE	0.67	0.13
Na$_2$SO$_4$	NF270	2.7	5.26
	NF90	1	0.67
	NF200	10	5
	BW30	0.66	0.11
	BW30LE	0.126	0.53

1.3.3 MWCO membrane determination from Cconv data

From the *C*conv values obtained before and reported in the Table 20, it is possible to calculate the molecular weight cut-off (MWCO) of the NF membranes studied, from the Eq. (12), as reported recently (Lhassani *et al.* 2000).The results of the MWCO calculated are reported in Table 22.

The results obtained show that the best conditions to determine the MWCO is under diluted solution (10^{-3} M) using a divalent salt such as Na$_2$SO$_4$. As observed for Na$_2$SO$_4$ rejections, it is not possible to determine a better value of MWCO at high electrolyte concentration. In the case of the NF270 we observed a rejection of 60% for Na$_2$SO$_4$ of 0.1 M. This low level of rejection is not usable to determine the MWCO because the definition of the MWCO determination is based on rejections higher than 90%. In case of NF200 membrane, the MWCO values calculated are considerably higher than those obtained using the usual method from calibrated neutral molecules. This can be explained by considering the strongly negative charge of this membrane. And the main limitation of this method is that the charge of the membrane is not taken into account.

Table 22: *Molecular weight cut-off determined from the Eq. (12) from Cconv results obtained*

Concentration Na$_2$SO$_4$ (mol.L^{-1})	MWCO calculated (Da)		MWCO*
	10^{-3} (±20)	10^{-1} (±15)	
NF270	308	2000	300
NF90	213	190	200
NF200	401	807	200

(*) Determined from the rejections of neutral calibrated compounds (See Table 16)

This method is in good adequation with the order obtained using the usual method from calibrated neutral molecules. This is a very simple method suitable for determination of the MWCO of microporous membranes.

1.3.4 Determination of Cint and polarization factor Φ

From both previously developed approaches (phenomenological and hydrodynamical) it was observed that it is possible to link J_{diff} the solute flux due to diffusion with the concentration of the solute on the surface of the membrane C_m ($J_{diff} = Ps\ \Delta Cs = Ps\ (C_m - C_p)$) and C_{conv} the solute concentration due to convection with the membrane internal concentration of the solute C_{int} ($C_{conv} = (1 - \sigma)C_{int}$). Then C_m and C_{int} was determined from C_{conv}, J_{diff}, σ and P_s. The values of C_{int} calculated for the NF and LPRO membranes are reported in Table 23.

Table 23: *Values of C_{int} ($g\ L^{-1}$) for NF and LPRO membranes and two sodium salts at two concentrations.*

		C_{int} ($g\ L^{-1}$)	
Feed concentration ($mol.L^{-1}$)		10^{-3}	10^{-1}
	NF270	0.0011	0.0675
	NF90	nd	nd
NaCl	NF200	0.0011	0.0794
	BW30	0.0008	0.0170
	BW30LE	0.0005	0.0342
	NF270	0.0015	0.060
	NF90	0.0008	0.010
Na_2SO_4	NF200	0.0018	0.067
	BW30	0.0012	0.007
	BW30LE	0.0007	0.012

The lower C_{int} values calculated for the LPRO membranes are due to the lower penetration of salts inside these dense RO membranes. The same behaviour is observed for the NF90 membrane which has a reverse osmosis behavior as observed before. For the NF270 the C_{conv} is high and thus the penetration of salts (monovalents and divalents) inside the membrane will be better due to convective behaviour.

The polarization factor which is defined as ($\Phi = C_m/C_0$) is calculated using Cm values and they are tabulated in Table 24.

Table 24: *Polarization factor (Φ) values determined for 3 membranes and 2 salts under various operating conditions*

Concentration (mol.L^{-1})		Φ 10^{-3}	Φ 10^{-1}
NaCl	NF270	0.98	0.96
	NF90	nd	nd
	NF200	0.64	0.62
	BW30	1.11	0.99
	BW30LE	0.89	0.80
Na$_2$SO$_4$	NF270	1.3	0.83
	NF90	0.99	0.41
	NF200	1.65	0.62
	BW30	nd	0.70
	BW30LE	1.68	0.62

Calculated polarization factor values are around 1 which is due to high flow rate and the low conversion (5%) that was used in the experiments. The highest values of polarization factor were obtained for the LPRO membranes due to their high rejection factor. We have also observed that the NF270 membrane has higher *Φ* values compared to the NF90 and NF200 membranes. This is due to higher C_{int} values observed before, especially under diluted conditions.

1.4 Membranes surface characterizations

1.4.1 Roughness measurements

AFM experiments were performed to obtain a topographic image and to calculate the roughness of the investigated membranes. The roughness values for two areas scanned for all the membranes are summarized in Table 25.
Fig.35 shows 3D AFM images of NF270, NF200, NF90 and BW30 membranes taken for an area of 1 µm x1µm. The vertical profile of the membrane surface is depicted with colour intensity. The light regions are the highest points (peaks) and the dark regions are the pores and depressions.

Table 25: *Roughness measurements for two scan areas (1µm x 1µm and 50µm x 50µm)*

Membrane	Roughness (nm) 50µm x 50µm	Roughness (nm) 1µm x 1µm
NF270	45 ± 5	13 ± 5
NF200	33 ± 5	21 ± 6
NE90	71 ± 5	nd
NF90	390 ± 20	298 ± 10
BW30	290 ± 10	125 ± 25
BW30LE	283 ± 10	120 ± 10

(a)   (b)

(c)   (d)
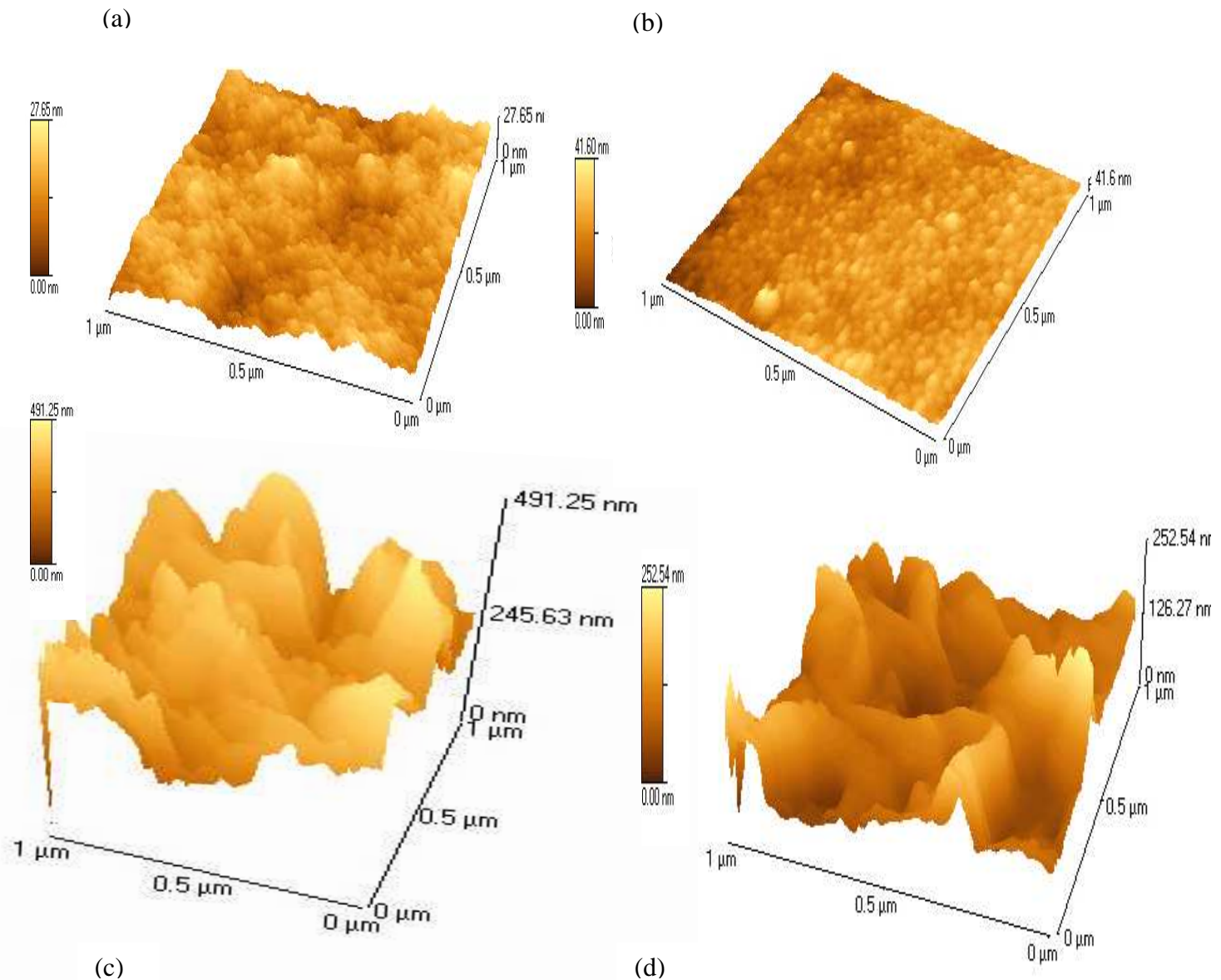
Figure 35: *Three-dimensional AFM images of the surface of (a) NF 270, (b) NF200, (c) NF90 and (d) BW30 membranes on a scan area of 1 µm x1µm.*

Table 25 shows that the larger the scanned area, the larger the roughness. The phenomenon of increasing roughness with increasing scan area can be related to the dependency of the roughness on the spatial wavelength of the scanned area or the frequency. For a small surface area, only the roughness of the "higher" frequencies is measured. When a larger surface area is scanned the roughness caused by additional lower frequencies also has to be taken into account. Another explanation for increasing roughness with increasing scan size may be the formation of fractal structure on the membrane surface when polymers are assembled to nodules or aggregates of nodules (Boussu *et al.* 2005). So, when the scan size is changed, it is possible to get a different surface topography, resulting in a difference roughness. Therefore it is crucial that the same scan size range is used when comparing the surface roughness for different samples.

From figure 35 and also from Table 25, we can show that the roughness values for the six membranes are very different; varying from 13 to 298 nm for a scan area of 1µm x 1µm. NF270 and NF200 are the smoothest membranes with small roughness values. NE90 is

characterized by an intermediate roughness value while the roughest surface can be found with NF90 and the LPRO membranes BW30 and BW30LE. The NF270, NF200 and NE90 membranes present lower roughness than the LPRO membranes. This is not confirmed by literature data, which indicate that average roughness increases with the nominal molecular weight cut off (Singh *et al.* 1998; Hilal *et al.* 2004). The surface of NF90 membrane contains many thin picks, which are responsible of the higher roughness of the nanofiltration membrane compared to the LPRO membranes.

It is assumed in the literature that Surface roughness has an important effect in membrane permeability. Hiros *et al.* (1996) and Gao and chen (1998) found that the water flux increased as the roughness of the membrane increased. Thus, the high roughness value of the NF90 membrane can explain its high permeability compared to the other membranes.

Surface roughness also has an important effect in membrane fouling behaviour (Elimelech et al. 1997; Zhu and Elimelech et al.1997; Vrijenhoek et al. 2001). Because of the ridge-and-valley structure of rough membrane surfaces, colloids are thought to be preferentially transported into the valleys (path of least resistance), which results in "valley clogging" and hence in a more severe flux decline in comparison with smooth membranes. However, other researchers did not observe any correlation between colloidal fouling and surface roughness, and the surface hydrophobicity appeared to be the most critical membrane characteristic to control colloidal fouling. Only when filtering small colloids by rough membranes, valley clogging plays an additional secondary role in membrane fouling (Van der Bruggen *et al.* 2004; Boussu *et al.* 2007). Besides the membrane properties, fouling also depends on the feed properties and the interplay between membrane and feed determines the fouling tendency (Boussu *et al.* 2006).

1.4.2 Wettability of the membranes

The hydrophobicity of the membranes was determined using contact angle (CA) measurements by sessile drop method. The results of contact angle measurements are summarized in table 26.

Table 26: *Water contact angle (CA) values for NF and LPRO membranes*

Membrane	NF270	NF200	NF90	NE90	BW30	BW30LE
CA (°)	39±5	38±3	64±4	nd	77±4	87±6

The hydrophobicity is ranged from 38 to 87° for the NF and LPRO membranes. Usually, the lower is the contact angle the more hydrophilic is the material and the hydrophilicity of membranes has a positive effect on the flux (Mänttäri *et al* 2004). Both surfaces of NF270 and NF200 have comparable contact angles with water, these membranes are the most hydrophilic membranes. The most hydrophobic membranes are the NF90, BW30 and BW30LE. A factor that complicates comparisons of data obtained is the differences in surface roughness among the membranes. The roughness of the surface of the NF90, BW30 and BW30LE membranes may be responsible on the difference of the measured contact angle. Contact angle hysteresis can be due to roughness and heterogeneity of a solid surface (Kwok et al. 1999). If roughness is higher than 100 nm, the measured contact angles are meaningless. On very rough surfaces,

contact angles are larger than on chemically identical smooth surfaces (Neumann *et al.* 1972, Bain *et al* 1989).

1.4.3 Characterization of the membrane charge

The separation mechanism of nanofiltration membranes is assumed to be based on a combination of several processes, like size exclusion, charged exclusion and, as sometimes refferred to as, dielectric exclusion. Concerning the separation of charged species, e.g. ions, both size and charge effects may play a role (Peeters et al. 1999).The charge of the nanofiltration membranes (NF270, NF200 and NF90) and the low pressure reverse osmosis membranes (BW30 and BW30LE) was evaluated by means of streaming potential measurements. To investigate the influence of the type of the electrolyte and its concentration at various levels of pH, different types of salts at different concentrations and pH were used for the streaming potential measurements.

1.4.3.1 Isoelectric point determination

The variation of streaming potential as a function of pH for the five membranes is plotted in Fig 36. This figure shows the pH dependence of streaming potential for the membranes studied. The NF270, NF90, NF200 and BW30LE membranes are slightly positively charged at low pH values and become increasingly negatively charged at higher pH values.
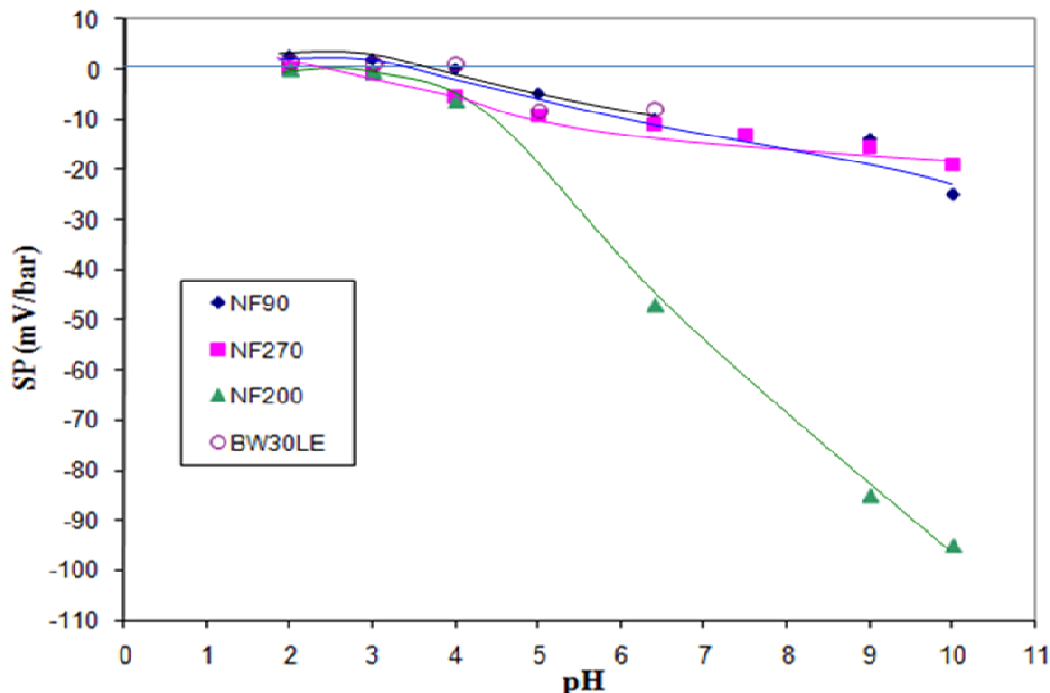
Figure 36: *Behaviour of the streaming potential as a function of pH for the different commercial membranes (KCl = 10^{-3}M, T° = 20°C)*

The shape of the streaming potential curve for the NF270, NF90, NF200 and BW30LE membranes is indicative of amphoteric surfaces (Childress *et al.* 1996, Saffaj *et al.* 2005 and Brant *et al.* 2006). For these membranes, the positive charge below the isoelectric point is

attributed to the protonation of amine functional groups ($NH_2 \rightarrow NH_3^+$). As pH increases, the membranes acquire a more negative charge from the deprotonation of carboxyl functional groups ($COOH \rightarrow COO^-$).

The NF200 membrane has much more surface charge than the other membranes. This result is in agreement with the kind of material this membrane is composed of. Sulfonic acid groups (SO_3^-) which are present on the NF200, are strongly acidic and are completely dissociated over nearly the entire pH range, while carboxylic groups (COO^-) are weakly acidic and will not be dissociated at a low pH (Schaep and Vandecasteele 2001).

The results of SP measurements for the tested membranes are listed in table 27.

Tableau 27: *Streaming potential (SP) and isoelectric point (IEP) of the NF and LPRO membranes*

Membrane type	NF270	NF200	NF90	BW30LE	BW30
Charge (neutral pH)	Negative	Negative	Negative	Negative	Negative
SP (mV/bar) (KCl 10^{-3}M, pH =6.7) (±1)	-10	-50	-7	-4	-4
IEP (KCl 10^{-3}M) (±0.3)	2.9	2.5	4.0	4.0	4.0

As indicated in this Table 27 and in Fig 36, the isoelectric point, i.e. the pH at which the net charge of the membrane is equal to zero, is located between 2.5 and 4. The position of the isoelectric point is similar for the NF90, BW30 and BW30LE membranes with pH 4.The values of isoelectric point found for the NF270 (3.0) and NF200 (2.5) are not quite far from those found in recent studies. (M. Mänttäri *et al. 2006,* Tanninen *et al.* 2006 and Lin *et al 2007).*

The NF270, NF90, BW30LE and BW30 membrane skin layers are made of polyamides but probably different monomers and different degrees of cross-linking in the polymerisation process result in somewhat different surface chemistries. This could be seen in dissimilar ion retention and permeability behaviours, because they have slightly different surface charges and hydrophilicities (M. Mänttäri *et al. 2006).* The results for BW30LE, BW30 and NF90 supported only a minor difference in the surface chemistry of these membranes.

1.4.3.1 Influence of Ionic strength on membrane charge

1.4.3.1.1Streming potential at different ionic strength

In order to investigate the ionic strength influence on the Streaming Potential, SP measurements were performed for several NaCl solutions. Fig 37 presents the variation of the streaming potential (SP) versus the salt concentration for the NF270 membrane. As expected, the streaming potential decreases as the salt concentration increases due to the phenomenon of the double-layer compression: the double layer thickness is reduced due to screening of the surface charge at a shorter distance. Fewer counter-ions can be displaced under the pressure difference. Furthermore, as shown by the Helmholtz-Smoluchovsky relation (Eq 13) a high ionic concentration make the solution inside the pores more conductive leading to a smaller SP (Peeters *et al* . 1999, Sbaï *et al.* 2003) . As can be seen, the streaming potential is close to

zero for the 10^{-1}M NaCl. This means that the effect of the membrane charge is completely eliminated when the salt concentration is high enough.
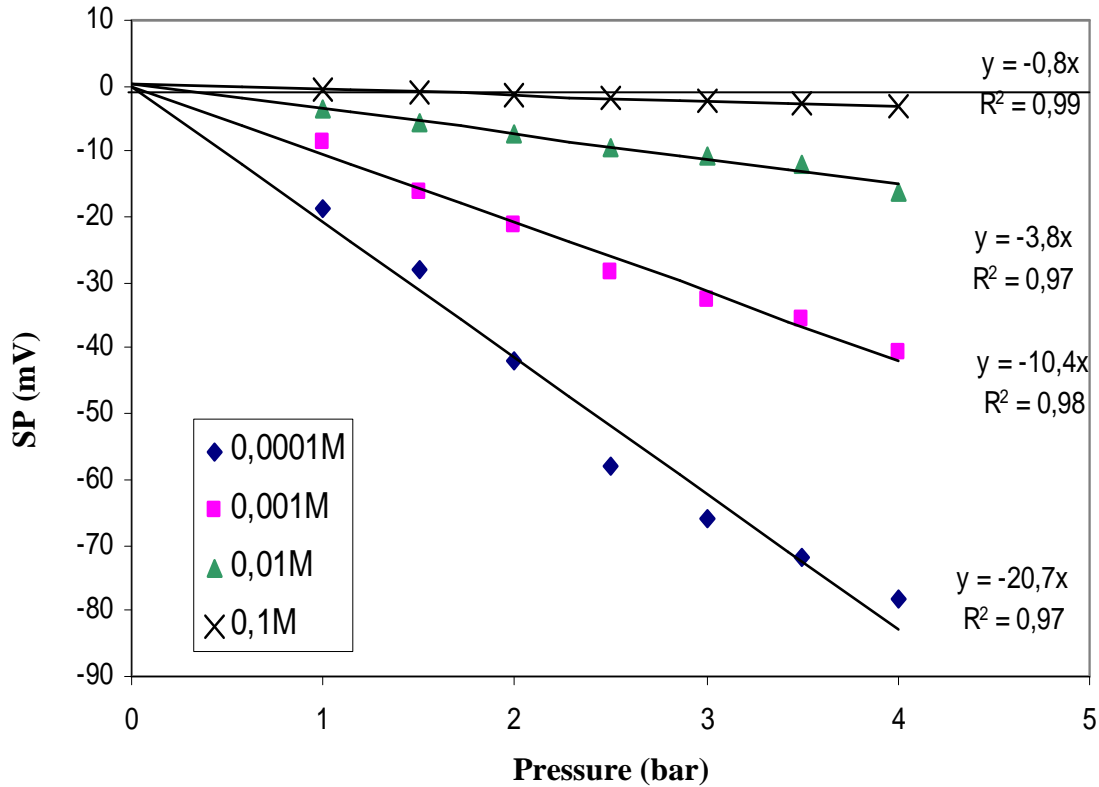
Figure 37: *Streaming potential as a function of the applied pressure for different concentrations of NaCl (Membrane NF270, pH = 6.4, T° = 20°C)*

The membrane charge depends on the concentration of the solution whith which the membrane is in contact. At a concentration of 0.1M, the membrane charges are supposed to be totally screened by the solution charges and for which the rejection is governed by only steric effect (Déon *et al.* 2007).

1.4.3.1.2 Ionic strength influence on IEP

In order to investigate the IEP dependence on the ionic strength, streaming potential measurements were performed for two NaCl solutions (10^{-3}M and 10^{-1}M) at various pH values. As displayed in Fig 38, SP results indicated that $\Delta\square / \Delta P$ is changing with ionic strength. The IEP increased with the increase of NaCl concentration from 10^{-3}M and 10^{-1}M. It increased from 4.0 to 5.0 for the NF90 membrane and from 2.5 to 3.5 for the NF200 membrane with respectively. This means that NaCl concentration affects the membrane charging process. The IEP dependence upon the solution concentration has been attributed to charge acquisition by ion adsorption (Violleau *et al.* 2005, Morao *et al.* 2006).
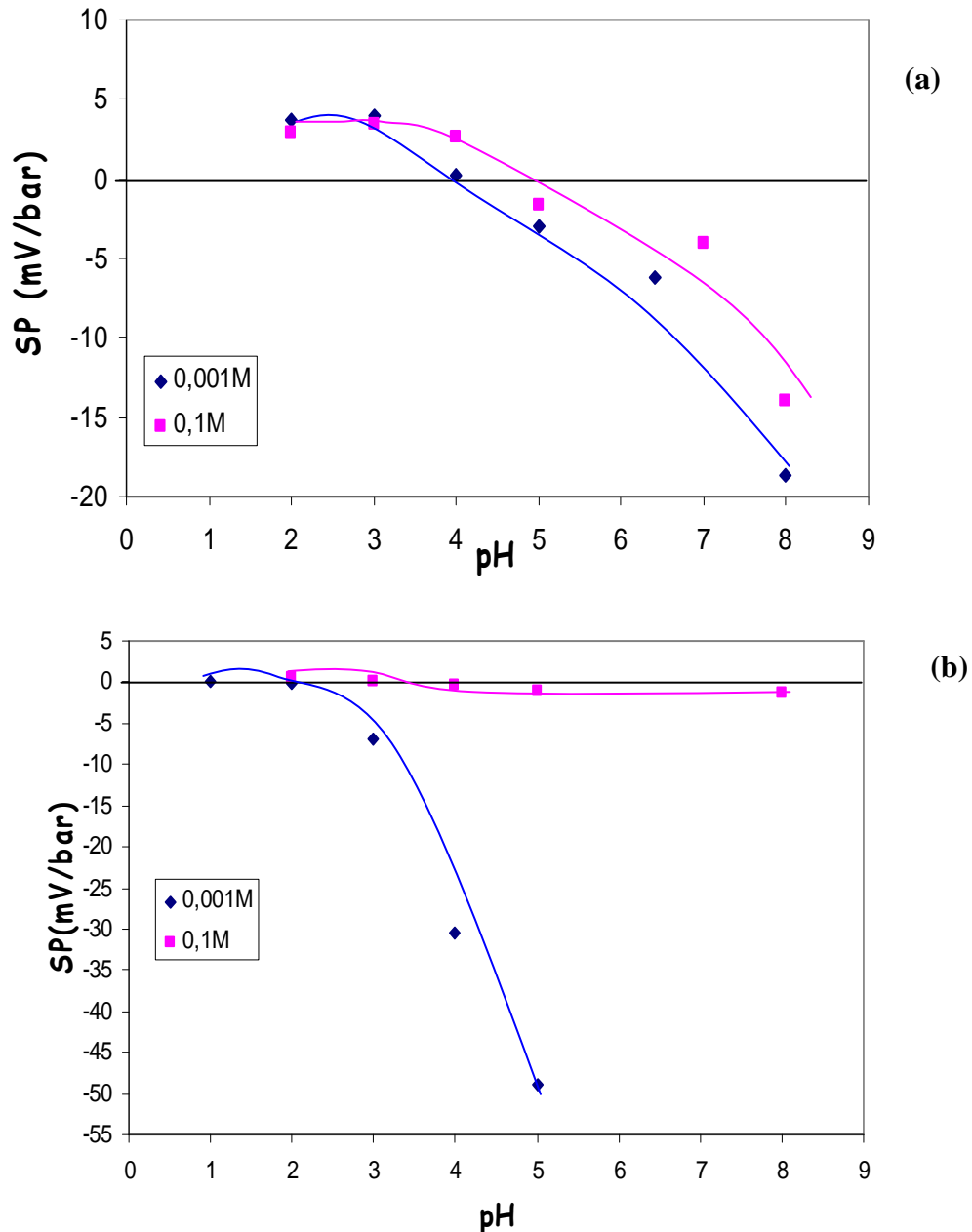
Figure 38: Streaming potential as a function of pH at different concentrations of NaCl (a) NF200 membrane (b) NF90 membrane

1.5 Membranes performance on Tan Tan Brackish water desalination

In this section, the performance of NF and RO membranes for desalination of Tan Tan water were evaluated and compared. This study, consisted of a laboratory bench-scale flat-sheet testing unit, which is an initial step for a large-scale pilot study wich is discussed in the last part of this chapter. Bench scale study results helped in selection of appropriate NF membranes suitable for treatment of Tan Tan water and to help the best choice for further experiments in Tan Tan large scale pilot plant.

Desalination experiments were carried out with three NF membranes (NF90, NE90 and NF200) and one LPRO membrane (BW30LE). The NF270 was excluded due to its low rejection and permeate flux values for all investigated single salts. The desalting efficiency and monovalent anions selectivity of the investigated membranes were evaluated under different operating conditions (transmembrane pressure and water recovery rate). SKK model was applied to fit the experimental data and evaluate the parameters σ and Ps. The optimal membrane was selected on several criteria such as: water permeability, removal of total salinity and monovalent anions selectivity.

1.5.1 Tan Tan water characterisation

Tan Tan brackish water after microfiltration were collected and analysed for pH, total dissolved solids and main ions concentration (Cl^-, NO_3^-, F^-, SO_4^{2-}, Ca^{2+}, Mg^{2+}, Na^+, K^+). The results of feed water analysis are presented in Table 28.

Table 28: *Water quality of Tan Tan brackish water sampled in Tan Tan BWRO plant and comparison with Moroccan and WHO guidelines*

	Tan Tan feed water	Moroccan standards	WHO Guidelines
T(°C)	27	-	25°C
pH	7.9	6.0 - 9.2	6.5-8.5
TDS(ppm)	3300- 4000	1000 - 2000	< 1000
Cl^-(ppm)	1287 - 1349	350 - 750	< 250
NO_3^-(ppm)	20	< 50	< 50
F^-(ppm)	1.1	0.7- 1.5	< 1.5
SO_4^{2-}(ppm)	500	200	< 200
Ca^{2+} (ppm)	270	< 500	< 270
Mg^{2+} (ppm)	115	100	< 50
Na^+(ppm)	595-761	< 200	< 200
K^+ (ppm)	19	-	-

As can be seen in Table 28 a number of water quality parameters exceed the WHO and Moroccan drinking water standards. In particular the salinity (TDS 3.3-4 g/L) and ion concentration Cl^-, SO_4^{2-} and Na^+ was high and thus needs desalination.

In the Moroccan Drinking Water Standards, TDS is set at two distinct limits: the permitted limit 1000 ppm and the maxiwum allowable limit of 2000 ppm, where no better source is available.

1.5.2 Hydraulic permeability of Tan Tan water

Experimental data for the permeate flux, with Tan Tan water, as a function of the transmembrane pressure are given in Fig. 39 for the four tested membranes.
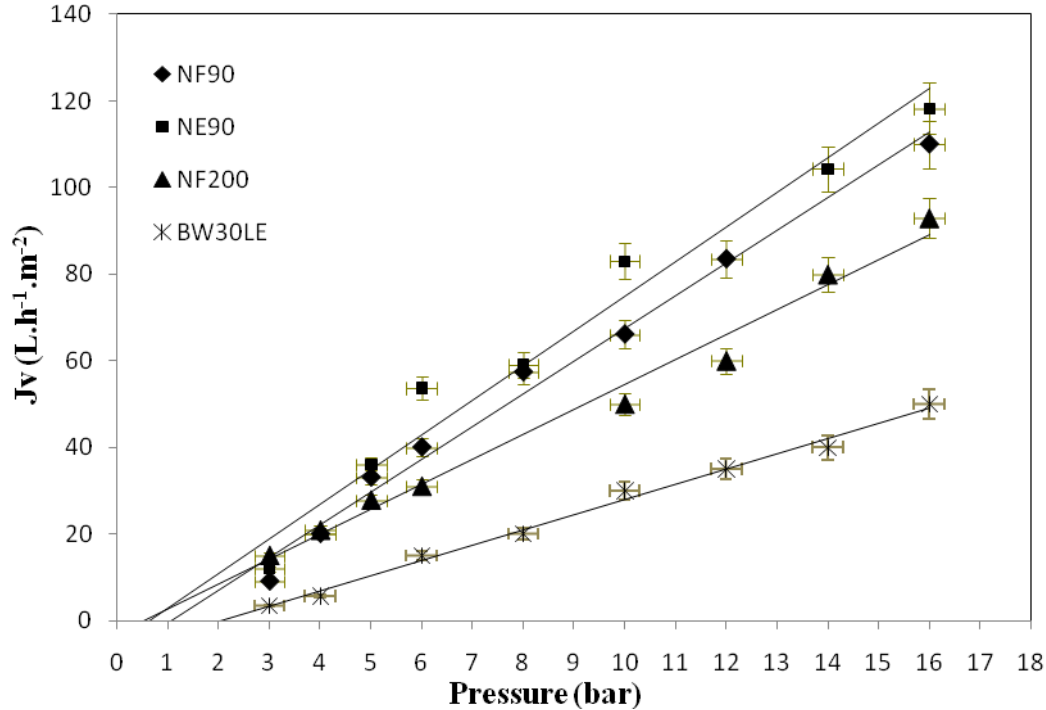
Figure 39: *Effect ot transmembrane pressure on the permeate flux with Tan Tan water*
(pH = 7.9, T = 28°C)

The fluxes increased linearly with the pressure. As earlier observed, the permeate fluxes obtained for the NF membranes were higher than the LPRO membrane. For the NF membranes, the highest fluxes were found for the NF90 and NE90 membranes while NF200 showed the lowest flux.

The hydraulic permeabilities and critical pressure values for all membranes obtained with Tan Tan brackish water are reported in Table 29.

Table 29:*Hydraulic permeability (Lp') to Tan Tan water and critical pressures (Pc) for the NF200, NE90, NF90 and BW30LE membranes*

Membrane	Lp' ($\pm$ 0.5) (L.h^{-1}.m^{-2}.bar^{-1})	Pc (bar) ($\pm$ 0.2)
NF200	5.8	0.5
NF90	7.6	1.1
NE90	8.0	0.7
BW30LE	3.5	2.2
BW30	3	nd

The critical pressure of LPRO membrane was 2 to 3 times higher than the one of NF membranes which is due to higher rejection and obviously higher osmotic pressure difference across the NF membrane.

The flux appeared at a pressure lower than 1.1 bar. Indeed, NF offers the advantages of partial demineralisation correlated to a lower effect of the osmotic pressure under the hydraulic permeabilities in comparison to RO, as expected, because the difference in concentration in both sides of the membrane is lower.

1.5.3 Removal of total salinity

Different membranes used for desalination of Tan Tan brackish water are compared in Fig 40. In this figure the retention of salts is shown as a function of transmembrane pressure at a fixed recovery rate of 15%.

At higher transmembrane pressure, the flux is higher and the contribution of diffusion becomes less important relative to convection, so that an increase in retention is found.

In general for a given conversion rate and operating pressure, the membranes under study rejected the total salinity following the order: BW30LE > NF90 > NE90 > NF200.

The highest rejections are obtained for the LPRO membrane. For this one, the membrane has no pores and the mechanism of exclusion is only chemical. In NF and as already seen, the selectivity is not only based on chemical phenomena, the pore size effect and the charge effects can influence the selectivity alone or associated, depending on the operating conditions and on the kind of NF membrane.
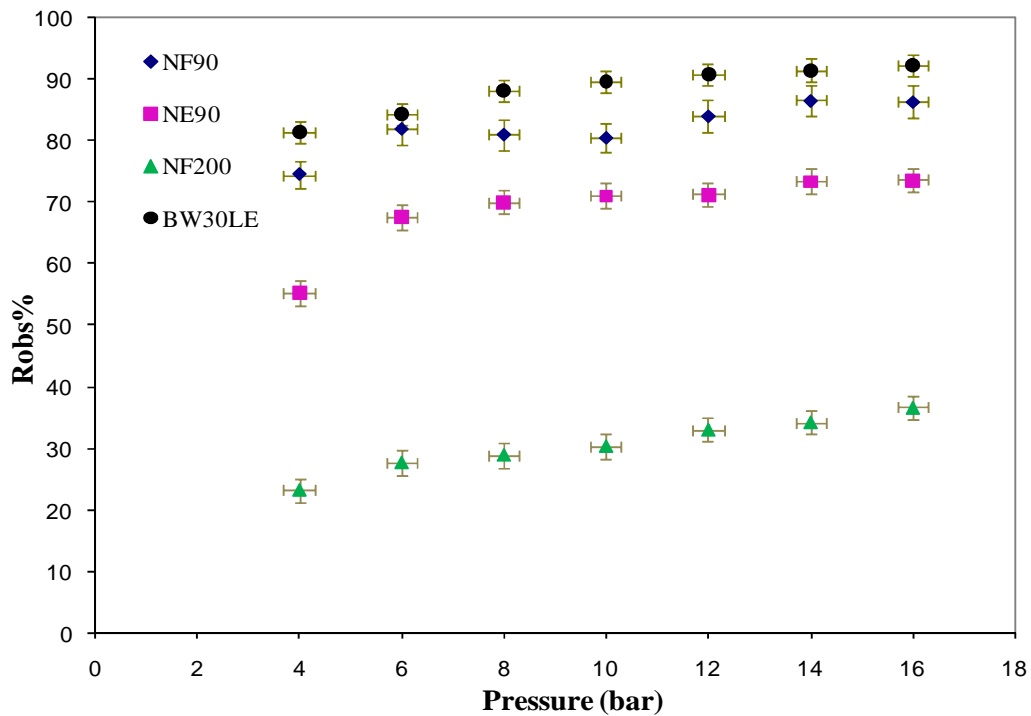
Figure 40: *Total salinity rejection during brackish water treatment by NF and LPRO membranes (T= 28°C, pH = 7.9, Y = 15%)*

Salts rejection is higher for NF90 (> 75 %) and is close to the LPRO membrane rejection. It has smallest pores size and its mass transfer behavior is close to classical RO membranes. Less rejections were obtained for the NE90 membrane (< 75%) and NF200 (< 35%). These results agree with those already found for this negatively charged membrane (in section I.4.1.3).There is an important effect of the screen phenomenon of the membrane charge at high concentration level, which is the case for Tan Tan water. Thus, the repulsion effect between the membrane and the salts decreased and the transfer through the membrane is then made easier and leads to an important decrease of salt removal efficiency.

1.5.4 Effect of the recovery rate on rejection

In real applications, NF and RO operations will be operated at high recovery rates since at higher the recovery more permeate is obtained. For Tan Tan brackish water, the influence of higher recovery values on NF and LPRO membranes was investigated and results are presented in Figure 41.
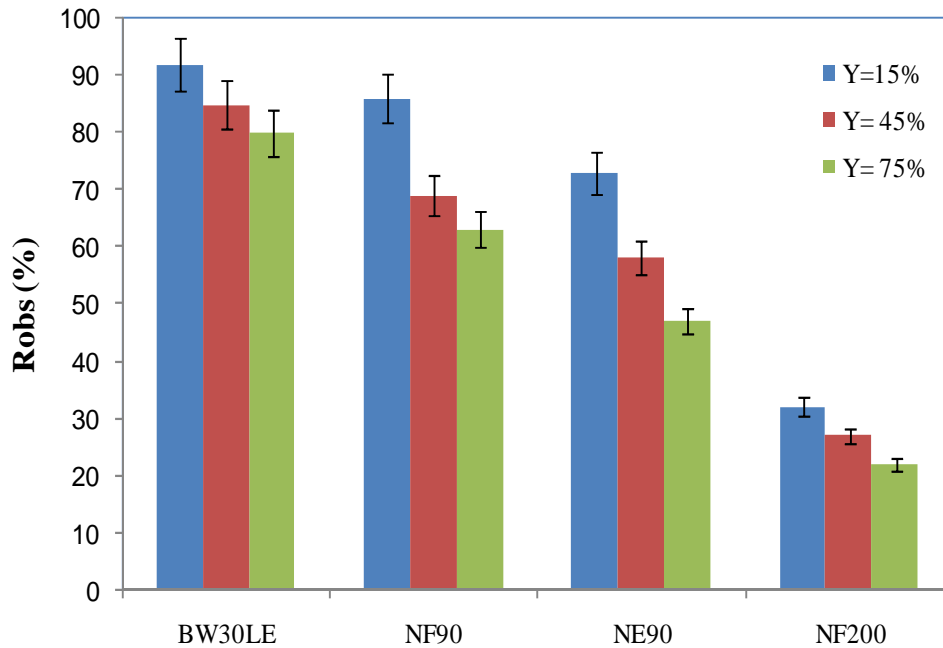
Figure 41: *Total salinity rejection during Tan Tan water treatment by NF and LPRO for recovery values of 15-75% (ΔP =16bar, T= 28°C, pH = 7.9)*

Figure 41 shows that the salt rejection decreases with increase of recovery rate for all the membranes. The drop of rejection rates of the LPRO membrane was lower than all of NF membranes, e.g., from 92 to 80% at Y = 75% (CF = 4) (12% drop) in the case of the LPRO membrane; BW30LE from 86 to 63% (23% drop) in the case of the NF90 membrane; and from 73 to 47% (26% drop) for the NE90 membrane. The NF200 membrane is less influenced by the recovery rate increase (12% drop).

At high recovery rate, the concentration factor (CF) increases, thus the bulk feed concentration of solutes increases. This increase may, in turn, be responsible for stronger concentration–polarisation, membrane–solute interactions and, even, solute adsorption onto membrane surface, which have deleterious effect on the membrane performance (Bannoud. 2001,Lhassani *et al.* 2001, Abouzaid *et al.* 2003, Maurel. 2006, Teixeira and Rosa. 2006).

Table 30 summarizes the experimental findings in term of total salinity in the permeate, for a pressure of 16 bar.

Table 30: *Permeate total salinity for Tan Tan water at different conversion rates and at a pressure of 16 bar, for the membranes NF200, NE90, NF90and BW30LE*

	Membrane	NF200	NE90	NF90	BW30LE
TDS in the permeate	Y=15%	2160	900	470	270
(ppm)	Y=45%	2460	1420	1020	670
	Y=75%	2630	1790	1250	730

The results given in this table confirm the satisfactory performances of Nanofiltration for desalination of Tan Tan brackish water compared to the LPRO membrane. NF membranes partial demineralize the brackish water treated. The NF90 membrane was able to reduce the salinity using one stage from 3300 to 1250 ppm (Y= 75%) at pressure of 16 bar.

The efficiency of this membrane on desalting Tan Tan brackish water is better than that of the NE90 which allows the reduction of salinity from 3300 to 1790 ppm at the same conditions. The NF200 membrane shows the least performances. In order to make Tan Tan brackish water drinkable with regard to salinity, it is recommended to either carry out the experiment at high pressure or use more than one NF stage.

The permeate salinity whith the BW30LE membrane was slightly higher than classical reverse osmosis membranes. The rejections with RO membranes are fairly high and nearly constant irrespective of the operating conditions (such as pressure and recovery rate). This confirms that the LPRO membrane is more open than usual.

1.5.5 Ion selectivity

The selectivity of the NF90, NE90, NF200 and BW30LE membranes for various major monovalent anions present in Tan Tan water, F^-, Cl^- and NO_3^- was investigated.

Figure 42 shows rejection *versus* pressure data of all investigated ions found in Tan Tan water with a pressure range of 4 to 16 bar for four membranes. It is obvious that the rejection of all ions increases with increasing pressure for NF membranes, while the anions rejections by the BW30LE membrane is almost independent of pressure.

The sequence of rejection of monovalent anions can be written as R (F^-) > R (Cl^-)> R (NO_3^-). The observed retention of the three ions is similar to the ionic order and opposite to the hydration energy order for the monovalent ions (Table 9). The F^- which has higher hydration energy is better retained than Cl^- and NO_3^- (Diawara *et al.* 2003, Wang *et al.* 2005).The LPRO shows almost similar rejection of Cl^- and NO_3^-.

The figures 42 (a), 42 (b) and 42 (c) shows that the smaller ions are better retained by NF membranes and greatest selectivity is obtained at low pressure. The retention of ions also tends to a plateau at higher pressures. The ions selectivity in NF is dependent on the pressure; the ions are transferred by two mechanisms convection and diffusion while only diffusion is involved in RO.
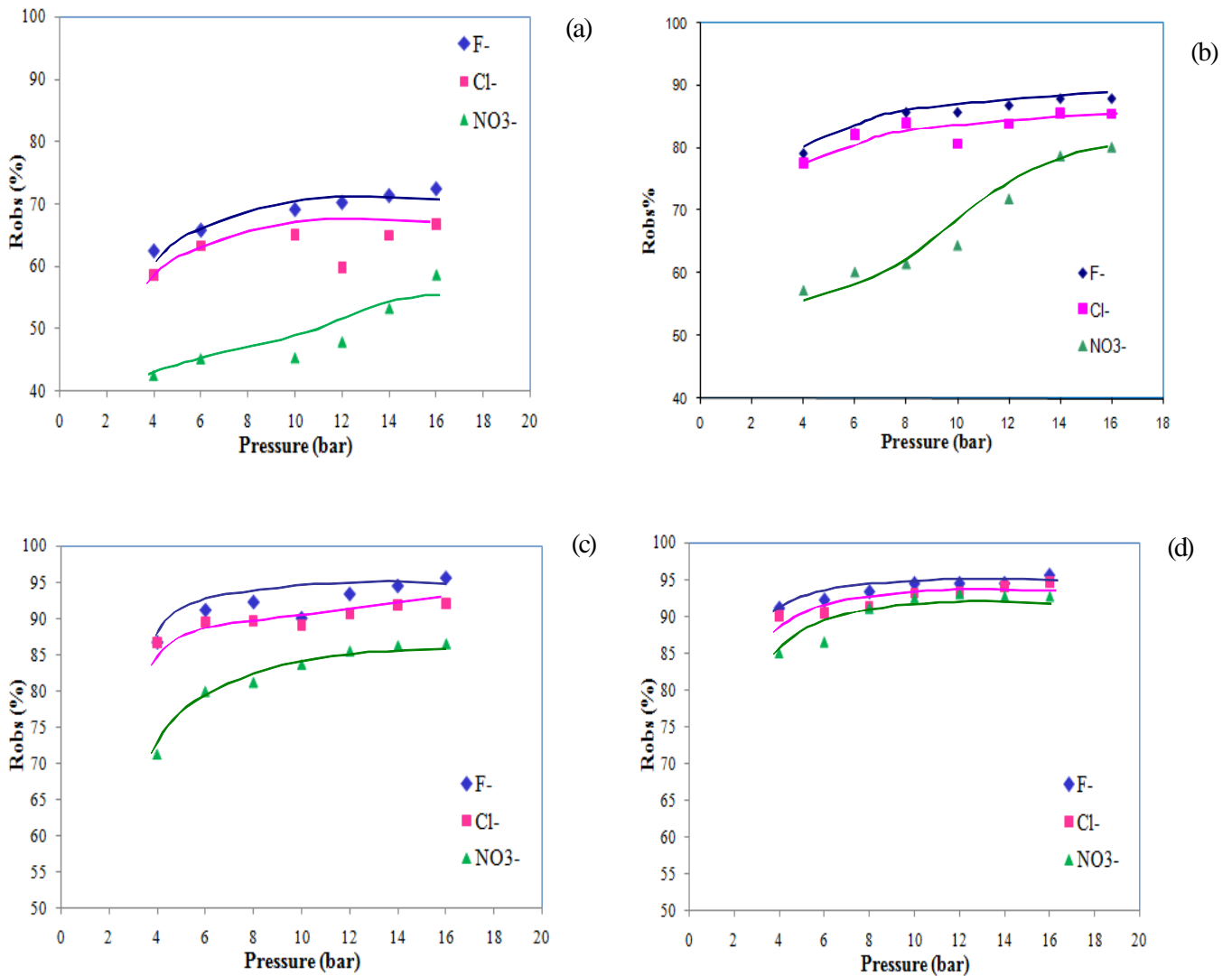
Figure 42: *Rejections of F⁻, Cl⁻ and NO₃⁻ anions found in Tan Tan brackish water versus pressure for: (a) NF200, (b) NE90, (c) NF90 and (d) BW30LE. (Y=15%, T=28°C, pH=7.9)*

Convection. They are carried by the solvent stream as a function of the transfer coefficient. The larger ions are more retained (physical parameters).

Solution–diffusion. A function of the solvation energies and the partition coefficient. The larger the ion, the less well it is retained (chemical parameters).

The convection transfer mechanisms are modified by altering the physical parameters (pressure, recovery rate), without altering diffusion, which is influenced only by the chemical parameters (concentration, pH).

Convection is low at low pressure and in contrast, the physical parameters predominate at high pressure, and the larger ions are better retained. Nevertheless, chemical selectivity is always much more important than physical selectivity for separating ions. This means that selectivity is always higher at low pressure (Lhassani *et al* 2001).

Fluoride retention is practically unaffected by pressure because the passage of this anion is mainly due to diffusion. Convection has virtually no effect since a significant increase in

pressure caused no marked change in F⁻ retention. On the other hand, Cl⁻ and NO_3^- retention is much more influenced by pressure because the passage of these anions is more due to physical than chemical forces. In fact the, diffusion is governed by chemical parameters, whereas convection is due to physical properties such as the size of the ions.

The rejection rates were also analysed as function of conversion rates. Table 31 summarizes the experimental findings in term of F⁻, Cl⁻ and NO_3^- removal at different conversion rates and for a pressure of 16 bar.

Table 31: *F⁻, Cl⁻ and NO_3^- rejection rates by NF200, NE90, NF90and BW30LEmembranes at different conversion rates and at a pressure of 16 bar*

Membrane	Y%	Robs(%)		
		Cl⁻	F⁻	NO_3^-
NF90	15%	92	95	86
	45%	84	89	80
	75%	64	84	69
NE90	15%	85	87	80
	45%	70	75	67
	75%	66	72	68
NE200	15%	66	72	58
	45%	62	68	53
	75%	49	61	44
BW30LE	15%	94	95	92
	45%	90	92	87
	75%	89	90	86

An increase in the conversion rate caused a decrease in the retention for the same pressure and for a given anion.

1.5.6 Modeling the ion rejection of Tan Tan brackish water

SKK model was applied, as explained earlier, to fit the rejection of total salinity and the monovalent anion of brackish water with flux. The fitting parameters (σ and Ps) of total salinity and monovalent anions F⁻, Cl⁻ and NO_3^- for four membranes are given in Table 32.

The model fitted well the experimental data of total salinity rejection and monovalent anions for all the membranes; in general it was able to predict the rejection within 0.1 % of the experimental values. However, at high recovery rate (75%), the error between experimental values and those calculated was >5%. Thus the parameters (σ and Ps) evaluated at high recovery rate are not realistic and confirmes the invalidity of SKK model at high recovery rates when the concentration polarization phenomenon is stronger.

The values of fitted parameters at recovery rate of 15% and 45% are logical as shown in table 32. The highest σ values and lowest Ps values were obtained for the BW30LE membrane.

Tableau 32: *Reflection coefficient (σ) and solute permeability (Ps) for each anion of filtered brackish water for NF90, NE90, NF200 and BW30LE membranes*

Membrane		NF90		BW30LE		NE90		NF200	
		σ	Ps (L.h^{-1})	σ	Ps (L.h^{-1})	σ	Ps (L.h^{-1})	σ	Ps (L.h^{-1})
Y =15%	TDS	0.86	0.07	0.95	0.04	0.73	0.15	0.33	0.36
	F$^-$	0.96	0.03	0.95	0.017	0.89	0.05	0.72	0.11
	Cl$^-$	0.90	0.03	0.96	0.02	0.84	0.06	0.64	0.15
	NO$_3^-$	0.87	0.07	0.95	0.03	0.76	0.10	0.34	0.45
Y =45%	TDS	0.71	0.11	0.93	0.15	0.69	0.25	0.3	0.66
	F$^-$	0.92	0.07	0.99	0.05	0.81	0.09	0.52	0.14
	Cl$^-$	0.89	0.11	0.91	0.07	0.78	0.14	0.56	0.25
	NO$_3^-$	0.85	0.13	0.87	0.04	0.62	0.36	nd	nd
Y =75%	TDS	0.71	0.26	0.99	0.19	0.65	0.46	0.25	0.49
	F$^-$	0.88	0.10	0.93	0.04	0.82	0.39	0.62	0.10
	Cl$^-$	0.99	0.79	0.99	0.27	0.66	0.08	0.48	0.11
	NO$_3^-$	0.67	0.13	0.88	0.05	0.46	0.35	nd	nd

In NF, the σ and Ps values depend on the type of membranes and anions and in the operating conditions (recovery rate). The NF90 presents the highest σ values and lowest salt permeabilities followed by the NE90 membrane. The σ values of the NF200 membrane are relatively low due to its low rejection rates and it consequently presents the highest salt permeabilities. The fitted parameters (σ and Ps) values seem to be highly dependent on the type of anion present in Tan Tan brackish water. Strongly solvated anions, like F$^-$ and Cl$^-$ lead to high values of σ in comparison with less solvated anions (NO$_3^-$) (Diawara *et al.* 2003, Al-Zoubi, H. 2006). It appears clearly that the mass transfer behaviour occurring in NF dedicated to a selective monovalent anions removal must be similar to that of a RO membrane. (σ and Ps) depend also on the operating parameters; the σ values decrease with increasing recovery rate and ions permeability decreases.

1.5.7 Partial conclusion

With NF membranes a desired drinking water respecting the standards can be easily produced from brackish water.Using the NF90 and the NE90 membranes, retentions of total salinity for about 65-90% were found for the NF90 and 50-75% for the NE90. The monovalent ions were retained for about 70% for the NF90 and 60% for the NE90.

The influence of water recovery rate was investigated. The rejection rate decreased at higher recovery rates, which was found to be a pure concentration effect. Changing the operating conditions has almost no effect in the monovalent ions rejection with LPRO membrane, while marked selectivity of monovalent ion was obtained with NF membranes, especially at low pressure conditions. These results will be further examined in large-scale pilot study in Tan Tan SWRO plant for the NF90 and NE90 which showed best performances in terms of rejection and permeability than the NF200. Table 33 summarizes the characteristics of all tested membranes.

Table 33: *Summary of the characteristics of all tested membranes*

Membrane Type	BW-30 Dow Filmtec	BW-30-LE Dow Filmtec	NF-90 Dow Filmtec	NF-200 Dow Filmtec	NF-270 Dow Filmtec	NE-90 Saehan
Material	Polyamide	Polyamide	Polyamide	Polypiperazine amide sulfonated	Polyamide	Polyamide charged
Charge (neutral pH)	Negative	Negative	Negative	Negative	Negative	nd
SP (mV/bar) (KCl 10^{-3}M)	- 4	- 4	-7	-50	-10	nd
IEP (KCl 10^{-3}M)	4.0	4.0	4.0	2.5	2.9	nd
Ra (nm) (50 x 50μm^2)	290 ± 50	283 ± 50	390 ± 20	33 ± 5	45 ±5	71 ± 5
Contact angle ($\theta°$)	76 ± 5	87 ± 5	64 ± 5	38± 5	38 ± 5	nd
UPW permeability (25°C) Lp (± 0.7) (L.h^{-1}.m^2.bar^{-1})	3.5	2.3	14.8	10.6	5.1	10.4
Lp' (Tan Tan Water 4 g.L^{-1}) (28°C) (L.h^{-1}.m^2.bar^{-1})	3± 0.5	3.5 ± 0.5	7.5 ± 0.5	5.8 ± 0.5	nd	8.0 ± 0.5
Pc (Tan Tan Water)	nd	3.8 ± 0.2	2.0 ± 0.2	1.6 ± 0.2	nd	1.8 ± 0.2
Mass transfer type	Diffusional	Diffusional	Diffusional (+)	Convection (+)	Convection (+)	Diffusional (+)
MWCO (Da)	156	187	213	401	308	254
σ (±0.02) NaCl (6 g.L^{-1})	0.99	0.98	0.85	0.62	0.26	nd
Rejection range of TDS (Tan Tan Water) Pressure (16 bar) (Y =75 and 15%)	nd	80/92	86/63	22/35	nd	73/47
Permeate TDS (ppm) — Y=15%	nd	270	470	2160	nd	900
Permeate TDS (ppm) — Y=45%	nd	670	1020	2460	nd	1420
Permeate TDS (ppm) — Y=75%	nd	730	1250	2630	nd	1790

2. *Applied study on a pilot scale in Tan Tan city (South of Morocco)*

Desalination of brackish water by NF membranes might be technically and economically viable to cope with water scarcity and overcome water deficit in Morocco. In this section the treatment of Tan Tan brackish water by NF and RO into potable water was investigated. Eight types of 4"x40" NF and LPRO modules were tested with the aim of desalination of Tan Tan water. The studied membranes were four NF membranes (NF90, NE90, ESNALF and NE70) and four LPRO membranes (BW30, BW30LE, REBLF and ESPA3).These membranes were purchased from various suppliers. Brackish water samples were collected from Tan Tan BWRO plant, Morocco. A pilot plant equipped with composite LPRO and NF membranes was operated at a temperature of 21°C, up to water recovery rates of 90%, up to a pressure of 20 bar and up to feed flow of 2 $m^3.h^{-1}$. The pilote unit was fed with the pretreated brackish water from the full scale plant

The technical and economical feasibilities of NF versus RO process for the production of potable water from Tan Tan brackish water were therefore investigated. The main performance indicators of this small NF/RO desalination system are productivity in the form of flux and recovery, desalination efficiency in the form of retention with regards to total dissolved solids, individual elements and energy requirements.

Operation of the demonstration unit should allow for the determination of the operating conditions and the establishment of performance parameters for large scale NF plant. It should also assist in technoeconomic evaluation of the process itself.

In the second part of this applied study, the results of the applications of NF on the desalination of moderately brackish waters (TDS < 10 g/L), and on brackish water defluoridation are discussed. Experiments with Tan Tan water spiked with specific ions were performed to check the potential of NF operation versus RO on filtration of moderately brackish waters, and to clarify the limits of application of NF membranes on brackish water desalination. The performances of NF and LPRO membranes on fluoride removal were also performed using various initial fluoride contents in Tan Tan water.

2.1 Tan Tan Brackish Water Treatment Plant

The Tan Tan Brackish Water Reverse Osmosis (BWRO) plant which has a production capacity of 1700 m^3/d, started in 2003. The plant is fed with brackish water from Khang Lahmam underground water located at 80 km far from the city. Figure 43 shows the flow diagram of the plant.

As shown in this Figure, the raw brackish water coming from the wells flows into a reservoir. It is sent to the pretreatment unit (Sand filters followed by cartridge filters), the high pressure pumps and then to the RO modules. The permeate is stored in the product water tank.
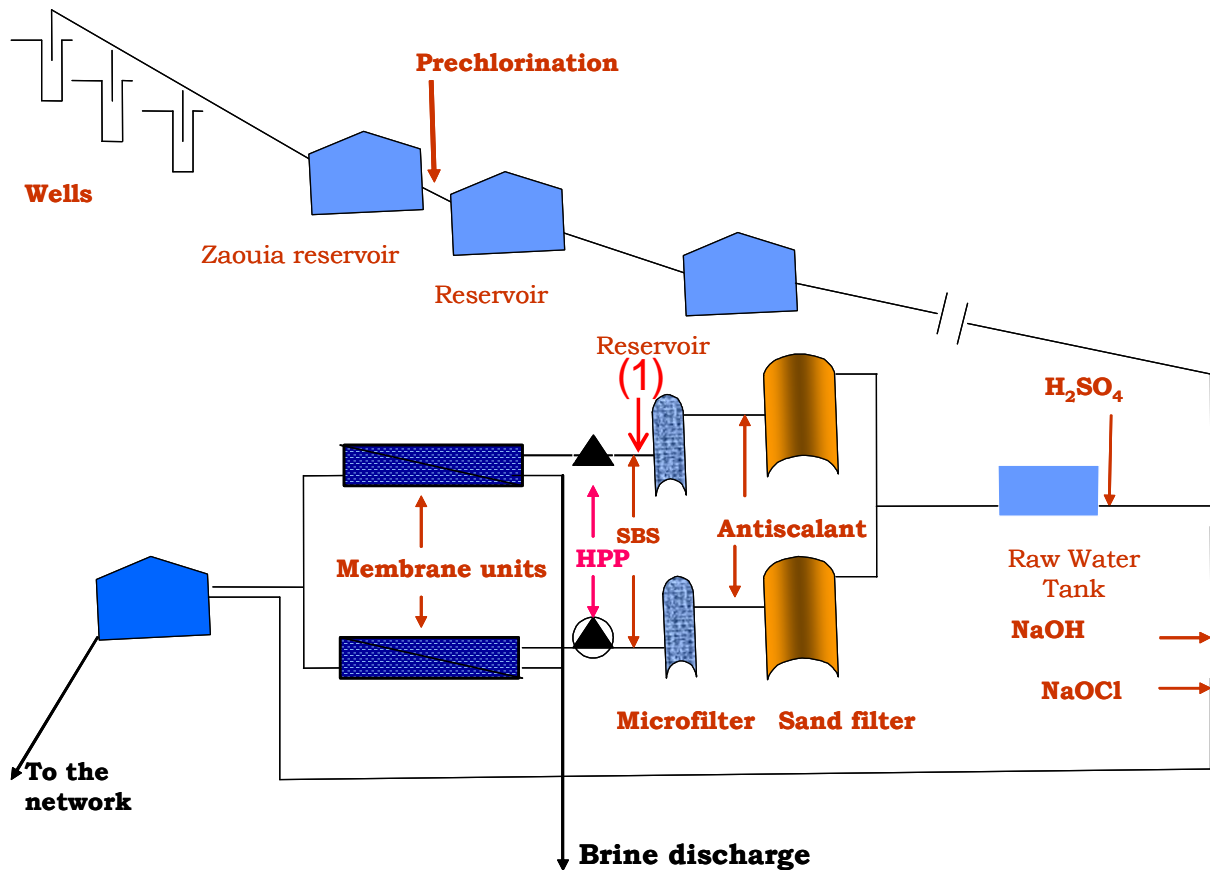
Figure 43: *Flow diagram of the Tan Tan BWRO plant*

Pretreatment unit

The raw brackish water is pretreated through the following stages:

➢ Prechlorination: A prechlorination station is located 50 km upstream of the plant (chlorine dosing up to 3 mg/L). Due to the occurrence of biofouling on the RO membranes when using prechlorination at the beginning of operation, it was decided to stop the use of prechlorination.

➢ Acidification: Sulphuric acid is injected at the inlet of the plant to prevent carbonate precipitation. The pH level is adjusted at 6.9. After acidification, the water is split in two similar process streams.

➢ Sand filters: Each stream is composed of one pressure filter. Each filter can treat a flowrate of 54 m^3/hr corresponding to a filtration velocity of 11 m/hr.

➢ Antiscalant : Antiscalant (polyphosphate 3 mg.L^{-1}) is injected to prevent scaling of calcium sulphate and barium sulphate as well metallic oxides.

➢ Microfiltration: Each RO skid is equipped with 5 µm cartridge filters

➢ Dechlorination: Dechlorination with sodium metabisulfite can be performed upstream of the high pressure pump. Since continuous chlorination has been stopped, the use of sodium metabisulfite was stopped as well. Moreover, the injection point was initially located upstream of the cartridge filters which led to extensive biological growth onto

the cartridge filters and the RO membranes. The injection point was then moved downstream of the cartridge filters.

Reverse Osmosis Unit

The RO section is divided into two trains, each train is composed of 2 stages. The first stage is composed of 4 pressure vessels each containing 6 RO modules (Dow BW30-400). The second stage is composed of 3 pressure vessels containing 6 RO modules (Dow BW30-400). The average conversion rate is 70% (feed flow rate per train = 54 m^3/hr ; permeate flow rate per train = 38 m^3/hr). Therefore, the average flux is 24 L/m^2-hr.

Post-treatment

The permeate water is then mixed to the raw brackish water with a 1:1 ratio. The pH adjustment is then performed with the injection of sodium hydroxide. Sodium hypochlorite is used for post-chlorination.

The brackish water used in our study was collected after the cartridge filters (see point (1) in Figure 43)

2.2 Membrane selection

In a preliminary study which consisted of a laboratory bench-scale flat-sheet testing, developed in the first part of this chapter, six NF and RO membranes were initially evaluated. Based on these bench-scale results, two LPRO membranes (BW30LE, and BW30) and two NF membranes (NE90 and NF90) were selected for use in the pilot study.
Projections based on membrane manufacturer simulation softwares (ROSA, CSMPro, IMS Design) were also performed in order to evaluate the performance of different NF and LPRO membranes on Tan Tan brackish water desalination. These assumptions were made to project the replacement of the existing low-pressure RO membrane (BW30) while keeping the same infrastructure for the RO system. Thirteen membranes from different manufacturer's (Hydranautics, DOW and Saehan) were evaluated. Projections were performed as reported in Table 34, with the following assumptions:
➢ Average water temperature of 23°C
➢ Use of the existing membrane configuration in Tan Tan plant (1st stage : 4 pressure vessels; 2nd stage : 3 pressure vessels; feed flowrate = 54 m^3/hr ; conversion rate = 70%)
➢ Pump efficiency = 80%

Table 34 gives the results of the different projections.

Table34: Projection results obtained with membrane suppliers' softwares

Membrane Type	Flux (L/m²-hr)	Feed Pressure (bar)	Specific Energy (kWh/m³)	Permeate TDS (mg/L)	Permeate Cl⁻ (mg/L)	Permeate Na⁺ (mg/L)	Permeate SO₄²⁻ (mg/L)	Permeate Ca²⁺ (mg/L)	Permeate Mg²⁺ (mg/L)
LOW-PRESSURE RO MEMBRANES									
BW-30-400 Dow Filmtec	24.2	15.4	0.76	56.4	14.1	8.3	2.5	1.7	0.8
BW-30-LE-440 Dow Filmtec	22.0	11.3	0.56	153.1	32.0	18.7	5.6	3.9	1.7
ESPA-2 Hydranautics	24.2	11.9	0.60	48.3	20.7	14.6	2.2	1.4	0.6
ESPA-1 Hydranautics	24.2	10.3	0.52	158.3	51.5	45.1	7.8	4.3	1.8
ESPA-4 Hydranautics	24.2	9.1	0.46	203.3	66.5	57.9	10.1	5.6	2.4
ESPA-3 Hydranautics	24.2	9.5	0.48	381.8	128.0	108.8	5.9	3.1	1.3
BLN Saehan	24.4	10.0	0.50	72.7	32.4	15.9	6.9	3.6	1.5
BLR Saehan	24.4	11.1	0.55	38.8	17.3	8.5	3.7	1.9	0.8
BLF Saehan	24.4	9.0	0.45	122.1	54.4	26.6	11.7	6.1	2.6
NF MEMBRANES									
NF-90-400 Dow Filmtec	24.2	8.9	0.44	259.4	138.0	78.0	10.3	10.5	4.6
ESNA-LF Hydranautics	24.2	8.9	0.45	710.5	371.4	224.7	26.7	22.6	9.6
NE-90 Saehan	24.3	7.8	0.39	423.6	221.2	108.2	5.9	3.1	1.3
NE-70 Saehan	24.1	6.2	0.29	921.3	571	263	35.3	9.4	6.4

These results show that all the NF membranes can meet a TDS level lower than 1000 mg/L and allows the desalination of Tan Tan water at low pressure values. All these NF membranes will be further tested in Tan Tan large scale pilot plant.We have limited the choice from RO membranes to the BW30 which is the existing low-pressure RO membrane installed in Tan Tan plant, the BW30LE, ESPA3 and REBLF membranes. The selection of the optimal membranes from the LPRO membranes was based on several criteria such as: relatively high removal of total salinity at low working pressures and monovalent anions selectivity.

2.3 Performance Evaluation

The main performance indicators of a pilot scale desalination system are productivity in the form of flux and recovery, desalination efficiency in the form of retention with regards to total dissolved solids, individual elements, and energy requirements in the form of specific energy consumption.

2.3.1 Water productivity

Permeate flux is an important parameter in design and economical feasibility analysis of membrane separation processes. When the level of solute rejection is met, the permeate flux becomes a fundamental factor in optimization of the process. The higher the permeate flux, the lower the filtration area necessary for a certain amount of solution to be processed.
Water productivity (or flux) of the NF and LPRO membranes for Tan Tan water was measured at first. The results are plotted as permeate flux versus the applied transmembrane pressure for the studied membranes as shown in Figure 44.
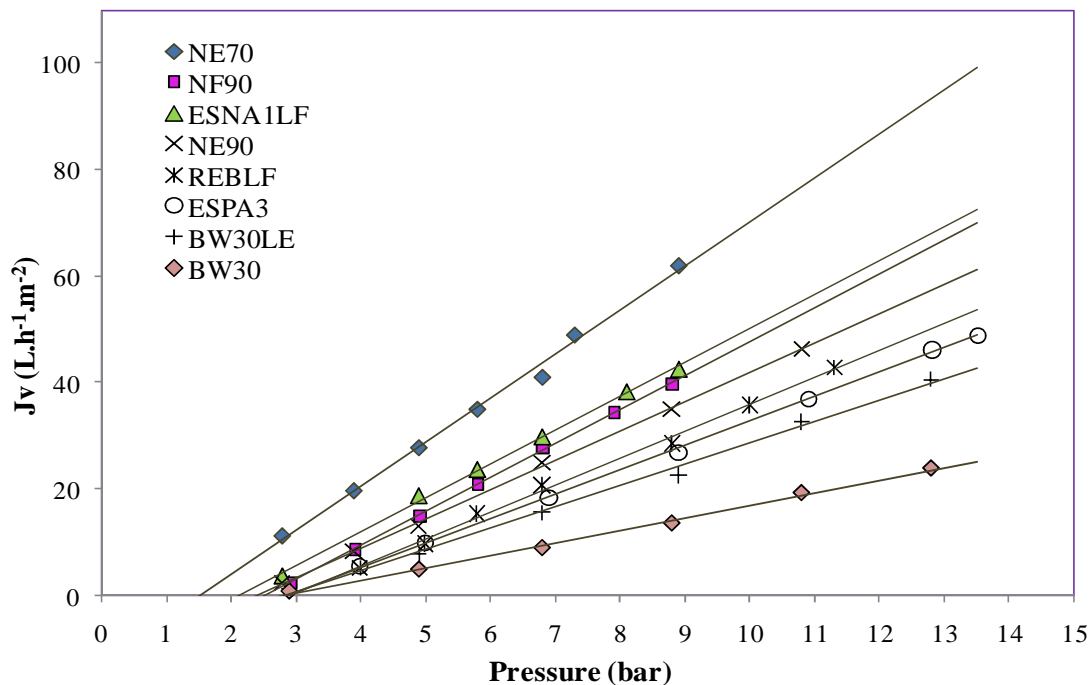
Figure 44: *Flux as a function of the applied transmembrane pressure for NF and LPRO membranes (Tan Tan Water TDS= 4000mg/L), pH = 7,9, T=21°C)*

The permeate flux increase linearly with the applied driving force, namely pressure, indicating that the increase in operating pressure will enhance the driving force and then overcome the membrane resistance. The permeability of the membranes follows this order: NE70 > NF90 ≈ ESNALF > NE90 > REBLF > ESPA3 > BW30LE > BW30. The permeability and critical pressure values obtained with Tan Tan brackish water are reported in Table 35 for the different membranes characterized. As expected, the permeability of NF membranes was higher than that of LPRO membranes. This is consistent with the results that NF membranes usually have higher water flux than RO membranes since the surface of RO membranes are denser and tends to be more compacted. The NE70 showed the highest flux, while the LPRO membrane BW30 showed the lowest permeate flux. The permeability of the NE70 was about 70% higher than the BW30 membrane. The NF90 and ESNA1LF membranes permeabilies were 60% higher than the BW30. The REBLF membrane (LPRO) tends to be similar to NF membranes in behavior, as it has nearly the same permeability as the NE90 membrane, followed by the ESPA3 and BW30LE membranes.

Table 35: *Permeability (Lp') to Tan Tan water and critical pressures (Pc) for the NF and LPRO membranes*

Membrane		Lp' (L.h^{-1}.m^{-2}.bar) ($\pm$0.4)	Pc (bar) ($\pm$0.2)
NF	NE70	8.2	1.5
	NF90	6.4	2.5
	ESNA1 LF	6.3	2.1
	NE90	5.5	2.4
LPRO	REBLF	5.1	3.0
	ESPA3	4.6	2.9
	BW30LE	3.9	2.8
	BW30	2.4	3.0

The NF membranes could run at a low pressure of 1.5bar for the NE70 and under 2.5bar for the other NF membranes, while LPRO membrane started desalting at pressure of 3bar.

2.3.2 Water quality

Research was conducted to evaluate the ability of NF studied membranes on Tan Tan brackish water desalination and to select the NF which can overlap with the selected LPRO membranes performances and achieve the required salt rejection at lower pressures and higher fluxes. Thus, the various NF and LPRO were tested to evaluate how each membrane performs and how permeate quality is impacted by various factors that affect performance (Recovery rate, feed and permeate flow and pressure). The understanding of these factors will provide guidelines into optimization and full scale design.

The desalination characterization of LPRO/NF modules were done under the following operating conditions:

● Recovery rates from 10% to 90%.

● Permeate flow: 0.1, 0.15 and 0.2 m^3.h^{-1} which corresponds to a permeate flux of 13, 20 and 26 L/m².hr

● Feed temperature: 21°C

The required working pressures for the desalination of Tan Tan brackish water and the chemical analysis of the permeate obtained after the treatment by the various NF and LPRO membranes are summarized in (Appendix A1-A8)

The retention data were expressed as the TDS in the permeate, the ion rejection

2.3.2.1 Permeate TDS

The results of permeate total salinity, for the investigated membranes at different recovery rates and different permeate flow are shown in figure 45. The horizontal line in this figure is the WHO limit (1000 ppm TDS). This target is achieved for:

- All the LPRO membranes over the entire recovery rates and flow rates investigated,
- The nanofiltration membranes NF90 and NE90 practically over the entire range of recovery ratio and flow rates investigated; except at low permeate flow (0.1 m^3.h^{-1}) and high recovery rate (90%)

The 1000 ppm TDS target was not achieved with the NE70 and ESNA1LF membranes at any of the tested conditions.

We can see from this figure that membrane characteristics affect permeate quality and consequently retention. The highest rejections are obtained for the LPRO membranes which have tighter structures. Salts rejection is higher in the range of NF membranes for NF90 and NE90 membranes and is close to the LPRO membranes rejection. As explained in the first part, these membranes are the most compact and their mass transfer behavior is close to RO membranes. The most open structure was characteristic of the ESNA LF and the NE70 which shows the lowest rejections.

The permeate quality is improved with increasing permeate flow which is a consequence of increasing operating pressure. The ion permeation is only a function of feed concentration and is independent on the operating pressure.

The recovery rate influence the amount of water produced; the permeate's total salinity increased with increasing recovery rate. This effect is caused by low tangential flow across the membrane (low Q_{feed}) at high recovery rates as well as the retained salt which accumulates in the boundary layer. This effect is most pronounced for the BW30 membrane. Due to feed pressure limitation on the pilote unit, the recovery rates reached with this membrane were limited to 70% at permeate flow rates higher than 0.15 m^3.h^{-1}. The higher retention of the BW30 increases the concentration of the concentrate and then the osmotic pressure. Thus very little permeate flux is produced.The influence of increasing recovery rate is least pronounced for the NE70 membrane primarily because of lower rejection.

Generally, the membranes tested shows the best salt rejection performance at low recovery rates and high permeate flow (Y = 10% and Q permeate = 0.2 m^3.h^{-1}), while the lowest rejection values for each membrane was obtained at high recovery rates and low permeate flow (Y = 90% and Q permeate = 0.1 m^3.h^{-1}). The NF and LPRO membranes performances can be compared and more discussed using the lowest and the highest rejection values for each membrane. These values are summarized in Table 36.
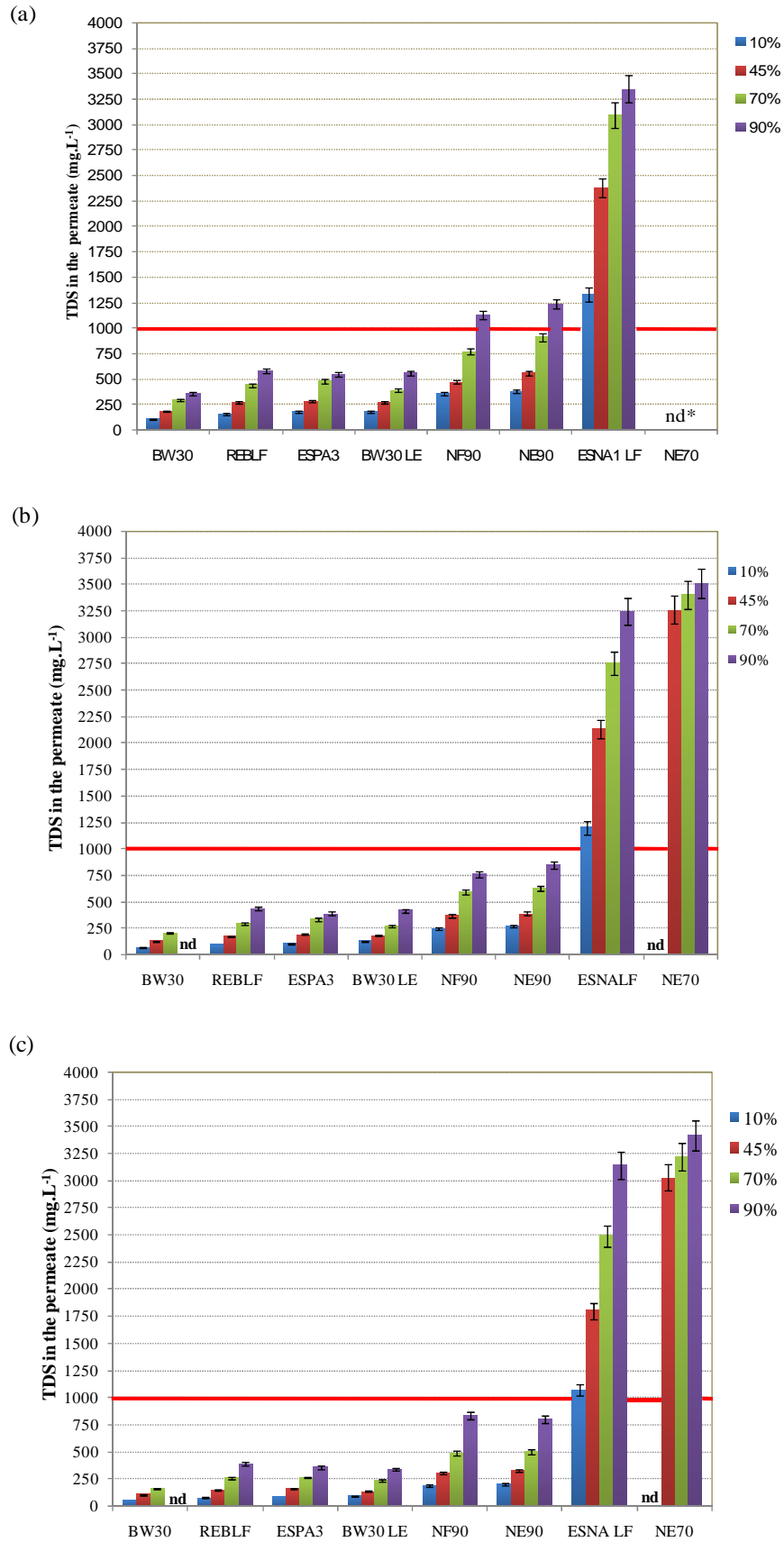
Figure 45: *Permeate total salinity at different recovery rates and different permeate flows/fluxes (a)0.1 m³.h⁻¹/ 13 L/m²-hr, (b) 0.15 m³.h⁻¹/20L/m²-hr, (c) 0.2 m³.h⁻¹/26 L/m²-hr; for the NF and LPRO membranes (T = 21°C, pH=7.9, TDS = 4000 mg/L) (*nd : not determined)*

Table 36 : Performance of the studied membranes for desalting of Tan Tan brackish water in terms of TDS rejection

Membrane		Total salinity in the permeate (mg/L)	TDS rejection rates (%)
NF	NE70	3330 - 3520	12 – 17
	NF90	190 - 1130	72 - 95
	ESNA1 LF	1070 - 3350	17 – 74
	NE90	200 - 1240	70 - 95
LPRO	RE BLF	78 - 578	88 - 98
	ESPA3	88 - 550	87 - 98
	BW30LE	95 - 560	86 - 98
	BW30	54 – 360	90 - 99

TDS rejection was better with the BW30 membranes for various operating conditions; the permeate TDS was between 54 and 360 ppm which corresponds to a TDS rejection of 99% to 90% respectively. The water produced with this membrane needs to be mixed to feed water to meet the minimum permeate TDS limit for drinking water.

The other LPRO membranes REBLF, ESPA3 and BW30LE showed more or less the same high capacity in the rejection of total salinity, but showed lower rejections compared to the BW30 membrane. The REBLF membrane which may be considered as a representative of the group shows a rejection rate from 86% to 98%. The permeate TDS from this membrane are 78 and 578 ppm. These LPRO membranes allows the production of appropriate water directly at high recovery rates and low permeate flow, while a remineralisation of produced water is needed at low recovery rates.

The reduction in TDS in Tan Tan water caused by the NF membranes varied over a wide range from one NF membrane to another. The NF90 and NE90 membranes have more or less the same high capacity in the rejection of total salinity and shows the best performances compared to the other NF membranes. The TDS in the permeate from both NF90 and NE90 membranes are between 200 and 1200 ppm for a percentage reductions in feed TDS of 95% and 70% respectively. These membranes can overlap with LPRO membranes; their efficiency to desalinate Tan Tan water is close to the BW30LE, ESPA3 and REBLF membranes. The NF90 and the NE90 can be used for a partial demineralization of Tan Tan brackish water and are more suitable for directly producing drinking water.

In comparison with the NF90 and NE90 membranes, the ESNA1LF membrane shows lower performance. The TDS in the permeate from the ESNA1LF membrane is moderate at low recovery rate and that is very low at high conversion rates. The percentage reductions in feed TDS from this membrane are17% and 73% for a total salinity in the permeate between 1070 and 3300 ppm. The NE70 membrane shows the least performance of all the membranes; it allows a rejection rate of 13% and 25%.

2.3.2.2 Ions removal

A similar trend is observed when an elemental analysis of the permeate samples is taken. Fig. 46 and Fig.47 show the rejection rates of divalent and monovalent ions respectively for all the tested membranes at a recovery rate of 70% and a permeate flow of 0.2 $m^3.h^{-1}$. These Figures show that LPRO membranes retained all ions to the highest degree. The divalent ions SO_4^{2-}, Mg^{2+} and Ca^{2+} are retained at > 98% and monovalent ions at > 95%, except for the NO_3^- which is retained at 80%.

The nanofiltration membranes NF90 and NE90 show the same tendency as LPRO for the divalent ions rejection. Using these NF membranes, retentions higher than 98% were found for SO_4^{2-}, Mg^{2+} ions. A rejection of 90% was found for calcium. The monovalent ions Na^+, Cl^-, K^+ and F^-, are well retained > 80%. The NO_3^- is not as well retained as other monovalent ions with a rejection value of 30%.

While the overall values are nearly similar for LPRO and both NF membranes for divalent ions, the distinction is clearer for the NF90 and NE90 membranes which are expected to be selective between mono-and divalent ions.

In the case of ESNA1LF and NE70 membranes, two distinctive retention patterns are observed. Firstly Mg^{2+} is retained at 95% and SO_4^{2-} with Ca^{2+} at 70%. Secondly, the monovalent ion retention is consistently lower; Na^+, Cl^-, K^+ and F^-, are retained at 40% for the ESNA1LF membrane while the retention of these ions by the NE70 membranes is about 20%.
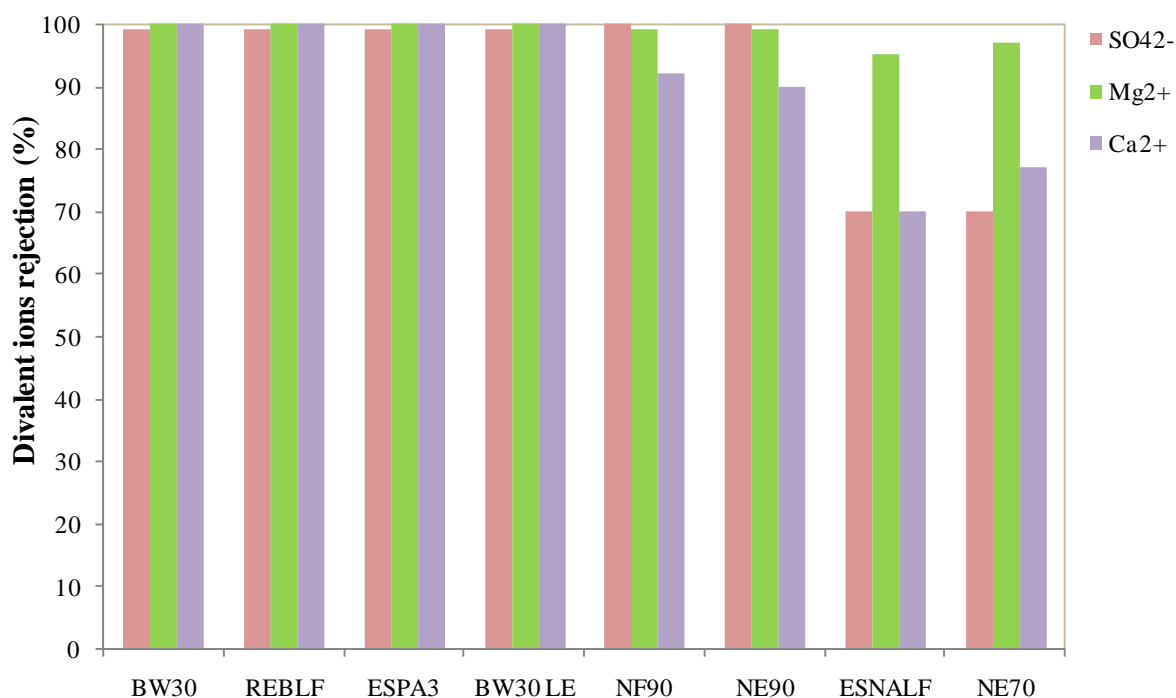
Figure 46: *Dependencies of retention coefficients of selected divalent ions on the membrane type (Y = 70%, T=21°C, Q $_{permeate}$ = 0.2 $m^3.h^{-1}$/ Flux = 26 L/m².hr)*
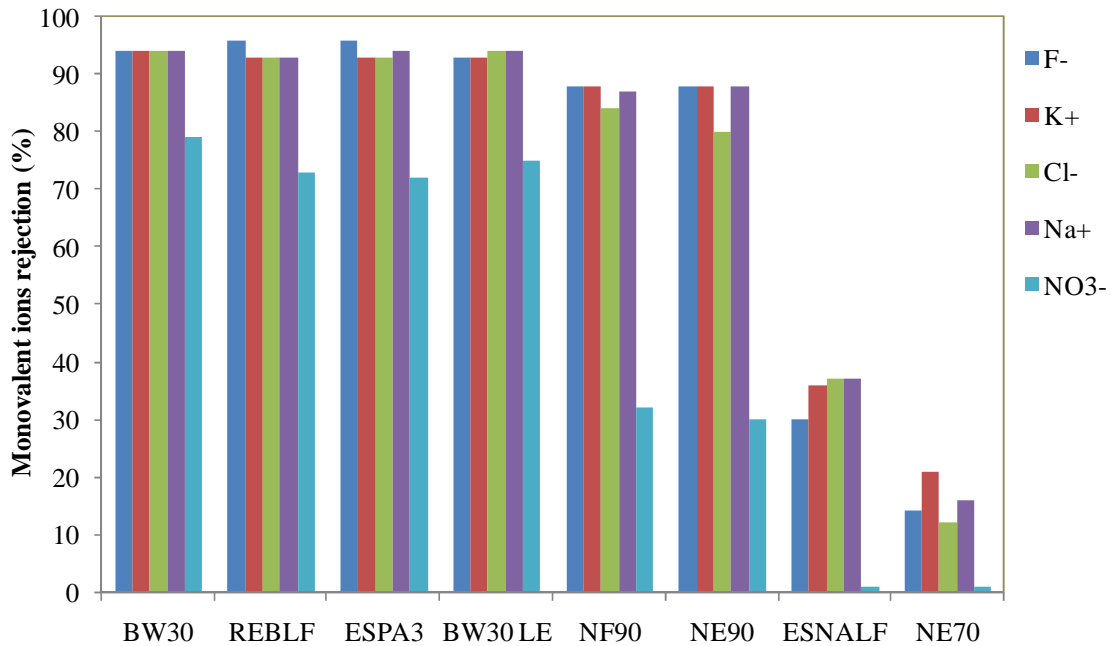
Figure 47: *Dependencies of retention coefficients of selected monovalent ions on the membrane type (Y = 70%, T=21°C, Q $_{permeate}$ = 0.2 m^3.h^{-1}/ Flux = 26 L/m².hr)*

Tables A1-A8 (see Appendix) summarize the concentration of the various monovalent and divalent ions in the permeate for all the investigated membranes.

As shown in Table 28, the concentrations of Mg^{2+}, NO_3^- , K^+ and F^- ions in Tan Tan brackish water are well below the drinking-water guidelines. After the treatment of these ions by the NF and LPRO membranes, their concentrations were more reduced and met the product water quality criteria.

The concentrations of Ca^{2+}, SO_4^{2-}, Cl^- and Na^+ in Tan Tan water exceed drinking water guidelines. The permeate chemical analysis results for these elements are further discussed below.

Sulfate and calcium removal:

In all cases, the treatment of Tan Tan water by the LPRO, NF90 and NE90 membranes, allowed the reduction of SO_4^{2-} content from 500 ppm to less than 10 ppm in the permeate, and the Ca^{2+} concentration from 270ppm to less than 20 ppm. Thus, the use of the NF90 and NE90 membranes was very efficient to remove the water hardness, which is mainly caused by calcium.

Chloride removal:

Chloride is the major ion in Tan Tan water with a concentration greater than 1200 ppm. The WHO established a recommended level of 250 mg /L for this element. It was shown in Fig.5 that Cl^- rejection values for LPRO membranes were similar and high to achieve the WHO limit, while nanofiltration membranes were capable of variable retention of Cl^- ion. In order to elucidate the suitability of the NF membranes for Cl^- removal, the results of the permeate chemical analysis for these element are presented in Fig.48. This figure shows the influence

of the type of membrane and different operating conditions on Cl⁻ removal compared to the WHO limit.
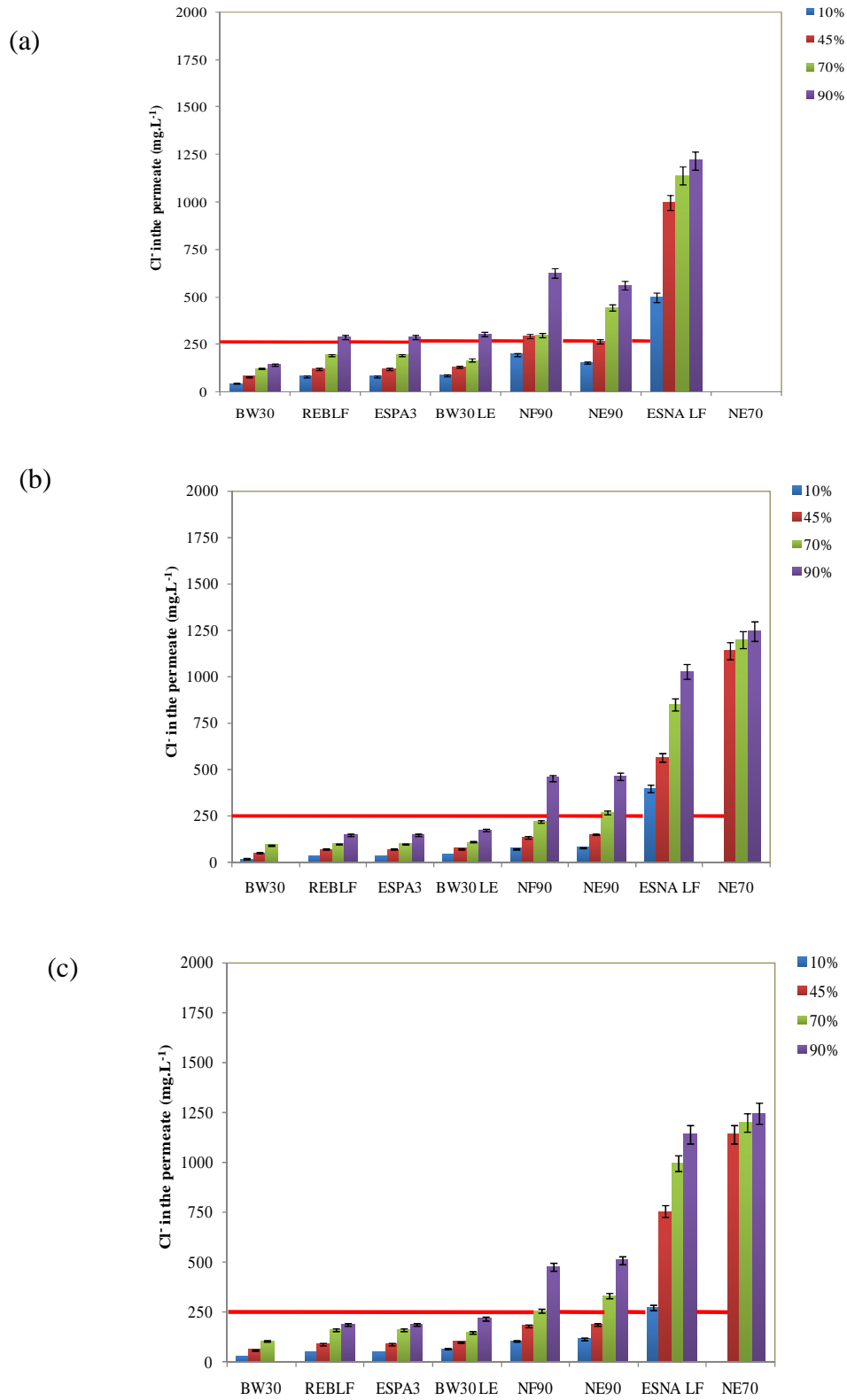
Figure 48: *Chloride concentration in the permeate at different recovery rates and different permeate flows/Fluxes (a)0.1 m³.h⁻¹/ 13 L/m²-hr, (b) 0.15 m³.h⁻¹/20 L/m²-hr, (c) 0.2 m³.h⁻¹/26 L/m²-hr, for the NF and LPRO membranes (T = 21°C, pH=7.9, TDS = 4000 mg/L)*

118

As in TDS rejection, this target is achieved for all the LPRO membranes at the entire recovery rates and flow range investigated. For the nanofiltration membranes NF90 and NE90 the WHO limit for Cl⁻ was respected at practically the entire recovery rates and flow range investigated except at high recovery rate (90%) and low permeate flow (0.1 m³.h⁻¹). For the NE70 and ESNA1LF, the Cl⁻ concentration in the permeate exceed the WHO limit at the entire recovery rates and flow range investigated.

Sodium removal

Tan Tan water contains Sodium at a concentration of 761 ppm. The WHO established a recommended level of 200 mg /L for this element. The results of sodium concentration in the permeate for different membranes are presented in Fig.49. This figure shows the influence of the type of membrane and different operating conditions on Na$^+$ removal compared to the WHO limit.

These results show that all the LPRO membranes can meet a sodium concentration lower than 200 mg/L. As for TDS and Cl⁻ removal, the NF90 and NE90 membranes were able to achieve the WHO limit for Na$^+$ at all operating conditions. An exception was found at high recovery rate (90%) and low permeate flow (0.1 m³.h⁻¹). The Sodium was less retained by the NE70 and ESNALF membranes; the Na$^+$ concentration in the permeate exceeded the WHO limit at the entire recovery rates and flow range investigated.
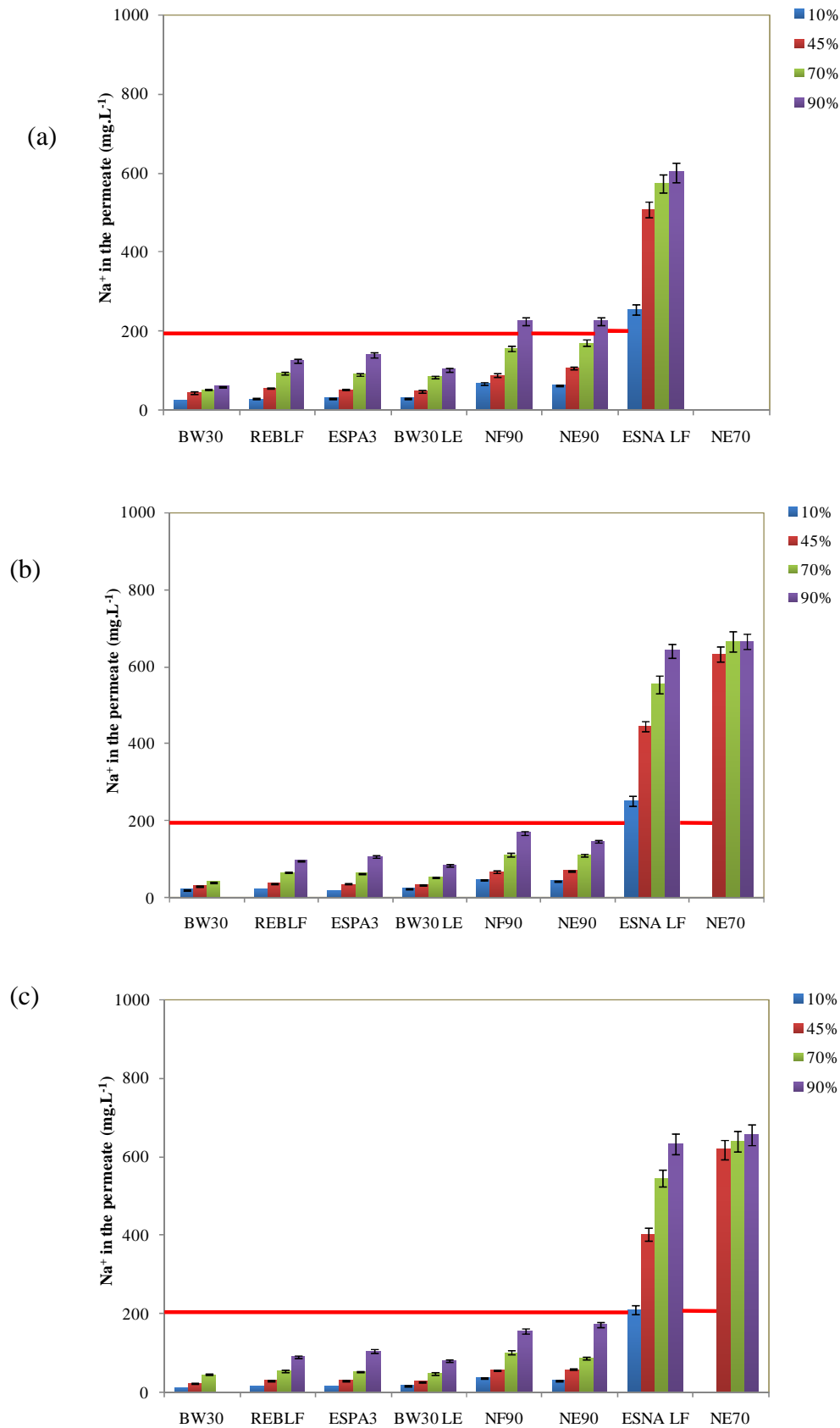
Figure 49: *Sodium concentration in the permeate at different recovery rates and different permeate flows/Fluxes (a)0.1 $m^3.h^{-1}$/ 13 L/m²-hr, (b) 0.15 $m^3.h^{-1}$/20 L/m²-hr, (c) 0.2 $m^3.h^{-1}$/26 L/m²-hr, for the NF and LPRO membranes (T = 21°C, pH=7.9, TDS = 4000 mg/L)*

120

2.3.3 Working pressures

The production rate of permeate in a nanofiltration and reverse osmosis process is proportional to the net driving pressure. The required pressures to desalt Tan Tan water for different investigated membranes were evaluated here. The pressure applied was fixed by a specific recovery ratio and permeate flow frate. Figure 50 shows the required working pressures for the NF and LPRO membranes under study, at different recovery rates and different permeate flow rates. From figure 50, we can see that the applied pressure increases with increasing permeate flow and recovery ratio. The permeate flux increases linearly with the operating pressure. So the applied pressure needed to overcome the membrane resistance becomes higher with an increase in the permeate flow. Recovery can be interpreted as system efficiency regarding the flow. This operating parameter is inevitably a result of set Q_{feed} and $Q_{permeate}$; it increases with increasing permeate flow, which is a result of increasing applied pressure.

The pressure required at a definite permeate flow and recovery rate depend on the membrane. Figure 50 shows that The LPRO membranes needs higher pressure to desalt Tan Tan brackish water compared to NF membrane. The higher retention increases the working pressure required due to the osmotic pressure build up. In nanofiltration, salts are only partially rejected so that the concentration difference between feed and permeate is smaller than for a complete rejection. This is an advantage for NF: osmotic pressures are lower compared to reverse osmosis, so that lower pressures need to be applied, and the energy consumption is proportionally lower. Also, the operating pressures for a high permeability membrane are smaller than for a comparatively lower permeability membrane (LPRO).

The highest operating pressures were found for the BW30 membrane which allows high rejection rates and has a lower permeability. The pressures applied for this membrane are two or three times higher than those for NF membranes. On the other hand, the LPRO membranes, REBLF, ESPA3 and BW30LE allow the desalination of Tan Tan water at pressures comparable to those applied in nanofiltration (< 14 bar). These membranes operate at the interface of nanofiltration and reverse osmosis.

The NF90 and NE90 membranes can achieve high TDS rejections at lower pressures (< 11 bar). The lowest TDS rejections rates were obtained with the ESNA1LF and NE70 membranes, this reason can be used to explain the lower operating pressures that was observed with these membranes compared to the NF90 and NE90 membranes.
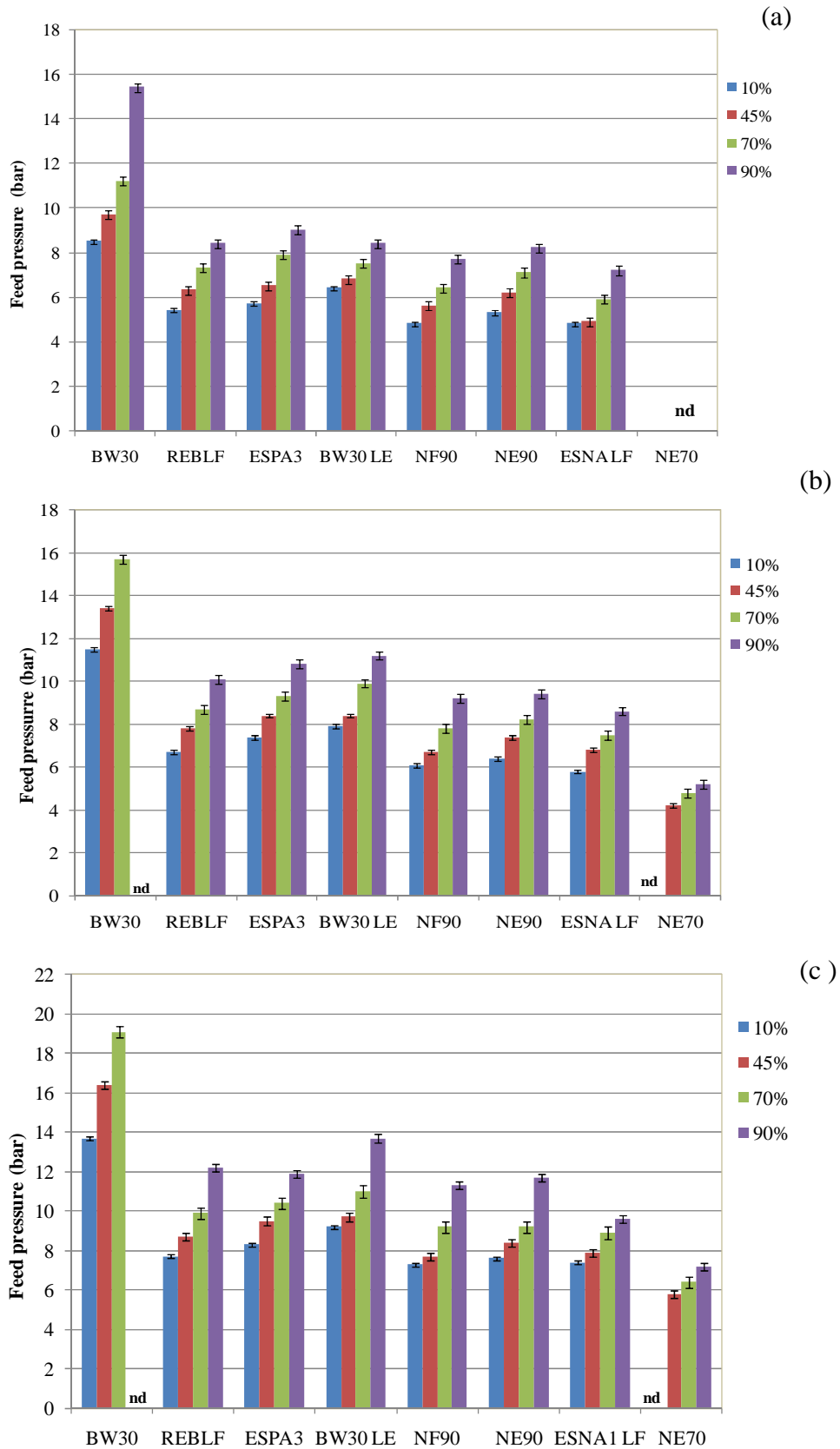
Figure 50: *Required pressures for desalination of Tan Tan water for the NF and LPRO membranes studied at different recovery rates and permeate flows (a) 0.1 m³.h⁻¹, (b) 0.15 m³.h⁻¹, (c) 0.2 m³.h⁻¹ (T=21°C, pH = 7.9)*

(nd *) The required working pressure was higher than 20 bar for the BW30 and lower than 4 bar for the NE70; it was not possible to work under this pressure conditions with the pilot unit.

2.3.4 Specific energy consumption

The specific energy consumption (SEC) is what ultimately determines the cost of the system as energy requirements (Schäfer *et al.* 2007). The variation of the SEC at different permeate flows and a selected recovery rate of 70% is plotted in Figure 51.
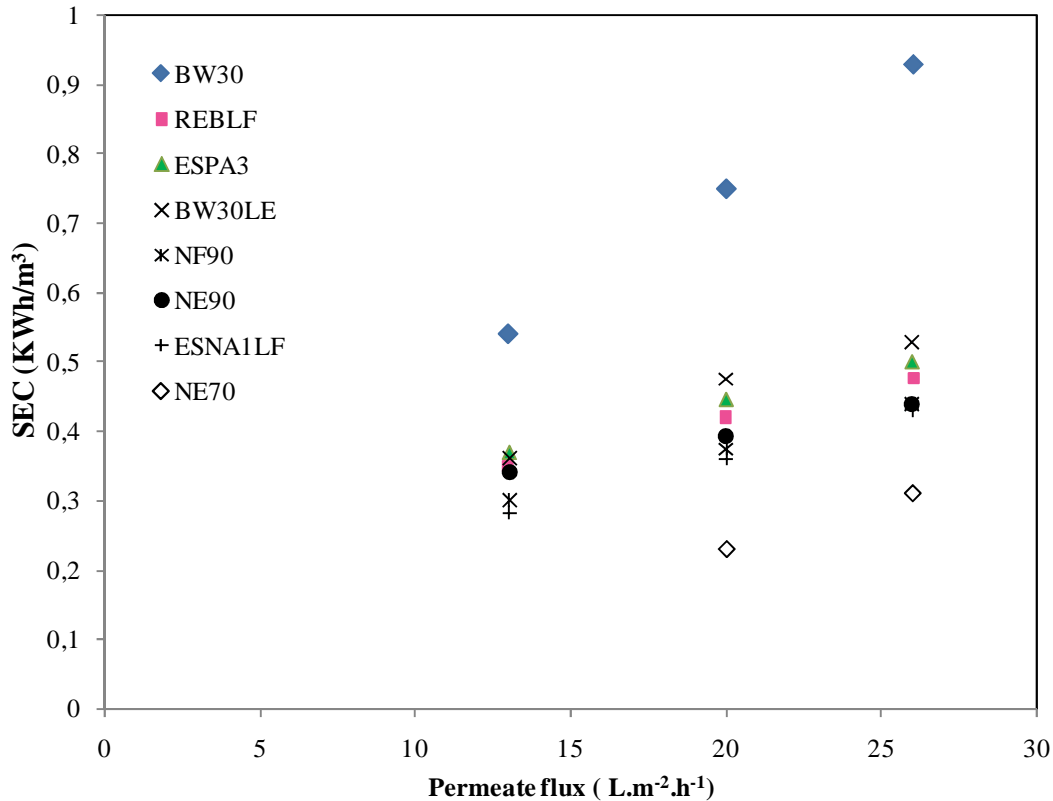
Figure 51: *Specific energy consumption (SEC) as a function of permeate flux for NF and LPRO membranes studied (Y = 70%, pump efficiency = 80%, T=21°C, TDS = 4000 mg/L)*

Energy requirement increase linearly with increasing permeate flow which is a result of increasing pressure. The electricity consumed for membrane filtration is proportional to transmembrane pressure. Maximum SEC values were found for BW30 membrane (from 0.54 to 0.93 kWh/m^3) followed by the other LPRO membranes (from 0.35 to 0.53 kWh/m^3).The higher rejection increases SEC due to the osmotic pressure increase (Schäfer *et al.* 2005). As a consequence, the required pressure increases and also the energy consumption.

The system does not require much energy with NF membranes due to a lower operating pressure. The NF90, NE90 and ESNA1LF membranes have more or less similar SEC values ranging from 0.34 to 0.43 kWh/m^3. Minimum SEC values are from 0.23 to 0.31 for the NE70 membrane.

2.3.5 Partial conclusion

In summary, the filtration results allow to clarify the difference between NF and LPRO membranes as for their desalination performances of the brackish water in Tan Tan.

The LPRO membranes sharply reduced the content of salts present in Tan Tan water (rejections > 90%). After treatment, the obtained permeate has a low value of TDS, especially

with the BW30 membrane, so the water produced with this membrane can be mixed to feed water to meet the minimum permeate TDS limit for drinking water. The results obtained for the REBLF; high salt rejection with relatively high permeability compared to other LPRO membranes, indicates that this membrane is an ultralow-pressure reverse osmosis membrane.

NF was observed to be an effective method to perform partial desalination of Tan Tan brackish water. The degrees of mineral salt removal with the NF90 and NE90 membranes was 72–95% and was dependent on the value of the recovery rate and permeate flow. These membranes have also shown their ability to reject both monovalent and divalent of Tan Tan water with very reasonable values which respect the WHO limits. On the contrary, NE70 and ESNA1LF membranes produced relatively very low rejection of salts indicating inappropriateness of theses membranes for the desalination of Tan Tan water.

The evaluation of pressure required for all the membranes permits to conclude that the tighter the membrane, the higher ΔP required. In this case, looser membranes are better since lower pressures are required to provide a very good permeate fluxes, if the membrane rejection can fulfill the requirement. Only the NF90 and NE90 membranes can meet the rejection requirement at higher permeate fluxes and lower applied pressures. The NF70 and ESNALF fail to provide the level of rejection, and then it will not be considered at all.

The energy consumption study showed that the NF90 and NE90 membranes require minimum energy consumption, compared to the LPRO membranes. These membranes are very effective for Tan Tan water demineralization respect the WHO limits. It is worth mentioning that lower energy consumption was obtained at high rejection level for the REBLF, ESPA3 and BW30LE membranes compared to the BW30 membrane.

The NF90 and NE90 membranes were observed to be effective to perform partial desalination of Tan Tan brackish water (TDS = 4g/L). In order to check the potential of these membranes on filtration of moderately brackish waters (TDS < 10 g/L), other filtration experiments were performed to clarify the limits of application of NF membranes on brackish water desalination. Further experiments were carried out with the NF90 and NE90 membranes to evaluate the performance of these membranes on brackish water defluoridation. These experiments will be addressed in the next section.

2.4 Possibilities of replacement of the BW30 membrane

In view of the positive and encouraging results obtained on pilot plant scale, trial on replacement of the existing BWRO membrane BW30 on a demonstration plant is essential.

The pilot results have shown that the ulta LPRO membrane REBLF, and the NF membrane NF90 are technically and economically favorite to replace the BW30 membrane. These membranes presented a combination of advantages in terms of permeability, working pressures, permeate quality and SEC for Tan Tan water desalination.

The REBLF membrane showed the highest rejection levels with high permeability. This membrane is also operable at ultralow pressures and allowed the desalination of Tan Tan brackish water at pressures and SEC comparable to those of nanofiltration. Table 37 sums up the performance of this membrane in terms of permeate quality, working pressure,

permeability and Specific energy consumption compared to the BW30 membrane and the NF membrane NF90.

Table 37: *Summury of the BW30, REBLF and NF90 membranes performace in Tan Tan water desalination at a recovery rate of 70% and a permeate flux of 26 L.h^{-1}.m^{-2}*

Membrane	Permeability (L.h^{-1}.m^{-2}.bar)	Working pressure (bar)	Permeate TDS (mg/L)	SEC kWh/m^3
NF90	6.4	9.2	490	0.44
REBLF	5.1	10	260	0.48
BW30	2.4	19	165	0.93

The NF90 membrane is the best NF membrane for Tan Tan water demineralization. Table 37 shows the remarkable closeness of the NF90 membrane performance to the REBLF membrane. The permeability of the NF90 membrane is higher, with relatively lower working pressures and energy consumption. However, the TDS of permeate solution is 2 times lower for the REBLF membrane compared to the NF90 membrane. Thus, more quantity of raw water will be utilized for blending with the REBLF permeate compared to the NF90 to produce exported water meeting the WHO standards.

The pilote study proved the effectiveness of the NF membrane, NF90, for desalination of Tan Tan brackish water. The results also proved that the ultraLPRO membrane REBLF can be used to desalinated Tan Tan water at lower pressure than the BW30. Benefits can be gained using both membranes. To select the best membrane to replace the BW30, the work can be continued by upscaling the processes from a pilot plant scale, in which 4"x40" membrane elements were utilized to a demonstration unit, in which large commercial size 8"x40" membrane elements are utilized. The translation of the findings obtained from a pilot scale to a plant scale should take various operating variables into careful consideration such as: maintain of steady operation over time, system arrangement, cleaning frequency.

2.5 Simulation performance

In recent years, reverse osmosis has increasingly gained significance in water desalination. One main reason for large scale applications of RO membranes is that the commercial simulation software for the RO process has been very mature, such as IMSdesign (Hydranautics), ROSA (DOW) and CSMPRO (Saehan). The simulation software helps consumers to save large numbers of preliminary experiments, but it cannot be applied to design the "loose RO", that is NF process, due to the effect of salt concentration is not considered (Wang *et al*. 2006). To increase efficiency in NF development, it has become essential to use calculation tools in conjunction with the process in question.

Since there is a scarcity of backup simulation programs, which allow operating conditions to be estimated, the essential design parameters are often determined using pilot plants in a time-consuming and cost-intensive manner. Moreover, a great deal of uncertainty is involved in designing industrial membrane processes if testing on a pilot scale is not conducted. In most cases, optimization during the pilot phase is mostly based on the empirical method, involving

the special know-how of the user. This also results in a lengthy period of process development.

The simulation software is no replacement for practical tests on a pilot scale and the design of a membrane plant by an expert. The objective in this case is to evaluate the precision of the membrane suppliers projection softwares and to estimate the ability of these tools to predict the membrane performances.

The process simulation tools (ROSA, CSMPRO and IMSdesign) were used in this study to predict the performance of NF and LPRO elements for treating Tan Tan brackish water. The results from the process simulation were verified by experimental results gained with the pilot unit for Tan Tan water. The simulations were performed with eight (4x40) modules: NF90, NE90, ESNALF, NE70, BW30, BW30LE, REBLF and ESPA3. The modules performance was evaluated in terms of permeate water quality. Projections were performed with the following assumptions:

➢ Average water temperature of 21°C
➢ Use of the same operating conditions used in the pilot tests (see Table 13) with one stage and one pressure vessel
➢ Pump efficiency = 80%

The simulation results for all the membranes are reported in Tables A9-A16 (see Appendix).

The simulations were compared to the pilot unit results especially with regard to the permeate TDS and working pressure as indicated in Fig. 52 and Fig 53 respectively, at a permeate flux of 26 $L.m^{-2}.h^{-1}$ and a recovery ratio of 70%.

The figures 52 and 53 give the simulation results of various simulation softwares that show the tendencies in terms of permeate TDS trends and the applied pressures.

The simulation results with ROSA software were in the same order of magnitude as those obtained in the pilot tests for the NF90, BW30 and BW30LE modules. The permeate TDS and the working pressures simulated match closely the experimental results.

The CSMPRO softwere was not successful to predict the performance of the NE90, NE70 and REBLF elements. The permeate TDS projected for the NE70 and the REBLF modules were 2 times higher than real results. On the other hand, the permeate TDS projection for the NE90 membrane was in a good agreement with measured values. The working pressures simulated with Saehan software were at least 2 times higher than the measured values.

In the case of ISMDesign, the closeness of working pressures projections to the experimental findings is remarkable. On the contrary, the permeate TDS projections was 2 times higher than the real results.
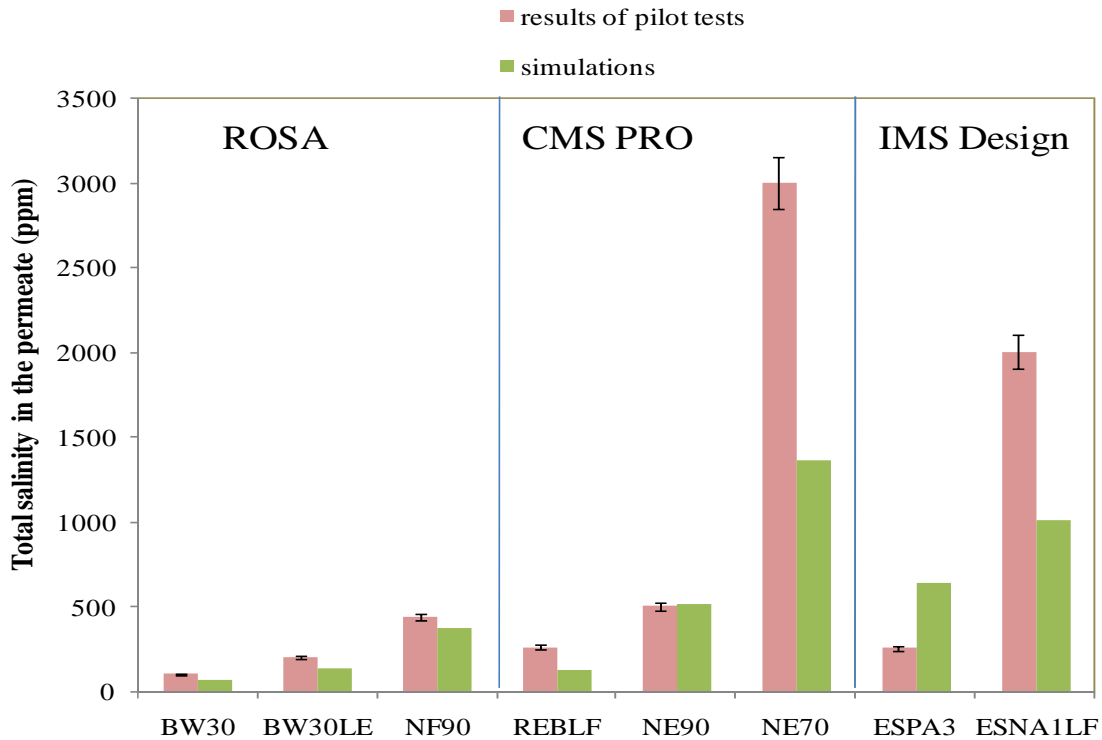
Figure 52: *Comparison of the simulation results of the permeate TDS obtained using ROSA, CMSPRO and IMSDesing softwares with the experimental results for the NF and LPRO membrane (Y= 70%, T=21°C, permeate flow/Flux= 0.2 $m^3.h^{-1}$/26 L/m²-hr,TDS = 4000 mg/L)*
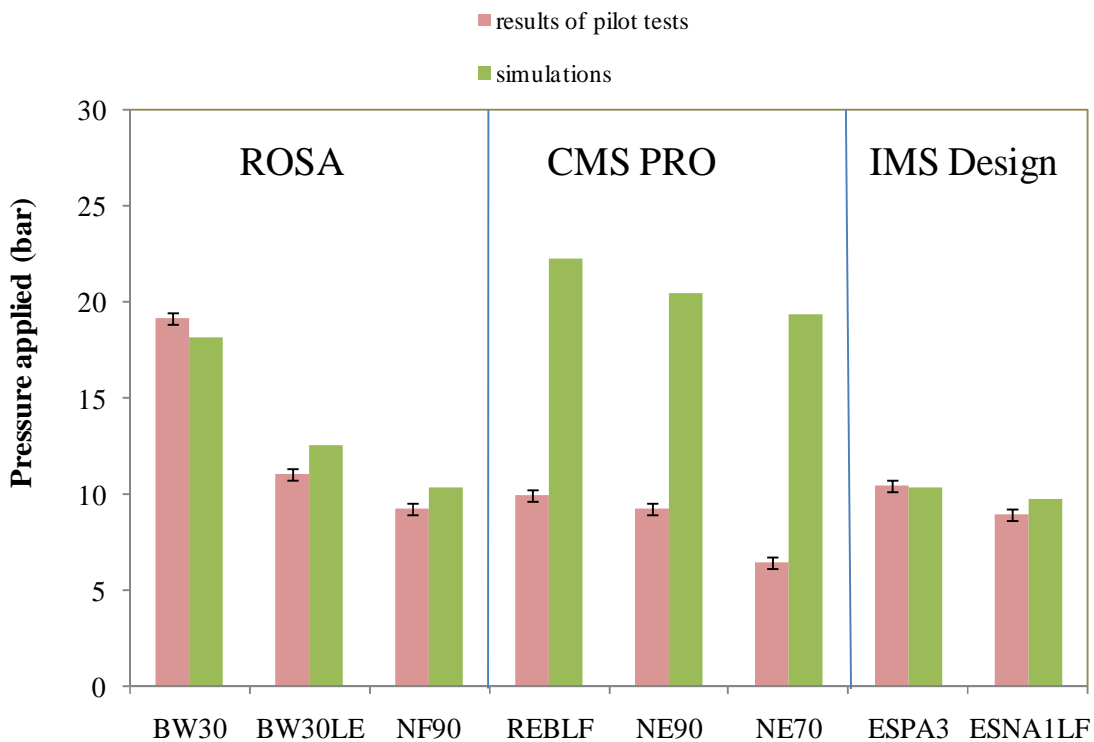
Figure 53: *Comparison of the simulation results of working pressure obtained using ROSA, CMSPRO and IMSDesing softwares with the experimental results for the NF and LPRO membrane (Y= 70%, T=21°C, permeate flow/Flux= 0.2 $m^3.h^{-1}$/26 L/m²-hr,TDS = 4000 mg/L)*

The use of ROSA software for the prediction of DOW, NF/RO elements performances proved successful. It can perform simulation of whole variations of recovery rate, feed and permeate flow used in this investigation. The performance predications it gave showed good agreement with measurements taken from the pilot tests.

ROSA software gives a good level of confidence in the prediction of pressure required for filtration and permeates total salinity compared to the other sofwares studied (IMS Design and CSMPRO3). The use of ROSA can help process designers in planning, designing and optimizing NF/RO processes, when using DOW elements.

2.5 Tan Tan water doping tests

2.5.1 Desalination by NF and RO of moderately brackish waters

The possibilities of producing drinking water from brackish water of high salinity levels using NF and RO processes were investigated. Through this study, we tried to evaluate the salinity effect on the performance of different NF and LPRO elements. The most effective NF membranes on Tan Tan brackish water desalination (NF90 and NE90) were used in this stage of the research. The performances of these membranes will be compared to those of the LPRO membranes, BW30 and REBLF. The chosen membranes were tested at two salinity levels, i.e. 6 and 10 g.L^{-1}. Tan Tan brackish water was spiked with sodium chloride until the desired concentration was achieved. At first, the water permeability of the membranes with both types of brackish water was investigated. After that, membranes performances in terms of TDS rejection, required pressures and energy requirements were studied with high salinity brackish water samples. These experiments were carried out at a recovery rates ranged from 10 to 70%. The permeate flow was kept constant at 0.2 m^3.h^{-1}.

2.4.1.1 Water productivity

Each membrane has a specific permeability for a given values of temperature and feed water salinity. The variation of membrane permeability with feed water salinity was investigated. Increase of the feed water salinity involved a decrease of membranes permeabilities as clearly seen in Fig.54. The permeability and critical pressure values obtained with Tan Tan brackish water and water doped for high salinity are reported in Table 38 for the NF90, NE90, REBLF and BW30 membranes.

Table 38 : *Permeability (Lp'') and critical pressures (Pc) of the NF90, NE90, REBLF and BW30 membranes with Tan Tan water doped at two salinity levels*

Membrane	Tan Tan water		Tan Tan water doped at 6g/L		Tan Tan water doped at 10 g/L	
	Lp'' (L/h.m^2.bar)	Pc (bar)	Lp'' (L/h.m^2.bar)	Pc (bar)	Lp'' (L/h.m^2.bar)	Pc (bar)
NF90	6.4	2.5	5.9	3.6	5.3	4.9
NE90	5.5	2.4	4.8	4.2	4.1	6.1
RE BLF	5.1	3.0	4.6	5.0	3.9	6.8
BW30	2.4	3.0	2.1	4.6	1.9	7.4
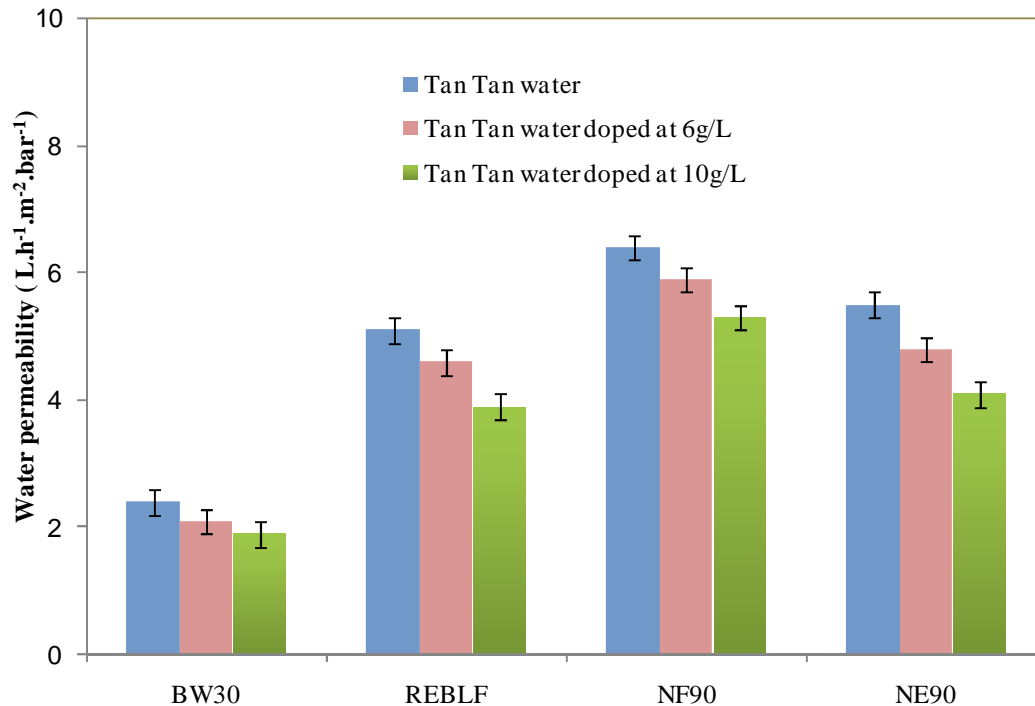
Figure 54: *The water permeability of the NF90, NE90, REBLF and BW30 membranes at different salinity levels (T=21°C)*

Salinity influences membrane permeability and transmembrane osmotic pressure. In both cases it leads to an increase of the critical driving pressure (Pc). The salinity effect follows a general trend for all membranes tested.

As expected, the water permeability was higher when operating with NF membranes. It was about three times higher for the NF90 membrane compared to the BW30 membrane at all salinity levels. The permeability of the REBLF membrane is slightly lower than the NE90 membranes at all salinity levels and is two times higher than the BW30 membrane permeability. The critical pressures for the higher flux membranes are smaller than for the low flux membranes. Thus, if the salt rejection of NF membranes is high enough in high salinity brackish water desalination, NF membranes are preferred to LPRO membranes. The higher permeability and lower critical pressures can be a cost advantage of NF membranes.

2.5.1.2 TDS reduction

The effect of feed water salinity on TDS reduction was investigated by adding different concentrations of NaCl to Tan Tan brackish water. Fig. 55 shows that the increase of salinity level decreases the TDS in the permeate and then the retention coefficient of all the membranes. Figure 55 also shows the dependencies of retention coefficients of TDS on the membrane type. Table 39 summarizes the permeate TDS values obtained with the different membranes at three levels of salinity (4, 6 and 10g/L) and three recovery rates

Table 39: *Performance of the studied membranes for desalting of Tan Tan brackish water in terms of TDS rejection.*

Membrane			Total salinity in the permeate (ppm)		
			Tan Tan water	Tan Tan water doped at 6g/L	Tan Tan water Doped at 10 g/L
NF	NF90	Y = 10%	190 ± 10	310 ± 20	770 ± 32
		Y = 45%	308 ± 8	530 ± 30	1120 ± 50
		Y = 70%	490 ± 30	790 ± 42	1620 ± 30
	NE90	Y = 10%	200 ± 10	360 ± 15	800 ± 30
		Y = 45%	325 ± 14	610 ± 20	1500 ± 30
		Y = 70%	500 ± 20	840 ± 32	2320 ± 40
LPRO	REBLF	Y = 10%	78 ± 4	129 ± 11	300 ± 35
		Y = 45%	150 ± 10	320 ± 30	680 ± 42
		Y = 70%	260 ± 20	450 ± 27	1000 ± 56
	BW30	Y = 10%	54 ± 5	80 ± 8	nd
		Y = 45%	106 ± 16	138 ± 20	nd
		Y = 70%	165 ± 10	226 ± 15	nd

It is evident that the BW30 is the most effective membrane for TDS reduction with the two values of feed TDS (4 and 6 g/L) and over the entire recovery rates investigated. The TDS rejection with this membrane showed more or less a steady value with an increase in feed salinity; the rejection rates obtained was higher than 96%. The salinity effect was negligible for the BW30 membrane. We were not able to carry out the experiments at high salinity level (10g/L) with the BW30. Due to high retention values obtained with this membrane; greater amount of pressure (> 20 bar) was needed.

What stands out in these experiments is how the REBLF membrane appears to be more influenced by the salinity effect than the other LPRO membrane tested, especially at high recovery rates. As salinity increases, the diffusion of salts which is due to a gradient of concentration across the membrane increases and the rejection advantage is gradually diminished. The performance of the REBLF membrane is not typical of that of RO membranes. This is due in part to the fact that this membrane which has high permeability has more open pores than the BW30 membrane.
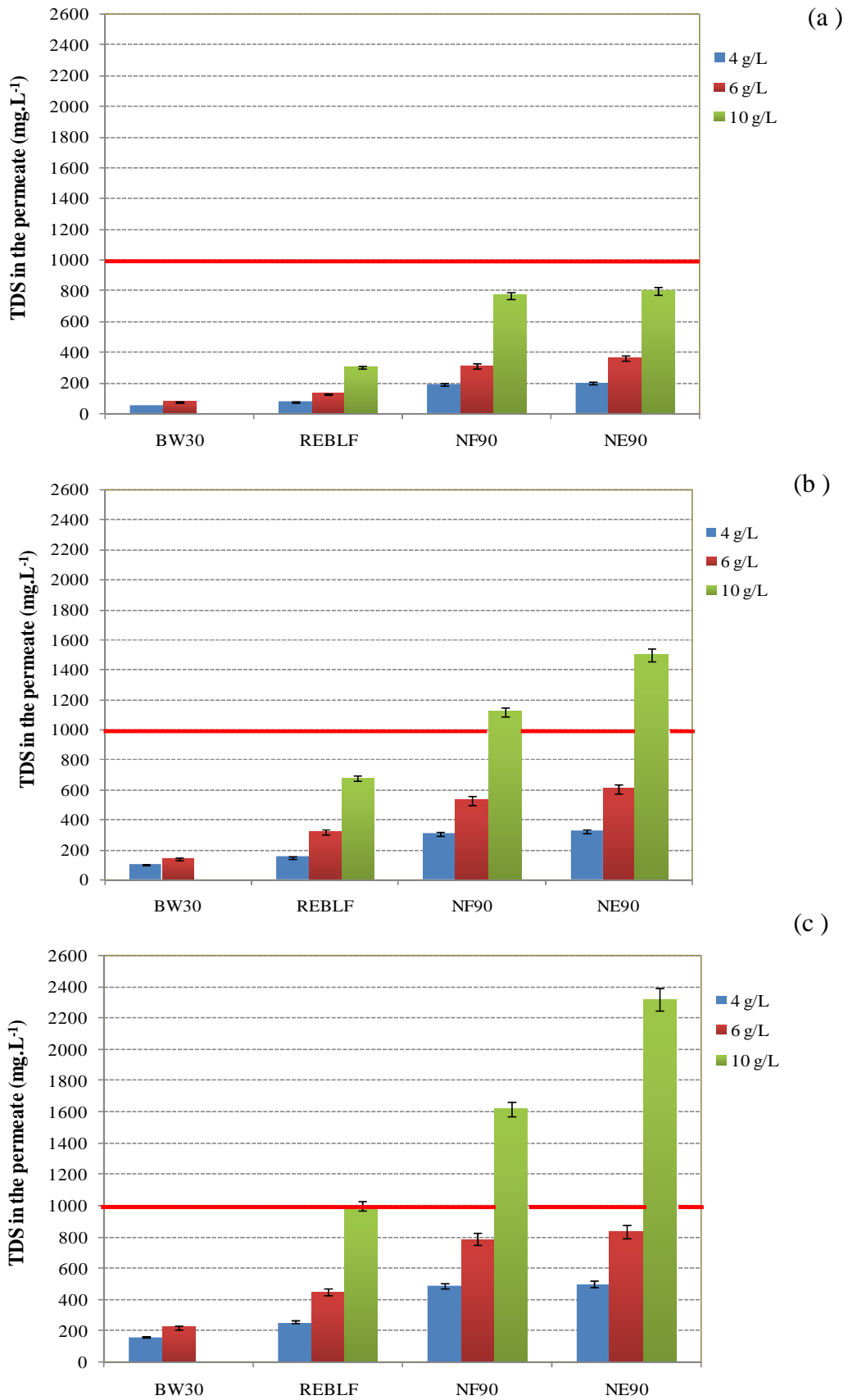
Figure 55: *Permeate total salinity at different feed salinity levels and different recovery rates (a)Y=10% (b) Y= 45% (c) Y=70%, for the NF90, NE90, REBLF and BW30 membranes (T = 21°C, Q permeate = 0.2m³.h⁻¹)*

The TDS in the permeate obtained with the REBLF membrane did not exceed the permissible WHO standards, at the entire salinity levels. The rejection rates obtained was higher than 90%. The permeate TDS measured at 10 g/L and a recovery rate of 70% was equal to the WHO limit. Thus, the efficiency of this membrane to produce potable water from high salinity brackish water can be limited to a feed TDS of 10 g/L under these conditions (Y= 70%, T=21°C and $Q_{permeate} = 0.2$ m^3.h^{-1}).

The NF membranes were more impacted by the increasing salinity than the LPRO membranes especially, at high salinity levels (10g/L). The benefit of the Donnan potential in the form of increased rejection is greatest at low to mid salinities (TDS < 6000 mg/L).The Donnan exclusion is affected at high feed salinity; increasing the feed salinity weakens the Donnan potential and leads to a decrease in membrane rejection (Bartels *et al.* 2005). With the brackish water at 6g/L, the NF membranes could still satisfy the WHO water standard. The obtained permeates with the NF90 and NE90 have a TDS lower than 840 mg.L^{-1} at a recovery rate of 70%. The rejections rates attained with these membranes exceed 84%. However, The NF membranes allow a partial quality improvement when high feed water salinity is treated (10 g/L). The TDS were not significantly retained with these membranes; the obtained permeates have a TDS between 800 and 1600 mg.L^{-1} for the NF90 membranes and a TDS between 800 to 2300 mg.L^{-1} for the NE90. The permeate quality attained at high recovery rates (> 45%) could not be considered as drinking water quality.

When considering the magnitude of the salinity effect at high feed salinities, a noticeable difference emerges between the NF90 and NE90 membranes (Fig. 55). The NE90 membrane is more affected by the increasing salinity than the NF90; the TDS in the permeate obtained from the NE90 membrane increases more than four times when increasing feed salinity whereas the increase of TDS in the permeate of the NF90 membrane is nearly three to four times.

The NF membranes are actually efficient at salinity levels under 6 g.L^{-1}, since they can reduce the TDS to a value which is accepted by the WHO standards. These membranes were insufficient to produce drinking water from high salinity brackish water (10g.L^{-1}): the TDS of the permeate obtained with the NF modules was superior to the standard value authorized by the WHO. A higher pressure should be employed to allow these membranes to reach better water quality.

2.5.1.3 Working pressures

Figure 56 shows the required pressures for desalting brackish waters in the salinity range of 4-10 g.L^{-1}, for the NF90, NE90, REBLF and BW30 membranes, at different recovery rates. This figure shows the dependency of the applied pressure on the salinity level for all the membranes. Increasing feed water salinity increases the osmotic pressure between two sides of the membrane, and then leads to the increase of applied pressure required to compensate the resistance to filtration created by osmotic pressure.
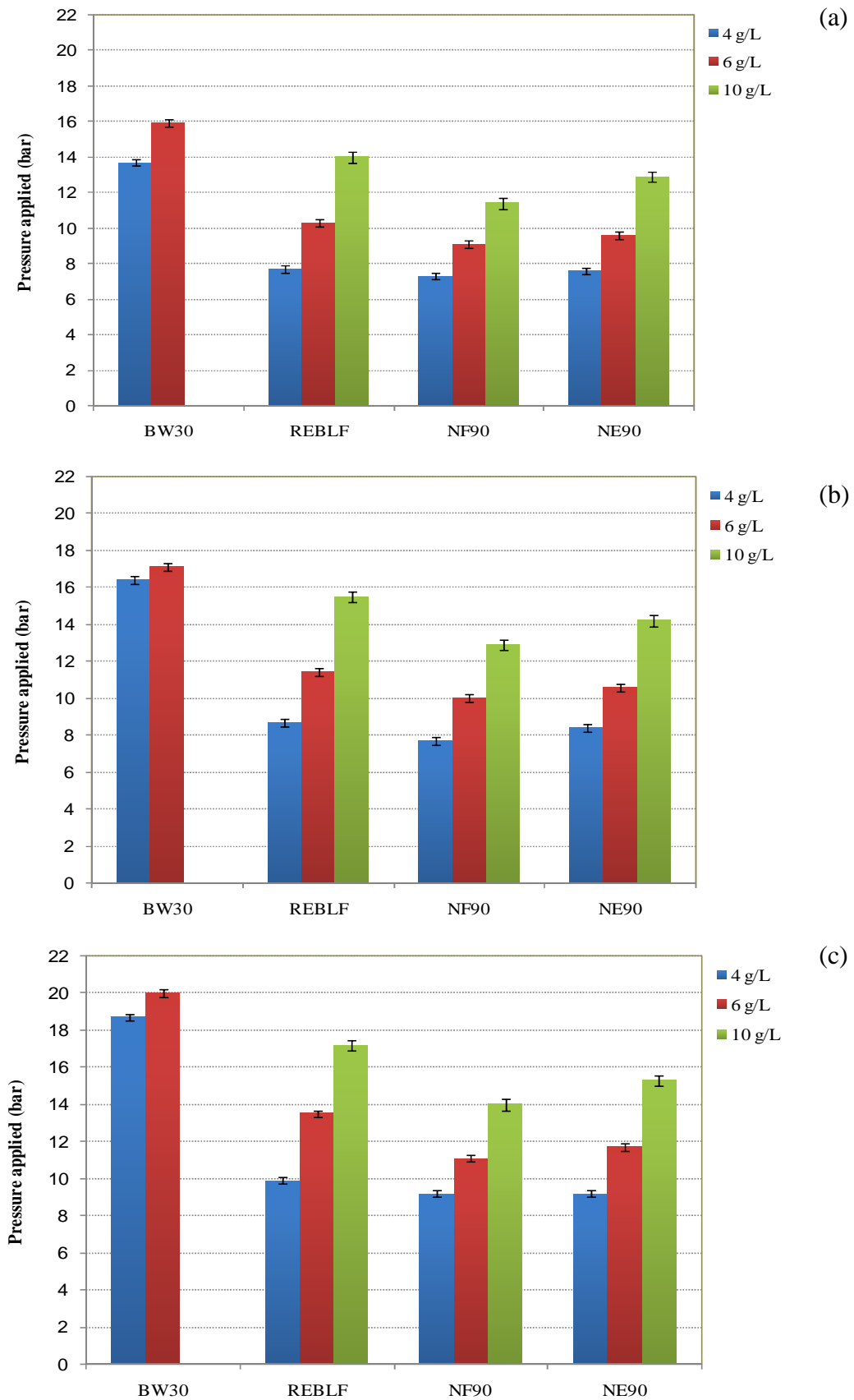
Figure 56 :*Required pressures for desalination of Tan Tan water for the NF and LPRO membranes studied at different recovery rates (a)Y=10% (b) Y= 45% (c) Y=70%, (T=21°C, pH = 7.9)*

For drinking water production of 0.2 m^3.h^{-1}, the system should run at high transmembrane pressure with LPRO membrane compared to the NF membranes, for three salinity values. The pressure required using the BW30 membrane is two times higher than this required for the NF90 at all recovery rates. The REBLF membrane can operate at moderate pressures compared to the BW30 membrane due to its lower rejection rates.

The working pressures of the REBLF membrane are comparable to those applied in NF at low feed salinity (TDS = 4 g.L^{-1}), whereas they become 30% higher for desalting highly salinity feed waters.

2.5.1.4 Energy consumption as a function of salinity

The relationship between the energy consumption and water salinity for the NF/RO desalination unit is illustrated in Fig. 57. It shows that the energy consumption increase with increasing feed solution concentration. This is valid for either RO or NF treatment processes because this energy is proportional to the quantity of salt to eliminate (Walha *et al.* 2007, Hrayshat 2007, Masson *et.al* 2005,). With brackish waters in the salinity range of 4000 -6000 mg/L, the amount of energy required is 0.9 and 1.0 kWh/m^3 respectively, for the BW30 membrane.The energy demand was the lowest for the NF90 and NE90 membranes with minimum of SEC values of 0.44 and 0.53 kWh/m^3 for a salinity range of 4000 -6000 mg/L respectively.

The SEC of the REBLF membrane was slightly higher than the NF membranes at low salinity levels, but with highly brackish feed water (10g.L^{-1}) the SEC of this membrane is higher 0.83 kWh/m^3 compared to the NF90 membrane which shows a minimum value (0.67 kWh/m^3).
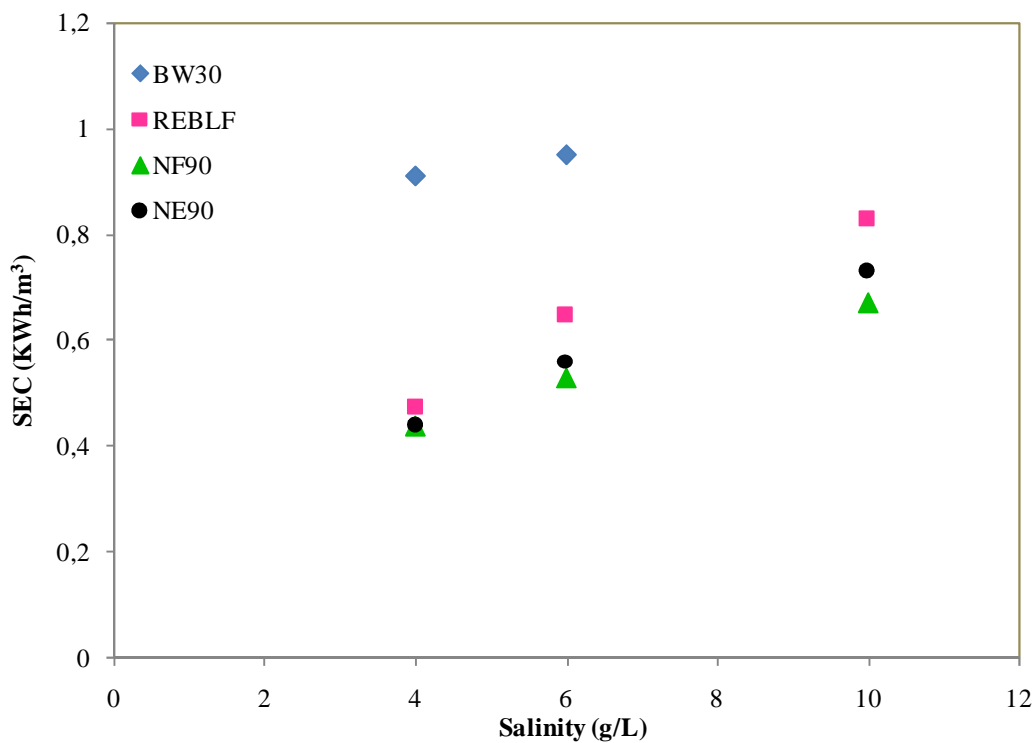
Figure 57: *Energy consumption of the NF/RO desalination unit as a function of salinity (Y=70%, T= 21°C, $Q_{permeate}$ = 0.2 m^3.h^{-1})*

The BW30 membrane was able to produce better quality water for the three values of feed water salinity, but with higher energy demand. This membrane sharply reduced the TDS present in raw brackish waters (rejections >96%). After treatment, the obtained permeate has a low value of TDS (< 200 ppm), which is accepted by WHO because this salinity is necessary for human consumption of drinking water.

2.5.2 Brackish water with high level F⁻ concentration

The fluoride content in many regions of Morocco greatly exceeds the acceptable standards. For its high and specific membrane selectivity, nanofiltration appears to be the best membrane process to remove fluoride from brackish underground water (Diawara *et al.* 2003, Tahaikt *et al.*2007, Pontié *et al.*2008).

A comparison of the performances of NF and LPRO membranes on fluoride removal was carried out using various initial fluoride contents in Tan Tan water (doped with NaF at 5, 10 and 15 ppm of fluoride). The NF membranes NF90 and NE90 which shows the best performances in Tan Tan water desalination was chosen for this study with the LPRO membrane BW30. The permeate flow was fixed to 0.2 $m^3.h^{-1}$. Figure 58 shows the variations of the permeate fluoride concentration as a function of the initial fluoride content at three recovery rates. Table 40 gives the fluoride content of the water produced for the NF 90, NE90 and BW30 membranes at different recovery rates.

Table 40: *Fluoride content of the water produced*

Membrane	Recovery rate $Y (\pm 2\%)$	Concentration F_0 (ppm)			
		1	*5*	*10*	*15*
	10%	0.08	0.12	0.14	0.4
NF90	45%	0.10	0.16	0.2	0.47
	70%	0.14	0.22	0.27	0.72
	10%	0.04	0.12	0.24	1
NE90	45%	0.06	0.18	0.41	1.5
	70%	0.09	0.26	0.55	1.8
	10%	0.02	0.03	0.03	0.04
BW30	45%	0.04	0.04	0.05	0.06
	70%	0.07	0.08	0.08	0.09

These results show that practically no influence of the initial fluoride content of the feed water on the fluoride rejection was observed for the BW30 membrane. The fluoride concentration in the permeate is very low and the beneficial effect of fluoride in drinking water (prophylactic good health effect) is not attained due to the fact that fluorides are totally rejected by the BW30 membrane due to the pure solution-diffusion mass transfer mechanism assured in RO (Lhassani *et al.* 2001).
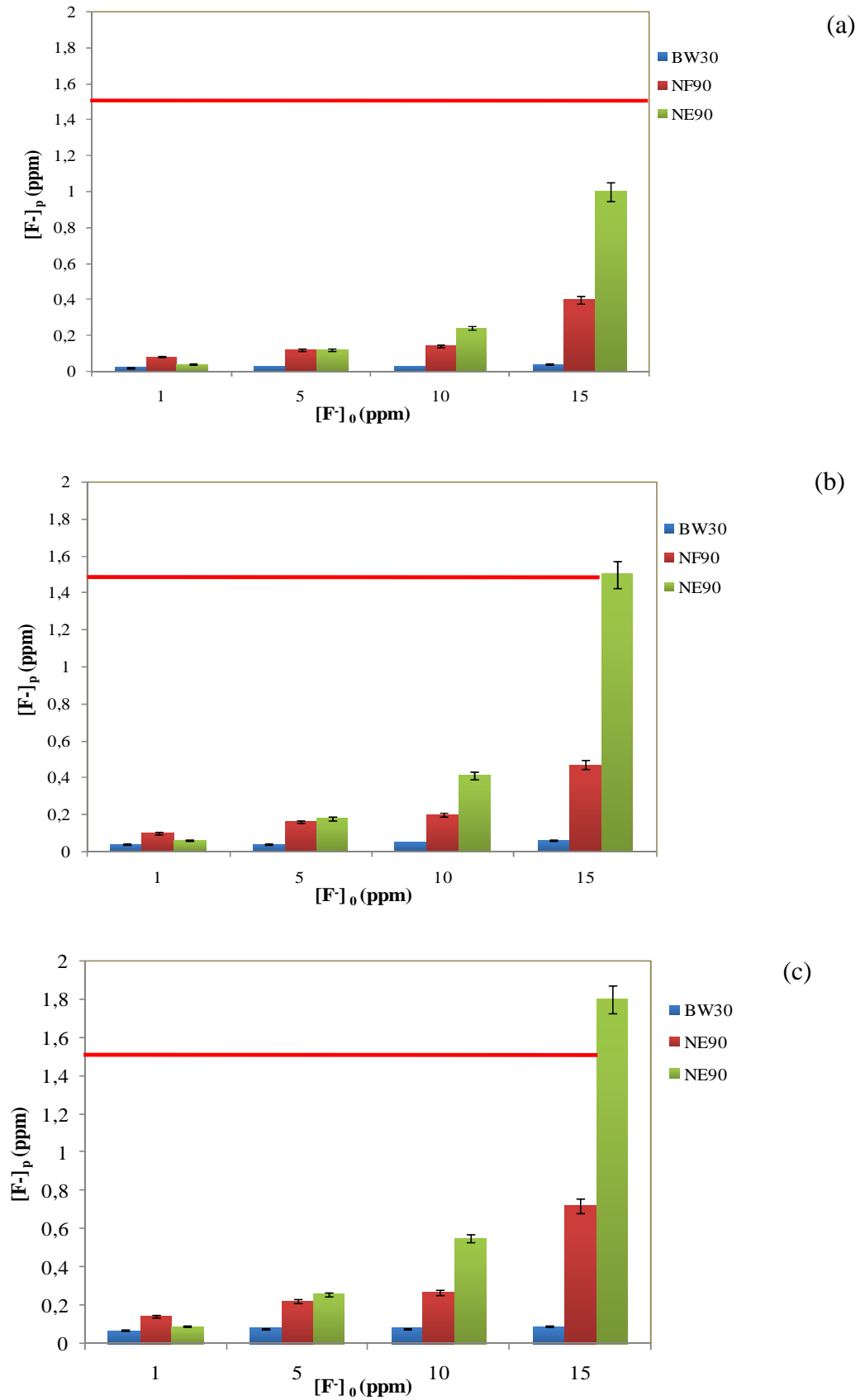
Figure 58: *Variations of fluoride concentration in the permeate for the studied membranes with F⁻ concentrations variations in Tan Tan water (a)Y= 10%, (b) Y= 45%, (b) Y= 70%, (Permeate flow = 0.2 m³.h⁻¹, T= 21°C)*

For the NF membranes the fluoride leakage increases with increasing the initial concentration of fluoride. The fluorides were reduced to a satisfactory value with the NF90 membrane; F⁻ level concentration after filtration, sufficient to maintain a prophylactic benefit effect under human health due to the permeate composition (F⁻ concentration under 1.5 mg/L). With the NE90 membrane, the fluoride content of the product water was lower than the standards at the entire recovery rates, when the initial concentration is bellow 10 ppm. The permeate concentration slightly exceed the WHO guidelines when treating a highly F⁻ content solution (15ppm) at high recovery rates (< 45%).

This study confirms to large scale experiments (membrane surface 7.6 m^2) the performances of the nanofiltration for a better selective defluoridation of a brackish water opening large perspectives for future large scale nanofiltration units in the world.

Conclusion

The necessity of water reclamation is growing driven by a stress on water supply and public desire for a significant improvement in water desalination. Reverse osmosis (RO) is widely used in brackish water desalination. Nanofiltration can be used for partial and/or selective demineralization of brackish water, and is more suitable for producing drinkable water directly without the need for remineralization compared to RO. This dissertation aimed to contribute towards the promotion of the use of NF membranes for the production of potable water from brackish water. The objectives of this dissertation were:

- To identify key factors influencing the retention of salts by NF/RO membrane filtration processes
- To elucidate the removal mechanisms of salts by NF/RO membranes, and
- To demonstrate the capacity and limitations of NF membranes in removing salts from brackish waters

This thesis presented a fundamental study to characterize and predict NF membranes performances using different approaches for selecting suitable NF membranes for brackish water desalination. These approaches include filtration experiments for single and mixtures salts, filtration of real brackish water, modeling and using of Atomic force microscopy, streaming potential and contact angle as methods of membrane surface characterization. The thesis also presented an applied study on pilot scale to demonstrate that NF membranes might be technically and economically viable to cope with water scarcity.

Among the investigated membranes, three NF membranes denoted NF90, NF200 and NF270 and two LPRO membranes denoted BW30 and BW30LE were employed in a laboratory scale. The performances of these membranes in terms of water permeability and in handling two single salts with different salinity levels were investigated. The results showed that the rejections of the investigated salts and the permeate fluxes for all membranes increased with the transmembrane pressure and decreased with the salt concentration. The results also showed that the LPRO membranes have high rejection rates of monovalent salts ($> 90\%$) with low permeabilities (< 3.5 L.h^{-1}.m^{-2}.bar^{-1}) while the NF membranes have relatively lower rejections ($< 80\%$) with higher permeabilities (2 or 7 times higher). Both types of membranes have shown the same equality in rejection of divalent salts at low concentration while the NF membranes rejection of divalent salt was lower at high concentration levels. The NF membranes are strongly influenced by the solution concentration. Interestingly, the NF90 membrane has the highest permeability amongst NF membranes and has the highest rejections. The NF200 and NF90 membranes have comparable retentions at low concentration levels while the retentions of the NF200 membrane are lower at high concentration level. The NF270 showed lower retention rates.

The roughness, hydrophobicity and surface charge of the membranes obtained respectively by the AFM, contact angle and streaming potential measurements were used to analyze both experimental data of pure water permeation and data obtained from salt rejection.

The AFM results shows that the NF270 and NF200 are the smoothest membranes (Ra < 20 nm), the NE90 membrane has an intermediate roughness while the NF90, the BW30 and the

BW30LE membranes were the roughest membranes (Ra > 120 nm). The high permeability value of the NF90 membrane was explained by its high roughness value (Ra = 290 nm). Even their high surface roughness which is indicative to a high fouling tendency, the NF90 and BW30LE membranes were chosen for Tan Tan brackish water experiments because of their high rejection rates and because of the low fouling tendency of Tan Tan water (SDI < 0.4).

The contact angle measurements show that the NF200 and NF270 membranes were more hydrophilic than other membranes (θ < 40 °). Hydrophobic membranes often exhibit lower water flux. The NF90 membrane shows higher water flux and shows hydrophobic character ($\theta \approx$ 70 °). We attributed the obtained result to the influence of surface roughness on contact angles values.

Employing a homemade streaming potential apparatus developed specially for this study, we explored the role of charge interaction in the separation of ions by NF membranes. The results show that all the membranes were negatively charged at neutral pH and show also that the charge of the membranes is dependent of solution pH. The NF200 membrane has much more surface charge than the other membranes, while the NF90, NF270, BW30 and BW30LE are weakly charged.

The negatively charged membrane, NF200, exhibits high retention at low concentration while the retention decreases at high concentration levels. This membrane can be classified as Donnan exclusion membrane. In other words its separation process is mainly governed by Donnan interaction rather than size exclusion. The effect of charge was completly eliminated at high ionic strength (10^{-1}M of NaCl). This can explain the decrease of retention for the NF200 membrane at high ionic strength due to screening phenomenon.

The NF90 membrane is weakly charged and is a tight NF membrane. This membrane is situated near the reverse osmosis side of the nanofiltration region and has a separation process governed by selective diffusion.

The NF270 is also weakly charged and has high MWCO. In fact given its very low rejection, the NF270 is at the boundary of UF membranes in the classification chart. For this reason this membrane was excluded in studying the salt mixture and real brackish water.

The salt mixture study was investigated with the NF90 and NF200 membranes; which present a selective retention between monovalent and divalent ions compared to the LPRO membranes. The presence of divalent ions in feed solution in salt mixture has an effect on monovalent ions rejection by NF membranes due to charge effect (Donnan effect). The presence of Sulfate reduced chloride rejection. However retention enhancement of chloride was obtained in the presence of calcium; chloride ions retention is higher when the quantity of divalent cation is dominating. The results presented demonstrate the complexity of ions retention in real brackish water filtration. The application of such findings to real feed water requires a careful consideration of operating variables, the solution chemistry and major constituents that may be present in feed solution.

The NF90, NE90, NF200 and BW30LE membranes were chosen for laboratory bench-scale testing of Tan Tan brackish water, based on the filtration experiments. This study clearly illustrates the essential differences between NF and RO processes. Indeed RO cannot be used

for partial and or selective demineralization. NF is more suitable for directly producing drinking water and the post treatment can be simplified. The argument, that NF membranes are more selective was also presented. It was clearly shown that NF selectivity for monovalent ions is higher than RO.

With NF90 and NE90 membranes a desired drinking water respecting the standards can be easily produced from brackish water with higher water fluxes. The influence of water recovery rate was also investigated. The rejection rate decreased at higher recovery rates, which was found to be a pure concentration effect. Changing the operating conditions has almost no effect in the monovalent ions rejection with LPRO membrane, while marked selectivity of monovalent ion was obtained with NF membranes, especially at low pressure conditions.

Spiegler–Kedem- Katchalsky model has been used to analyse the experimental filtration results. This model was applied two single salts data and real brackish water data and was used to fit the experimental data of rejection with the permeate flux in order to determine the fitting parameters of the reflection coefficient (σ) and the solute permeability (P_s). For both single salts, the results showed that SKK model was successfully fitted the experimental data for all the membranes expect for NF90 membrane with monovalent salt. The fitting parameters σ and P_s values were dependent on the concentration and the type of salts and the type of membrane. It was seen that Ps increases with salt concentration while σ decreases due to the reduction in salt rejection. The values of σ were higher for the NF90, BW30 and BW30LE membranes and with divalent salt which means that a relatively complete rejection was given and consequently the values of P_s were lower. The model was also able to represent most experimental data of monovalent ions in real brackish water sample and the values of σ and P_s were dependent on the nature of monovalent ions and on recovery rates. The σ values were higher for fluoride ion and at low recovery rates.

The experimental data of rejection and flux of the investigated membranes was represented in another way to quantify the transfer parameters: J_{diff}, the solute diffusion flux and C_{conv}, the solute concentration due to convection. This approach is valid only in some limited domain of operating conditions with low polarization concentration and with membrane considered having no charge. This representation was useful for the comparison of the behavior of different NF and RO membranes. The NF membranes showed high values of Cconv while the values of Cconv for LPRO membranes were nearly equal to zero. The Pe values calculated from J_{diff} and C_{conv} values showed that Pe >1 for the NF membranes where convective mass transfer is quite dominant. The Pe <1 obtained for the LPRO membranes confirmed that diffusionnal mass transfer is quite dominant for these membranes. The NF90 membrane which is a tigh membrane is more diffusional (Pe < 1).

A new method of determination of the membrane molecular weight cut-off was used, this method was in good adequation with the order obtained using the usual method from calibrated neutral molecules for all the membranes, expect for the NF200 membrane. No real value of MWCO was obtained for this membrane. The method used is not valid for negatively charged membranes.

Benchscale results helped to select proper membranes for testing in large-scale pilot study in Tan Tan SWRO plant. The NF90, NE90 and BW30LE which show the best performances in terms of rejection and permeability than the NF200 were chosen.

Eight types of 4"x40" NF and LPRO modules were tried with the aim of desalination of Tan Tan water at pilot scale in Tan Tan SWRO plant. The studied membranes are four NF membranes (NF90, NE90, ESNALF and NE70) and four LPRO membranes (BW30, BW30LE, REBLF and ESPA3).

The filtration results allow clarifying the difference between the NF and LPRO membranes in their desalination performance of Tan Tan brackish water.

The LPRO membranes sharply reduced the content of salts present in Tan Tan water (rejections > 90%). After treatment, the obtained permeate has a low value of TDS, especially with the BW30 membrane, so the water produced with this membrane needs to be mixed with feed water to meet the minimum permeate TDS limit for drinking water .The results obtained for the REBLF; high salt rejection with relatively high flux from the conventional LPRO membrane, indicate that this membrane is ultralow-pressure reverse osmosis membrane.

NF was observed to be an effective method to perform partial desalination of Tan Tan brackish water. The degrees of mineral salt removal with the NF90 and NE90 membranes was 72–95% and was dependent on the value of the recovery rate and permeate flow. These membranes have also shown their ability to reject both monovalent and divalent of Tan Tan water with very reasonable values which respect the WHO limits. On the contrary, NE70 and ESNA1LF membranes produced relatively very low rejection of salts indicating inappropriateness of theses membranes for the desalination of Tan Tan water.

The evaluation of pressure required for all the membranes permits to conclude that the tighter the membrane, the higher ΔP required. In this case, looser membranes are better since lower pressures are required to provide a very good permeate fluxes, if the membrane rejection can fulfill the requirement. Only the NF90 and NE90 membranes can meet the rejection requirement at higher permeate fluxes and lower applied pressures.

The energy consumption study confirms that the NF90 and NE90 membranes, which required minimum energy consumption, are more economical than the LPRO membranes. This will make these membranes more suitable for the desalination of Tan Tan water.

The REBLF, ESPA3 and BW30LE membranes allow the desalination of brackish water at pressures comparable to those applied in nanofiltration. These membranes operate at the interface of nanofiltration and reverse osmosis and might be helpful in optimizing the desalination process of Tan Tan brackish water.

In this thesis, we used three commercial simulation softwares to project the performances of reverse osmosis and nanofiltration brackish water systems which are: ROSA 6.1 (DOW, USA), IMS Design (Hydranautics, USA) and CSMPRO3 (Saehan, Korea). The results from the process simulation using these softwares were verified by the practical operating experiences gained with the pilot system.

The use of ROSA software for the prediction of DOW, NF/RO elements performances proved successful. It can perform simulation of whole variations of recovery rate, feed and permeate flow used in this investigation. The performance predications it gave showed good agreement with measurements taken from the pilot tests.

ROSA software gives a good level of confidence in the prediction of pressure required for filtration and permeates total salinity compared to the other sofwares studied (IMS Design

and CSMPRO3). The use of ROSA can help process designers in planning, designing and optimizing NF/RO processes, when using DOW elements.

This thesis also investigated the application of nanofiltration for demineralization of model solution simulating moderately brackish waters (salinity range of 4-10 g.L^{-1}), and defluoridation of Tan Tan brackish water doped with fluoride at high concentrations (5 - 15 mg/L).

Doping salts experiments with Tan Tan water were performed to check the potential of NF operation versus RO on filtration of moderately brackish waters, and to clarify the limits of application of NF membranes on brackish water desalination. The NF90 and NE90 membranes, which were observed to be effective to perform partial desalination of Tan Tan brackish water, were chosen with the BW30 and REBLF membrane for this investigation.
The results showed that the NF90 and NE90 membranes were efficient at salinity level of 6 g.L^{-1}, since they can reduce the TDS to 800 mg/L at a recovery rate of 70%, which is accepted by the WHO standards. These membranes were not capable to produce drinking water from high salinity brackish water (10g.L^{-1}): the TDS of the permeate obtained with the NF90 module was equal to 1,600 mg/L, while it was equal to 2,300 mg/L for the NE90. These concentrations were superior to the standard value authorized by the WHO. The pressures required using the BW30 membrane, which presented the highest retention rates, were two times higher than those required for the NF membranes. A higher pressure should be employed to allow the NF membranes to reach better water quality at high salinity levels.

The performances of NF and LPRO membranes on fluoride removal were also presented using various initial fluoride contents in Tan Tan water. The results showed that the fluorides were reduced to a satisfactory value with the NF90 and NE90 membranes. The F$^-$ level concentration after filtration was sufficient to maintain a prophylactic benefit effect under human health due to the permeate composition (F$^-$ concentration under 1.5 mg/L).

This dissertation confirms from laboratory scale to pilot scale the effectiveness of nanofiltration for a partial and selective demineralization of brackish water at low operating pressures and high water production compared to RO. It also allows the determination of the operating conditions and the establishment of performance parameters for large scale NF plant and should also assist in technoeconomic evaluation of the process itself.

Perspectives

There is no doubt that in the near future, nanofiltration (NF) will play a central role in propagating the success of brackish water desalination.

Findings reported in this dissertation are critical and have revealed new scope for further fundamental as well as applied research works for NF.

In a fundamental aspect, the following areas can be of particular interest:

- Effects of parameters such as Temperature and pH of the solution on NF removal efficiency,

- The removal processes using NF membranes are complex and poorly understood. The testing of NF membranes in salt mixtures presented in part I of chapter 3, was interesting. It was however very brief and used only binary mixtures. Different salts mixtures should be performed in order to investigate the influence of medium composition on ions retention and to elucidate electrokinetic interactions between ions and the membrane.

- AFM was used to investigate the surface morphology and the roughness of the studied membranes in the air medium. Imaging of the surface of membranes under salt solutions should be investigated in order to find these characteristics under the same medium of filtration experiments.

In applied research:

- A full scale membrane filtration process involves many operating variables including (but not limited to) cross flow rate, transmembrane pressure, recovery, system arrangement, cleaning frequency, and module design. The pilot study did not examine all these variables, it has been demonstrated that some of these variables might have certain effects on the overall removal efficiency. Therefore it is essential that the translation of the results obtained from a pilot scale to a real life situation should take various operating variables into careful consideration.

- Fouling is an inevitable phenomenon in most (if not all) of the membrane filtration process. It is known that it strongly influence not only the production of drinking water but also removal efficiency of the membranes. Numerous dedicated investigations have been devoted to study the fouling effects on performances of RO membranes. However, studies addressing the particular issues related to NF remain very scarce and revealed that NF membranes are less fouling prone than reverse osmosis (Eriksson *et al.* 2005; Boussu 2006). Consequently, investigation elucidating the fouling tendency of both membranes will create interesting results.

- The testing presented in Part II of Chapter 3, demonstrated performance efficiency of the NF90 and NE90 membranes with LPRO membranes for Tan Tan water demineralization over a broad range of operation, but did not provide any indication of membrane lifetime under real operating conditions. It is recommended, therefore, that

long-term membrane testing under variable flow conditions should be conducted to establish membranes performances over time.

- The doping tests of Tan Tan brackish water define the limit of application of the NF membranes (NF90 and NE90) for demiralization of moderately brackish waters to a TDS of 10g/L. The pressures applied in these experiments were in the range of 6 to 15 bar. Therefore, it would be advantageous to conduct the filtration experiments at high pressures or use more than one NF stage to reach better water quality.

H. DACH thesis team, Tan-Tan, Morocco, august 2007

References

Abouzaid, A., Mouzdahir, A., Rumeau, M., (2003), Etude de la rétention des sels monovalents et bivalents par nanofiltration, Comptes Rendus de Chimie, 6, 431- 436.

Afonso, M., Hagmeyer G. and Gimbel R., 2001, Streaming potential measurements to assess the variation of nanofiltration membranes surface charge with the concentration of salt solutions, Separation and Purification Technology, 22, 529-541

Agarwal M, Rai, K., Shritastav, R. and Dass, S., (2003), Defluoridation of water using amended clay. Journal. of Cleaner Producting, 11, 439-444

Ahmad , A.L., Ooi, B.S., Mohammad , A.W., Choudhoury, J.P., (2004), Development of a highly hydrophilic nanofiltration membrane for desalination and water treatment, Desalination, 168, 215-221.

Ahmed, G.E. and Schmid, J., (2002), Feasibility study of brackish water desalination in the Egyptian deserts and rural regions using PV systems. Energy Conversion and Management, 43, 2641-2649.

Ahmed, A.L, Ooi, B.S, Wahab Mohammad, A., Choudhury, J.P, (2004), Development of highly hydrophilic nanofiltration membrane for desalination of water treatment, Desalination, 168, 215-221.

Ahmad, A.L., Chong, M.F., Bhatia, S., (2005). Mathematical modeling and simulation of the multiple solutes system for nanofiltration process. Journal of Membrane Science 253: 103–115.

Al-Sofi, M., (2001) Seawater desalination — SWCC experience and vision Desalination, 135, 121-139

Al-Subaie, Z.K., (2007), Precise way to select a desalination technology, Desalination, 206, 29-35.

Altinkaya, S. A. and Ozbas, B., (2004), Modeling of asymmetric membrane formation by dry-casting method, Journal of Membrane Science, 230, 71-89.

Al-Zoubi, H., Development of novel approach to the prediction of nanofiltration membrane performance using advanced atomic force microscopy, Thesis, University of Nottingham, (2006).

Amy, G.L., Alleman, B.C. and Cluff, C.B., (1990), Removal of dissolved organic matter by nanofiltration, Journal of Environnement and Engineering , 116, 200-205 .

Amor, Z., Bariou, B., Mameri, N., Taky, M., Nicolas, S., Elmidaoui, A., (2001), Fluoride removal from brackish water by electrodialysis, Desalination, 133, 215-223

Apambire, W.B, Boyle, D.R and Michel, F.A., (1997), Geochemistry, Genesis and health implications of fluoriferous groundwaters in the upper regions of Ghana. Environement. Geology, 33, 13-24.

Andrianne, J. and Alardin, F., (2002), Thermal and membrane process economics: optimized selection for seawater desalination, Desalination, 153, 305-311.

Aptel, P., Buckley, C.A., (1996), Categories of membrane operations, In: Water Treatment Membrane Process, Chapitre 2, McGraw-Hill.

Azbar, N. and Turkman, A., (2000), Defluoridation in drinking waters, Water Science and technology , 42, 403-407

Bain, C.D, Troughton, E.B, Tao, Y-T., Evall, J., Whitesides, G.M. and Nuzzo, R.G., (1989), Formation of monolayer films by the spontaneous assembly of organic thiols from solution onto gold, Journal of American Chemistry and Society, 111, 321-335.

Balannec, B., Vourch, M., Rabiller-Baudry, M. and Chaufer, B., (2005), Comparative study of different nanofiltration and reverse osmosis membranes for dairy effluent treatment by dead-end filtration Separation and Purification Technology, 42, 195-200.

Bannoud, A.H., (2001), Elimination de la dureté et des sulfates contenus dans les eaux par nanofiltration, Desalination, 137, 133-139.

Bandini, S., (2005), Modelling the mechanism of charge formation in NF membranes: theory and application, Journal of Membrane Science, 264, 75.

Baranowski B., (1991), Non-equilibrium thermodynamics as applied to membrane transport, Journal of Membrane Science, 57, 119.

Bhattacharya A., Ghosh, P., (2004), Nanofiltration and reverse osmosis membranes: theory and application in separation of electrolytes, Rev. Chem. Eng, 20 111–173.

Bellona C., Drewes, JE., Xu P. and Amy G,(2004),Factors affecting the rejection of organic solutes during NF/RO treatment—a literature review, Water Research, 38, 2795-2809

Ben Farès, N., (2006), Contribution de l'étude de l'élimination des ions zinciques : Etude expérimentale et modélisation, Thesis, Rennes University, France.

Benavente, J., Jonsson, G., (1997), Effect of adsorption of charged macromolecules on streaming and membrane potential values measured with a microporous polysulfone membrane, Separation Science and Technology, 32, 1699-1710.

Bes-Piá, A., Iborra-Clar, M.I. , Iborra-Clar, A., Mendoza-Roca, J.A., B. Cuartas-Uribe and M.I. Alcaina-Miranda, (2005), Nanofiltration of textile industry wastewater using a physicochemical process as a pre-treatment, Desalination, 178, 343-349.

Berg, P., Hagmeyer, G .and Gimbel, R., (1997), Removal of pesticides and other micropollutants by nanofiltration, Desalination, 113, 205-208.

Bertrand, S., Lemaitre, I. and Wittmann, E., (1997) Performance of a nanofiltration plant on hard and highly sulphated water during two years of operation, Desalination, 113, 277-281 .

Bohdziewicz, J ., Bodzek, M . and E. Wasik, (1999), The application of reverse osmosis and nanofiltration to the removal of nitrates from groundwater, Desalination, 121, 139-147 .

Boussahel, R., Bouland, S., Moussaoui, K.M. and Montiel, A., (2000), Removal of pesticide residues in water using the nanofiltration process, Desalination, 132, 205-209.

Bindra, S.P and Abosh, W., (2001), Recent developments in water desalination, Desalination, 136, 49 -56.

Blank, J.E., Tusel, G.F. and Nisari, S., (2007), The real cost of desalted water and how to reduce it further, Desalination, 205, 298-311.

Bouchard, C., Kouadio, P., Ellis, D., Rahni, M. and Lebrun, R.E., (2000), Les procédés à membranes et leurs applications en production d'eau potable, Vecteur Environnement, 33:4:28-38.

Bouchekima, B., (2003), Solar desalination plant for small size use in remote arid areas of South Algeria for the production of drinking water, Desalination, 156, 353-354.

Boughriba A.,(2004), Expériences et perspectives du dessalement au Maroc, Cours sur le dessalement de l'eau de mer et des eaux saumâtres, organized by MEDRC, Ecole nationale de l'industrie minérale, Rabat.

Boussu , K., Van der Bruggen, B., Volodin, A., Snauwaert, J., Van Haesendonck, C. and Vandecasteele, C., (2005), Roughness and hydrophobicity studies of nanofiltration membranes using different modes of AFM, Journal of Colloid and Interface Science, 286, 632-638.

Boussu, K., Zhang, Y., Cocquyt, J., Van der Meeren, P., Volodin, A., Van Haesendonck, C., Martens, J.A. and Van der Bruggen, B., (2006), Characterization of polymeric nanofiltration membranes for systematic analysis of membrane performance, Journal of Membrane Science, 278, 418-427.

Boussu, K., Belpaire, A., Volodin, A., Van Haesendonck, C., Van der Meeren, P., Vandecasteele, C. and Van der Bruggen, B., (2007), Influence of membrane and colloid characteristics on fouling of nanofiltration membranes, Journal of Membrane Science, 289, 220-230.

Bowen, W. R. and Welfoot, J. S., (2002), Modelling the performance of membrane nanofiltration—critical assessment and model development, Chemical Engineering Science, 57, 1121-1137.

Bremere, I., Kennedy, M., Stikker, A. and Schippers, J., (2001), How water scarcity will affect the growth in the desalination market in the coming 25 years, Desalination, 138, 7-15.

Brant, J.A., Johnson, K. M. and Childress, A.E., (2006), Characterizing NF and RO membrane surface heterogeneity using chemical force microscopy, Colloids and Surfaces A, 280, 45-57.

Buisson, H., Lebeau, T., Lelievre, C., Herremans, L., (1998), Les membranes : point sur les évolutions d'un outil incontournable en production d'eau potable, L'eau l'industrie les nuisances, pp 42- 47.

Caroa, J., Schiestelb, T., Werthc, S., Wanga, H., Noack, M., (2006) Can inorganic membranes compete with organic ones? Perovskite hollow fibres for O_2-separation and supported H_2-selective zeolite membranes, Desalination, 199, 365–367.

Carta, J. A., González, J. and Subiela, V., (2003), Operational analysis of an innovative wind powered reverse osmosis system installed in the Canary Islands, Solar Energy, 75, 153-168.

Cath, T.Y., Childress, A.E. and Elimelech, M., (2006), Forward osmosis: Principles, applications, and recent developments, Journal of Membrane Science, 281, 70-87.

Causserand, C., (1992), Etude des mécanismes de sélectivité d'une membrane d'ultrafiltration, Thesis University of Toulouse (France).

Cabassud C.and Wirth D., (2003), Membrane distillation for water desalination: How to chose an appropriate membrane?, Desalination, 157, 307-314.

Castel, C., Schweizer, M., Simmonot, M.O. and Sardin, M., (2000), Selective removal of fluoride ions by a two-way ion-exchange cyclic process. Chem. Eng. Sci. 55(17) 3341-3352.

Chatudvedi, A.K., Yadava, K.P., Pathak K.C and Singh, V.N, (1990), Defluoridation of water by adsorption on fly ash. Water, Air, and Soil Pollution. 49, 51-60.

Chernet, T., Trafi, Y. and Valles, V.,(2002), Mechanism of degradation of the quality of natural water in the lakes region of the Ethiopian rift valley, Water Research. 35, 2819-2832

Childress, A.E. and Elmilech, M., (1996), Effect of solution chemistry on the surface charge of polymeric reverse osmosis and nanofiltration membranes, Journal of Membrane Science, 119, 253-268.

Childress, A.E. and Elimelech, M., (2000), Relating nanofiltration membrane performance to membrane charge (Electrokinetic) characteristics, Environment Science and technology, 34, 3710- 3716.

Choi, S., Yun, Z., Hong, S. and Ahn, K., (2001), The effect of co-existing ions and surface characteristics of nanomembranes on the removal of nitrate and fluoride, Desalination, 133 53-64.

Conlon, W., (1985), Pilot field test data for prototype ultra low pressure reverse osmosis elements, Desalination, 56, 203-226.

Conlon, W. J. and McClellan, S.A., (1989), Membrane softening: treatment process comes of age, Journal. AWWA, 81, 47–51.

Cot, L., Membranes inorganiques: exercise académique ou réalité industrielle, L'actualité chimique, (jully1998).

Cot, L., Ayral, A., Durand, J., Guizard, C., Hovnanian,N., Julbe, A. and Larbot, A., (2000), Inorganic membranes and solid state sciences, Solid State Sciences, 2, 313-334.

Coté P., Masini M., Mourato D., (2004) Desalination 167, 1-11

Côté, P.,Cadera, J., Coburn, J. and Munro, A. (2001), A new immersed membrane for pretreatment to reverse osmosis, Desalination, 139, 229-236.

Christoforou, C. C. ,G. B. Westermann-Clark and J. L. Anderson (1985), The streaming potential and inadequacies of the Helmholtz equation, Journal of Colloid and Interface Science, 106, 1-11

Cleveland, C.T., T.F. Seacord and A.K. Zander, (2002), Standardized membrane pore size characterization by polyethylene glycol rejection. Journal Environnemental Engeneering, 128, 399–407.

Czarnowski, W, Wrzeinovska, K. and Krechniak, J. (1996) Fluoride in drinking water and human urine in Northern and Central Poland. Science of the Total Environement. 191, 177-184.

Deshmukh, S.S., Childress, A.E., (2001) Zeta potential of commercial RO membranes: influence of source water type and chemistry, Desalination, 140, 87-95.

Déon, S., Dutournié, P, and Bourseau, Patrick, (2007), Transfer of monovalent salts through nanofiltration membranes: A model combining transport through pores and the polarization layer, Industrial Engeneering Chemistry research, 46, 6752-6761.

Diawara, C. K., Sidy Lô, M., Rumeau, M., Pontie, M. and Sarr, O., (2003), A phenomenological mass transfer approach in nanofiltration of halide ions for a selective defluorination of brackish drinking water, Journal of Membrane Science, 219, 103-112.

Du Plessis, JB. (1995), What would be the maximum concentration of fluoride in water that would not cause dental fluorosis? Fluoride and fluorosis. The status of S. Afr. Res., North West Province. 4.

Durand-Bourlier, L., Laine, JM, (1997) Proc. Membrane Technology Conf., New Orleans, 1-16

Elimelech, M., Zhu, X., Childress, A.E. and Hong, S., (1997), Role of membrane surface morphology in colloidal fouling of cellulose acetate and composite aromatic polyamide reverse osmosis membranes, journal of Membrane Science, 127, 101–109.

El-Nashar, A. (2001), The economic feasibility of small solar MED seawater desalination plants for remote arid areas , Desalination, 134, 173-186.

Ericsson, B., Hallberg, M .and Wachenfeldt, J ., (1996), Nanofiltration of highly colored raw water for drinking water production, Desalination, 108, 129-141 .

Eriksson, P., (1988), Nanofiltration extends the range of membrane filtration, Environmental Progress, 7, 58-62.

Erikson, P., Kyburz, M. and Pergande, W., (2005), NF membrane characteristics and evaluation for sea water processing applications, Desalination, 184, 281- 294.

Escobar, I .C., Hong, S. and Randall, A .A ., (2000), Removal of assimilable organic carbon and biodegradable dissolved organic carbon by reverse osmosis and nanofiltration membranes, Journal of Membrane Science , 175, 1-17.

Fane, A.G. , Awang, A.R. , M. Bolko, R. Macoun, R. Schofield, Y.R. Shen and F. Zha , (1992), Metal recovery from wastewater using membranes. Water Science Technology 25, 5–18.

Frappart, M, r Akoum, Oma, Lu Hui Ding and M.Y. Jaffrin (2006), Treatment of dairy process waters modelled by diluted milk using dynamic nanofiltration with a rotating disk module Journal of Membrane Science, 282, 465-472.

Freger, V. Gilron, J. and Belfer, S., (2002), TFC polyamide membranes modified by grafeting of hydrophilic polymers: an FT-IR/AFM/TEM study, Journal of Membrane Science, 209, 283-292.
Fukuda T., W. Yang, A. Yamauchi (2003). KCl transport mechanism across charged mosaic membrane in KCl–sucrose mixed system. J. Membr. Sci. 212: 255–261.

Gao, Y.X, and Chen Y.H, (1998) the latest development in Japan for NF, low pressure RO membranes and their application, Membrane science and technology, 18, 11-18.

Gozálvez-Zafrilla, J.M. , Sanz-Escribano, D. , Lora-García and M.C. León Hidalgo, (2008), Nanofiltration of secondary effluent for wastewater reuse in the textile industry, Desalination, 222, 272-279.

Garcia-Aleman J. and J.M. Dickson, (2004), Permeation of mixed-salt solutions with commercial and pore-filled nanofiltration membranes: membrane charge inversion phenomena, J. Membr. Sci. 239 , 163.

Garmes H, Persin F, Sadeaur J, Pourcelly G and Mountadar, M., (2002), Defluoridation of groundwater by a hybrid process combining adsorption and Donnan dialysis. Desalination 145, 287-291.

Gilron J., N. Gara and O. Kedem (2001). Experimental analysis of negative salt rejection in nanofiltration membranes. J. Membr. Sci., 185, 223-236.

Gotor, A.G., Pestana, I. and Espinoza, C.A., (2003), Optimization of RO desalination systems powered by renewable energies, Desalination, 156, 351- 360.

Ghorai, S., Pant, K.K., (2002) Investigations on the column performance of fluoride adsorption by activated alumina in a fixed bed. Report, Indian Institute of Technology Kharagpur.

Hafiane, A ., Lemordant, D . and Dhahbi, M ., (2000), Removal of hexavalent chromium by nanofiltration, Desalination, 130, 305-312 .

Haddada, R., Ferjani, E., Roudesli, M.S. and Deratani, A., (2004), Properties of cellulose acetate nanofiltration membranes: application to brackish water desalination, Desalination, 167, 403- 409.

Hafsi. M, (2001), Analysis of Boujdour desalination plant performance, Desalination, 134, 93-104.

Hassan, A. M., Al-Sofi, M. A. K. , Al-Amoudi, A. S., Jamaluddin, A. T. M., Farooque, A. M., Rowaili, A., Dalvi, A.G.I., Kither, N. M., Mustafa, G. M. and Al-Tisan, I.A.R., (1998), A new approach to membrane and thermal seawater desalination processes using nanofiltration membranes (Part 1) Desalination, 118, 35-51

Hassan , A. M., Farooque, A. M., Jamaluddin, A.T.M., Al-Amoudi, A.S., Al-Sofi, M.A.K., Al-Rubaian, A.F., Kither, N.M., Al-Tisan, I.A.R. and Rowaili, A., (2000), A demonstration plant based on the new NF—SWRO process, Desalination, 131, 157-171

Herold, D., (1998), Small scale photovoltaic desalination for rural water supply-Demonstration plant in Gran Canaria, Renewable Energy, 14, 293-298.

Hichour, M., Persin, F., Sandeaux, J., Gavach, C., (2000), Fluoride removal from waters by Donnan dialysis, Separation and Purification Technology,18, 1-11

Hilal, N., Al-Zoubi, H., Darwish, N.A., Mohammad, A.W. and Abu Arabi, M., (2004), A comprehensive review of nanofiltration membranes:Treatment, pretreatment, modelling, and atomic force microscopy, Desalination, 170, 281-308.

Hiller S, Cooper C, Kelligrau S, Rusel G, Hughes H and Coggon D (2000) Fluoride in drinking water and risk of hip fracture in the UK: A case-control study. The Lancet 335, 265-269

Hirose. M., Itoh, H. and Minamizaki, Y., (1996), Proceedings of the international congress on membranes and membrane process, Japan, 18- 23 August, pp. 178-179.

Hoffer, L., Schwinn, H., L. Biesert and D. Josic , (1995), Improved virus safety and purity of a chromatographically produced factor-IX concentrate by nanofiltration. Journal of Chromatography B-Biological Applications, 669, 187–196.

Hoppe W., Lohmann, W., Markl, H, Ziegler, H.,(1983), (Eds.), Biophysics, Berlin, Springer, 1983.

Hrayshat E.S. and E. Al-Rawajfeh A., (2008), A solar multiple effect distiller for Jordan Desalination, 220, 558-565

Huang, R., Chen, G., Sun, M. and Gao, C., (2008), Preparation and characterization of quaterinized chitosan/poly(acrylonitrile) composite nanofiltration membrane from anhydride mixture cross-linking, Separation and Purification Technology, 58, 393-399.

Huang, T.C, Shai, M.S and Pei, P.S, (2003), Cogeneration approach for near shore internal combustion power plants applied to seawater desalination, Energy Conversion & Management, 44, 1259-1273.

Huisman, I. H., Trägårdh, G., Trägårdh, C. and Pihlajamäki, A., (1998), Determining the zeta-potential of ceramic microfiltration membranes using the electroviscous effect, Journal of Membrane Science, 147, 187-194

Hwan Kim,J., DiGiano,F. A., Geens, J. and Vandecasteele, C.,(2004), Influence of MF pretreatment on NF performance for aqueous solutions containing particles and an organic foulant, Separation and Purification Technology, 36, 203-213.

Jain, S., Gupta, S.K., (2004), Analysis of modified surface force pore flow model with concentration polarization and comparison with Spiegler-Kedem model in reverse osmosis systems, Journal of Membrane Science, 232, 45-62.

Jain S., S.K. Gupta (2004). Analysis of modified surface pore flow model with concentration polarization and comparison with Spiegler–Kedem model in reverse osmosis system. J. Membr. Sci. 232: 45–61.
Jibril B., Ibrahim, A. A., (2001),Desalination 139 (2001) 287-295

Kecili, K., Etude et caractérisation de membranes synthétiques organiques immergées de microfiltration (MF) et d'ultrafiltration (UF) employées pour la production d'eau destinée à la consommation humaine :Intensification des opérations de déconditionnement et de nettoyage, Thesis, Université Pierre et Marie Curie (Paris VI), 2006.
Kedem O., A. Katchalsky (1958). Biochem. Biophys. Acta 27: 229.

Kedem O., A. Katchalsky (1963). Permeability of composite membranes : 1–3. Trans. Faraday Soc. 59:163

Khawaji, A.D., Kutubkhanah, I.K, Wie, J.M, (2008), Advances in seawater desalination technologies, Desalination 221, 47–69.

Kiso, Y., Sugiura, Y ., Kitao, T . and Nishimura, K ., (2001), Effects of hydrophobicity and molecular size on rejection of aromatic pesticides with nanofiltration membranes, Journal of Membrane Science ,192 1-10 .

Klinowski J., T. Foley, P. Meares (1974). Differential conductance coefficients in a cation-exchange membrane. Proc. R. Soc., Lond. A. 336 (1974) 327.

Kosutic, K. and B. Kunst (2002), Removal of organics from aqueous solutions by commercial RO and NF membranes of characterized porosities, Desalination,142, 47-56

Kosutic, K., Furac, L., Sipos, L. and Kunst, B., (2005), removal of arsenic and pesticides from drinking water by nanofiltration membranes, Separation and Purification Technology, 42, 137-144.

Kosutic, K., Dolar, D. and Kunst, B., (2006), On experimental parameters characterizing the reverse osmosis and nanofiltration membranes' active layer, Journal of Membrane Science, 282, 109-114.

Koyuncu, I., and Yzgan.,M, (2001), Application of Nanofiltration and reverse osmosis membranes to the salty and polluted surface water, Journal of Environemental Sciences and Health, 36, (7), 1321-1333.

Krieg. H.M, Modise.S.J, Keizer, K and Neomagus, H.W.J.P, (2004), Salt rejection in nanofiltration for single and binary salt mixtures in view of sulfates removal, Desalination, 171, 205-215.

Kwok, D. Y. and Neumann, A. W., (1999), Contact angle measurement and contact angle interpretation, Advances in Colloid and Interface Science, 81, 167-249.

Labbez,C., P. Fievet, A. Szymczyk, A. Vidonne, A. Foissy and J. Pagetti, Retention of mineral salts by a polyamide nanofiltration membrane, Sep. Purif. Technol. 30 (2003), p. 47.

Lebrun, R.E., Xu, Y., Dynamic characterization of nanofiltration and reverse osmosis membranes, Sep. Sci. Technol.34 (8) (1999) 1629.

Levenstein R., D. Hasson, R. Semiat, (1966), Utilization of the Donnan effect for improving electrolyte separation with nanofiltration membranes. Journal of Membrane Science, 116, 77.

Lhassani, A., Rumeau, M. and Benjelloun, D., (2000), Essai d'interprétation des mécanismes de transfert des sels en nanofiltration,Tribune de l'eau, N° 603–605, 100-107.

Lhassani, A., Rumeau, M. , Benjelloun, D. and Pontié, M., (2001), Selective demineralization of water by nanofiltration, Application to the defluorination of brackish water, Water Research, 35, 3260-3264.

Lin, Y.L., Chiang, P.C. and Chang, E.-E., (2007), Removal of small trihalomethane precursors from aqueous solution by nanofiltration, Journal of Hazardous Materials, 146, 20-29.

Li YH, Wang S, Cao A, Zhao D, Zhang X, Xu C, Luan Z, Ruan D, Lian J, WuD and Wei B (2001) Adsorption of fluoride from water by amorphous alumina supported on carbon nanotubes. Chem. Phys. Lett. 38(3) 469-476.

Loeb, S. and Sourirajan, S., (1962), Sea water demineralization by means of an osmotic membrane, Advances in Chemistry Series, 38, 117-125.

Lourdes, G.R. (2002), Seawater desalination driven by renewable energy: A review, Desalination, 143, 103-113.

Lu, G.Q., Diniz da Costa, J.C., Duke, M., Giessler, S., Scolow, R., Williams, R.H., Kreutz, T., (2007), Inorganic membranes for hydrogen production and purification: a critical review and perspective, Journal of colloid and interface science, 314, 589-603.

Mahmoudi, H. and Ghaffour, N., (2008), Capacity building strategies and policy for desalination using renewable energies in Algeria, Renewable and Sustainable Energy Reviews, In Press, Uncorrected Proof.

Mameri N., Yeddou A. R., Lounci, H., Belhocine, D, Grib H., Bariou, B., (1998) Defluoridation of septentrional Sahara water of North Africa by electrocoagulation process using bipolar aluminium electrodes, Wat. Res. 32 (5) 1604-1612.

Mänttäri, M., Pekuri, T., Nystrom, M., (2004), NF270 anew membrane having promising characteristics and being suitable for treatment of dilute effluents from the paper industry, Journal of Membrane Science, 242, 107-116.

Mänttäri, M., Pihlajamäki and A., Nystöm, M., (2006), Effect of pH on hydrophilicity and charge and their effect on the filtration efficiency of NF membranes at different pH, Journal of Membrane Science, 280, 311-320.

Mathioulakis, E., Belessiotis, V. and Delyannis, E., (2007), Desalination by using alternative energy: Review and state of the art, Desalination, 203, 346 - 365.

Matsumoto, H., Konosu, Y., Kimura, N., Minagawa, M. and Tanioka, A., (2007), Membrane potential across reverse osmosis membranes under pressure gradient, Journal of Colloid and Interface Science, 309, 272-278.

Matsuyama, H., Yuasa, M., Kitamura, Y., Teramoto, M. and Lloyd, D. R., (2000), structure control of anisotropic and asymmetric polypropylene membrane prepared by thermally induced phase separation, Journal of membrane science, 179, 91-100.

Matsuura T., (2001), Progress in membrane science and technology for seawater desalination- a review, Desalination, 47-54

Maurel, A., (1993), Techniques séparatives à membranes : Osmose inverse, nanofiltration, ultrafiltration, microfiltration tangentielle – Considérations théoriques, in techniques de l'ingénieur, p.p.1-24.

Maurel, A., (2006), Dessalement de l'eau de mer et des eaux saumâtres et autres procédés non conventionnels d'approvisionnement en eau douce, 2nd ed , Lavoisier

Meares P., J.F. Thain, D.G. Dawson (1972). Transport across ion-exchange resin membranes: the frictional model of transport. G. Eisenmann (Ed.), Membranes, Vol. 1, Dekker, New York, 1972 (Chapter 2).

Medeazza, G.M., (2004), Water desalination as a long-term sustainable solution to alleviate global freshwater scarcity ? A North- South approach, Desalination, 169, 287-301.

Menkouchi Salhli, M.A. Annouar, S., Mountadar, M., Soufiane, A. and Elmidaoui, A., (2008), Nitrate removal of brackish underground water by chemical adsorption and electrodialysis. Desalination, 227, 327 -333.

Menjeaud, C., Pontié, M. and Rumeau, M., (1993), Mécanismes de transfert en osmose inverse, Entropie, 179, 13-29.

Mjengera, H. and Mkongo, G. (2002) Appropriate defluoridation technology for use in fluorotic areas in Tanzania. 3rd WaterNet Symposium, Water Demand Management for Sustainable Development.

M'nif, A., Boughecha, S., Hamrouni, B., Dhahbi, M., (2007), Coupling of membrane processes for brackish water desalination, Desalination, 203,331-336.

Moges, G., Zewge, F. and Socher, M., (1996), Preliminary investigations on the defluoridation of water using fired clay chips. J. of Afr. Earth Sci. 21(4) 479- 482.

Mohan, G. Rao, N.V.R and Bhaskaran, C.S.,(1988), Studies on defluoridation of water. Journal. of Fluorine Chemistry. 41, 17-24

Mohsen, M.S. and A1-Jayyousi, O.R., (1999), Brackish water desalination: an alternative for water supply enhancement in jordan, Desalination, 124, 163-174.

Mohsen, M. S., Jaber J.O. and Afonso, M. (2003), Desalination of brackish water by nanofiltration and reverse osmosis, Desalination, 157, 167.

Morao, A.I.C., Alves, A.M.B., Afonso, M.D., (2006), Concentration of clavulanic acid broths: Influence of the membrane surface charge density on NF operation, Journal of Membrane Science, 281, 417-428.

Moros, A. Gozálvez-Zafrilla , J.M. and Lora-García, J., 2007, Nitrate removal from ternary ionic solutions by a tight nanofiltration membrane, Desalination, 204, 63-71.

Moturi, W.K.N, Tole, M.P and Davies, T.C. (2002), The contribution of drinking water towards dental fluorosis: A case study of Njoro division, Nakuru district, Kenya. Environ. Geochem. and Health 24 123-130

Murthy, Z.V. P., Gupta, S.K., (1997), Estimation of mass transfer coefficient using a combined nonlinear membrane transport and film theory model, Desalination, 109, 39-49.

Mulder, M., (2003) Basic principle of membrane technology, 2nd ed, Boston: Kluwer Academic publisher.

Muller, WJ, Heath, RGM and Villet, M.H (1998) Finding the optimum: Fluoridation of potable water in South Africa. Water SA 24(1) 21-27.

Nabe, A., Staude, E. and G. Beelfort, (1997), Surface modification of polysulfone ultrailtration membranes and fouling by BSA solutions, Journal of membrane science, 133, 57-72.

Neumann, A. W., Good, R.J., (1972), Thermodynamics of contact angles, Journal of Colloid and Interface Science, 38, 341- 358.

Nicos, X.T., (2001), Desalination and the environment, Desalination, 141, 223 -236.

Nguyen, Q.T., (1999), Membranes organiques : mode de préparation des membranes pour les séparations spécifiques, L'actualité Chimique, on February.

Notcout, G and Davies, F. (1999) Biomonitoring of volcanogenic fluoride,Furnas Caldera, Sao Miguel, Azores. J. of Volcan. and Geoth. Res. 92 209-214

Ortigez, J.M., Exposito, E., Gllud, F., Garcia, V., Montiel, V., Aldaz, A., (2007) Electrodialysis of brackish water powered by photovoltaic energy without batteries: direct connection behavior, Desalination, 208, 89-100.

Palmeri, J., Blanc, P., A. Larbot and P. David, (2000), Hafnia ceramic nanofiltration membranes: Part II. Modeling of pressure-driven transport of neutral solutes and ions, Journal of Membrane Science, 179, 243-266.

Paugam, L., Taha, S., Dorange, G., Jaouen, P., Quéméneur, F., (2003), Mechanism of nitrate ions transfer in nanofiltration depending on pressure, pH, concentration and medium composition, Journal of Membrane Science 231 , 37–46

Pearce, G., Introduction to membranes: Membrane selection, Filtration and Separation, April (2007).

Peeters, J. M. M., Boom, J. P., Mulder, M. H. V. and Strathmann, H., (1998), Retention measurements of nanofiltration membranes with electrolyte solutions, Journal of Membrane Science, 145, 199-209.

Peeters, J.M.M., Mulder, M.H.V. and Strathmann, H., (1999), Streaming potential measurements as a characterization method for nanofiltration membrane, Colloids and Surfaces A, 150, 247-259.

Perry, M. and Linder, C., (1989), Intermediate reverse osmosis ultrafiltration (RO UF) membranes for concentration and desalting of low molecular weight organic solutes, Desalination, 71, 233-245.

Pontalier, P.Y., Ismail A. and Ghoul M.,(1997), Mechanism for the selective rejection of solutes in nanofiltration membranes. Separation and purification technology, **12**,175.

Pontié, M., Sissoko, H., Rumeau, M. and Mar-Diop, C., (1994), Dessalement sélectif des eaux saumâtres fluorurées du bassin du Sénégal par nanofiltration, 1ères. Journées Internationales Interfiltra-Intermembrane, Paris, 101.

Pontié, M ., Phénomènes électrocinétiques et transferts ioniques dans les membranes poreuses à faible seuil de coupure. Application au traitement des eaux saumâtres, Thesis, Tours University, 1996.

Pontié, M., Chasseray, X., Lemordant, D., Lainé, J.M., (1997), Electrokinetic phenomena in microporous composite organic membranes of weak charge density, Journal de Chimie Physique et de Physico-Chimie Biologique, 94, 1741-1762.

Pontié, M., Sarr , O. and Rumeau, M., (1997), Evaluation des possibilités de déssalement d'une eau saumâtre par osmose inverse et par nanofiltration, L'eau l'industrie les nuisances, 210, 57-63.

Pontié, M., Diawara, C. K. and Rumeau, M., (2002), Streaming effect of single electrolyte mass transfer in nanofiltration: potential application for the selective defluorination of brackish drinking waters, Desalination, 151, 267-274.

Pontié, M., Lhassani, A., Diawara, C.K., Elana, A., Innocent, C., Aureau, D., Rumeau, M. , Croue, J.P., Buisson, H. and Hemery, P., (2004), Seawater nanofiltration for the elaboration of usable salty waters, Desalination, 167, 347-355.

Pontié, M., Dach, H., Leparc, J., Hafsi, M. and Lhassani, A.,(2008), Novel approach combining physico-chemical characterizations and mass transfer modelling of nanofiltration and low pressure reverse osmosis membranes for brackish water desalination intensification, Desalination, 221, 174-191.

Pouet, F., Persin, F., Rumeau, M., (1992) Intensive treatment by electrocoagulation -flotation - tangential flow microfiltration in areas of high seasonal population,Water Research,25, 247-253.

Rautenbach, R. and Gröschl, A., (1990), Separation potential of nanofiltration membranes, Desalination, 77, 73-84.

Richards, B.S and Schäfer, A.I., (2003), Photovoltaic-powered desalination system for remote Australian communities, Renewable Energy, 28, 2013-2022.

Richards, B., Remy, C. and Schäfer, A.I., (2004), Sustainable drinking water production from brackish sources using photovoltaics, 19th European Photovoltaic and Solar Energy Conversion Conference, Paris, France, p.p 3369–3372.

Rice, C.L., Whitehead, R., (1965), Electrokinetic flow in narrow cylindrical capillary, Journal of Physical chemistry, 69, 4017- 4024.

Redondo, J.A., (2001), Brackish-, sea- and wastewater desalination, Desalination, 138, 29-40.

Rodriguez J. J., V. Jimenez, O. Trujillo, J. M. Veza, (2002) Desalination 150 219-225
Robinson, R., Ho, G. and Mathew, K., (1992), Development of a reliable low-cost reverse osmosis desalination unit for remote communities, Desalination, 86, 9-26.

Rovel, J.M, state and behavior of seawater desalination in the future, Proceedings of CHEMRAWNXV, 21-23 june 2004, Paris, 22-28.

Rosa M.J. and. de Pinho M.N, (1995), The role of ultrafiltration and nanofiltration on the minimization of the environmental-impact of bleached pulp effluents, Journal of Membrane Science, 102 , 155–161.

Rumeau, M., (1990), Membrane: transfert, Encyclopedia Universalis - C14: 911.

Rumeau M. and Pontié, M., (1998), Potabilisation d'une eau saumâtre hyperfluorurée du Sénégal par déminéralisation sélective. Hydrotop. Marseille, 21–23 Avril.

Saffaj, N., Persin, M., Younssi, S. A., Albizane, A., Bouhria, M., Loukili, H., Dach, H. and Larbot, A., (2005), Removal of salts and dyes by low $ZnAl_2O_4$–TiO_2 ultrafiltration membrane deposited on support made from raw clay, Separation and Purification Technology, 47, 36-42.

Santafé-Moros, A., Gozálvez-Zafrilla, J.M., Lora-García, J.,(2007), Nitrate removal from ternary ionic solutions by a tight nanofiltration membrane, Desalination, 204, 63 -71.

Sbaï, M., Fievet, P., Szymczyk, A., Aoubiza, B., Vidonne, A. and Foissy, A., (2003), Streaming potential, electroviscous effect, pore conductivity and membrane potential for the determination of the surface potential of a ceramic ultrafiltration membrane, Journal of Membrane Science , 215, 1-9.

Schaep, J., Van der Brugen,B., Uyetherhoven, S., Croux, R., Vandecasteele, C., Wilms, D., Van Houtte, E. and Vanlerberghe, F.,(1998), Removal of hardness from groundwater by nanofiltration, Desalination, 119,295-301.

Schaep, J., Vandecasteele, C., A.W. Mohammad and W.R. Bowen, (1999) Analysis of salt retention of nanofiltration membranes using the Donnan-Steric partitioning Pore Model, Separation Science and Technology., 34 , 3009.

Schaep, J., Vandecasteele, C., Peeters, B., Luyten, J., Dotremont, C. and Roels, D., (1999), Characteristics and retention properties of a mesoporous γ-Al$_2$O$_3$ membrane for nanofiltration Journal of Membrane Science, 163, 229-237.

Schaep, J. and Vandecasteele, C., (2001), Evaluating the charge of nanofiltration membranes, Journal of Membrane Science, 188,129-136.

Schäfer. I.A and Richards, B.S., (2005), Testing of a hybrid membrane system for groundwater desalination in ana Australian national park, Desalination, 183, 55-62.

Schäfer. I.A, Broeckmann, A. and Richards, B.S.,(2007), Renewable energy powered membrane technology. Development and characterization of a photovoltaic hybrid membrane system, Environemental Science and Technology, 41, 998-1003.

Scheomean, J.J and Leach, G.W., (1986), An invesigation of the performance of two newly installed defluoridation plants in South Africa and some factors affecting their performance. Water Sci. Tech. 19 953-965.

Sforça, M. L., Yoshida, I. V. P. and Nunes, S. P. (1999), Organic–inorganic membranes prepared from polyether diamine and epoxy silane, Journal of Membrane Science, 159, 197-207.

Shih, M-C., (2005), An overview of arsenic removal by pressure-driven membrane processes, Desalination, 172, 85-97.

Sivakumar, M., Mohan, D.R., and Rangarajan R., (2006), Studies on cellulose acetate-polysulfone ultrafiltration membranes II. Effect of additive concentration, Journal of Membrane Science, 268, 208-219.

Singh, S., K. C. Khulbe, T. Matsuura and P. Ramamurthy, (1998), Membrane characterization by solute transport and atomic force microscopy, Journal of Membrane Science, 142, 111-127

Slezak A., Turczynski, B., Nawrat, Z., (1989), Modification of the Kedem–Katchalsky–Zelman model equations of the transmembrane Transport. J. Non-Equilib. Thermodyn. 14: 205–218.

Spiegler, K.S, Kedem, O., (1966), Thermodynamics of hyperfiltration (reverse osmosis): criteria for efficient membrane, Desalination, 1, 311-326.

Srimurali, M, Prghati, A. and Khartikeyane, J. (1998), A study on removal of fluorides from drinking water by adsorption onto low-cost materials. Environ. Pollut. 99 285-289.

Starthmann, H., (1999), Membrane process for sustainable industrial growth, Membrane technology N° 113.

Staverman A.J. (1952) .Trans. Faraday Soc. 48: 176.

Schlögl R. (1964). Stoff transport durch Membranen. Steinkopff, Darmstadt, 1964.

Suen, S-Y., Liu, Y-C. and Chang, C-S., (2003), Exploiting immobilized metal affinity membranes for the isolation or purification of therapeutically relevant species, Journal of Chromatography B, 797, 305-319.

SUSHEELA AK (2001) Sound planning and implementation of fluoride and fluorosis mitigation programme in an endemic village. Int. workshop on fluoride in drinking water

Sutzkover I., D. Hasson, R. Semiat (2000) . Simple technique fro measuring the concentration polarization level in a reverse osmosis system. Desalination 131: 117–127.

Szaniawska, D., H.G. Spencer, Non-equilibrium thermodynamics analysis of the transport properties of formed-inplace Zr(IV) hydrous oxide–PAA membranes. II. NaCl–water solutions, Desalination 101 (1995) 31.

Szymczyk, A, Sbai, M., Fievet, P. and Vidonne, A., (2006), Transport properties and electrokinetic characterization of an amphoteric nanofilter, Langumir, 22, 3910-3919.

Szymczyk, A. and Fievet, P. (2006) Ion transport through nanofiltration membranes: the steric, electric and dielectric exclusion model, Desalination, 200, 122-124

Szymczyk, A, Fievet, P and Ramseyer, C., (2006), Dielectric constant of electrolyte solutions confined in a charged nanofiltration membrane Desalination, 200, 125-126.

Szymczyk. A., Fatin-Rouge, N. and Fievet, P., (2007) Tangentiel streaming potential as a tool in modeling of ion transport thtough nanoporous membranes, Journal of colloids and Interface Science, 309, 245-252.

Sy, M.H., Sene, P., Diouf, S., (1996), Fluorose osseuse au niveau de la main, Société d'Edition de l'association d'enseignement médical des hopitaux de Paris, 15 (2) 109-115.

Tahaikt, M., Achary, I., Menkouchi Sahli, M.A., Amor, Z., Taky, M., Alami, A., Boughriba, A., Hafsi, M. and Elmidaoui, A.,(2006), Defluoridation of Moroccan groundwater by electrodialysis: continuous operation, Desalination, 189, 215-220.

Tahaikt, M., El Habbani, R., Ait Haddou, A., Achary, I., Amor, Z., Taky, M., Alami, A., Boughriba, A., Hafsi M.and Elmidaoui, A., (2007), Fluoride removal from groundwater by nanofiltration, Desalination, 212, 46-53.

Tahaikt, M., Ait Haddou, A., El Habbani, R., Amor, Z., Elhannouni, F., Taky, M., Kharif, M., Boughriba, A., Hafsi, M. and Elmidaoui, A., (2008), Comparison of the performances of three commercial membranes in fluoride removal by nanofiltration. Continuous operations Desalination, 225, 209-219.

Tahri K., (2001), The prospects of fresh water supply for Tan Tan City from non-conventional water resources, Desalination, 135, 43-50.

Tanninen, J., Mänttäri, M., Nyström, M., (2006), Effect of salt mixture concentration on fractionation with NF membranes, Journal of Membrane Science, 283, 57-64.

Teixeira, M. R. and Rosa, M.J., (2006), Neurotoxic and hepatotoxic cyanotoxins removal by nanofiltration, 40, 2837-2846.

Teixeira, M., Rosa M. and Nyström, M., (2005),The role of membrane charge on nanofiltration performance Journal of Membrane Science, 265, 160-166

Thekkedath, A., Etude du colmatage de membranes d'ultrafiltration (UF) par la matière organique naturelle (MON), Thesis, Université d'Angers, 2007.

Thomson, M., Miranda, M.S. and Infield, D.,(2003), A small-scale seawater reverse-osmosis system with excellent energy efficiency over a wide operating range, Desalination, 153, 229-236.

Travi Y.,Hydrogéologie et hydrologie isotopique des aquifères fluorés du bassin du Sénégal, Ph D thesis, Univ. Paris-Sud, Orsay (1988); Mémoire N° 95, CNRS, ISSN 0302-2684 (1993).

Tsuru, T. M., Urairi, S. Nakao and S. Kimura , (1991), Reverse osmosis of single and mixed electrolytes with charged membranes: Experiment and analysis. Journal of Chemical Engineering of Japan, 24 , 518–524.

Ulbricht, M., (2006), Advanced functional polymer membranes, Polymer, 47, 2217-2226.

Van der Bruggen, B., Schaep, J., Maes, W., Wilms, D. and Vandecasteele, C., (1998), Nanofiltration as a treatment method for the removal of pesticides from ground waters. Desalination,117, 139.

Van der Bruggen, B., Schaep, J., Wilms D., and Vandecasteele C., (1999), Influence of molecular size, polarity and charge on the retention of organic molecules by nanofiltration, Journal of Membrane Science, 156, 29-41.

Van der Bruggen, B., Schaep, J., Wilms, D. and Vandecasteele, C., (1999), Influence of molecular size, polarity and charge on the retention of organic molecules by nanofiltration, Journal of Membrane Science , 156, , 29-41 .

Van der Bruggen, B ., Everaert, K ., Wilms, D. and Vandecasteele, C., (2001), Application of nanofiltration for removal of pesticides, nitrate and hardness from ground water: rejection properties and economic evaluation, Journal of Membrane Science, 193, 239-248 .

Van Der Bruggen, B. and Vandelcasteele, C., (2002), Distillation vs. membrane filtration: overview of process evolutions in seawater desalination, Desalination, 143, 207-218.

Van Der Bruggen, B., Vandecasteele, C., Van Gestel, T., Doyen, W., Leysen, R., (2003), A review of pressure-driven membrane processes in wastewater treatment and drinking water production, Environmental Progress, 22 (1), 46-56.

Van Der Bruggen, B., Vandecasteele, C., (2003), Removal of pollutants from surface water and groundwater by nanofiltration: overview of possible applications in the drinking water industry, Environmental Pollution, 122, 435- 445.

Van der Bruggen, B. , A. Koninckx and C. Vandecasteele, (2004)Separation of monovalent and divalent ions from aqueous solution by electrodialysis and nanofiltration, Water Research, 38, 1347-1353

Van der Bruggen, B., Schaep, J ., Maes, W., Wilms, D. and Vandecasteele, C ., (1998), Nanofiltration as a treatment method for the removal of pesticides from ground waters, Desalination, 117, 139-147.

Van der Horst H.C., Timmer, J.M.K., Robbertsen T. and J. Leenders , (1995),Use of nanofiltration for concentration and demineralization in the dairy industry: Model for mass transport. Journal of Membrane Science 104 ,205–218.

Van Gestel, T., Vandecasteele, C., Buekenhoudt, A.,.Dotremont, C., Luyten, J., Leysen, R., Van der Bruggen, B. and Maes, G., (2002), Salt retention in nanofiltration with multilayer ceramic TiO_2 membranes, Journal of Membrane Science, 209, 379-389.

Ventresque, C. and Bablon, G .,(1997),The integrated nanofiltration system of the Mery-sur-Oise surface water treatment plant (37 mgd), Desalination, 113, 263-266 .

Ventresque, C., Gisclon, V., Bablon, G. and Chagneau, G ., (2000), An outstanding feat of modem technology : the Mery-sur-Oise nanofiltration treatment plant (340,000 m'/d), Desalination, 131, 1-16 .
Vedavaysan C.V., Desalination 139 (2001) 419-421 ;

Veressinina, Y., Trapido,. M Ahelik, V. and Munter, R. (2001) Fluoride in drinking water: The problem and its possible solutions. Proc. Estonian Acad. Sci. Chem. 50(2) 81-88

Veza J. M., J. J. Rodriguez-Gonzalez, Desalination 157 (2003) 65-72 ;

Violleau, D., Essis-Tome, H., Habarou, H., Croué, J.P., Pontié, M., (2005), Fouling studies of a polyamide nanofiltration membrane by selected natural organic matter: an analytical approach, Desalination, 173 (2005) 223.

Vrijenhoek, E.M., Hong, S. and Elimelech, M., (2001) Influence of membrane surface properties on initial rate of colloidal fouling of reverse osmosis and nanofiltration membranes, Journal of membrane science, 188**,** 115–128.

Wangnick, K. (2002) IDA Worldwide Desalting Plants Inventory. Report No. 17. Gnarrenburg, Germany: Wangnick Consulting GMBH.

Walha, K., Ben Amer, R., Firdaous, L., Quéméneur, F. and Jaouen, P., (2007), Brackish groundwater treatment by nanofiltration, reverse osmosis and electrodialysis in Tunisisa: performance and cost comparison, Desalination, 207, 95 - 106.

Wang,Y., Reardon, E.J.,(2001),Activation and regeneration of a soil sorbent for defluoridation of drinking water. App. Geochem. 16, 531-539.

Wang, W., Li, R., Tan, J., Luo, K., Yang, L., Li, H. and Li, Y. (2002). Adsorption and leaching of fluoride in soils of C hina. Fluoride 35(2) 122-129

Wang, M. Su, Z.Y. Yu, X.L. Wang, M. Ando and T. Shintani, (2005),Separation performance of a nanofiltration membrane influenced by species and concentration of ions, Desalination 175, 219.

Wang D., Wang, X. , Tomi, Y, Masaaki, A. and T Shintani, (2006) Modeling the separation performance of nanofiltration membranes for the mixed salts solution, Journal of Membrane Science, 280, 734-743.

Wang X.L., Wang W.N. and D.X. Wang, (2002) Experimental investigation on separation performance of nanofiltration membranes for inorganic salt solutions, Desalination 145, 115

Watson, B.M. and Homburg, C .D., (1989), Low-energy membrane nanofiltration for removal of color, organics and hardness from drinking water supplies, Desalination, 72,11-22 .

Wijmans, J. G. and Baker, R. W., (1995), The solution-diffusion model: a review, Journal of Membrane Science, 107, 1-21.

Wittmann, E., Cote, P ., Medici, C ., Leech , J. and Turner, A.G.,(1998) Treatment of a hard borehole water containing low levels of pesticide by nanofiltration, Desalination, 119 347-352

Yang, F., Zhang, S., Yang, D. and Jian, X.,(2007), Preparation and characterization of polypiperazine amide/PPESK hollow fiber composite nanofiltration membrane, Journal of Membrane Science, 301, 85-92.

Yang, M., Hashimoto, T., Hodhi, N and Myoga, H. (1999) Fluoride removal in a fixed bed packed with granular calcite. Water Res. 33(16) 3395-3402

Yang, CL. and Dluhy, R. (2002), Electrochemical generation of aluminium sorbent for fluoride adsorption. J. of Hazardous Materials 94(3) 239-252.

Yaroshchuk, A.E , (2001), Non-steric mechanisms of nanofiltration: Superposition of Donnan and dielectric exclusion, Separation and purification Technology, 22, 143.

Zidouri H, (2000),Desalination of Morocco and presentation of design and operation of the Laayoune seawater reverse osmosis plant, Desalination, 131, 137-145

Zelman A., (1972), Membrane permeability. Generalization of the reflection coefficient method of describing volume and solute flow, Biophys. J. 12: 414–419.

Zhu, X. and Elimelech, M., (1997), Colloidal fouling of reverse osmosis membranes: measurements and fouling mechanisms, Environment science and Technology, 31, 3564–3662.

Zimmermann, R., Dukhlin, S., Werner, C., (2001), A concept for the generalization of the standard electrokinetic model, Colloids and Surfaces A: Physicochemical and Engineering Aspects, 195, 103-112.

Electronic resources

DOW (2005). FILMTEC Membrane Elements - Technical Manual, Dow Liquid Separations. available at: http://www.dow.com/liquidseps/lit/techman.htm (accessed: November 07)

DOW, ROSA, Version 6.1. Dow Liquid Separations. Available at: http://www.dow.com/liquidseps/design/rosa.htm (accessed: November 07)

Hydranautics, (2000), Technical Service bulletins, Available at: http://www.membranes.com/index.php?pagename=tech_bulletins (accessed: November 07)

SAEHAN, (2006),Technical manual: Reverse osmosis membranes, Available at: http://www.saehancsm.com/ (accessed: November 07)

UNESCO (2003). The United Nations World Water Development Report - Water for People - Water for Life (Executive Summary), UNESCO Publishing / Berghahn Books.

WHO (2006) Guidelines for drinking-water quality: incorporating first addendum, Vol. 1, 3rd ed, Recommendations. World Health Organization. Available at: http://www.who.int/water_sanitation_health/dwq/gdwq0506.pdf

Review of the Desalination and Water Purification Technology Roadmap, (2004), Water Science and Technology Board (WSTB).

International Desalination Association: www.idadesal.org.com

Thesis related publications

Reffered journal papers

Maxime Pontié, **Hanane Dach**, Jérôme Leparc, Mahmoud Hafsi et Abdelhadi Lhassani; Novel approach combining physico-chemical characterizations and mass transfer modelling of nanofiltration and low pressure reverse osmosis membranes for brackish water desalination intensification, Desalination, 221, (2008), 174-191.

Book chapters

Maxime Pontié, Courfia Diawara, Abdelhadi Lhassani, **Hanane Dach**, Michel Rumeau, Hervé Buisson et Jean Christophe Schrotter; Chapter 2 Water Defluoridation Processes: A Review. Application: Nanofiltration (NF) for Future Large-Scale Pilot Plants, Advances in Fluorine Science, 2, (2006), 49-80.

Reffered conference papers

1 Hanane DACH, Maxime PONTIE, Abdelhadi LHASSANI, Élimination sélective par nanofiltration (NF) d'ions indésirables présents dans les eaux saumâtres: approches analytique et phénoménologique intégrées, GRUTTEE 27-29 Septembre 2005 Aix-les-Bains FRANCE.

2 Hanane DACH, Maxime PONTIE, Abdelhadi LHASSANI, Mohammed BOUGHRIBA, Jérôme LEPARC, Comparaison des opérations de nanofiltration (NF) et d'osmose inverse (OI) pour un dessalement sélectif et durable des eaux saumâtres au Maroc : Approche couplant des caractérisations physico-chimiques et une modélisation phénoménologique, Symposium international Environnement, Catalyse et Génie des Procédés - ECGP5, 24-26 avril 2006, Fès, MAROC.

3 Hanane DACH, Maxime PONTIE, Nanofiltration as a sustainable water defluoridation operation dedicated to large scale pilot plants for the future, World Filtration Congress: Discover the future of filtration and separation, 14-18 Avril 2008, Leipzig, Germany.

Posters

Hanane Dach, Jérôme Leparc, Abdehadi Lhassani, Mahmoud Hafsi, M.Pontié, Novel approach combining physic-chemical characterizations and mass transfer modelling of nanofiltration and low pressure reverse osmosis membranes for brackish water desalination intensification, European Desalination Society: Desalination and the envirennement, 22-25 Avril 2007, Halkidiki, GRECE.

Appendix (1)

Table A1: *Summury of tests results for the BW30 membrane (Working pressure and Chemical analysis of the permeate) at different operation conditions*

				BW30 (RO)							
Flux (L/m^2-hr)	Recovery rate (± 2 %)	Feed Pressure (bar)	Permeate TDS (mg/L)	Permeate							
				Cl$^-$ (mg/L)	NO$_3^-$ (mg/L)	F$^-$ (mg/L)	K$^+$ (mg/L)	Na$^+$ (mg/L)	SO$_4^{2-}$ (mg/L)	Ca^{2+} (mg/L)	Mg^{2+} (mg/L)
13	10%	8.5 ± 0.1	105 ± 7	45	4.2	0.05	0.61	25.2	3.2	≈ 0	≈ 0
	45%	9,7 ± 0.1	184 ± 11	80	5.6	0.07	1.1	45.2	4.6	≈ 0	≈ 0
	70%	11.2 ± 0.1	289 ± 7	123	7.3	0.12	1.5	53.5	5.9	≈ 0	≈ 0
	90%	15.4 ± 0.2	360 ± 10	143	11.5	0.17	1.8	60.5	6.7	≈ 0	≈ 0
19	10%	11.5 ± 0.3	70 ± 14	32	2.9	0.02	0.45	21.1	2.1	≈ 0	≈ 0
	45%	13.4 ± 0.4	132 ± 15	61	4.1	0.06	1	31.5	3.2	≈ 0	≈ 0
	70%	15.7 ± 0.3	206 ± 14	104	6.5	0.09	1.2	41.5	5.7	≈ 0	≈ 0
	90%	- (*)	-	-	-	-	-	-	-	-	-
26	10%	13.7 ± 0.1	54 ± 5	20	2.4	0 ,02	0.31	13.8	1.5	≈ 0	≈ 0
	45%	16.4 ± 0.4	106 ± 16	53	3.1	0.04	0.6	23.7	3.1	≈ 0	≈ 0
	70%	19.1 ± 0.2	165 ± 10	94	4.5	0.07	1.3	45.7	5.2	≈ 0	≈ 0

Table A2: *Summury of tests results for the REBLF membrane (Working pressure and Chemical analysis of the permeate) at different operation conditions*

				RE BLF SAEHAN (RO)							
Flux (L/m^2-hr)	Recovery rate (± 2 %)	Feed Pressure (bar)	Permeate TDS (mg/L)	Permeate							
				Cl$^-$ (mg/L)	NO$_3^-$ (mg/L)	F$^-$ (mg/L)	K$^+$ (mg/L)	Na$^+$ (mg/L)	SO$_4^{2-}$ (mg/L)	Ca^{2+} (mg/L)	Mg^{2+} (mg/L)
13	10%	5.4 ± 0.4	155 ± 5	82	5.4	0.04	0.72	29.1	5.9	≈ 0	≈ 0
	45%	6.3 ± 0.3	267 ± 26	120	7.6	0.07	1.39	56.2	6.2	≈ 0	≈ 0
	70%	7.3 ± 0.3	440 ± 20	194	9.7	0.09	2.25	95.3	7.1	≈ 0	≈ 0
	90%	8.4 ± 0.2	578 ± 28	287	10.7	0.10	3.03	126.1	7.4	≈ 0	≈ 0
19	10%	6.7 ± 0.3	99 ± 5	50	3.3	0.04	0.53	22	3.6	≈ 0	≈ 0
	45%	7.8 ± 0.1	178 ± 12	90	5.2	0.05	0.88	36.9	4.1	≈ 0	≈ 0
	70%	8.7 ± 0.2	298 ± 20	164	6.8	0.07	1.59	66.1	4.9	≈ 0	≈ 0
	90%	10.1 ± 0.2	435 ± 30	187	8.7	0.09	2.30	96.3	5.2	≈ 0	≈ 0
26	10%	7.7 ± 0.3	78 ± 4	36	2.3	0.03	0.41	15.9	2.8	≈ 0	≈ 0
	45%	8.7 ± 0.3	150 ± 10	73	4.9	0.04	0.74	30.8	3.1	≈ 0	≈ 0
	70%	9.9 ± 0.2	260 ± 20	100	5.7	0.05	1.33	54.9	3.6	≈ 0	≈ 0
	90%	12.2 ± 0.3	390 ± 35	150	8.1	0.07	2.21	91.9	4.4	≈ 0	≈ 0

Table A3: *Summury of tests results for the ESPA3 membrane (Working pressure and Chemical analysis of the permeate) at different operation conditions*

Flux (L/m²-hr)	Recovery rate (± 2 %)	Feed Pressure (bar)	Permeate TDS (mg/L)	ESPA3 (LPRO) Permeate Cl⁻ (mg/L)	NO₃⁻ (mg/L)	F⁻ (mg/L)	K⁺ (mg/L)	Na⁺ (mg/L)	SO₄²⁻ (mg/L)	Ca²⁺ (mg/L)	Mg²⁺ (mg/L)
13	10%	5.7 ± 0.1	180 ± 6	82	5.4	0.04	0.76	31.1	3.2	≈ 0	≈ 0
	45%	6.5 ± 0.2	285 ± 15	120	7.6	0.07	1.27	52.2	4.7	≈ 0	≈ 0
	70%	7.9 ± 0.2	480 ± 10	194	9.7	0.09	2.23	90.6	5.4	≈ 0	≈ 0
	90%	9.0 ± 0.2	550 ± 20	287	10.7	0.10	3.48	140.9	5.9	≈ 0	≈ 0
19	10%	7.4 ± 0.1	107 ± 5	50	3.3	0.04	0.46	19.2	2.8	≈ 0	≈ 0
	45%	8.4 ± 0.1	196 ± 6	90	5.2	0.05	0.89	35.8	3.2	≈ 0	≈ 0
	70%	9.3 ± 0.1	336 ± 14	164	6.8	0.07	1.55	63.5	3.8	≈ 0	≈ 0
	90%	10.8 ± 0.1	390 ± 23	187	8.7	0.09	2.61	108.3	4.1	≈ 0	≈ 0
26	10%	8.3 ± 0.1	88 ± 2	36	2.3	0.03	0.36	15.3	2.7	≈ 0	≈ 0
	45%	9.5 ± 0.1	166 ± 7	73	4.9	0.04	0.77	31.3	2.6	≈ 0	≈ 0
	70%	10.4 ± 0.2	256 ± 10	100	5.7	0.05	1.28	51.9	3.1	≈ 0	≈ 0
	90%	11.9 ± 0.3	360 ± 35	150	8.1	0.07	2.46	105.3	3.9	≈ 0	≈ 0

Table A4: *Summury of tests results for the BW30LE membrane (Working pressure and Chemical analysis of the permeate) at different operation conditions*

				BW30 LE (RO)							
Flux (L/m²-hr)	Recovery rate (± 2 %)	Feed Pressure (bar)	Permeate TDS (mg/L)	Permeate							
				Cl⁻ (mg/L)	NO₃⁻ (mg/L)	F⁻ (mg/L)	K⁺ (mg/L)	Na⁺ (mg/L)	SO₄²⁻ (mg/L)	Ca²⁺ (mg/L)	Mg²⁺ (mg/L)
13	10%	6.4 ± 0.2	179 ± 5	88	8.7	0.07	0.86	31.6	5.1	≈ 0	≈ 0
	45%	6.8 ± 0.1	270 ± 13	134	10.2	0.09	1.37	48.5	5.9	≈ 0	≈ 0
	70%	7.5 ± 0.1	390 ± 10	168	12.1	0.10	2.39	83 .2	6.4	≈ 0	≈ 0
	90%	8.4 ± 0.1	560 ± 20	305	15.5	0.11	3.05	103	6.7	≈ 0	≈ 0
19	10%	7.9 ± 0.1	130 ± 7	65	6.3	0.04	0.65	24	3.8	≈ 0	≈ 0
	45%	8.4 ± 0.1	185± 15	101	8.8	0.07	0.95	34.6	4.1	≈ 0	≈ 0
	70%	9.9 ± 0.3	275 ± 7	148	10.1	0.09	1.57	54	4.2	≈ 0	≈ 0
	90%	11.2 ± 0.1	420 ± 10	218	14.1	0.10	2.58	83.9	4.9	≈ 0	≈ 0
26	10%	9.2 ± 0.1	95 ± 4	44	4.3	0.02	0.47	17.8	3.1	≈ 0	≈ 0
	45%	9.7 ± 0.1	137 ± 7	74	6.9	0.04	0.76	27.7	3.1	≈ 0	≈ 0
	70%	11.0 ± 0.3	240 ± 10	111	8.9	0.05	1.48	48.2	3.2	≈ 0	≈ 0
	90%	13.7 ± 0.1	340 ± 10	175	12.5	0.06	2.51	79.8	3.8	≈ 0	≈ 0

Table A5: *Summury of tests results for the NF90 membrane (Working pressure and Chemical analysis of the permeate) at different operation conditions*

Flux (L/m²-hr)	Recovery rate (± 2 %)	Feed Pressure (bar)	Permeate TDS (mg/L)	Permeate Cl⁻ (mg/L)	NO₃⁻ (mg/L)	F⁻ (mg/L)	K⁺ (mg/L)	Na⁺ (mg/L)	SO₄²⁻ (mg/L)	Ca²⁺ (mg/L)	Mg²⁺ (mg/L)
				NF90 (NF)							
13	10%	$4,8 \pm 0,1$	361 ± 6	197	13,1	0,12	1.69	67.6	5.1	10.4	6.8
	45%	$5,6 \pm 0,1$	470 ± 30	294	14.6	0,15	2.2	89.3	6.6	12.1	9.1
	70%	$6,4 \pm 0,1$	770 ± 20	300	16.9	0,22	2.5	156	7.9	16.4	9.5
	90%	$7,7 \pm 0,2$	1130 ± 20	626	20,5	0,3	5.4	225.9	8.2	20	11.2
19	10%	$6,1 \pm 0,1$	253 ± 10	105	10,3	0,11	1.1	47.8	4.1	7.3	3.8
	45%	$6,7 \pm 0,1$	370 ± 10	184	13,5	0,13	1.6	67.6	5.3	8.9	5.1
	70%	$7,8 \pm 0,2$	594 ± 14	255	15,1	0,16	3.9	112.4	6.7	13.1	6.2
	90%	$9,2 \pm 0,3$	762 ± 30	477	18,6	0,28	4.1	167.9	6.1	15	7.7
26	10%	$7,3 \pm 0,1$	190 ± 10	74	9,3	0,08	0.9	37.6	2.8	4.1	1.3
	45%	$7,7 \pm 0,1$	308 ± 8	136	11,7	0,10	1.4	56.4	3.6	7.8	2.5
	70%	$9,2 \pm 0,1$	490 ± 30	220	13.7	0,14	2.8	102.2	3.9	10.1	3.7
	90%	$11,3 \pm 0,2$	840 ± 35	455	17.2	0,24	3.8	156.9	4.7	11.3	4.2

Table A6: *Summury of tests results for the NE90 membrane (Working pressure and Chemical analysis of the permeate) at different operation conditions*

Flux (L/m²-hr)	Recovery rate (± 2 %)	Feed Pressure (bar)	Permeate TDS (mg/L)	Permeate							
				Cl^- (mg/L)	NO_3^- (mg/L)	F^- (mg/L)	K^+ (mg/L)	Na^+ (mg/L)	SO_4^{2-} (mg/L)	Ca^{2+} (mg/L)	Mg^{2+} (mg/L)
13	10%	5,3 ± 0,1	378 ± 10	154	13,1	0,09	1.55	63.0	6.2	12.7	7.5
	45%	6,2± 0,1	560 ± 30	265	14.6	0,11	2.8	106.7	9.3	14.4	9.2
	70%	7,1 ± 0,1	912 ± 32	446	16.9	0,15	4.3	171	11.7	18.6	11
	90%	8,2 ± 0,2	1240 ± 50	560	20,5	0,18	6.1	225.9	12.3	22	13.1
19	10%	6,4 ± 0,2	274 ± 10	115	10,3	0,05	1.1	43.9	6.9	8.5	4.7
	45%	7,4 ± 0,1	392 ± 15	186	13,5	0,08	1.8	69.8	8.1	10	6.6
	70%	8,2 ± 0,2	625 ± 50	334	15,1	0,12	2.9	111.4	10.3	13.9	7.5
	90%	9,4 ± 0,1	850 ± 30	511	18,6	0,17	4.7	146.9	14.4	17	8.6
26	10%	7,6 ± 0,1	200 ± 10	80	9,3	0,04	1.5	30.4	4.6	5.3	2.1
	45%	8,4 ± 0,1	325 ± 14	152	11,7	0,06	1.4	59.6	6.1	9.9	4.1
	70%	9,2 ± 0,1	500 ± 20	270	13.7	0,09	2.3	88.2	8.3	11.5	5.2
	90%	11,7 ± 0,3	800 ± 15	462	17.2	0,12	3.9	172.9	10.6	12.3	6.8

Table A7: *Summury of tests results for the NE70 membrane (Working pressure and Chemical analysis of the permeate) at different operation conditions*

Flux (L/m²-hr)	Recovery rate (± 2 %)	Feed Pressure (bar)	Permeate TDS (mg/L)	Permeate							
				Cl^- (mg/L)	NO_3^- (mg/L)	F^- (mg/L)	K^+ (mg/L)	Na^+ (mg/L)	SO_4^{2-} (mg/L)	Ca^{2+} (mg/L)	Mg^{2+} (mg/L)
13	10%	nd	nd	nd	nd	nd	nd	nd	nd	nd	nd
	45%	nd	nd	nd	nd	nd	nd	nd	nd	nd	nd
	70%	nd	nd	nd	nd	nd	nd	nd	nd	nd	nd
	90%	nd	nd	nd	nd	nd	nd	nd	nd	nd	nd
19	10%	nd	nd	nd	nd	nd	nd	nd	nd	nd	nd
	45%	4.2 ± 0.1	3260 ± 100	1220	18	0.89	16.4	633	85.2	38	15
	70%	4.8 ± 0.1	3400 ± 130	1260	19	0.96	16.3	665	145	45	19
	90%	5.2 ± 0.2	3510 ± 200	1285	20	1.05	16.5	666	203	60	23
26	10%	nd	nd	nd	nd	nd	nd	nd	nd	nd	nd
	45%	5,8 ± 0,2	3030 ± 150	1140	17	0.91	15.4	618	92	30	12
	70%	6,4 ± 0,1	3221 ± 140	1200	19	0.95	15.9	640	143	35	14
	90%	7.2 ± 0,2	3420 ± 225	1254	20	0.95	16.2	656	154.2	45	22

Table A8: *Summury of tests results for the ESNA1LF membrane (Working pressure and Chemical analysis of the permeate) at different operation conditions*

				ESNA 1 LF (NF)							
Flux (L/m²-hr)	Recovery rate (± 2 %)	Feed Pressure (bar)	Permeate TDS (mg/L)	Permeate							
				Cl⁻ (mg/L)	NO₃⁻ (mg/L)	F⁻ (mg/L)	K⁺ (mg/L)	Na⁺ (mg/L)	SO₄²⁻ (mg/L)	Ca²⁺ (mg/L)	Mg²⁺ (mg/L)
13	10%	$4,8 \pm 0,4$	1330 ± 50	500	20	1,2	6.3	255.9	35.8	30	14
	45%	$4,9 \pm 0,4$	2380 ± 80	1000	23	1,3	12.8	508.6	105.2	43	20
	70%	$5,9 \pm 0,5$	3095 ± 95	1140	27	1,5	13 .4	573.8	165.3	49	22
	90%	$7,2 \pm 0,3$	3350 ± 50	1220	27	1,5	13.4	602	180	53	35
19	10%	$5,8 \pm 0,3$	1200 ± 50	275	18	1,1	5.9	252	45.2	27	10
	45%	$6,8 \pm 0,5$	2135 ± 35	756	20	1,4	10.3	445.8	85.2	38	15
	70%	$7,5 \pm 0,6$	2755 ± 65	995	21	1,5	12.8	553.9	145	45	19
	90%	$8,6 \pm 0,6$	3245 ± 45	1140	24	1,4	15	641.4	203	60	23
26	10%	$7,4 \pm 0,2$	1070 ± 70	400	16	0,9	5.1	210	24	22	8.9
	45%	$7,9 \pm 0,8$	1800 ± 20	563	19	1,2	9.5	404.7	92	30	12
	70%	$8,9 \pm 0,6$	2490 ± 100	853	23	1,3	12.26	545.3	143	35	14
	90%	$9,6 \pm 0,7$	3140 ± 100	1030	23	1,3	14.4	633.3	154.2	45	22

Table A9: *Summury of simulation results for the BW30 membrane (Working pressure and Chemical composition of the permeate) at different operation conditions*

BW30-4040 (LOW-PRESSURE RO)											
Flux (L/m²-hr)	Recovery rate	Feed Pressure (bar)	Specific Energy (kWh/m³)	Permeate TDS (mg/L)	Permeate						
					Cl⁻ (mg/L)	Na⁺ (mg/L)	F⁻ (mg/L)	NO₃⁻ (mg/L)	SO₄²⁻ (mg/L)	Ca²⁺ (mg/L)	Mg²⁺ (mg/L)
13	10%	7,3	2.54	35,2	14.6	9	0.02	2.1	2.3	1.6	0.68
	45%	8.8	3.07	60.9	25.2	15.2	0.04	3.4	4.1	2.6	1.17
	70%	11.8	4.18	108.9	46.2	27.7	0.08	5.5	7.2	5.1	2.16
	90%	24.4	9.43	298	130	77.6	0.21	10.6	21	14.4	6.3
19	10%	9.9	3.43	24.5	10,1	6.1	0,02	1,5	1,6	1,1	0,5
	45%	11.4	3.98	41.8	17,4	10.5	0.03	2.4	2.7	1.9	0.8
	70%	14.8	5.16	76.5	32.2	19.3	0.05	4.1	5.1	3.5	1.5
	90%	29.3	9.96	210	90.9	54	0.15	8.6	14.7	10.1	4.4
26	10%	12.6	4.37	19	7.8	4,7	0.01	1.17	1.3	0,8	0.37
	45%	14.2	4.98	32.5	13.4	8.1	0.02	1.94	2.2	1.5	0.64
	70%	18.1	6.23	58	24.2	14.5	0.04	3.26	3.9	2.6	1.16
	90%	33.3	11.6	169	72.3	43.5	0.12	7.5	11.9	8.1	3.5

Table A10: _Summury of simulation results for the REBLF membrane (Working pressure and Chemical analysis of the permeate) at different operation conditions_

RE BLF (OI)											
Flux (L/m²-hr)	Recovery rate	Feed Pressure (bar)	Permeate TDS (mg/L)	Permeate							
				Cl⁻ (mg/L)	Na⁺ (mg/L)	F⁻ (mg/L)	NO₃⁻ (mg/L)	SO₄²⁻ (mg/L)	Ca²⁺ (mg/L)	Mg²⁺ (mg/L)
13	10%	7.8	81	36	19	0.01	1.1	7	3.6	1.5
	45%	11.8	133	60	31	0.02	1.8	11	6	2.6
	70%	19.7	238	107	55	0.04	3.2	20	11	4.6
	90%	46.3	582	262	134	0.1	8.1	50	26	11
19	10%	8.8	55	24	12	0.01	0.7	5	2.5	1
	45%	12.8	88	40	20	0.01	1.2	7.6	4	1.7
	70%	20.7	158	71	37	0.03	2.1	13.6	7.1	3
	90%	49.6	414	187	95	0.07	5.6	36	19	8
26	10%	9.8	41	18	9	0.01	0.6	3.5	1.8	0.7
	45%	13.8	68	31	15	0.01	0.9	15.7	3	1.3
	70%	22.2	124	55	28	0.02	1.7	10.7	5.6	2.4
	90%	53	330	148	76	0.06	4.5	28.5	15	6.3

Table A11: *Summury of simulation results for the ESPA3 membrane (Working pressure and Chemical analysis of the permeate) at different operation conditions*

Flux (L/m²-hr)	Recovery rate	Feed Pressure (bar)	Permeate TDS (mg/L)	Permeate						
				Cl^- (mg/L)	Na^+ (mg/L)	F^- (mg/L)	NO_3^- (mg/L)	SO_4^{2-} (mg/L)	Ca^{2+} (mg/L)	Mg^{2+} (mg/L)
13	10%	4.2	265	83	77	0.17	12	11	6	2.7
	45%	5.2	678	226	197	0.44	23	31	17	7.2
	70%	nd (*)	nd	nd	nd	nd	nd	nd	nd	nd
	90%	nd	nd	nd	nd	nd	nd	nd	nd	nd
19	10%	5.4	177	55	51	0.11	8	7	4	2
	45%	6.5	469	153	136	0.3	18	20	11	5
	70%	nd	nd	nd	nd	nd	nd	nd	nd	nd
	90%	nd	nd	nd	nd	nd	nd	nd	nd	nd
26	10%	6.6	132	41	38	0.09	6	5	3	1
	45%	7.8	358	116	104	0.23	14	15.7	8	3.7
	70%	10.4	635	212	185	0.41	22	29	16	7
	90%	nd	nd	nd	nd	nd	nd	nd	nd	nd

Header spanning: **ESPA3 (OI)**

Table A12: *Summury of simulation results for the BW30LE membrane (Working pressure and Chemical analysis of the permeate) at different operation conditions*

BW30LE-4040 (LOW-PRESSURE RO)											
Flux (L/m^2-hr)	Recovery rate	Feed Pressure (bar)	Specific Energy (kWh/m^3)	Permeate TDS (mg/L)	Permeate						
					Cl$^-$ (mg/L)	Na$^+$ (mg/L)	F$^-$ (mg/L)	NO$_3^-$ (mg/L)	SO$_4^{2-}$ (mg/L)	Ca^{2+} (mg/L)	Mg^{2+} (mg/L)
13	10%	5.8	2.03	65	26	16	0.04	4.5	4.2	2.9	1.25
	45%	7.23	2.54	109	45	27	0.08	6.7	7.1	4.9	2.13
	70%	10.1	3.58	194	83	49	0.13	9.7	13.1	9	3.91
	90%	21.3	7.48	503	222	131	0.35	14.7	37.5	25.4	11.1
19	10%	7.6	2.64	46	18	11	0.03	3.3	2.9	2	0.87
	45%	9.25	3.15	75	31	19	0.05	5.1	4.8	3.4	1.46
	70%	20.3	6.96	127.7	51	30	0.06	7.8	9.6	6.5	2.86
	90%	25.6	8.54	361	157	93	0.25	13	26.3	17.8	7.7
26	10%	9.4	3.27	36	14	9	0.02	2.6	2.2	1.7	0.68
	45%	10.97	3.85	60	25	15	0.04	4.2	4.1	2.7	1.17
	70%	14.59	5.02	106	44	26	0.07	6.5	7.1	4.8	2.1
	90%	28.4	9.86	296	128	76	0.21	11.9	21.3	14.4	6.3

Table A13: *Summury of simulation results for the NF90 membrane (Working pressure and Chemical analysis of the permeate) at different operation conditions*

Flux (L/m²-hr)	Recovery rate	Feed Pressure (bar)	Specific Energy (kWh/m³)	Permeate TDS (mg/L)	Permeate						
					Cl⁻ (mg/L)	Na⁺ (mg/L)	F⁻ (mg/L)	NO₃⁻ (mg/L)	SO₄²⁻ (mg/L)	Ca²⁺ (mg/L)	Mg²⁺ (mg/L)
13	10%	4.2	1.45	257	130.5	75.74	0.21	10.6	8.2	8.5	3.7
	45%	5.3	1.85	394	201.6	117.26	0.32	13.1	13.3	13.6	5.9
	70%	7.3	2.6	641	329	190	0.51	15.5	24.1	24.1	10.4
	90%	13.2	4.57	1288	653.8	368	0.93	18.2	65.7	59.2	25.5
19	10%	5.2	1.8	184	91.9	53.8	0.15	8.7	5.7	5.9	2.6
	45%	6.5	2.2	280	141.6	82.6	0.23	11.1	9.1	9.3	4.1
	70%	9.0	3.04	462	236.9	137.5	0.37	13.8	16.6	16.4	7.1
	90%	16.5	5.62	1020	521.9	297.3	0.76	17.4	46.4	43.2	18.7
26	10%	6.2	2.15	144	71.7	41.9	0.12	7.4	4.4	4.6	2.1
	45%	7.5	2.64	227	114.2	66.7	0.19	9.9	7.2	7.4	3.2
	70%	10.3	3.54	375	191.3	111	0.31	12.7	12.9	13.1	5.7
	90%	18.6	6.64	874	448	256	0.67	16.8	37.5	35.5	15.4

NF90-4040 (Nanofiltration)

Table 14: *Summury of simulation results for the NE90 membrane (Working pressure and Chemical analysis of the permeate) at different operation conditions*

NE90 (NF)										
Flux (L/m²-hr)	Recovery rate	Feed Pressure (bar)	Permeate TDS (mg/L)	Permeate						
				Cl⁻ (mg/L)	Na⁺ (mg/L)	F⁻ (mg/L)	NO₃⁻ (mg/L)	SO₄²⁻ (mg/L)	Ca²⁺ (mg/L)	Mg²⁺ (mg/L)
13	10%	7.2	335	172	88	0.01	4.9	6	3.1	1.3
	45%	11.05	548	281	144	0.02	7.9	9.8	5.2	2.2
	70%	18.2	946	485	248	0.03	13.6	17	8.9	3.8
	90%	39.9	2082	1074	549	0.08	28.4	39	21	8.9
19	10%	7.9	225	115	59	0.01	3.3	3.9	2.1	0.9
	45%	11.7	365	187	96	0.01	5.3	6.5	3.4	1.5
	70%	19.3	649	331	169	0.02	9.6	11.3	5.9	2.5
	90%	45.8	1642	839	429	0.06	24	28.7	15.1	6.4
26	10%	8.6	170	87	44	0.01	2.5	3	1.6	0.7
	45%	12.5	280	143	73.5	0.01	4.1	5.1	2.6	1.1
	70%	20.4	516	264	135	0.01	7.5	9	4.7	2
	90%	47.5	1250	641	327	0.04	17.9	22.7	11.8	5

Table A15: *Summury of simulation results for the ESNA1LF membrane (Working pressure and Chemical analysis of the permeate) at different operation conditions*

ESNA 1 LF (NF)										
Flux (L/m²-hr)	Recovery rate	Feed Pressure (bar)	Permeate TDS (mg/L)	Permeate						
				Cl⁻ (mg/L)	Na⁺ (mg/L)	F⁻ (mg/L)	NO₃⁻ (mg/L)	SO₄²⁻ (mg/L)	Ca²⁺ (mg/L)	Mg²⁺ (mg/L)
13	10%	3,7	852	451	277	1,39	7,4	26	21,3	9,1
	45%	4,4	1166	612	372	1,34	9,8	41	34	14,53
	70%	nd (*)	nd	nd	nd	nd	nd	nd	nd	nd
	90%	nd	nd	nd	nd	nd	nd	nd	nd	nd
19	10%	5,1	568	301	185	0,93	4,9	17,4	14,1	6,1
	45%	6,1	827	437	267	1,09	7	27,43	22,93	9,76
	70%	7,7	1305	681	412	1,24	11	49	41	17,3
	90%	nd	nd	nd	nd	nd	nd	nd	nd	nd
26	10%	6,3	426	226	140	0,69	3,65	13	10,68	4,55
	45%	7,3	639	337	206	0,89	5,4	20,7	17,25	7,35
	70%	9,7	1008	530	321	1,18	8,5	35,5	29,2	12,5
	90%	nd	nd	nd	nd	nd	nd	nd	nd	nd

Table A16: *Summury of simulation results for the NE70 membrane (Working pressure and Chemical analysis of the permeate) at different operation conditions*

Flux (L/m^2-hr)	Recovery rate	Feed Pressure (bar)	Permeate TDS (mg/L)	NE70 (NF) Permeate						
				Cl$^-$ (mg/L)	Na$^+$ (mg/L)	F$^-$ (mg/L)	NO$_3^-$ (mg/L)	SO$_4^{2-}$ (mg/L)	Ca^{2+} (mg/L)	Mg^{2+} (mg/L)
13	10%	7.3	896	482	9	247	0.02	11.3	6.5	3
	45%	10.1	1305	707	13	361	0.03	16	11	5
	70%	14.7	1898	1042	17.6	533	0.06	20.2	20	9
	90%	nd	nd	nd	nd	nd	nd	nd	nd	nd
19	10%	8.1	635	339	6.3	173	0.01	8.6	4.4	1.9
	45%	11.4	956	513	9.5	262	0.02	12.6	7.1	3
	70%	17.2	1534	832	14.8	425	0.04	18.5	13	6
	90%	nd	nd	nd	nd	nd	nd	nd	nd	nd
26	10%	9.2	492	262	5	134	0.01	6.9	3.3	1.5
	45%	12.6	779	416	7.8	213	0.02	10.7	5.5	2.5
	70%	19.3	1361	730	13.5	373	0.03	18	10	4.5
	90%	41.4	3070	1669	29	853	0.07	36.2	26	11.7

Appendix (2): Referees reports

	UNIVERSITE DE BRETAGNE SUD U.F.R. SCIENCES ET SCIENCES DE L'INGENIEUR
	Patrick BOURSEAU, Professeur ☎ : *02 97 87 45 31* - 🖨 : *02 97 87 45 00* ✉ : patrick.bourseau@univ-ubs.fr

Rapport concernant le mémoire de thèse de Mademoiselle **Hanane DACH**, intitulé :

Comparaison des opérations de nanofiltration et d'osmose inverse pour le dessalement sélectif des eaux saumâtres : de l'échelle du laboratoire au pilote industriel

pour obtenir le grade de Docteur de l'Université d'Angers.

Cette thèse a pour objectif de comparer les performances de membranes d'osmose inverse et de nanofiltration pour la production d'eau potable à partir d'eaux saumâtres. Elle correspond à des enjeux environnementaux forts liés à la croissance du stress hydrique dans certaines régions du globe, et notamment en Afrique du Nord et au Moyen-Orient, enjeux que l'auteur résume parfaitement dans le premier chapitre de son mémoire. Le travail réalisé vise en particulier à démontrer la faisabilité technico-économique de la nanofiltration vis-à-vis de l'osmose inverse basse pression pour le dessalement d'eaux modérément saumâtres (4 à 6 g/L). Il associe des expérimentations de caractérisation physico-chimique de la surface des membranes à des études de filtration menées à l'échelle du laboratoire, puis à l'échelle pilote sur une eau saumâtre naturelle marocaine (eau de Tan-Tan). Un modèle simple de transfert (Spiegler-Kedem-Katchalsky) est également mis en œuvre pour interpréter le comportement des membranes sur la base des mécanismes de transfert convectif et diffusif du soluté.

Le travail a été dirigé par les professeurs Maxime Pontié de l'Université d'Angers (directeur de thèse) et Abdelhadi Lhassani de l'Université de Fès au Maroc. Le mémoire, de 178 pages est organisé de manière classique en trois chapitres consacrés à une étude bibliographique, à la présentation des matériels et méthodes mis en œuvre, et à la présentation et à la discussion des résultats. Il inclut également une introduction et une conclusion et s'appuie sur une bibliographie riche de plus de 200 références.

Le **chapitre 1** (57 pages) présente tout d'abord le contexte de la thèse : stress hydride croissant dans de nombreuses régions, forte croissante de la capacité mondiale de dessalement et part élevée de l'osmose inverse au sein des techniques de dessalement (43 %), les eaux saumâtres représentent le quart des eaux traitées. Dans ce contexte, la nanofiltration (NF) peut être utilisée en adoucissement partiel de ces eaux saumâtres en lieu et place de l'OI, et ce qui ouvre un marché potentiel important à cette technologie. L'auteur présente les installations existantes au Maroc ainsi que les projets en cours, et met en évidence la question de la teneur élevée en fluor de certaines eaux (Afrique en particulier) et de leur défluorisation. L'auteur détaille ensuite les applications en traitement d'eaux saumâtres et précise les mécanismes de transfert régissant la sélectivité d'une membrane de nanofiltration (exclusion stérique, électrique et diélectrique). Il introduit le modèle développé successivement par Spiegler, Kedem et Katchalski basé sur la thermodynamique des processus irréversibles. Ce modèle s'applique à des solutions contenant un seul soluté et lorsque les interactions électriques entre le soluté et la membrane sont négligeables. Il prédit les flux du solvant et du soluté à partir de 3 paramètres, les perméabilités de la membrane au solvant (L_p) et au soluté (P_s), et le coefficient de réflexion du soluté ($\tilde{\sigma}$) Une transformation linéaire du modèle permet également de mettre en évidence les importances respectives des composantes convective et diffusive dans le transport du soluté.

Il aurait été utile que soit précisée la différence entre le modèle de Spiegler-Kedem et celui de Kedem-Katchalsky, et à quoi correspond la variante (appelée SKK) que l'auteur a utilisée dans son travail.

Le chapitre se termine par une présentation des techniques de caractérisation des membranes d'OI et de NF mises en œuvre dans la thèse : détermination du potentiel d'écoulement transmembranaire (SP), qui dans le cas de la NF permet d'obtenir le point isoélectrique PIE de la membrane et une indication qualitative de sa charge effective à un pH différent du PIE, de l'hydrophobicité de la surface membranaire par la mesure de l'angle de contact par la méthode de la goutte d'eau sessile, et de la rugosité moyenne des membranes par microscopie à force atomique (AFM).

Le **chapitre 2** (15 pages) présente les matériels et méthodes mis en œuvre dans la thèse et en particulier les membranes et les pilotes de filtration. Le pilote de laboratoire utilisé en particulier pour l'étude des solutions modèles à 2 ou 3 ions accepte des membranes planes (S = 0,047 m^2). Dans le cadre de ce travail, ont été testées deux membranes d'osmose inverse basse pression (OIBP), la BW30 et BW30LE (DOW-Filmtec, de rétention en chlorure de sodium R respectivement égales à 99,5 et 99 %, deux membranes de NF présentant des rétentions en sels élevées (NF90, DOW-Filmtec et NE90, Saehan, R = 85-95 %) ainsi que deux membranes de NF Dow-Filmtec à plus faible rétention (NF270, R = 40-60 % ; NF200, R = 35-50 %). Toutes les membranes sont en polyamide excepté la NF200 dont le matériau (polypiperazineamide) est réticulé par des groupements sulfonés qui lui confèrent une charge plus élevée.

L'installation pilote accepte des modules spirale de 4'' (S = 7,2 m^2). Outre les membranes testées à l'échelle du laboratoire, seront également utilisées deux membranes supplémentaires (ESPA3, Hydranautics et REBLF, Saehan), deux membranes de nanofiltration à forte

rétention en sel (ESNA 1 LF, Hydranautics, et NE70, Saehan), ainsi qu'une membrane à faible rétention en sel (NE70, Saehan).

Le **chapitre 3 « résultats et discussions »** (64 pages) est organisé en deux parties traitant respectivement de la caractérisation et de l'analyse des performances des membranes planes, et de la filtration d'une eau saumâtre marocaine à l'échelle pilote (eau de Tan-Tan).

Les études en laboratoire sont présentées en 4 paragraphes, le premier concernant la filtration de solutions modèles *(§I.1)*. Les perméabilités à l'eau puis à une solution de NaCl (6 g/L), et les rétentions en chlorure de sodium et en sulfate de sodium sont mesurées à recyclage total. Les membranes présentent des perméabilités à l'eau qui décroissent de Lp = 14,8 L.h^{-1}.m^{-2}.bar^{-1} pour la NF90, et d'environ 10,5 L.h^{-1}.m^{-2}.bar^{-1} pour la NF200 et la NE90, à 5,1 L.h^{-1}.m^{-2}.bar^{-1} pour la NF 270, et 2.3 et 3.5 L.h^{-1}.m^{-2}.bar^{-1} pour les membranes d'OIBP. Logiquement, les membranes de NF ont donc une perméabilité plus élevée que les membranes d'OIBP, mais la NF270, bien qu'ayant visiblement des pores assez larges (son seuil de coupure pour des molécules organiques est donné par le fabricant à 300 Da contre 200 Da pour les autres membranes) a des flux très bas, à peine supérieurs à ceux des membranes d'OIBP. Les perméabilités à la solution de NaCl s'établissent dans le même ordre, à l'exception de la NF200 qui a maintenant un flux de perméation supérieur à celui de la NF90, probablement parce que la NF200 a la rétention en sel la plus faible et qu'elle présente à ce titre une différence de pression osmotiques moindre.

En ce qui concerne les rétentions en chlorure de sodium, il apparaît que la NF200 a des rétentions nettement supérieures à celles de la NF90 et de la NF270, et sont finalement assez proches des rétentions des membranes d'osmose basse pression (BW30 et BW30LE). A faible pression (< 6 bar) la rétention de la NF90 est plus faible que celle de la NF270, mais l'ordre s'inverse au-delà de 6 bar. L'auteur explique ce comportement par l'inversion du mode prédominant du transfert. Cependant, la courbe de rétention de la membrane NF90 présentant une discontinuité surprenante, on peut se demander s'il ne s'agit pas plutôt d'un artefact expérimental. Les rétentions en sulfate de sodium sont plus importantes, la différence de rétention entre les 2 sels étant moindre pour les membranes d'OIBP. L'auteur l'explique fort justement par la différence entre les mécanismes de transfert du soluté. En OIPB, c'est principalement la taille des ions et leur diffusivité qui régissent la vitesse de transfert des ions : les ions les plus petits diffusent plus rapidement mais les écarts entre ions ne sont pas énormes. En NF, la sélectivité résulte d'un phénomène d'exclusion stérique, mais aussi électrique (effet Donnan), ce qui induit une sélectivité marquée entre ions monovalents et divalents (fortement exclus de par leur charge élevé).

L'auteur étudie ensuite l'influence de la concentration en sel (NaCl puis Na2SO4) sur les rétentions, toujours pour les 2 membranes d'OIPB et les 3 de NF considérées, sur les mêmes gammes de pression que précédemment. Les rétentions diminuent lorsque la concentration augmente, faiblement pour les membranes d'OIPB, plus nettement pour les membranes de NF à cause de l'écrantage des charges de la membrane à force ionique élevée. Les courbes de rétention des membranes de NF pour 5 concentrations en NaCl (10^{-3} à 10^{-1} M) sont très intéressantes. Elles font en effet apparaître 3 comportements bien distincts lorsqu'on augmente la pression. Pour la membrane NF 90, les courbes de rétention sont plutôt resserrées

et à peu près parallèles, pour la membrane NF270 elles sont plus espacées et ont une allure divergente (à pression élevée, la rétention chute très fortement quand la concentration augmente), et enfin pour la membrane NF200 elles sont également très espacées mais plutôt « convergentes » (les chutes de rétention quand la concentration augmente sont plus marquées à faible pression qu'à pression élevée). L'auteur explique justement le comportement de la NF270 par sa taille de pores relativement grande : à concentration élevée, les effets de charge étant masqués, seule reste l'exclusion stérique, qui est faible, et le chlorure de sodium est faiblement retenu. Le comportement des 2 autres membranes n'est pas expliqué. Pour la membrane NF90 (effet modéré de la concentration) on pourrait imaginer que la charge de la membrane est suffisamment forte pour que l'écrantage soit moins sensible, y compris à 0,1M.

La rétention de solutions à 3 ions est ensuite étudiée, sur des mélanges NaCl-Na2SO4 (l'ion divalent étant alors le co-ion de la membrane) et NaCl-CaCl2 (contre-ion divalent), pour les membranes NF90 et NF 200 (la membrane NF270 n'est pas considérée ici, probablement parce qu'elle présente des rétentions nettement plus faibles). Les résultats présentés sont conformes à ceux déjà publiés. Pour le premier mélange, l'ajout d'ions sulfate, fortement retenus, facilite le passage des ions chlorures : plus la proportion d'ions sulfate augmente, plus la rétention des ions chlorures diminue. L'auteur l'explique par le fait que la présence des ions sulfate attire les ions chlorures dans la membrane, alors qu'il serait plus correct de considérer que c'est le transfert des ions Na^+ qui « tire » les ions Cl^- pour assurer le respect de l'électroneutralité. Ce phénomène de « transfert facilité » des ions chlorures est plus marqué pour la membrane NF200, ce qui est attribué à la charge élevée de la membrane qui rejetterait plus fortement les ions sulfate. Cette interprétation n'est pas totalement convaincante puisque les essais précédents montrent que la NF90 rejette légèrement mieux les ions sulfate que la NF200.

Le comportement du mélange à contre-ion divalent (NaCl-CaCl2) est différent. La rétention des ions chlorures diminue dans un premier temps lorsqu'on ajoute une faible proportion de CaCl2 à du chlorure de sodium, mais elle augmente ensuite avec la proportion de CaCl2 dans le mélange. Ce phénomène a déjà été observé dans la littérature pour différents mélanges (NaCl-CaCl2, Bandini & Vezzani, Chem. Engng Sci. 58, 3303 (2003), ou NaCl-MgCl2, S. Déon, Thèse UBS, novembre 2007). L'auteur explique ce comportement non-linéaire par le fait qu'à faible ratio CaCl2/NaCl le phénomène dominant serait l'écrantage par les ions Na+ de la charge de la membrane qui rejetterait alors moins bien les ions chlorures, alors qu'à des ratios plus élevés le fort rejet des ions Ca2+ faciliterait le passage des ions Na+ et donc des ions chlorures par respect de l'électroneutralité. Cette interprétation, centrée sur le comportement de l'ion Cl-, ne prend cependant pas en compte la forte adsorption des ions divalents sur la membrane y compris à faible concentration, phénomène probablement prépondérant par rapport à l'écrantage de la charge de la membrane par les ions sodium.

Au *paragraphe suivant (I.2)*, la rétention des solutions de sels purs (NaCl et Na2SO4) sont fittées à l'aide du modèle de Spiegler-Kedem (SK) pour identifier les coefficients de perméabilité (Ps) et de réflexion (□). La transformée linéaire du modèle est ensuite utilisée pour caractériser l'importance relative des termes diffusif et convectif dans le transfert du chlorure de sodium (solution à 0.1 M). Comme attendu, il s'avère que le terme diffusif est

prépondérant pour les membranes d'osmose (BW30 et BW30LE), ainsi que pour la membrane NF90; pour la membrane NF270 à larges pores le terme convectif est prépondérant et pour la membrane NF 200 le mode est mixte, convectif-diffusif. Bien que le modèle de SK soit valable pour des molécules non chargées, les résultats sont physiquement cohérents, probablement parce qu'à la concentration 0,1 M considérée la charge fixe de la membrane est écrantée et l'exclusion du NaCl principalement d'origine stérique. Cette partie se termine par l'estimation des seuils de coupure des membranes de nanofiltration, ainsi que des concentrations en sels dans les pores (cint) et à la surface de la membrane (cm) et du facteur de polarisation (□). Ces calculs me semblent plus discutables parce que (i) la polarisation dépend de la pression appliquée ce qui n'est pas pris en compte ici, et (ii) en solution diluée (ici 10^{-3} M), les concentrations en cations et en anions dans la membrane peuvent être très différentes à cause de la charge fixe qu'elle porte, et la notion de « concentration en sel » dans la membrane est discutable.

Il faut cependant saluer la volonté de l'auteur d'utiliser un modèle de transfert pour interpréter le comportement des membranes dans une situation (solutions ioniques diluées) où la sélectivité du transfert résulte de couplages forts entre des effets d'exclusion stérique, électrique et diélectrique, et de phénomènes de transport convectif et diffusif. Cette partie de la thèse illustre bien à mon avis la complexité des mécanismes impliqués et l'apport du modèle dans l'interprétation des résultats. La discussion montre aussi à mon avis les limites du modèle utilisé et le bénéfice que ce type d'études peut tirer de la confrontation à des modèles de connaissance plus complets, de type Stefan-Maxwell par exemple.

Le *paragraphe I.3* présente les essais de caractérisation de la surface des membranes. Dans un premier, la rugosité moyenne des membranes a été mesurée par AFM sur des échantillons de 50 □m x 50 □m et de 1 □m x 1 □m. La rugosité est un paramètre intéressant car elle a été corrélée par certains auteurs à la perméabilité et au colmatage des membranes de nanofiltration (la rugosité augmenterait avec le seuil de coupure de la membrane et une rugosité élevée favoriserait le colmatage par des colloïdes dans les vallées). Les mesures font apparaître des différences importantes, la rugosité moyenne des membranes testées ici variant dans un rapport supérieur à 10. En outre, la valeur de cette rugosité moyenne croît notablement avec l'aire de la surface analysée et il faut donc en tenir compte lorsqu'on veut comparer la rugosité de différentes membranes. L'auteur indique que ce fait pourrait résulter du caractère fractal de la rugosité, ou traduire le fait que la rugosité dépendrait de la longueur d'onde de la surface scannée. Quoiqu'il en soit, les deux membranes d'OIPB et la membrane NF90 ont une rugosité nettement plus élevée (280 à 390 nm sur une surface 50 □m x 50 □m) que les trois autres membranes de nanofiltration testées (33 à 71 nm).

L'hydrophobicité des membranes a ensuite été testée en mesurant l'angle de contact par la méthode de la goutte sessile. L'auteur indique que les valeurs sont délicates à interpréter puisque à hydrophobicité donnée, l'angle augmente avec la rugosité de la surface. C'est un inconvénient de la méthode de la goutte sessile. Les membranes NF200 et NF270 semblent cependant plus hydrophiles que la membrane NF90 et les deux membranes d'osmose.

Enfin, le potentiel d'écoulement transmembranaire des membranes est mesuré sur la gamme de pH admissible par les membranes (2-10) pour déterminer leurs points

isoélectriques (PIE) et obtenir une information qualitative sur leurs charges fixes. Ces informations peuvent contribuer directement à interpréter les performances observées lors de la filtration des solutions ioniques, ce qui rend ces mesures particulièrement intéressantes. Parmi les résultats présentés, on retiendra que les courbes de potentiel des membranes en polyamide sont assez proches, le potentiel de la membrane NF200 (en polypiperazineamide sulfonée) au-delà du PIE étant nettement plus élevé (en valeur absolue) que celui des autres membranes, trahissant ainsi sa charge de surface plus élevée. Corollairement, le PIE de cette membrane NF200 (2,5) est un peu plus bas que ceux des membranes en polyamide (entre 2,9 et 4,0). Enfin, le potentiel d'écoulement de la membrane NF270 (l'influence de la force ionique sur le PIE n'est présenté que pour cette membrane) diminue quand la force ionique augmente pour pratiquement s'annuler à 10^{-1} M, indiquant qu'à partir de cette concentration l'exclusion est purement d'ordre stérique, résultat conforme à la littérature et à notre expérience. Enfin, le PIE se décale vers les valeurs positives lorsque la force ionique augmente (d'environ une unité de pH lorsqu'on passe de 10^{-3} à 10^{-1} M), matérialisant ainsi l'écrantage de la charge de la membrane par les ions de la solution.

Il aurait été intéressant d'inclure dans ces méthodes de caractérisation une estimation du rayon de pores des membranes de NF par la mesure de la rétention d'une molécule neutre (glucose par exemple). Cette caractérisation relativement simple aurait probablement facilité l'interprétation des flux et des rétentions mesurés en discriminant éventuellement l'effet du diamètre moyen de pores de celui de la porosité (degré de vide) de la membrane, et permis de préciser le rôle de l'exclusion stérique.

La *quatrième sous-partie (§I.4)* de cette étude à l'échelle du laboratoire fait le lien avec l'étude de cas détaillée en deuxième partie en étudiant les performances de 5 membranes (3 de NF et 2 d'OIBP) sur l'eau naturelle de Tan-Tan, eau légèrement saumâtre (3,3 à 4 g/l de solides dissous). L'auteur a déterminé les perméabilités entre 0 et 15 bar, les rétentions en matières dissoutes et en certains anions (Cl-, F-, NO3-), puis étudié l'influence du taux de conversion (Y = débit de perméat/débit d'alimentation). En ce qui les flux et les rétentions totales, on peut noter que les performances des membranes sur l'eau de Tan-Tan ne se classent pas toujours dans l'ordre obtenu avec la solution modèle NaCl à 6g/L (les flux de la NF90 et de la NF200 sont en ordre inverse par exemple).

Ces faits expérimentaux semblent difficiles à expliquer et on peut se demander si les membranes n'ont pas évoluées entre les deux séries d'expériences. A ce titre, on aurait aimé avoir davantage de détails sur l'enchaînement des différentes expériences : les mêmes membranes ont-elles été utilisées pour toutes les expériences ? Ont-elles été nettoyées entre les expériences ? La stabilité de leurs performances dans le temps a-t-elle été contrôlée, et comment ? La question du maintien des propriétés des membranes sur des campagnes entières d'expériences est un problème crucial, particulièrement en nanofiltration de solutions peu concentrées où la moindre modification de la charge de surface à la suite d'un lavage ou d'une simple expérience peut entraîner des modifications notables de ses performances.

Les anions sont retenus par toutes les membranes dans le même ordre, F- étant mieux retenu que Cl-, lui-même mieux retenu que NO3-. L'auteur l'explique par la valeur des énergies d'hydratation : les petits ions ont une énergie d'hydratation plus importante et sont pour cela plus exclus de la membrane. L'auteur montre aussi clairement que la nanofiltration a une sélectivité nettement supérieure à l'osmose inverse en ce qui concerne la transmission des anions monovalents (NO3- est en particulier nettement moins retenu que les 2 autres anions) et indique que cette sélectivité peut être (en partie) contrôlée en jouant sur les paramètres opératoires. Cela ouvre des perspectives intéressantes pour le contrôle de l'équilibre ionique d'eaux (partiellement) dessalées.

La discussion suscite implicitement la question de la nature du transfert diffusif des ions dans une membrane de nanofiltration : cette diffusion a-t-elle lieu dans la phase dense comme en osmose inverse (et comme le suppose l'auteur), ou dans la solution contenue dans les pores comme les modèles de connaissance (type Nernst-Planck) en font l'hypothèse ? Les deux modes coexistent probablement, le mode dominant évoluant lorsqu'on passe progressivement d'une membrane d'osmose inverse dense à une membrane de nanofiltration à pores pérennes.

L'auteur calcule ensuite à l'aide du modèle dit « SKK » les valeurs des perméabilités et des coefficients de réflexion de la matière totale dissoute ainsi que des 3 anions, pour 4 membranes et 3 taux de conversion. Les valeurs semblent cohérentes, mais on aurait aimé savoir comment l'auteur a adapté le modèle de Spiegler-Kedem à un mélange de plusieurs composés.

A l'issue de cette étude à l'échelle du laboratoire, les deux membranes NF90 et NE90 se distinguent nettement par leurs de perméation élevées et leurs rétentions adaptées à un dessalement partiel des eaux saumâtres de Tan-Tan.

La **deuxième partie du chapitre 3** est consacrée à la comparaison de la faisabilité technique et économique de la nanofiltration et de l'osmose inverse basse pression pour la production d'eau potable à partir de l'eau saumâtre de Tan-Tan. Cette étude recouvre un enjeu industriel sous-jacent, à savoir le remplacement des membranes d'OI actuellement en place sur l'usine de dessalement (BW30) par des membranes de nanofiltration. Il s'agit donc dans cette étude de déterminer à l'échelle pilote les conditions opératoires optimales d'une installation industrielle (pression transmembranaire et taux de conversion), et d'établir les principaux indicateurs de sa performance (flux de perméation, efficacité de dessalement et consommation énergétique), et ceci en fonction de la capacité de production souhaitée.

Une première évaluation des performances de 8 membranes a été faite à l'aide des logiciels fournis pas les fabricants, et la validité de ces prédictions sera validée *a posteriori*. Les performances de plusieurs membranes ont alors été déterminées sur l'installation pilote pour des taux de conversion allant de 10 à 90 %, et 3 valeurs différentes de la vitesse tangentielle et du flux de perméation. L'étude, très complète, a montré que les membranes d'OI atteignaient dans tous les cas la cible fixée en matière de dessalement (1 g/L en matières totales dissoutes). Parmi les membranes de nanofiltration, la NF90 et la NE90 y parviennent également sauf à forte conversion ou à faible flux de perméation, mais les autres membranes testées s'avèrent inadaptées. L'auteur a montré également que les deux membranes de NF produisaient de l'eau potable a un coût comparable à la membrane d'OIBP la plus économique, soit 0,34 à 0,43 kWh/m^3 sur la gamme de flux investiguée (13 à 26 L.h^{-1}.m^{-2}). En outre, les membranes de

nanofiltration permettent de produire directement l'eau potable, alors que l'eau produite par osmose inverse est trop déminéralisée et doit être remélangée avec de l'eau saumâtre. Globalement, *l'intérêt des membranes de NF testées est ainsi démontré pour la production d'eau potable à partir de l'eau saumâtre de Tan-Tan.*

En comparant l'ensemble des performances, l'auteur sélectionne finalement deux membranes candidates au remplacement des membranes BW30 existantes, la membrane de nanofiltration NF90 (Dow-Filmtec) et une membrane d'osmose inverse basse pression proche de la nanofiltration (REBLF, Saehan), et conclut que le choix définitif devra être fait sur la base d'une étude technico-économique complète.

En complément, l'auteur s'est attaché à cerner le potentiel et les limites de la NF en matière de dessalement partiel et de défluorisation des eaux saumâtres, sur la base d'essais effectués avec de l'eau de Tan-Tan (4,4 g/L en TDS) enrichie en sel ou en fluor. Les membranes de nanofiltration NF90 et NE90 apparaissent capable de dessaler correctement des eaux d'une salinité de 6 g/L mais pas de 10 g/L. Elles sont en outre largement capables de traiter des eaux dopées à 15 ppm de fluor, quel que soit le taux de conversion adopté.

La conclusion du mémoire résume parfaitement le travail réalisé et met les résultats obtenus en perspective. Elle dégage des perspectives de poursuite claires et appropriées, tant sur le plan appliqué et sur un plan plus fondamental.

En conclusion, ce travail de thèse réalise un bon équilibre entre une recherche appliquée s'appuyant sur des enjeux industriels précis, et des aspects plus fondamentaux liés à la caractérisation des membranes et à l'interprétation de leurs performances. L'enjeu de l'extrapolation est clairement identifié (comment obtenir à l'échelle du laboratoire les informations nécessaires au dimensionnement d'une installation industrielle) et la méthodologie suivie est bien adaptée (travailler sur des solutions modèles pour comprendre, puis sur des solutions réelles pour valider et obtenir des ordres de grandeur réalistes pour le dimensionnement).

Ce travail apporte également une contribution intéressante et parfois originale à l'étude de la sélectivité des membranes de nanofiltration de sels purs ou en mélange (à 3 ions), dans des conditions de concentrations modérées où la sélectivité du transfert résulte des effets couplés d'exclusion stériques, électriques et diélectriques (diminution des énergies d'hydratation des ions dans les pores) et du mode de transport dominant.

Le travail expérimental est important est varié, les résultats présentés sont d'un bon niveau et attestent que la candidate a acquis une bonne maîtrise de son sujet malgré la complexité du domaine. Il faut souligner également le souci constant qu'elle a eu d'interpréter les résultats expérimentaux à la lumière d'un modèle de transfert.

Sur le plan de la forme, le manuscrit est bien structuré et agréable à lire. La qualité et le volume des travaux effectués au cours de cette thèse correspondent largement aux exigences de soutenance d'une thèse de Doctorat. Je donne donc un avis favorable à la demande de

soutenance présentée par Mademoiselle Hanane DACH pour présenter son travail en vue d'obtenir le grade de Docteur de l'Université d'Angers.

Fait à Lorient, le 20 avril 2008

Patrick BOURSEAU,
Professeur

UNIVERSITE IBN TOFAIL   14/04/2008
FACULTE DES SCIENCES
LABORATOIRE DES PROCEDES DE SEPARATION

Pr . Azzeddine ELMIDAOUI
Tel/Fax : 037 37 30 33
GSM : 064 49 32 20
E-mail : elmidaouiazzedine@hotmail.com
            elmidaouiazzedine@yahoo.fr

Rapport de Thèse de Doctorat
Hanane DACH

Comparaison des opérations de Nanofiltration et d'Osmose Inverse pour le dessalement sélectif des eaux saumâtres : de l'échelle laboratoire au pilote industriel

L'objectif du travail de madame Dach est de comparer deux techniques de dessalement non conventionnelles, NF et OI, dans le dessalement des eaux saumâtres.

Après une étude bibliographique exhaustive sur les problèmes de disponibilité d'eau au Maroc et sur les différentes techniques de dessalement, particulièrement les procédés membranaires, l'auteur présente dans le deuxième chapitre le matériel utilisé et les procédures expérimentales adoptées.

Dans le troisième chapitre, sont présentés et discutés les résultats de cette étude. En plus d'une caractérisation physico-chimique des membranes utilisées, l'auteur présente quelques résultats de la modélisation des phénomènes de transport. En suite elle présente les performances des essais de dessalement menés aussi bien au laboratoire qu'à l'échelle du pilote industriel sur le site de Tan Tan au Sud du Maroc.

La candidate Dach, a su dominer un sujet large et délicat notamment sur le plan expérimental. Malgré l'abondance du contenu, le manuscrit est clair et facile à lire. Les expériences sont particulièrement nombreuses et menées avec logique, les résultats sont correctement analysés et les interprétations convaincantes.

Le mémoire ouvre des perspectives très intéressantes dans le domaine de dessalement des eaux saumâtres, dans un moment où les périodes de secheresse s'installent avec insistance entrainant une diminution inquiétante des ressources en eau au niveau du Maroc.

Pour toutes ces raisons, j'estime le mémoire de l'étudiante Hanane Dach mérite d'être présenté pour obtenir le grade de Docteur.

Azzeddine Elmidaoui

UNIVERSITE SIDI MOHAMED BEN ABDELLAH

ECOLE SUPERIEURE DE TECHNOLOGIE DE FES

LABORATOIRE DES SCIENCES ET TECHNOLOGIE DU GENIE DES PROCEDES

Tél. : 035 60 05 86   Fax : 035 60 05 88

Route d'Immouzzer, B.P. 2427 Fès

Jilali BENTAMA,
Professeur

RAPPORT DE THESE

Le rapport de thèse de Doctorat National présenté par Hanane DACH est intitulé : Comparaison des opérations de Nanofiltration et d'Osmose inverse pour le dessalement sélectif des eaux saumâtres : de l'échelle du laboratoire au pilote industriel.

Le but du travail est d'établir une approche systématique de caractérisation des membranes commerciales du nanofiltration (NF) et d'osmose inverse à basse pression (LPRO) pour une meilleure aide aux utilisateurs. Pour évaluer et comparer les performances (productivité et sélectivité) des deux technologies membranaires, deux principales sortes de caractérisations sont développées:

- La première est physico-chimique en termes de hydrophobicité/hydrophilicité, morphologie et topographie ;
- La seconde concerne d'une part le transfert de masse en terme de perméabilités aux solutions salines constituée de sels monovalents ou bivalents et la détermination de seuil de coupure.

Le comportement des membranes commercialisées de NF et d'OI (LPRO) pour le traitement des eaux saumâtres est présenté. Le travail expose à chaque fois les résultats obtenus aux laboratoires et ceux déterminés sur le site de traitement d'eau de Tan Tan. L'étude de l'évaluation des performances de ces membranes pour la défluoruration d'une eau saumâtre contenant les ions fluorures est aussi présentée.

Le rapport est composé de trois parties :

La première partie présente une étude bibliographique et les études expérimentales. Elle concerne le dessalement de l'eau, l'expérience marocaine dans ce domaine, les procédés membranaires en générale et la NF et l'OI en particulier. Les techniques de caractérisation et les paramètres affectant les performances des membranes de NF et d'OI sont détaillés.

La partie expérimentale traite les travaux réalisés dans les deux laboratoires de recherche :

-    le laboratoire de chimie appliquée de la faculté des sciences et techniques de Fès,

191

- le laboratoire du groupe de recherche d'analyse et procédé d'Angers France, et ceux réalisés à la station de déminéralisation de Tan Tan.

Après avoir décrit les membranes commerciales et leur domaine d'utilisation en terme de pression, pH, température et la gamme de rétention en % de sel (NaCl et MgSO4), la candidate a présenté les caractéristiques et les modes opératoires des pilotes de filtration utilisés.

Dans un premier temps, trois membranes de nanofiltration dénommées NF90, NF200 et NF270 et deux membranes d'OI dénommées BW30 et BW30LE ont été testées au niveau du laboratoire, pour deux solutions contenant des sels monovalents, en termes de perméabilité à l'eau et avec différentes concentrations. Les résultats ont prouvé que les rejets des sels étudiés et les flux de perméat pour toutes les membranes augmentent avec la pression transmembranaire et diminuent avec la concentration. Une étude comparative entre les membranes BW30 et BW30LE d'une part et les NF90, NF200 et NF270 d'autre part est exposée. Cette étude est accompagnée par les caractérisations des membranes suivantes :
- la mesure de la charge des membranes par le potentiel d'écoulement ;
- La morphologie de surface des membranes par la Microscopie de force atomique ;
- La mesure de l'angle de contact pour déterminer la mouillabilité de la couche active des membranes ;

Les caractérisations des solutions utilisées dans ce travail concernent :
- La mesure du pH ;
- La mesure de la salinité (TDS) ;
- L'analyse des chlorures, nitrates et fluorures par électrodes spécifiques ;
- Le dosage des sulfates par précipitation ;
- Le dosage du calcium et du magnésium par colorimétrie.

Dans le cas de mélange de sel monovalent et divalent, la candidate a présenté les résultats de l'étude comparative entre les membranes NF90 et NF200 (qui présentent une sélective entre les ions monovalents et bivalents) et les membranes d'osmose inverse à basse pression.

La deuxième partie est consacrée à une étude pilote du dessalement d'une eau saumâtre du Sud du Maroc, afin de prouver sur le plan technique et économique, l'efficacité de la nanofiltration pour le dessalement de cette eau. La nanofiltration s'est avérée efficace pour le dessalement partiel et sélectif de l'eau saumâtre étudiée en un seul étage, avec une consommation énergétique plus faible qu'en OI.

L'étude pilote réalisée avec des membranes spiralées de NF et d'OI sur des eaux réelles et saumâtres de Tan Tan a montré l'efficacité du procédé de nanofiltration. En effet la NF permet un dessalement partiel et sélectif avec une consommation énergétique plus faible qu'en OI.

La dernière partie est consacrée à l'exploitation des résultats expérimentaux pour une étude d'évaluation de la précision de logiciels de simulation de 3 fournisseurs de membranes dénommés :

- ROSA: Dow Chemical
- IMSDesign : Hydranautics
- CSMPRO : Saehan

La conclusion de cette étude est que:

Des 4 membranes de NF testées, la NF90 et la NE90 sont sans doute les plus adéquates et les plus concurrentes à la BW30 pour le dessalement d'une eau saumâtre avec un taux de salinité de 4 g/L. Elle permettent un dessalement partiel et permettent aussi de préparer une eau destinée à la consommation humaine (TDS $\leq$ 1000 ppm) à des pressions 2 fois plus faibles et à des taux de conversions plus élevés (90%).

Des essais de dopage de l'eau de TanTan à différents taux de salinité et avec des ions fluorures ont été réalisés. Ces essais ont permis de déterminer les limites d'application des membranes de nanofiltration et confirmer l'efficacité de la NF pour la défluoruration sélective des eaux saumâtres au Maroc.

La candidate Hanane DACH a su mettre un plan de travail pour aboutir aux résultats désirés : la comparaison entre deux technologies de séparation membranaire destinées aux dessalements des eaux saumâtres. Elle a utilisé des procédés nouveaux, a assimilé les différentes techniques de caractérisation physico-chimique et a exploité ses résultats pour évaluer des logiciels commerciaux de simulation. L'ensemble du travail de cette thèse rassemble entre une recherche scientifique de qualité et une recherche-développement d'opportunité. Après examen du rapport de thèse de Hanane DACH, je donne un avis favorable pour sa présentation orale.

<div align="center">

Fès, le 14 avril 2008

Signé : **Jilali BENTAMA**

</div>